


UNIVERSITA' DELLA CALABRIA

Dipartimento di FISICA

Scuola di Dottorato

Scienze, Comunicazione e Tecnologie "Archimede"

Indirizzo

Fisica e Tecnologie Quantistiche

Con il contributo di (Ente finanziatore)

Commissione Europea, Fondo Sociale Europeo e Regione Calabria

CICLO

XXVIII

FIELD THEORY APPROACH TO JUNCTIONS OF INTERACTING QUANTUM WIRES

Settore Scientifico Disciplinare FIS/02

Direttore: Ch.mo Prof. Pietro Pantano

Firma _____

Supervisore: Dr. Domenico Giuliano

Firma _____

Dottorando: Dott. Andrea Nava

Firma _____

CONTENTS

I. INTRODUCTION

Omne ignotum pro magnifico.
Tacito

Recent progress in fabrication of nanostructured quantum wires has shown that it is possible to realize quasi-one-dimensional condensed matter systems hosting a few, and even just one, conducting channel, thus effectively behaving as "truly one-dimensional" conductors. This motivated the rise of a great attention, theorical as well as experimental, towards one-dimensional systems. Experimentally, the creation of one-dimensional systems is challenging but realizable. Molecular or atomic layer epitaxy (the deposition of a crystalline overlayer on a crystalline substrate) is one promising and consolidated approach to build one-dimensional quantum wires. For example, the growth of AlAs-AlGaAs-AlAs on vicinal (110) GaAs substrates[1], a defect free Fe layers obtained on As-saturated GaAs surfaces[2] and growth of Au-assisted and self-assisted InAs nanowires with diameters of 10 nm[3]. The most used material are Si and Ge from group IV, InAs, GaAs and GaN from group III-V and CdSe or ZnO from group II-VI. Alternatively, theoretical predictions can be, and have been, tested[4,5] on macromolecules with tubular structure like single walled carbon nanotubes[6]. It is also possible to fabricate atomically precise nanostructures like 1D Co atomic chains deposited on the stepped surface of Pt(997)[5] or atomic Au chains deposited on Si step edges[7,8].

There are two main reasons that have led to increased attention in one-dimensional systems: the exotic effects that occur with a decrease in the number of dimensions (integer and fractional quantum Hall effect, spin-charge separation, breaking down of Fermi liquid approach, Majorana fermions at the boundaries) and the possible technological and engineering applications that the control of nanoscopic systems would allow (NASA spent $11 million in 2005 to produce a one-meter long prototype quantum wire able to conduct electricity 10 times faster than copper at just a sixth of the weight and the chemistry Nobel prize Richard Smalley saw quantum wire as "a divine solution to humanity's electricial power transmission problem"). After single quantum wires were built, the next natural step is to extend the results of electronic engineering to the quantum world. That is, to design and reproduce the quantum analogue of more complex structures like logic gates, beam splitters, switches, bridges and others. In real life, a circuit is not only composed by a single perfect wire: it contains junctions and impurities, points where an electron have to "choose what to do". Thus, in order to be effective for real systems, a formalism must provide a tool to treat barriers in a single wire, junctions between two, or more, wires (see Figure [1], panel d) and in general other possible component useful for the realization of a quantum circuit.

Teoretically, a large class of electronic systems in spatial dimensions higher than one is well described within Landau Fermi liquid theory which is capable of successfully accounting for the main effects of electronic interaction[9–12]. In Landau's Fermi liquid theory, adding the interaction among electrons and/or between electrons and external potentials (such as the lattice potential of ions in a metal, for instance) on top of a Fermi gas does modify the whole picture of the Fermionic system only quantitatively, not qualitatively. Indeed, the basic assumption is that, close to the Fermi surface, low-energy elementary "quasiparticle" excitations of the interacting electron liquid are in one-to-one correspondence with particle- and hole-excitations in the noninteracting Fermi gas. This corresponds to a nonzero overlap between the quasiparticle wave function in the Fermi liquid and the electron/hole wave function in the noninteracting Fermi gas, which is reflected by a coefficient Z_F of the quasiparticle peak at the Fermi surface in the spectral density of states that is finite though, in general, < 1 ($Z_F = 1$ corresponds to the noninteracting limit). The "adiabatic deformability" of quasiparticles to electrons and/or holes by smoothly switching off the interaction allows, for instance, to address transport in a Fermi liquid in a similar way to what is done using scattering approach in a noninteracting Fermi gas, etc.[13]. At variance with what happens in spatial dimensions higher than 1, in purely one-dimensional interacting electronic systems the effects of the interaction are much more dramatic that what happens in Landau's theory[14]. Any attempt to encode the effects of the interaction in a simple finite parameter renormalization of the quasiparticles and of the quasihole does ultimately fail, due to the fact that the formulas for the renormalized quantities would blow up at the Fermi level, thus invalidating the whole procedure leading to Landau Fermi liquid theory. Landau's Fermi liquid theory is grounded on the possibility of obtaining reliable results by perturbatively treating the electronic interaction[12,15]. This is strictly related to the small rate of multi-particle inelastic processes, in which, due to the interaction, an electron/hole emits electron-hole pairs. While this is typically the case in systems with spatial dimension d higher than one, in one-dimensional systems, the proliferation of particle-hole pair emission at low energies leads to a diverging corresponding rate, which makes the quasiparticle peak disappear ($Z_F = 0$). As a result, the interaction cannot be dealt with perturbatively and one has rather to resort to nonperturbative techniques, allowing for summing over infinite sets of diagrams[16–18] Formally, interacting electrons in one dimension are commonly treated within Tomonaga-Luttinger liquid (TLL)-approach[19,20]. TLL formalism provides a general description of low-energy physics of a one-dimensional interacting electronic system in terms of collective bosonic excitations (charge- and/or spin-plasmons). Electronic operators are realized as nonlinear vertex operators of the bosonic fields[21,22]. Tomonaga was able to encode the excitations of a one-dimensional Fermi gas into the excitations of free Bosons. Resorting to Bosonic coordinates, one sees the magic that the Bosonic Hamiltonian corresponding to

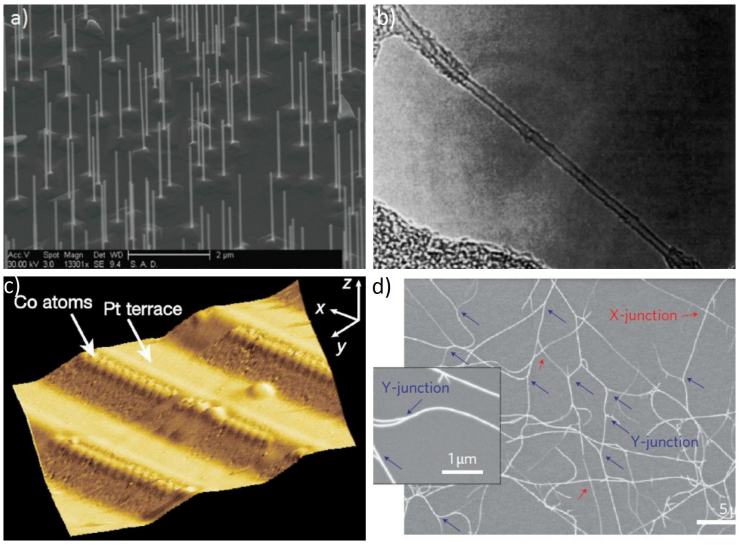

FIG. 1. a) InAs quantum wires grown on the InAs (111)B surface from 40 nm diameter Au colloids dispersed from solution [picture from: "Electron transport in indium arsenide nanowires", Shadi A. Dayeh]; b) TEM image of a single-walled nanotube [picture from: "Cobalt-catalysed growth of carbon nanotubes with single-atomic-layer walls", Bethune et al.]; c) STM topography showing 1D atomic chains of Co grown by step decoration on Pt(997) [picture from: "Atomic Chains at Surfaces", J. E. Ortega and F. J. Himpsel]; d) carbon nanotube film with X- and Y-junctions [picture from: "Flexible high-performance carbon nanotube integrated circuits", Dong-ming Sun, et al.]

free Fermions and the one corresponding to interacting Fermions take the same form. They are both quadratic in the particle density operator. As for what concerns transport properties, the most striking prediction of the TLL-approach is possibly the power-law dependence of the conductance on the low-energy reference scale ("infrared cutoff"), which is typically identified with the (Boltzmann constant times the) temperature, or with the (Fermi velocity times the) inverse system length ("finite-size gap") in a dc transport measurement, or with eV, with V being an applied voltage, in a nonequilibrium experiment. While TLL-formalism poses no particular constraints on the strength of the "bulk" interaction within the quantum wires, it suffers of limitations, when used to describe transport across impurities in an interacting quantum wire, or conduction properties at a junction of quantum wires. Within TLL-framework, a junction of quantum wires is mapped onto a model of K-one dimensional TLLs (one per each wire), interacting with each other by means of a "boundary interaction" localized at x = 0. Dealing with such a class of boundary problems requires pertinently setting the boundary conditions on the plasmon fields at x = 0. While in some very special cases the boundary conditions can be written as simple linear relations between the plasmon fields, in general they cannot. When it is possible the linear relation is expressed in terms of a "current splitting matrix" (M-matrix). This is a consequence of the nonlinearity of the relations between bosonic and fermionic fields: even linear conditions among the fermionic fields are traded for highly nonlinear conditions in the bosonic fields. As a consequence, except at the fixed points of the boundary phase diagram, where the boundary conditions are "conformal", that is, linear in the bosonic fields, the boundary interaction can only be dealt with perturbatively, with respect to the closest conformal fixed point[23,24]. Other information can be obtained only making educated guesses from the global topology of the fixed-point manifold of the phase diagram. Using the Bosonic approach junctions of 2 and 3 wires have beed analysed under particular symmetries in the bulk or at the junction[25–31]. Recently, the bosonization approach in combination with zero-temperature numerics has successfully been employed to compute the junction conductance by relating it to the asymptotic behavior of certain static correlation functions. Correspondingly, the length scale over which the asymptotic behavior emerges has been worked out, as well[32,33]. Also, numerical calculations of the finite-temperature junction conductance can be performed by using quantum Monte Carlo approach[34] or, likely, by implementing some pertinently adapted version of the finite-temperature density matrix renormalization group approach to quantum spin chains[35,36].

Alternatively, one may not be required to give up using fermionic coordinates, by employing a systematic renormalization group (RG) procedure to treat the effects of the bulk interaction on the scattering amplitudes at the junction. Among the various possible ways of implementing RG for junctions of interacting QWs, the two most effective (and widely used) ones are certainly the poor man's fermionic renormalization group (FRG)-approach, based upon a systematic summation of the leading-log divergences of the S-matrix elements at the Fermi momentum and typically yielding equations that can be analytically treated[37–40], and the functional renormalization group (fRG)-approach,

based on the functional renormalization group method, leading to a set of coupled differential equations for the vertex part that, typically, can only be numerically treated[41–50]. Both approaches are expected to apply only for a sufficiently weak electronic interaction in the quantum wires and, in this sense, they are less general than the TLL-approach, which applies even for a strong bulk interaction. Nevertheless, at variance with the TLL-approach, a RG-approach based on the use of fermionic coordinates leads to equations for the S-matrix elements valid at any scale and, thus, it allows for recovering the full scaling of the conductance, all the way down to the infrared cutoff.

Besides the remarkable merit of providing analytically tractable RG-flow equations, the FRG-approach, when applied to interacting spinful electrons, also accounts for the backscattering bulk interaction, which is usually neglected in the TLL-framework[37,38]. Moreover, it can be readily generalized to describe junctions involving superconducting contacts, at the price of doubling the set of degrees of freedom, to treat particle- and hole-excitations on the same footing[51]. The fermionic RG-approaches suffer, however, of the limitation on the bulk interaction, which must be weak, in order for the technique to be reliably applicable. Futhermore, they are not able to describe many-particle scattering processes (that can be instead defined through a M-matrix) even going beyond the leading log correction in perturbation theory[52–54].

The search for observable predictions regarding the junction of quantum wires has so far been focused on two main physical quantity: the charge transport properties of the system, expressed in terms of the conductance tensor, and described through different techniques like the Landauer-Buttiker formalism, the Kubo formula or the Green's function method, or the or measurements of the local density of states (LDOS) of the bulk electrons close to the junction, directly measurable with a scanning tunneling microscope (STM). Both these quantities are related to the S or M matrices, so the knowledge of such matrices, that is the knowledge of the boundary conditions, gives direct access to these and other physical properties of the system (like the power dissipation, or the measurements of the occupation of pairs of Majorana zero modes).

Starting from these observations, the thesis is organized as follows:

- in **Chapter II** we provide an effective tool able to generalize in a systematic way the implementation of the boundary conditions, discussing the theoretical and applicative interest. Such a tool, able to manage and tame the mare magnum of possible boundary conditions of a system involving one dimensional quantum wires, would be the trait d'union between the classical electronic engineering, which led to the patent and to the manufacture of all the know electronic devices, and the quantum mechanichs that, for what concerns this area of application, it is still terra incognita in many of its aspects;

- in **Chapter III** making a combined use of bosonization and fermionization techniques, we build nonlocal transformations between dual fermion operators, describing junctions of strongly interacting spinful one-dimensional quantum wires. Our approach allows for trading strongly interacting (in the original coordinates) fermionic Hamiltonians for weakly interacting (in the dual coordinates) ones. It enables us to generalize to the strongly interacting regime the FRG-approach to weakly interacting junctions. As a result, on one hand, we are able to pertinently complement the information about the phase diagram of the junction obtained within bosonization approach; on the other hand, we map out the full crossover of the conductance tensors between any two fixed points in the phase diagram connected by a renormalization group trajectory[55];

- in **Chapter IV** we investigate more exotic setups, studying the local density of states (LDOS) in systems of Luttinger-liquid nanowires connected to a mesoscopic superconducting island with finite charging energy, in which Majorana bound states give rise to different types of topological Kondo effects[56]. Kondo effect emerges usually due to the coupling of bulk electrons with a quantum spin with degenerate energy levels. Similarly, topological Kondo is achieved when the nonlocal quantum spin is build in terms of $K > 3$ Majorana fermions at the interface between the Luttinger-liquid nanowires and the mesoscopic superconductor. We show that electron interactions enhance the low-energy LDOS in the leads close to the island, with unusual exponents due to Kondo physics that can be probed in tunneling experiments[57];

- in **Chapter V** we provide the main conclusions of this thesis and outline some further perspective of our investigation.

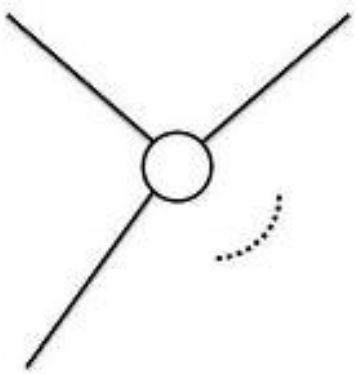

FIG. 2. Sketch of the system: K quantum wires of length ℓ join together at $x = 0$

II. RENORMALIZATION GROUP APPROACHES TO JUNCTIONS OF INTERACTING QUANTUM WIRES

What is not possible is not to choose.
Jean-Paul Sartre

Within Luttinger Liquid framework an impurity corresponds to a nonintegrable boundary interaction term[58] which, in general, can be dealt with only perturbatively, using, as paradigmatic reference, the case in which the impurity strength is so high to effectively break the wire into two ("disconnected" quantum wire), or is so weak that the wire may be regarded as "almost homogeneous", or in general a more complex situation that can be expressed as a linear relation between bosonic fields that preserve the right commutation rules ("conformal" boundary condition). In Fermionic coordinates, instead, the amplitudes corresponding to the possible single-electron scattering processes at an impurity are encoded within the scattering matrix S, which is typically $K \times K$ (for a normal junction or $2K \times 2K$ for a superconducting junction), K being the number of independent single-electron channels. If, at a first stage, one neglects the interaction, then the S matrix exactly encodes all the scattering processes, no matter on how strong is the interaction centre (the junction). Introducing the interaction one then finds that, within perturbation theory, the amplitude of each single-particle scattering process diverges, as the corresponding energy gets close to the Fermi energy. Keeping these divergence under control in a systematic way is possible, by resorting to the renormalization group (RG) approach, in which divergences are traded for an effective dependence of the physical amplitudes on a dimensionful energy scale (which can be the level spacing, or $k_B T$, T being the temperature, or $\hbar\omega$, where ω is the frequency associated to an ac measurement, etc.). Such a dependence propagates onto the physical quantities, calculated starting from the single-particle amplitudes, and thus takes physical effects which can be detected, for instance, in an equilibrium dc transport measurement. As a result, the Fermionic approach can be, for a large class of impurity problems, as effective as the Bosonic one.

II.1. Model

In this section we outline the main properties of the physical systems we mean to study. As sketched in Fig. [2], we will consider systems made by an arbitrary number of one dimensional quantum wires of length ℓ, coupled together at a point called "junction". We will assume that all the wires are single-channel and spinless (treating each channel within a single wires, including the spin, individually). The generic system is described by an Hamiltonian of the form

$$H = \sum_{j=1}^{K} H_{B,j} + H_J + H_I \tag{2.1}$$

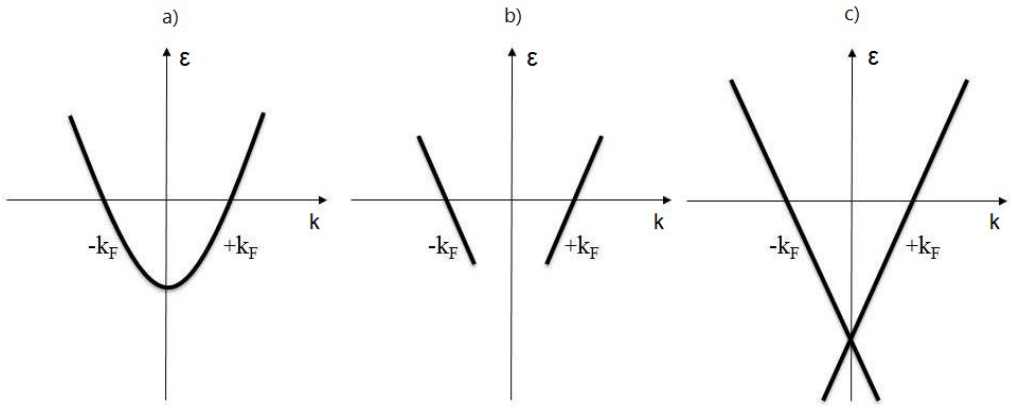

FIG. 3. a) Parabolic dispersion relation for a 1d quantum wire; b) linearized dispersion relation around the left and right Fermi points and with a bandwidth cutoff; c)linearized dispersion relation without a bandwidth cutoff (Luttinger model)

Here, $H_{B,j}$ is the bulk Hamiltonian for the j-th wire. Each wire is characterized by a spatial coordinate going from 0, near the junction, to ℓ (with $\ell \to +\infty$), far from the junction. For a system of free fermions in one dimension the dispersion relation for Hamiltonian is usually parabolic and the Fermi surface of the noninteracting model consists of two disconnected Fermi points, $\pm k_F$ (see Fig. [3], panel a), such that $e^{+i(k_F+k)x}$ represent a wave going from 0 to ℓ, that is an "outgoing" or "right Fermi point" fermion and we will use the index R to denote it, while $e^{-i(k_F+k)x}$ represent a wave going from ℓ to 0, that is an "ingoing" or "left Fermi point" fermion and we will use the index L to denote it.

As it was suggested by Tomonaga, in the Luttinger Liquid context, the divergences at the Fermi level are a low-energy feature and, thus, one may take care of them by keeping only low-energy, long-wavelength excitations nearby the Fermi energy, that is, by linearizing the single-particle spectrum and neglecting states further away from the two Fermi point. For this reason, we introduce the "high-k cutoff", called "bandwidth cutoff", such that $|k| < \Lambda$ and the dispersion relation $\epsilon(p)$ may be regarded as linear, about the Fermi points, for $|p - k_F| < \Lambda$ and for $|p + k_F| < \Lambda$, respectively (see Fig. [3], panel b). Thus, as a consequence of linearization, we introduce two sets of fermionic operators describing electrons with momentum near the "left" and "right" Fermi points so that we can write the fermionic field as

$$\psi_j(x) = e^{-ik_{F,j}x}\psi_{L,j}(x) + e^{+ik_{F,j}x}\psi_{R,j}(x) \tag{2.2}$$

where we have defined the chiral fields

$$\begin{aligned} \psi_{R,j}(x) &= \frac{1}{\sqrt{\ell}}\sum_k e^{ikx} a_{R,j}(k) \\ \psi_{L,j}(x) &= \frac{1}{\sqrt{\ell}}\sum_k e^{-ikx} a_{L,j}(k) \end{aligned} \tag{2.3}$$

that, by definition, vary slowly on the length scale k_F^{-1} and may be regarded as independent Fermionic fields, obeying the anticommutation relations:

$$\left\{\psi_A(x), \psi_B^\dagger(y)\right\} = \delta_{AB}\delta(x-y) \tag{2.4}$$

$$\{\psi_A(x), \psi_B(x)\} = \left\{\psi_A^\dagger(x), \psi_B^\dagger(x)\right\} = 0 \tag{2.5}$$

In terms of these fields the bulk Hamiltonian has the form

$$H_B = -i\sum_{j=1}^{K} v_j \int_0^{\ell} dx \left\{ \psi^{\dagger}_{R,j}(x)\,\partial_x \psi_{R,j}(x) - \psi^{\dagger}_{L,j}(x)\,\partial_x \psi_{L,j}(x) \right\} \tag{2.6}$$

with dispersion relation $\epsilon_{j;k} = v_j k$ For a mathematically more rigorous treatment[20] we have to introduce some high energy non-physical states extending the relation dispersion from $-\infty$ to $+\infty$ in both right and left branches (see Fig. [3], panel c). Doing so, that is removing the bandwidth cutoff, it is necessary to introduce another cutoff to avoid unphysical divergences. This is realized introducing a "transfer cutoff" in the interaction Hamiltonian. The differences in the use of the bandwidth or transfer cutoff are deeply discussed in Refs. [16, 59, and 60].

H_J is the junction Hamiltonian; it contains all the boundary operators that describe the physical processes involving the electrons at the point $x = 0$. Typically, the most relevant terms are bilinear or quartic in the fermionic operators. They may preserve or not charge and spin (for example in presence of a superconducting junction) and may involve other operators like majorana edge states or quantum dots. The form of the junction Hamiltonian depends strongly by the system taken into analysis so, for the moment, we will not give to it a specific form.

H_I is the interaction Hamiltonian. Requiring the conservation of the number of electrons in each wire, it has the form of a density-density interaction and contains intra-wire and inter-wire terms. Its generic form is

$$H_I = \frac{1}{2}\sum_{j=1}^{K}\sum_{j'=1}^{K} \iint dx dy \rho_j(x) V_{j,j'}(x-y) \rho_{j'}(y) \tag{2.7}$$

where $V_{j,j'}(x-y)$ is a real, symmetric under wire indices exchange and parity-symmetric short range potential and $\rho_j(x) = \psi^{\dagger}_j(x)\psi_j(x)$. The fact that $V_{j,j'}(x)$ has a finite range, λ, limits the momentum transfer to a stripe of half-width $D_0 \sim 1/\lambda$ about the Fermi momentum, this act as our transfer cutoff.

From the Hamiltonian, H, we can recover the Hamiltonian for spinful wires or multichannel wires with an appropriate wire indices replacement. For example, the Hamiltonian for K spin-$\frac{1}{2}$ wires is recovered from the Hamiltonian for $2K$ spinless wires through the replacement

$$\begin{aligned} j\ even &\rightarrow j,\uparrow \\ j\ odd &\rightarrow j,\downarrow \end{aligned} \tag{2.8}$$

In this case Eq. [2.6] and Eq. [2.7] assume the form

$$H_B = -i\sum_{j=1}^{K}\sum_{\sigma} v_j \int_0^{\ell} dx \left\{ \psi^{\dagger}_{R,j,\sigma}(x)\partial_x \psi_{R,j,\sigma}(x) - \psi^{\dagger}_{L,j,\sigma}(x)\partial_x \psi_{L,j,\sigma}(x) \right\} \tag{2.9}$$

and

$$H_I = \frac{1}{2}\sum_{j=1}^{K}\sum_{j'=1}^{K}\sum_{\sigma\sigma'} \int_0^{L} dx\, dy\, \rho_{j,\sigma}(x) V_{j,j';\sigma,\sigma'}(x-y) \rho_{j',\sigma'}(y) \tag{2.10}$$

respectively. Finally, even if it is not true in general (like for example for a spin-orbit coupled quantum wire in a magnetic field[61]), in the following, to simplify the notation, we will assume that the Fermi momentum is the same for all the wires specifying, where needed, the main effects of this simplification.

II.2. Scattering matrix

In the non interacting case, if the only relevant operators within the junction Hamiltonian are the operators bilinear in the fermionic fields, the full dynamics of the scattering problem is encoded by the $K \times K$ scattering matrix $S(\epsilon_k)$, defined so that $S(\epsilon_k)$ acts on the incoming-wave amplitudes, giving back the outgoing-wave amplitudes. For a normal junction of K wires for example:

$$a_{R,j}(k) = \sum_{j'=1}^{K} S_{j,j'}(\epsilon_k)\, a_{L,j'}(k) \tag{2.11}$$

or in matrix form

$$\begin{pmatrix} \vdots \\ a_{R,j}(k) \\ \vdots \end{pmatrix} = \begin{bmatrix} S_{1,1}(\epsilon_k) & \cdots & S_{1,K}(\epsilon_k) \\ \vdots & \ddots & \vdots \\ S_{K,1}(\epsilon_k) & \cdots & S_{K,K}(\epsilon_k) \end{bmatrix} \begin{pmatrix} \vdots \\ a_{L,j}(k) \\ \vdots \end{pmatrix} \tag{2.12}$$

The element on the diagonal, $S_{i,i}(\epsilon_k) \equiv r_{i,i}$, represent the reflection coefficient within wire i, while the off-diagonal terms, $S_{i,j}(\epsilon_k) \equiv t_{i,j}$, correspond to the transmission coefficient between different wires. The modulus squared of these coefficients correspond to the probability amplitude for that process. From probability current continuity equation, one readily sees that $S(\epsilon_k)$ is a unitary matrix, that is

$$S(\epsilon_k) S^{\dagger}(\epsilon_k) = S^{\dagger}(\epsilon_k) S(\epsilon_k) = 1$$

This constrain correspond to the quantum analogous of the Kirchhoff law and strongly restricts the number of independent element of the S-matrix. A $K \times K$ complex matrix depends from a total of $2K^2$ real parameters; the unitary requirement, that can also be written as

$$\sum_{k=1}^{K} S_{ik} S_{jk}^{*} = \sum_{k=1}^{K} S_{ki} S_{kj}^{*} = \delta_{ij}, \quad 1 \leq i, j \leq K \tag{2.13}$$

impose some constraints on them. These equations are redundant, as it can be easily seen observing that an exchange of i and j leaves the conditions unaffected. This means that the only independent constrains are given by $1 \leq i \leq j \leq K$, or:

$$\begin{cases} \sum_{k=1}^{K} \left| S_{ik}^{2} \right| = 1 & 1 \leq i = j \leq K \\ \sum_{k=1}^{K} S_{ik} S_{jk}^{*} = 0 & 1 \leq i < j \leq K \end{cases} \tag{2.14}$$

The first line is real and put K constrains, the second line contains $(K-1) + (K-2) + \cdots + 2 + 1 = K(K-1)/2$ complex independent equation, that correspond to $K(K-1)$ constrains. This means that a unitary matrix has only $2K^2 - K - K(K-1) = K^2$ real independent parameters. In a physical contest, these parameters are somehow related to the coefficients that appear in the junction Hamiltonian, H_J and not all of them are important or truly independent. Indeed, there are two main reasons that further reduce the number of free parameters: possible symmetries of the system (time reversal, particle-hole, Z_n, D_n, ...) and the fact that physical quantities, being real, depend on the amplitudes and not on the phases of the S-matrix coefficients (so for example an overall phases in the S-matrix has no real physical meaning). There are different ways to parametrize a matrix in terms of the independent parameters. We can write a generic 2×2 S-matrix ($S \in U(2)$)

$$S = \begin{bmatrix} r_{1,1} & t_{1,2} \\ t_{2,1} & r_{2,2} \end{bmatrix} \tag{2.15}$$

as

$$S(\theta, \phi, \varphi_1, \varphi_2) = e^{i\phi} \begin{bmatrix} \cos\theta e^{i\varphi_1} & \sin\theta e^{i\varphi_2} \\ -\sin\theta e^{-i\varphi_2} & \cos\theta e^{-i\varphi_1} \end{bmatrix} \tag{2.16}$$

or, putting $\varphi_{1,2} = \psi_1 \pm \psi_2$, as

$$S(\theta, \phi, \psi_1, \psi_2) = e^{i\phi} \begin{bmatrix} e^{i\psi_1} & 0 \\ 0 & e^{-i\psi_1} \end{bmatrix} \begin{bmatrix} \cos\theta & \sin\theta \\ -\sin\theta & \cos\theta \end{bmatrix} \begin{bmatrix} e^{i\psi_2} & 0 \\ 0 & e^{-i\psi_2} \end{bmatrix} \tag{2.17}$$

Another useful parametrization is given in terms of the Pauli matrices σ_i, $i = 1, 2, 3$

$$\sigma_i = \begin{bmatrix} \delta_{i,3} & \delta_{i,1} - i\delta_{i,2} \\ \delta_{i,1} + i\delta_{i,2} & -\delta_{i,3} \end{bmatrix} \tag{2.18}$$

and Euler angles θ_i, $i = 1, 2, 3$, as

$$S(\phi, \theta_1, \theta_2, \theta_3) = e^{i\phi} e^{\frac{i}{2}\theta_1\sigma_3} e^{\frac{i}{2}\theta_2\sigma_1} e^{\frac{i}{2}\theta_3\sigma_3} \tag{2.19}$$

Let us note that for $\phi = 0$ we obtain the subgroup $SU(3)$.

For a generic 3×3 S-matrix ($S \in U(3)$)

$$S = \begin{bmatrix} r_{1,1} & t_{1,2} & t_{1,3} \\ t_{2,1} & r_{2,2} & t_{2,3} \\ t_{3,1} & t_{3,2} & r_{3,3} \end{bmatrix} \tag{2.20}$$

a possible useful parametrizations is

$$S\left(\{\varphi_i\}_{i=1}^{5}, K\right) = \begin{bmatrix} 1 & 0 & 0 \\ 0 & e^{i\varphi_1} & 0 \\ 0 & 0 & e^{i\varphi_2} \end{bmatrix} K \begin{bmatrix} e^{i\varphi_3} & 0 & 0 \\ 0 & e^{i\varphi_4} & 0 \\ 0 & 0 & e^{i\varphi_5} \end{bmatrix} \tag{2.21}$$

where K, in the Kobayashi-Maskawa parametrization, depends on four free parameters and can be written as

$$K\left(\{\theta_i\}_{i=1}^{3}, \delta\right) = \begin{bmatrix} \cos\theta_1 & -\sin\theta_1\cos\theta_3 & -\sin\theta_1\sin\theta_3 \\ \sin\theta_1\cos\theta_2 & \cos\theta_1\cos\theta_2\cos\theta_3 - \sin\theta_2\sin\theta_3 e^{i\delta} & \cos\theta_1\cos\theta_2\sin\theta_3 + \sin\theta_2\cos\theta_3 e^{i\delta} \\ \sin\theta_1\sin\theta_2 & \cos\theta_1\sin\theta_2\cos\theta_3 - \cos\theta_2\sin\theta_3 e^{i\delta} & \cos\theta_1\sin\theta_2\sin\theta_3 - \cos\theta_2\cos\theta_3 e^{i\delta} \end{bmatrix} \tag{2.22}$$

or, in the Chau-Keung parametrization, as

$$K\left(\{\vartheta_i\}_{i=1}^{3}, \xi\right) = \begin{bmatrix} 1 & 0 & 0 \\ 0 & \cos\vartheta_1 & \sin\vartheta_1 \\ 0 & -\sin\vartheta_1 & \cos\vartheta_1 \end{bmatrix} \begin{bmatrix} \cos\vartheta_2 & 0 & \sin\vartheta_2 e^{-i\xi} \\ 0 & 1 & 0 \\ -\sin\vartheta_2 e^{i\xi} & 0 & \cos\vartheta_2 \end{bmatrix} \begin{bmatrix} \cos\vartheta_3 & \sin\vartheta_3 & 0 \\ -\sin\vartheta_3 & \cos\vartheta_3 & 0 \\ 0 & 0 & 1 \end{bmatrix} \tag{2.23}$$

Another useful parametrization[62] is given in terms of the Gell-Mann matrices λ_i, $i = 1, ..., 8$, and the generalized Euler angles ψ_i, $i = 1, ..., 9$, as

$$S\left(\phi, \{\psi_i\}_{i=1}^{8}\right) = e^{i\phi} U e^{\frac{i}{2}\lambda_5\psi_1} \bar{U} e^{i\lambda_8\psi_2} \tag{2.24}$$

where

$$U\left(\{\psi_i\}_{i=3}^{5}\right) = e^{\frac{i}{2}\lambda_3\psi_3} e^{\frac{i}{2}\lambda_2\psi_4} e^{\frac{i}{2}\lambda_3\psi_5} \tag{2.25}$$

and

$$\bar{U}\left(\{\psi_i\}_{i=6}^{8}\right) = e^{\frac{i}{2}\lambda_3\psi_6} e^{\frac{i}{2}\lambda_2\psi_7} e^{\frac{i}{2}\lambda_3\psi_8} \tag{2.26}$$

The sets (ψ_3, ψ_4, ψ_5) and (ψ_6, ψ_7, ψ_8) play the roles of Euler angles for two different $SU(2)$ groups. The angles (ψ_1, ψ_4, ψ_7) take the name of latitudes and they range in $[0, \pi]$, while the angles $(\psi_2, \psi_3, \psi_5, \psi_6, \psi_8)$ are called azimuthal coordinates.

Increasing the order of the matrix makes the parametrization harder (see for example Ref. [63] for the parametrization of a 4×4 unitary matrix). However, for a generic S-matrix of order K some recursive algorithms can be in hand. Any $S_K \in U(K)$ can be written in the form

$$S_K = B_K \cdot \begin{pmatrix} 1 & 0 \\ 0 & S_{K-1} \end{pmatrix} \tag{2.27}$$

where $B_K \in U(K)$ is an unitary matrix uniquely defined by its first column that is a vector of the unit sphere S^{2K-1} of the Hilbert space C^K

$$S^{2K-1} = \left\{ x \in C^K, \|x\| = 1 \right\} \tag{2.28}$$

and $S_{K-1} \in U(K-1)$. Iterating the relation, S_K can be written as the product of K unitary matrices

$$S = B_K \cdot B_{K-1}^1 \cdots B_1^{K-1} \tag{2.29}$$

where

$$B_{K-n}^n = \begin{pmatrix} I_K & 0 \\ 0 & B_{K-n} \end{pmatrix} \tag{2.30}$$

Such a parametrization always exists. It is easy to check that the number of parameters is preserved, because it is given be $1 + 3 + \cdots + 2K - 1 = K^2$.

What we have said until now can be extended to the case of superconducting junctions, that is systems that allow physical processes at the boundary that do not preserve charge (the easiest examples are the normal-superconductor junction[51] and the normal-"topological superconductor" junction[61,64]). In this case a description in terms of S-matrix can still be used but with some minor adjustments. First of all the dimension of the S-matrix must be doubled, to take into account both the particle and hole channels on the same footing. That is

$$a_{R,j}(k) = \sum_{j'=1}^{K} \left[S_{j,j'}^{e,e}(\epsilon_k)\, a_{L,j'}(k) + S_{j,j'}^{e,h}(\epsilon_k)\, a_{L,j'}^{\dagger}(-k) \right] \tag{2.31}$$

and

$$a_{R,j}^{\dagger}(-k) = \sum_{j'=1}^{K} \left[S_{j,j'}^{h,e}(\epsilon_k)\, a_{L,j'}(k) + S_{j,j'}^{h,h}(\epsilon_k)\, a_{L,j'}^{\dagger}(-k) \right] \tag{2.32}$$

The diagonal elements, $S_{i,i}^{e,e}(\epsilon_k) \equiv r_{i,i}^N$, still represent the reflection coefficients within wire i, while the off-diagonal terms, $S_{i,j}^{e,e}(\epsilon_k) \equiv t_{i,j}^N$, correspond to the transmission coefficients between different wires. The new elements on the form, $S_{i,i}^{h,e}(\epsilon_k) \equiv r_{i,i}^A$, represent the Andreev reflection coefficient within wire i, while the terms, $S_{i,j}^{h,e}(\epsilon_k) \equiv t_{i,j}^A$, correspond to the crossed Andreev reflection coefficient between different wires. They transform an incoming electron into an outgoing hole. The S-matrix elements $S_{i,j}^{h,h}(\epsilon_k)$ and $S_{i,j}^{e,h}(\epsilon_k)$ play the same role of $S_{i,j}^{e,e}(\epsilon_k)$ and $S_{i,j}^{h,e}(\epsilon_k)$ but for an incoming hole. All these $2K \times 2K$ coefficients are not independent. Indeed, the unitary condition, $S^{\dagger}S$, is true also for the superconducting case. Furthermore, making the complex conjugate of Eq.[2.32] and replacing k with $-k$, we derive the particle-hole symmetry constraint

$$\begin{aligned} S_{i,j}^{h,h}(\epsilon_k) &= S_{i,j}^{e,e\dagger}(\epsilon_{-k}) \\ S_{i,j}^{h,e}(\epsilon_k) &= S_{i,j}^{e,h\dagger}(\epsilon_{-k}) \end{aligned} \tag{2.33}$$

These are all the general statement on the S-matrix that can be derived without giving a specific form to the junction Hamiltonian H_J. Knowing the S-matrix, its symmetries and how its coefficients are related to the physical parameters (like the chemical potential, backscattering amplitude and so on) is fundamental to describe the behaviour of the system. Following the fermionic approaches[37,39] the S-matrix remains the major player also in presence of a weak bulk interaction, as long as it is confined to a finite region L so that it is possible to define asymptotic scattering

states. Indeed, as we will show in the next section through a Green's functions approach, the effect of the interaction can be absorbed within a renormalization of the scattering matrix coefficients. That is, the S-matrix of the non interacting system is replaced by a new, scale dependent, S-matrix, where the role of the scale, Λ, can be played for example by the temperature, the length of the system, the energy or the applied voltage. The equations that give the form of the renormalized S-matrix coefficients as a function of the scale variable are called renormalization group (RG) equations. They depend on the interaction potential present in H_I, and on the S-matrix itself (in particular on the bare value of the S-matrix, that is the matrix in the non interacting regime). They can be written as

$$\frac{dS_{i,j}\left(\epsilon_k,\Lambda\right)}{d\ln\Lambda}=\beta\left(\left\{S_{i,j}\left(\epsilon_k,\Lambda\right)\right\},V_{i,j}\left(\Lambda\right)\right) \tag{2.34}$$

The small number of S-matrices for which all the RG equations are zero are scale invariant and the interaction does not modify the behaviour of the system. For this reason, they are called fixed points (FP). Each of them define a class, within the space of all possible $K\times K$ (or $2K\times 2K$) matrices, to which all other non FP S-matrices move towards during the renormalization procedure driven by Eqs. [2.34]. All the S-matrices, obtained by the same Hamiltonian, that collapse on the same FS at the end of the RG trajectory, and therefore belong to the same class, share the same low energy, low temperature, large length behaviour in presence of interaction. Furthermore, playing with the interaction potential it is possible to stabilize one particular FP and force the system to work as we want. Later we will give some example of possible and interesting FPs showing their importance. The parametrization of the S-matrix given above, plays now a relevant role. Indeed, it allows us to exchange the RG equations for the coefficients into equation for the K^2 real parameter that parametrize the matrix. Furthermore, under particular circumstances, the RG equations for these parameters can be traded for equations for the physical parameters contained in H_J.

II.2.1. Current splitting matrix

Until now we have described all actors and stages involved in the S-matrix description of junctions of one dimensional quantum wires. The last step consist in the definition of the "current splitting matrix" $\mathbb{M}^S$, whose elements are given by

$$\mathbb{M}^S_{i,j}\equiv\left|S_{i,j}\right|^2 \tag{2.35}$$

$\mathbb{M}^S$ has two important properties: first, its elements are real and positive, second, it satisfy the constrains

$$\sum_i \mathbb{M}^S_{i,j}=\sum_j M^S_{i,j}=1 \tag{2.36}$$

This condition is the classical Kirchhoff law for the currents. Indeed, starting from the S-matrix it is easy to check that the "current splitting matrix" defined above relates the incoming and outgoing currents, $I_{R(L)j}$. If the S-matrix energy dependence can be disregarded, Eq.[2.11] can be also be written as

$$\psi_{R,j}\left(0\right)=S_{j,j'}\psi_{L,j'}\left(0\right) \tag{2.37}$$

that implies

$$I_{Ri}\propto\left\langle\psi^\dagger_{R,i}\psi_{R,i}\right\rangle=\sum_j\left|S_{i,j}\right|^2\left\langle\psi^\dagger_{L,j}\psi_{L,j}\right\rangle\propto\sum_j\mathbb{M}^S_{i,j}I_{Lj} \tag{2.38}$$

Furthermore, in the DC limit, the Landauer-Buttiker theory relates the conductance tensor $G_{i,j}$, that is a physical well defined and measurable quantity, with the S-matrix, and then the M-matrix, through (see Appendix [II.8]

$$G_{i,j}\propto\delta_{i,j}-\mathbb{M}^S_{i,j} \tag{2.39}$$

So, a control on the current splitting matrix implies a control on the transport properties of the system under analysis. To better understand the mathematical properties of $\mathbb{M}$, it is helpful to define the following sets of matrices:

we call a matrix "doubly stochastic" if all its element are real and positive and the sum over the element of a row or a column is one. That is, if it belongs to the set

$$D_{stoc}\left(K\right)\equiv\left\{\mathbb{M}_{K\times K}\colon\ \mathbb{M}_{i,j}\in R^{+}\ \wedge\ \sum_{i=1}^{K}\mathbb{M}_{i,j}=\sum_{j=1}^{K}\mathbb{M}_{i,j}=1\right\}\tag{2.40}$$

Furthermore, we call a matrix "unistochastic" if it is doubly stochastic and its elements can be written as the modulus squared of the elements of an unitary matrix. That is if it belongs to the set

$$U_{stoc}\left(K\right)\equiv\left\{\mathbb{M}_{K\times K}\colon\ \mathbb{M}_{i,j}\in R^{+}\ \wedge\ \sum_{i=1}^{K}\mathbb{M}_{i,j}=\sum_{j=1}^{K}\mathbb{M}_{i,j}=1\ \wedge\ \mathbb{M}_{i,j}=\left|S_{i,j}\right|^{2}\ \wedge\ S\in U\left(K\right)\right\}\tag{2.41}$$

It is true that $U_{stoc}\left(K\right)\subset D_{stoc}\left(K\right)$ but not the vice versa.

This two sets of matrices are present in a great number of fields in physics involving transition probabilities, like particle physics, foundation of quantum theory, quantum information, computation theory, quantum mechanics on graphs[65–69] and condensed matter physics[23,24,70]. For this reason a great interest has risen around the mathematical properties of these matrices sets and their relation with Birkhoff's Polytope, van der Waerden matrix and Hadamard matrix[71,72]. Of particular importance is the Birkhoff–von Neumann theorem[73] that states that a matrix is doubly stochastic if and only if it is a convex combination of permutation matrices

$$\mathbb{M}_{K\times K}\in D_{stoc}\left(K\right)\iff\begin{cases}\mathbb{M}_{K\times K}=\sum_{i}a_{i}P_{i}\\ a_{i}\geq0,\ \sum_{i}a_{i}=1\\ P_{i}\in P_{erm}\end{cases}\tag{2.42}$$

where the permutation set is defined as

$$P_{erm}\left(K\right)\equiv\left\{P_{K\times K}\colon\ P_{i,j}\in\left\{0,1\right\}\ \wedge\ \sum_{i=1}^{K}P_{i,j}=\sum_{j=1}^{K}P_{i,j}=1\right\}\tag{2.43}$$

that is, all the elements of each row or column are zero except one that is equal to 1. Let us note en passant that the intersection between the unistochastic set and the orthogonal group $O\left(K\right)$ is the permutation group

$$U_{stoc}\left(K\right)\bigcap O\left(K\right)\equiv P_{erm}\left(K\right)\tag{2.44}$$

The importance of this statement will be clear later, for now let us underline that within $P_{erm}\left(K\right)$ there are some elements such that their corresponding unitary matrix satisfy the FP condition $\beta\left(\left\{S_{i,j}\left(\epsilon_{k},\Lambda\right)\right\},V_{i,j}\left(\Lambda\right)\right)=0$ like, for example

$$S_{N}=\begin{pmatrix}1&0\\0&1\end{pmatrix},\ S_{D}=\begin{pmatrix}0&1\\1&0\end{pmatrix}\tag{2.45}$$

that respectively describe a junction of two wires that are totally decoupled or fully connected; playing with the interaction potential we can force the system to collapse on one of these FP. That is, they act as a "quantum" ON/OFF switch. For a three wire junction we have the following interesting FPs

$$\begin{gathered}S_{N}=\begin{pmatrix}1&0&0\\0&1&0\\0&0&1\end{pmatrix},\ S_{\chi^{-}}=\begin{pmatrix}0&1&0\\0&0&1\\1&0&0\end{pmatrix},\ S_{\chi^{+}}=\begin{pmatrix}0&0&1\\1&0&0\\0&1&0\end{pmatrix},\\ S_{N_{1}}=\begin{pmatrix}1&0&0\\0&0&1\\0&1&0\end{pmatrix},\ S_{N_{2}}=\begin{pmatrix}0&0&1\\0&1&0\\1&0&0\end{pmatrix},\ S_{N_{3}}=\begin{pmatrix}0&1&0\\1&0&0\\0&0&1\end{pmatrix}\end{gathered}\tag{2.46}$$

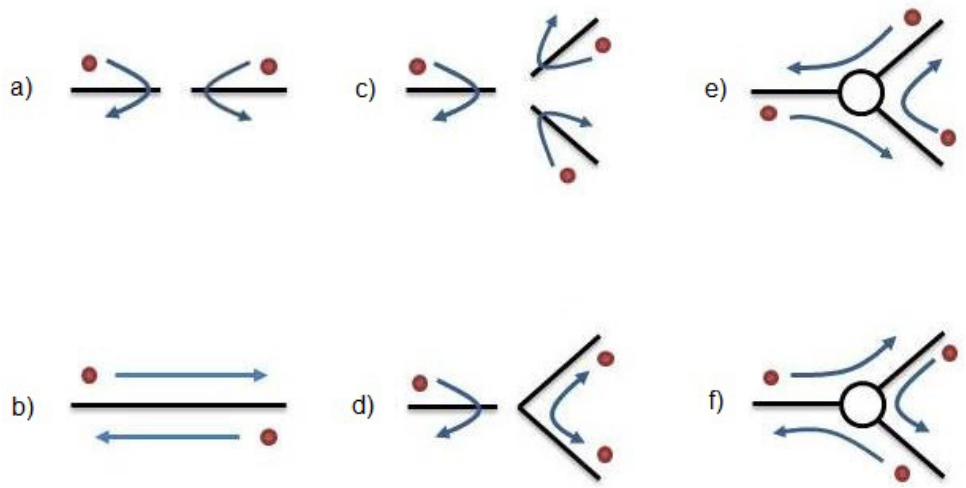

FIG. 4. Examples of fixed points for two- and three-wire junctions. Panel a) and b) correspond to the matrices S_N and S_D of Eq. [2.45]. We have respectively a fully disconnected junction or a perfect wire. Panels from c) to f) refer to Eq. [2.46] and represent in order three fully disconnected wires (S_N), one disconnected wire with perfect transmission between the other two (S_{N_i}), counterclockwise and clockwise perfect transmission of current ($S_{\chi^{\pm}}$)

The first represent three disconnected wires; the second and the third correspond to a system in which the current coming from wire i is totally transmitted to the next of previous wire, while the last three matrices correspond to a system in which one wire is decoupled and the other two are fully connected. They are the quantum counterpart of the electronic component that in engineering go under the name of circulators and switches (a pictorial interpretation of these matrices is given in Fig. [4]). These are only a small example of possible realizable systems. Changing the number of involved wires, other interesting behaviours that can be described through the splitting matrix formalism, and that have a relevant physical and engineering role if reproduced experimentally, emerges. For examples, the "magic tee" and the "rat-race coupler" described by a scattering matrix of the form

$$S_{magix-tee} = \frac{1}{\sqrt{2}} \begin{pmatrix} 0 & 0 & 1 & -1 \\ 0 & 0 & 1 & 1 \\ 1 & 1 & 0 & 0 \\ -1 & 1 & 0 & 0 \end{pmatrix} \quad S_{rat-race} = \frac{-i}{\sqrt{2}} \begin{pmatrix} 0 & 1 & 0 & -1 \\ 1 & 0 & 1 & 0 \\ 0 & 1 & 0 & 1 \\ -1 & 0 & 1 & 0 \end{pmatrix} \tag{2.47}$$

or the symmetrical and asymmetrical couplers (with $\alpha^2 + \beta^2 = 1$)

$$S_{sym} = \begin{pmatrix} 0 & \alpha & i\beta & 0 \\ \alpha & 0 & 0 & i\beta \\ i\beta & 0 & 0 & \alpha \\ 0 & i\beta & \alpha & 0 \end{pmatrix} \quad S_{asym} = \begin{pmatrix} 0 & \alpha & \beta & 0 \\ \alpha & 0 & 0 & -\beta \\ \beta & 0 & 0 & \alpha \\ 0 & -\beta & \alpha & 0 \end{pmatrix} \tag{2.48}$$

or more complicated systems that involves an higher number of wires like the one in Refs. [74–76].

Through the fermionic approaches, that are based on imposing boundary conditions via the S-matrix, it is possible to perform a systematic study of physical systems whose current splitting matrix belongs to the set of unistochastic matrices $U_{stoc}(K)$. Within this set, we can focus on some particular matrices, some of them belonging to the permutation group $P_{erm}(K)$, that are very interesting from a physical and applicative point of view. Furthermore, we know that this is only a subset of a more wide set including splitting matrix, like the ones belonging to $D_{stoc}(K)$, with even more interesting properties. To do this other approaches must be implemented, like the one that we will discuss in the next sections.

For a junction where Andreev-like processes are allowed at the boundary, the dc conductance is proportional to

$$G_{i,j} \propto \delta_{i,j} - \left|S_{i,j}^{e,e}\right|^2 + \left|S_{i,j}^{e,h}\right|^2 \tag{2.49}$$

If we assume that the junction is superconductive, that is all the boundary processes are mediated by the superconductor so that no direct coupling between normal wires are allowed, for energies under the superconducting gap no normal processes are present, $S_{i,j}^{e,e} = 0$, and the dc conductance reduces to

$$G_{i,j} \propto \delta_{i,j} + \left|S_{i,j}^{e,h}\right|^2 \tag{2.50}$$

This suggest us to define a current splitting matrix, belonging to the set $-U_{stoc}(K)$, of the form

$$\mathbb{M}_{i,j}^{A} \equiv -\left|S_{i,j}^{e,h}\right|^2 \tag{2.51}$$

It follows that there is a duality between the normal and purely superconducting junction[77] and that the full analysis done for the normal case can be extended to the superconducting case only changing a sign in front of each splitting matrix. The general case, when normal and Andreev-like processes are both non zero it is much more complicate as the corresponding splitting matrix does not belong to any known set.

II.3. G-ology model and renormalization group equations for bulk and boundary parameters

In this section we analyse the effect of a density-density interaction Hamiltonian on the bulk and boundary properties of the system. Starting from Eq. [2.7] and making advantage of the decomposition of the fermionic fields Eq. [2.2], one obtains

$$\begin{aligned}\rho_j(x) &= \psi_j^\dagger(x)\,\psi_j(x) \\ &= \psi_{j,R}^\dagger\psi_{j,R} + \psi_{j,L}^\dagger\psi_{j,L} + \psi_{j,R}^\dagger\psi_{j,L}e^{-2ik_F x} + \psi_{j,L}^\dagger\psi_{j,R}e^{2ik_F x}\end{aligned} \tag{2.52}$$

the interaction can be decomposed in a sum of nine different contributions involving left and right chiral fields, which can be listed as

$$\begin{array}{ccc} R^\dagger R^\dagger RR & R^\dagger L^\dagger RR & L^\dagger L^\dagger RR \\ R^\dagger R^\dagger RL & R^\dagger L^\dagger RL & L^\dagger L^\dagger RL \\ R^\dagger R^\dagger LL & R^\dagger L^\dagger LL & L^\dagger L^\dagger LL \end{array}$$

The Feynman diagrams corresponding to each contribution are shown in Fig. [5] and the corresponding processed in momentum space in Fig. [6].

Following the standard g-ology notation we classify the different types of interaction as follows. We have a forward scattering term that involves particles with the same chirality and preserve it. The associated momentum transfer is small and, in the limit of short range interaction, the corresponding interaction Hamiltonian has the form

$$H_{g_4} = \frac{1}{2}\sum_{X=L,R}\sum_{j,j'} g_{4;j,j'}\int_0^L dx :\psi_{X,j}^\dagger(x)\,\psi_{X,j}(x)::\psi_{X,j'}^\dagger(x)\,\psi_{X,j'}(x): \tag{2.53}$$

with $g_{4;j,j'} \approx V_{j,j'}(0)$. The normal ordering : : excludes the unphysical interaction of a particle with itself. The main effect of this interaction term is just to renormalize the Fermi velocity and the chemical potential by a finite, non-diverging, amount while it has no effect of the renormalization of the scattering matrix and gives only a sub leading contribution to the renormalization of the other interaction constants (as we will show in next sections). For

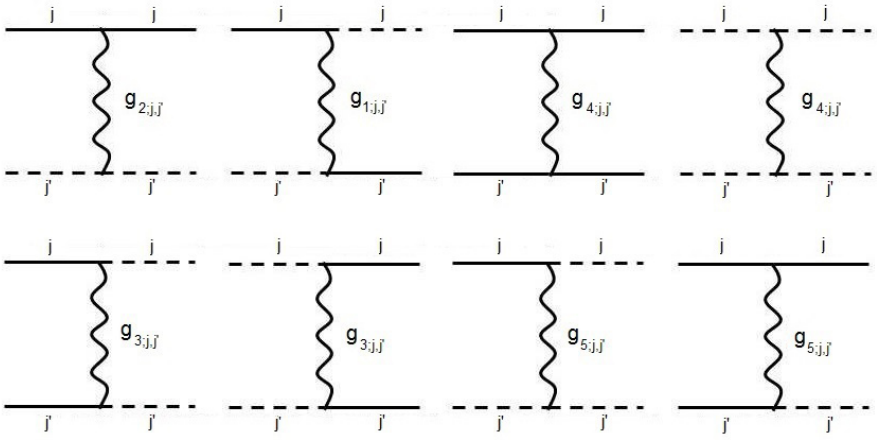

FIG. 5. Scattering processes and g-ology notation of the interaction terms in H_{int}. Solid and dashed lines represent rightgoing and leftgoing particles, wavy line represent the interaction.
From top-left to bottom-right: forward and backward scattering that preserve chiralities, monochirality forward scattering, Umklapp scattering and two examples of non conserving chiralities processes.

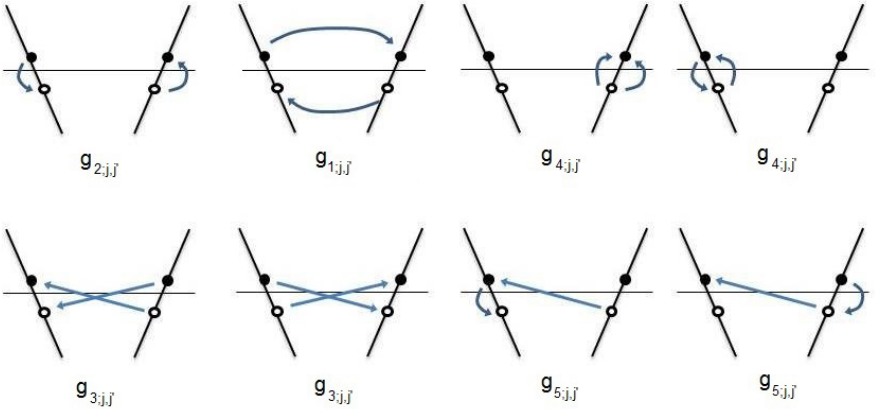

FIG. 6. Scattering processes depicted in Fig. [5] represented in the momentum-energy plane

this reasons it can be neglected, from the point of view of the RG analysis. Another forward scattering term that preserves the chiralities but involves particles with opposite chirality is given by

$$H_{g_2} = \sum_{j,j'} g_{2;j,j'} \int_0^L dx : \psi^\dagger_{R,j}(x)\,\psi_{R,j}(x) :: \psi^\dagger_{L,j'}(x)\,\psi_{L,j'}(x) : \tag{2.54}$$

Again the transfer momentum is small and $g_{2;j,j'} \approx V_{j,j'}(0)$. Next, the backward scattering term that involves particles with opposite chiralities and a momentum transfer of the order of $2k_F$ is given by

$$H_{g_1} = -\sum_{j,j'} g_{1;j,j'} \int_0^L dx : \psi^\dagger_{R,j}(x)\,\psi_{R,j'}(x) :: \psi^\dagger_{L,j'}(x)\,\psi_{Lj}(x) : \tag{2.55}$$

with $g_{1;j,j'} \approx V_{j,j'}(2k_F)$. For an long range interaction the backward scattering can be neglected compared to the forward term, $g_{1;j,j'} \ll g_{2;j,j'}$, while for a short range interaction they have the same order of magnitude. In the limit

of point-like interaction, in agreement with the Pauli principle, they have exactly the same values such that the two contribution, at least in the same wire, cancel each other, $g_{1;j,j} - g_{2;j,j} = 0$. It is worth to note that, if two wires have different Fermi momentum, $k_{F,j} \neq k_{F,j'}$, then the inter-wire backward scattering should contain an additional multiplicative fast oscillating factor of the form $\exp\left[2i\left(k_{F,j} - k_{F,j'}\right)x\right]$ and can be ignored[61] as the density operator vary slowly on the scale of k_F^{-1} so that the whole argument averages to zero, after integration. Another backward scattering term in the interaction Hamiltonian is given by the Umpklapp process that involves two particles near the same Fermi point that reverse the chiralities after the interaction

$$H_{g_3} = \frac{1}{2}\sum_{X=L,R}\sum_{j,j'} g_{3;j,j'} \int_0^L dx : \psi^\dagger_{X,j}(x)\,\psi_{\bar{X},j}(x) :: \psi^\dagger_{X,j'}(x)\,\psi_{\bar{X},j'}(x) : e^{\pm 4ik_F x} \tag{2.56}$$

(plus sign is for $X = L$ and minus sign for $X = R$). This process has a transfer momentum of $4k_F$ and its contribution is important only at half filling where $4k_F$ is equal to a reciprocal lattice vector and momentum conservation can be fulfilled. Assuming this is not the case, we will neglect it. Finally, the terms that expect the change of only one chirality, labeled $g_{5;j,j'}$, can be readily neglect, as the argument of the integral is proportional to the rapidly oscillating function $\exp(2ik_F x)$ and average to zero after integration. Accordingly, the RG analysis performed in the rest of this thesis will be based upon an interaction Hamiltonian involving only Eq. [2.54] and Eq. [2.55]. In presence of only intra-wire interaction the coupling constants are written as

$$g_{\lambda;j,j'} = \delta_{j,j'} g_{j,\lambda}$$

to remove the redundant wire labels. In the spinful case (Eq. [2.8]), the notation

$$\begin{aligned} g_{j,1,\parallel} &= V_{j,\uparrow\uparrow}(2k_F) = V_{j,\downarrow\downarrow}(2k_F) \\ g_{j,2,\parallel} &= V_{j,\uparrow\uparrow}(0) = V_{j,\downarrow\downarrow}(0) \\ g_{j,1,\perp} &= V_{j,\uparrow\downarrow}(2k_F) = V_{j,\downarrow\uparrow}(2k_F) \\ g_{j,2,\perp} &= V_{j,\uparrow\downarrow}(0) = V_{j,\downarrow\uparrow}(0) \end{aligned} \tag{2.57}$$

is conventionally introduced, to highlight the spin dependence of the interaction on the spin of the involved fermions.

II.4. Renormalization group equations for the conductance tensor and the single particle scattering matrix

One of the main questions about systems of quantum wires is about their transport behaviour. In the following section we study how junctions of quantum wires conduct electricity. In particular, we are interested in the low-energy, low-temperature, long-distance limit. In this limit indeed, different junctions with different structures and interaction show the same behavior, that is belong to the same universality class and share the same linear conductance. In this section we compute the dc-conductance for a junction of K quantum wires resorting to the Matsubara imaginary-time formalism, depicted in Appendix [II.6]. In this section the computation is restricted to a normal junction in presence of forward scattering only but a straight application of the approach allows to extend the result for a superconducting junction with backward scattering. Up to second order in the interaction, we may list the following contributions to the $\mathcal{D}$-tensor, defined in Appendix [II.8]. In the absence of interaction, we obtain

$$\begin{aligned} &\mathcal{D}^I_{(0);j,j'}(x,x';i\Omega_n) \\ &= \frac{e^2v^2}{\beta}\sum_\omega \{-G^{(0)}_{(L,j);(L,j')}(x,x';i\omega+i\Omega_n)G^{(0)}_{(L,j');(L,j)}(x',x;i\omega) - G^{(0)}_{(R,j);(R,j')}(x,x';i\omega+i\Omega_n)G^{(0)}_{(R,j');(R,j)}(x',x;i\omega) \\ &+ G^{(0)}_{(L,j);(R,j')}(x,x';i\omega+i\Omega_n)G^{(0)}_{(R,j');(L,j)}(x',x;i\omega) + G^{(0)}_{(R,j);(L,j')}(x,x';i\omega+i\Omega_n)G^{(0)}_{(L,j');(R,j)}(x',x;i\omega)\} \end{aligned} \tag{2.58}$$

The first-order correction to the $\mathcal{D}$-kernel due to the interaction is given by

$$\begin{aligned} &\mathcal{D}^I_{(1);j,j'}(x,x';\tau) \\ &= -e^2v^2\sum_{u,u'=1}^K g_{u,u'}\int_0^L dx^{"}\int_0^\beta d\tau^{"}\,\langle \mathbf{T}_\tau[: \psi^\dagger_{R,j'}(x,\tau)\psi_{R,j'}(x,\tau) : - : \psi^\dagger_{L,j'}(x,\tau)\psi_{L,j'}(x,\tau) :] \end{aligned}$$

$$\times [: \psi^{\dagger}_{R,j}(x',0)\psi_{R,j}(x',0) : - : \psi^{\dagger}_{L,j}(x',0)\psi_{L,j}(x',0) :] : \psi^{\dagger}_{R,u}(x^{"},\tau^{"})\psi_{R,u}(x^{"},\tau^{"}) :: \psi^{\dagger}_{L,u'}(x^{"},\tau^{"})\psi_{L,u'}(x^{"},\tau^{"}) \quad (2.59)$$

At variance, the second-order contribution is given by

$$\mathcal{D}^{I}_{(2);j,j'}(x,x';\tau)$$
$$= \frac{e^2v^2}{2}\sum_{u,u'=1}^{K}\sum_{s,s'=1}^{K} g_{u,u'}g_{s,s'}\int_0^L dx_1dx_2\int_0^{\beta} d\tau_1d\tau_2$$
$$\times \langle \mathbf{T}_{\tau}[: \psi^{\dagger}_{R,j}(x,\tau)\psi_{R,j}(x,\tau) : - : \psi^{\dagger}_{L,j}(x,\tau)\psi_{L,j}(x,\tau) :][: \psi^{\dagger}_{R,j'}(x',0)\psi_{R,j'}(x',0) : - : \psi^{\dagger}_{L,j'}(x',0)\psi_{L,j'}(x',0) :]$$
$$\times : \psi^{\dagger}_{R,u}(x_1,\tau_1)\psi_{R,u}(x_1,\tau_1) :: \psi^{\dagger}_{L,u'}(x_1,\tau_1)\psi_{L,u'}(x_1,\tau_1) :: \psi^{\dagger}_{R,s}(x_2,\tau_2)\psi_{R,s}(x_2,\tau_2) :: \psi^{\dagger}_{L,s'}(x_2,\tau_2)\psi_{L,s'}(x_2,\tau_2) \quad (2.60)$$

Let us, now, start to systematically compute the various corrections making use of the Green's function of Appendix [II.7]. For the unperturbed result, in the zero temperature limit (see Eq. [2.200] in Appendix [II.8]), we obtain the standard result

$$G_{j,j'} = \frac{e^2}{2\pi}\left\{-\delta_{j,j'} + |S^{e,e}_{j,j'}|^2\right\} \quad (2.61)$$

where the scattering matrix is evaluated at the Fermi level.
For the First-order corrections, let us set $X, X' = L, R$. A straightforward application of Wick's theorem yields (denoting, for simplicity, (x,τ) with w, $(x',0)$ with w', $(x^{"},\tau^{"})$ with $w^{"}$)

$$\langle \mathbf{T}_{\tau} : \psi^{\dagger}_{X,j}(w)\psi_{X,j}(w) :: \psi^{\dagger}_{X',j'}(w')\psi_{X',j'}(w') :: \psi^{\dagger}_{R,u}(w^{"})\psi_{R,u}(w^{"}) :: \psi^{\dagger}_{L,u'}(w^{"})\psi_{L,u'}(w^{"}) :\rangle$$
$$= -G^{(0)}_{(X,j);(X',j')}(w,w')G^{(0)}_{(X',j');(R,u)}(w',w^{"})G^{(0)}_{(R,u);(L,u')}(w^{"},w^{"})G^{(0)}_{(L,u');(X,j)}(w^{"},w)$$
$$- G^{(0)}_{(X,j);(X',j')}(w,w')G^{(0)}_{(X',j');(L,u')}(w',w^{"})G^{(0)}_{(L,u');(R,u)}(w^{"},w^{"})G^{(0)}_{(R,u);(X,j)}(w^{"},w)$$
$$- G^{(0)}_{(X,j);(R,u)}(w,w^{"})G^{(0)}_{(R,u);(L,u')}(w^{"},w^{"})G_{(L,u');(X',j')^{(0)}}(w^{"},w^{'})G^{(0)}_{(X',j');(X,j)}(w^{'},w)$$
$$- G^{(0)}_{(X,j);(R,u)}(w,w^{"})G^{(0)}_{(R,u);(X',j')}(w^{"},w^{'})G^{(0)}_{(X',j');(L,u')}(w^{'},w^{"})G^{(0)}_{(L,u');(X,j)}(w^{"},w)$$
$$+ G^{(0)}_{(X,j);(R,u)}(w,w^{"})G^{(0)}_{(R,u);(X,j)}(w^{"},w)G^{(0)}_{(X',j');(L,u')}(w^{'},w^{"})G^{(0)}_{(L,u');(X',j')}(w^{"},w')$$
$$- G^{(0)}_{(X,j);(L,u')}(w,w^{"})G^{(0)}_{(L,u');(R,u)}(w^{"},w^{"})G^{(0)}_{(R,u);(X',j')}(w^{"},w^{'})G^{(0)}_{(X',j');(X,j)}(w^{'},w)$$
$$- G^{(0)}_{(X,j);(L,u')}(w,w^{"})G^{(0)}_{(L,u');(X',j')}(w^{"},w^{'})G^{(0)}_{(X',j');(R,u)}(w^{'},w^{"})G^{(0)}_{(R,u);(X,j)}(w^{"},w)$$
$$+ G^{(0)}_{(X,j);(L,u')}(w,w^{"})G^{(0)}_{(L,u');(X,j)}(w^{"},w)G^{(0)}_{(X',j');(R,u)}(w^{'},w^{"})G^{(0)}_{(R,u);(X',j')}(w^{"},w') \quad (2.62)$$

As a result, in Fourier space one obtains

$$\mathcal{D}^{I}_{(1);j,j'}(x,x';i\Omega_n) = e^2v^2\sum_{u,u'=1}^{K} g_{u,u'}\sum_{X,X'=L,R}(-1)^{X+X'}\frac{1}{\beta^2}\sum_{\omega,\omega'}\int_0^L dx_1$$
$$\times \Big\{ G^{(0)}_{(X,j);(X',j')}(x,x';i\omega+i\Omega_n)G^{(0)}_{(X',j');(R,u)}(x',x_1;i\omega)G^{(0)}_{(R,u);(L,u')}(x_1,x_1;i\omega')G^{(0)}_{(L,u');(X,j)}(x_1,x;i\omega)$$
$$+ G^{(0)}_{(X,j);(X',j')}(x,x';i\omega+i\Omega_n)G^{(0)}_{(X',j');(L,u')}(x',x_1;i\omega)G^{(0)}_{(L,u');(R,u)}(x_1,x_1;i\omega')G^{(0)}_{(R,u);(X,j)}(x_1,x;i\omega)$$
$$+ G^{(0)}_{(X,j);(R,u)}(x,x_1;i\omega)G^{(0)}_{(R,u);(L,u')}(x_1,x_1;i\omega')G^{(0)}_{(L,u');(X',j')}(x_1,x^{'};i\omega)G^{(0)}_{(X',j');(X,j)}(x^{'},x;i\omega-i\Omega_n)$$
$$+ G^{(0)}_{(X,j);(R,u)}(x,x_1;i\omega)G^{(0)}_{(R,u);(X',j')}(x_1,x^{'};i\omega')G^{(0)}_{(X',j');(L,u')}(x^{'},x_1;i\omega'-i\Omega_n)G^{(0)}_{(L,u');(X,j)}(x_1,x;i\omega-i\Omega_n)$$
$$- G^{(0)}_{(X,j);(R,u)}(x,x_1;i\omega)G^{(0)}_{(R,u);(X,j)}(x_1,x;i\omega-i\Omega_n)G^{(0)}_{(X',j');(L,u')}(x^{'},x_1;i\omega')G^{(0)}_{(L,u');(X',j')}(x_1,x';i\omega'+i\Omega_n)$$
$$+ G^{(0)}_{(X,j);(L,u')}(x,x_1;i\omega)G^{(0)}_{(L,u');(R,u)}(x_1,x_1;i\omega')G^{(0)}_{(R,u);(X',j')}(x_1,x^{'};i\omega)G^{(0)}_{(X',j');(X,j)}(x^{'},x;i\omega-i\Omega_n)$$
$$+ G^{(0)}_{(X,j);(L,u')}(x,x_1;i\omega)G^{(0)}_{(L,u');(X',j')}(x_1,x^{'};i\omega')G^{(0)}_{(X',j');(R,u)}(x^{'},x_1;i\omega'-i\Omega_n)G^{(0)}_{(R,u);(X,j)}(x_1,x;i\omega-i\Omega_n)$$
$$- G^{(0)}_{(X,j);(L,u')}(x,x_1;i\omega)G^{(0)}_{(L,u');(X,j)}(x_1,x;i\omega-i\Omega_n)G^{(0)}_{(X',j');(R,u)}(x^{'},x_1;i\omega')G^{(0)}_{(R,u);(X',j')}(x_1,x';i\omega'+i\Omega_n)\Big\} \quad (2.63)$$

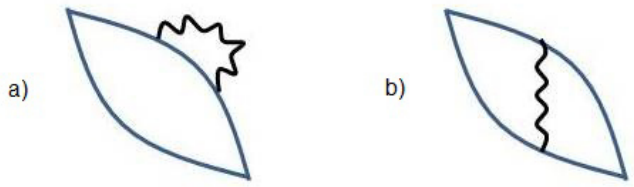

FIG. 7. First order corrections to the conductance loop: a) one loop correction; b) vertex correction

Diagrammatically, in Eq. [2.63] we can identify two different set of conductance correction terms: the one loop correction and the verted correction, both depicted in Fig. [7]. Now, after back-rotating to real frequencies by substituting $i\Omega_n$ with $\Omega + i\eta$, it is easy to verify that, upon pertinently closing the various integration paths in the ϵ-space, all the terms at the fourth, fifth, seventh and eighth row of Eq. [2.63] are equal to zero. Therefore, we obtain

$$\mathcal{D}^{I}_{(1);j,j'}(x,x';i\Omega_n) = e^2v^2 \sum_{u,u'=1}^{K} g_{u,u'} \sum_{X,X'=L,R} (-1)^{X+X'} \frac{1}{\beta^2} \sum_{\omega,\omega'} \int_0^L dx_1$$
$$\times \Bigg\{ G^{(0)}_{(X,j);(X',j')}(x,x';i\omega+i\Omega_n) G^{(0)}_{(X',j');(R,u)}(x',x_1;i\omega) G^{(0)}_{(R,u);(L,u')}(x_1,x_1;i\omega') G^{(0)}_{(L,u');(X,j)}(x_1,x;i\omega)$$
$$+ G^{(0)}_{(X,j);(X',j')}(x,x';i\omega+i\Omega_n) G^{(0)}_{(X',j');(L,u')}(x',x_1;i\omega) G^{(0)}_{(L,u');(R,u)}(x_1,x_1;i\omega') G^{(0)}_{(R,u);(X,j)}(x_1,x;i\omega)$$
$$+ G^{(0)}_{(X,j);(R,u)}(x,x_1;i\omega) G^{(0)}_{(R,u);(L,u')}(x_1,x_1;i\omega') G^{(0)}_{(L,u');(X',j')}(x_1,x';i\omega) G^{(0)}_{(X',j');(X,j)}(x',x;i\omega-i\Omega_n)$$
$$+ G^{(0)}_{(X,j);(L,u')}(x,x_1;i\omega) G^{(0)}_{(L,u');(R,u)}(x_1,x_1;i\omega') G^{(0)}_{(R,u);(X',j')}(x_1,x';i\omega) G^{(0)}_{(X',j');(X,j)}(x',x;i\omega-i\Omega_n) \Bigg\}$$

It is fundamental to observe that all the vertex correction disappeared while the remaining contributions are readily identified to be given by

$$\mathcal{D}^{I}_{(1);j,j'}(x,x';i\Omega_n) = -e^2v^2 \sum_{X,X'=L,R} (-1)^{X+X'} \frac{1}{\beta^2} \sum_{\omega,\omega'} \int_0^L dx_1$$
$$\times \Bigg\{ G^{(0)}_{(X,j);(X',j')}(x,x';i\omega+i\Omega_n) \delta G^{(1)}_{(X',j');(X,j)}(x',x;i\omega)$$
$$+ \delta G^{(1)}_{(X,j);(X',j')}(x,x';i\omega) G^{(0)}_{(X',j');(X,j)}(x',x;i\omega-i\Omega_n) \Bigg\} \tag{2.64}$$

with $\delta G^{(1)}_{(X',j');(X,j)}(x',x;i\omega)$ being the first-order one-loop corrections to one of the two Green's functions of the conductance loop. The absence of vertex corrections is true also in presence of a forward scattering interaction and in presence of anomalous contractions. Furthermore, following Ref. [78], we assume that vertex corrections give zero contribution up to the second order. It follows that, instead to compute the laborious dc conductance correction we can focus on the perturbative treatment of the Green's functions only as we will do in the next section.

II.4.1. First order correction to the Green's functions and renormalization group equations for the scattering matrix

In the following, using the Matsubara imaginary time technique we will compute the first order correction to the fermions propagators and then to the scattering matrix coefficients in presence of interaction. We will do it in the Matsubara formalism for a junction that, at the boundary, allows for any possible single particle normal and Andreev-like processes. Through this approach we will show how to reproduce and extend, to the case of energy dependent

scattering matrix and in presence of any kind of inter-wire and intra-wire interaction the RG equation of Refs. [37 and 39] for a normal junction; furthermore we will extend the results of Ref. [51] for the NS junction to the case of K wires allowing for spin-flip and p-wave Andreev processes at the boundary. Another advantage of the formalism we will develop in the following is the possibility to go beyond the leading log approximation including, in the correction of the scattering matrix, diagrams of higher order in the interaction parameters. Indeed, a comparison between the FRG technique and the bosonic approach[61] highlights how the first order correction to the S-matrix is insufficient to gather all the features of systems that involves interaction with Majorana's fermion at the boundary. Have an handleable tool able to include sub-leading correction within the RG equation could be crucial for the application of the fermionic approach of such kind of systems.

Let us take an interaction Hamiltonian of the form of Eq. [2.54] plus Eq. [2.55]. To take them both into account at the same time the smart approach is to forget for the moment about the wire and interaction indices and add them only at the end of the computation through the unique substitutions

$$\begin{aligned} g &\to \sum_{a,a'} g_{2;a,a'} \\ x &\to x, j \\ x' &\to x', j' \\ R, x_1 &\to R, x_1, a \\ L, x_1 &\to L, x_1, a' \end{aligned} \tag{2.65}$$

for the forward scattering and

$$\begin{aligned} g &\to -\sum_{a,a'} g_{1;a,a'} \\ x &\to x, j \\ x' &\to x', j' \\ R^\dagger, x_1 &\to R^\dagger, x_1, a \\ L^\dagger, x_1 &\to L^\dagger, x_1, a' \\ R, x_1 &\to R, x_1, a' \\ L, x_1 &\to L, x_1, a \end{aligned} \tag{2.66}$$

for the backscattering term. The starting point is to compute the first order of the Dyson's series for the normal Green's function

$$\delta G^{(1)}_{RL}(x,\tau,x') = +g \int_0^L dx_1 \int_0^\beta d\tau_1 \left\langle T_\tau \psi_R(x,\tau) : \psi^\dagger_R(x_1,\tau_1)\psi_R(x_1,\tau_1) :: \psi^\dagger_L(x_1,\tau_1)\psi_L(x_1,\tau_1) : \psi^\dagger_L(x',0) \right\rangle \tag{2.67}$$

and for the anomalous Green's function

$$\delta F^{(1)}_{RL}(x,\tau,x') = +g \int_0^L dx_1 \int_0^\beta d\tau_1 \left\langle T_\tau \psi_R(x,\tau) : \psi^\dagger_R(x_1,\tau_1)\psi_R(x_1,\tau_1) :: \psi^\dagger_L(x_1,\tau_1)\psi_L(x_1,\tau_1) : \psi_L(x',0) \right\rangle \tag{2.68}$$

making use of the Wick's theorem (a detailed computation can be found in Appendix [II.9]). Discarding all the trivially zero contractions, in Fourier space, we have the following first order contributions for the normal Green's function

$$\begin{aligned} \delta G^{(1)}_{RL}(x,x',i\omega) \approx +\frac{g}{\beta} \int_0^L dx_1 \sum_{\omega'} [\\ + G^{(0)}_{RR}(x,x_1,i\omega) G^{(0)}_{RL}(x_1,x_1,i\omega') G^{(0)}_{LL}(x_1,x',i\omega) \\ + G^{(0)}_{RL}(x,x_1,i\omega) G^{(0)}_{LR}(x_1,x_1,i\omega') G^{(0)}_{RL}(x_1,x',i\omega) \\ + G^{(0)}_{RL}(x,x_1,i\omega) F^{(0)}_{RL}(x_1,x_1,i\omega') \tilde{F}^{(0)}_{RL}(x_1,x',i\omega) \end{aligned}$$

$$+F_{RL}^{(0)}(x,x_1,i\omega)\,\tilde{F}_{RL}^{(0)}(x_1,x_1,i\omega')\,G_{RL}^{(0)}(x_1,x',i\omega)$$
$$-F_{RL}^{(0)}(x,x_1,i\omega)\,G_{RL}^{(0)}(x_1,x_1,i\omega')\,\tilde{F}_{RL}^{(0)}(x_1,x',i\omega)] \tag{2.69}$$

and for the anomalous Green's function

$$\delta F_{RL}^{(1)}(x,x',i\omega) \approx +\frac{g}{\beta}\int_0^L dx_1 \sum_{\omega'}[$$
$$+G_{RR}^{(0)}(x,x_1,i\omega)\,F_{RL}^{(0)}(x_1,x_1,i\omega')\,G_{LL}^{(0)}(x',x_1,-i\omega)$$
$$+G_{RL}^{(0)}(x,x_1,i\omega)\,G_{LR}^{(0)}(x_1,x_1,i\omega')\,F_{RL}^{(0)}(x_1,x',i\omega)$$
$$-G_{RL}^{(0)}(x,x_1,i\omega)\,F_{RL}^{(0)}(x_1,x_1,i\omega')\,G_{LR}^{(0)}(x',x_1,-i\omega)$$
$$+F_{RL}^{(0)}(x,x_1,i\omega)\,\tilde{F}_{RL}^{(0)}(x_1,x_1,i\omega')\,F_{RL}^{(0)}(x_1,x',i\omega)$$
$$+F_{RL}^{(0)}(x,x_1,i\omega)\,G_{RL}^{(0)}(x_1,x_1,i\omega')\,G_{LR}^{(0)}(x',x_1,-i\omega)] \tag{2.70}$$

Substituting the full form of the Green's functions through Eq. [2.187], a comparison with the the zeroth order normal and anomalous Green's functions

$$G_{R,L}^{(0)}(x,x',i\omega_n) = \frac{1}{l}\sum_k \frac{e^{+ik\left(x+x'\right)}}{(\epsilon_k - i\omega)} S^{e,e}(\epsilon_k)$$
$$\frac{1}{2\pi v}\int d\epsilon \frac{e^{+i\frac{\epsilon}{v}\left(x+x'\right)}}{(\epsilon - i\omega)} S^{e,e}(\epsilon)$$
$$\frac{i}{v}\Theta(\omega)\,S^{e,e}(i\omega)\,e^{-i\frac{\omega}{v}\left(x+x'\right)} \tag{2.71}$$

and

$$F_{R,L}^{(0)}(x,x',i\omega_n) = \frac{1}{l}\sum_k \frac{e^{+ik\left(x+x'\right)}}{(\epsilon_k - i\omega)} S^{e,h}(\epsilon_k)$$
$$\frac{1}{2\pi v}\int d\epsilon \frac{e^{+i\frac{\epsilon}{v}\left(x+x'\right)}}{(\epsilon - i\omega)} S^{e,h}(\epsilon)$$
$$\frac{i}{v}\Theta(\omega)\,S^{e,h}(i\omega)\,e^{-\frac{\omega}{v}\left(x+x'\right)} \tag{2.72}$$

give us the first order correction to the $S^{e,e}$ and $S^{e,h}$ coefficients. Upon restoring the wire indices, for the forward interaction, Eq. [2.54], through the replacement in Eq. [2.65] and for the backscattering term, Eq. [2.55], with the replacement in Eq. [2.66] and adding up the two contributions we can write the first order correction in the matrix form

$$\frac{dS(\omega,\Lambda)}{d\ln\Lambda} = -S(\omega,\Lambda)\,F^{\dagger}(-\Lambda,\Lambda)\,S(\omega,\Lambda) + F(\Lambda,\Lambda) \tag{2.73}$$

where $\Lambda = D/D_0$ and the scattering matrix is written in the block form

$$S(\omega,\Lambda) := \begin{pmatrix} S^{e,e}(\omega,\Lambda) & S^{e,h}(\omega,\Lambda) \\ S^{h,e}(\omega,\Lambda) & S^{h,h}(\omega,\Lambda) \end{pmatrix}$$
$$= \begin{pmatrix} S^{e,e}(\omega,\Lambda) & S^{e,h}(\omega,\Lambda) \\ S^{e,h*}(-\omega,\Lambda) & S^{e,e*}(-\omega,\Lambda) \end{pmatrix} \tag{2.74}$$

and where we defined a "Friedel" matrix[39] of the form

$$F(\omega,\Lambda) := \begin{pmatrix} F^{e,e}(\omega,\Lambda) & F^{e,h}(\omega,\Lambda) \\ F^{h,e}(\omega,\Lambda) & F^{h,h}(\omega,\Lambda) \end{pmatrix} = \begin{pmatrix} F^{e,e}(\omega,\Lambda) & F^{e,h}(\omega,\Lambda) \\ F^{e,h*}(-\omega,\Lambda) & F^{e,e*}(-\omega,\Lambda) \end{pmatrix} \tag{2.75}$$

with $F^{e,e}$ and $F^{e,h}$, $K \times K$ matrices whose elements are given by

$$\begin{aligned} F^{e,e}_{j,j'}(\omega,\Lambda) &:= \frac{1}{2(2\pi)v}\left[-g_{2;j,j'}S^{e,e}_{j,j'}(\omega,\Lambda) + \sum_a g_{1;j,a}\delta_{j,j'}S^{e,e}_{a,a}(\omega,\Lambda)\right] \\ F^{e,h}_{j,j'}(\omega,\Lambda) &:= \frac{1}{2(2\pi)v}\left[g_{2;j,j'}S^{e,h}_{j,j'}(\omega,\Lambda) - g_{1;j',j}S^{e,h}_{j',j}(\omega,\Lambda)\right] \end{aligned} \tag{2.76}$$

The current form of the RG equation for the S matrix breaks the particle-hole symmetry of Eq. [2.33]. To preserve the particle-hole symmetry explicitly we have to modify the equation as

$$\frac{dS(\omega,\Lambda)}{d\ln\Lambda} = -S(\omega,\Lambda)\frac{1}{2}\left[F^\dagger(\Lambda,\Lambda) + F^\dagger(-\Lambda,\Lambda)\right]S(\omega,\Lambda) + \frac{1}{2}\left[F(\Lambda,\Lambda) + F(-\Lambda,\Lambda)\right] \tag{2.77}$$

This is equivalent to subtracting from the original quartic Hamiltonian a cutoff-dependent chemical potential term[79]. Eq. [2.77] applies well to a large class of systems, including the resonant tunneling[40] and normal-superconducting junction[51]. In these cases the intrinsic energy dependence of the scattering matrix play a crucial role in the comprehension of the physical properties of the system in presence of interaction. Instead, in presence of a structureless impurity[37–39] the scattering matrix is assumed to be an analytic function, slowly varying on the scale of the Fermi energy. Therefore, it is possible to neglect the intrinsic energy dependence of the scattering matrix and the RG equation reduces to

$$\frac{dS(\Lambda)}{d\ln\Lambda} = -S(\Lambda)F^\dagger(\Lambda)S(\Lambda) + F(\Lambda) \tag{2.78}$$

This simple and elegant equation give us some interesting information on the behavior of the scattering matrix under the change of scale. First of all we see that

$$\begin{aligned} \frac{dI}{d\ln\Lambda} &= \frac{dS(\Lambda)S^\dagger(\Lambda)}{d\ln\Lambda} \\ &= S(\Lambda)\frac{dS^\dagger(\Lambda)}{d\ln\Lambda} + \frac{dS(\Lambda)}{d\ln\Lambda}S^\dagger(\Lambda) \\ &= -S(\Lambda)S^\dagger(\Lambda)F(\Lambda)S^\dagger(\Lambda) + S(\Lambda)F^\dagger(\Lambda) + \\ &\quad -S(\Lambda)F^\dagger(\Lambda)S(\Lambda)S^\dagger(\Lambda) + F(\Lambda)S^\dagger(\Lambda) \\ &= 0 \end{aligned} \tag{2.79}$$

and then that S remains unitary under the RG flow. Indeed, let us call dS the variation of S under an infinitesimal change of scale. Then

$$\begin{aligned} (S+dS)\left(S^\dagger + dS^\dagger\right) &= SS^\dagger + SdS^\dagger + dSS^\dagger \\ &\approx I + d\left(SS^\dagger\right) \\ &\approx I \end{aligned} \tag{2.80}$$

Finally, we can easily find the fixed points, corresponding to values of S which do not change under RG flow. Indeed, to do so, S must set to zero the right-hand term of Eq. [2.78], which implies the condition

$$S(\Lambda)F^\dagger(\Lambda) = F(\Lambda)S^\dagger(\Lambda) \tag{2.81}$$

For $K = 2$ and $K = 3$, examples of scattering matrices that satisfy the FP conditions are the ones in Eq. [2.45] and Eq. [2.46] or for example the matrix

$$S_M = \begin{bmatrix} -\frac{1}{3} & \frac{2}{3} & \frac{2}{3} \\ \frac{2}{3} & -\frac{1}{3} & \frac{2}{3} \\ \frac{2}{3} & \frac{2}{3} & -\frac{1}{3} \end{bmatrix} \tag{2.82}$$

that correspond to a system with maximum transparency allowed by unitarity and compatible with time reversal symmetry. We will discuss it in details in the next Chapter. An important limit of Eq. [2.78] is the case of a junction of spinless wires without inter-wire interaction; the F matrix is given by

$$F_{j,j'} = \frac{1}{4\pi v} \left(g_{j,2} - g_{j,1}\right) S_{j,j} \delta_{j,j'} \tag{2.83}$$

Another interesting limit is the junction of spin-$\frac{1}{2}$ wires, in absence of inter-wire interaction, such that

$$F_{(j,\sigma),(j',\sigma')} = \delta_{\sigma,\sigma'} \frac{1}{4\pi v} \left(g_{j,2,\parallel} - g_{j,1,\parallel} - g_{j,1,\perp}\right) S_{j,j} \delta_{j,j'} \tag{2.84}$$

valid under the assumption that spin is preserved by the boundary Hamiltonian. Yet, an important remark to make, before concluding this section, is that, typically, the RG trajectories do not flow all the way down to $D/D_0 = 0$, but must be cut off at a physically relevant scale D_*. As the temperature $T = 0$, D_* typically is the lowest energy scale available for an excitation of the system. For instance, in a finite-size system of length L, one clearly gets $D_* \sim v_F/L$. At finite temperature T, provided $v_F/L \ll k_B T$ (k_B being Boltzmann's constant), it is natural to stop the RG flow at $D_T \sim k_B T$, to take into account the smearing of the Fermi surface over an energy width $\sim k_B T$.
It is possible to give a graphical interpretation of the first order correction of the scattering matrix in terms of Feynman diagrams in space-frequency domain. The building blocks to assemble any physical process are the normal and anomalous Green's functions in Appendix [II.7]. In particular we recognize the normal Green's functions $G_{(R,j);(R,j)}$ and $G_{(L,j);(L,j)}$ that represent the propagation of a left or right going electron or hole inside a given wire j. In Fig. [8], panel a), they are pictorially represented as a straight line approaching or leaving the junction. For a left going particle the line is dotted, while for a right going particle it is continuous; for an hole we will use the same convention but with the direction of the arrow reversed. In addition we have the normal and anomalous Green's functions $G_{(R,j);(L,j')}$, $F_{(R,j);(L,j')}$ and $\tilde{F}_{(R,j);(L,j')}$ that involve a reflection or transmission by the junction of a particle or of an hole. These processes are shown in Fig. [8], panel b), where the scattering matrix dependence is highlighted. Combining these blocks with the interaction processes of Fig. [5] it is easy to give a pictorial representation of each line of Eqs. [2.69,2.70]. In Fig. [9] for example the first three lines of Eq. [2.69] are depicted for both forward and backward scattering. The scattering matrix dependence of these processes can be easily compared with the first three lines of Eqs. [2.214,2.215]. The space-frequency representation can be easily used for the higher order corrections to give a real space interpretation of the physical processes.

II.4.2. One-loop correction to the bulk interacting constants

It is well known[16,59,60] that the interaction strengths $g_{1;j,j'}$ and $g_{2;j,j'}$ are not constant and change in the course of renormalization. For this reason the RG equations for the S-matrix must be supplemented with the RG equations for $g_{1;j,j'}$ and $g_{2;j,j'}$. The starting point to compute these RG equations is the interaction Hamiltonian of Eq. [2.54] and Eq. [2.55]; the first order processes contained in it (remembering that the four fermions fields are not exactly evaluated at the same point x [2.7]) are shown in Fig. [5]. Now, we will compute all the 1-loop processes that contain a right/outgoing (ω_1, p_1) and left/ingoing (ω_2, p_2) fermion in the initial state and a right/outgoing (ω_3, p_3) and left/ingoing (ω_4, p_4) fermion in the final state. All the processes are shown in Fig. [10] where: a continuous line represents a right/outgoing chirality field, a dashed line a left/ingoing chirality field, a wavy line a $g_{2;j,j'}$ or $g_{1;j,j'}$ interaction. To proceed, we have, first of all, to compute the free Green's function at imaginary time for right and left movers, in momentum-frequency domain. Through a Fourier transformation of Eqs. [2.187] we obtain

$$G_{(R,j);(R,j')}(p, i\omega) = -\frac{\delta_{j,j'}}{v_F p + i\omega} \tag{2.85}$$

Similarly, for left movers:

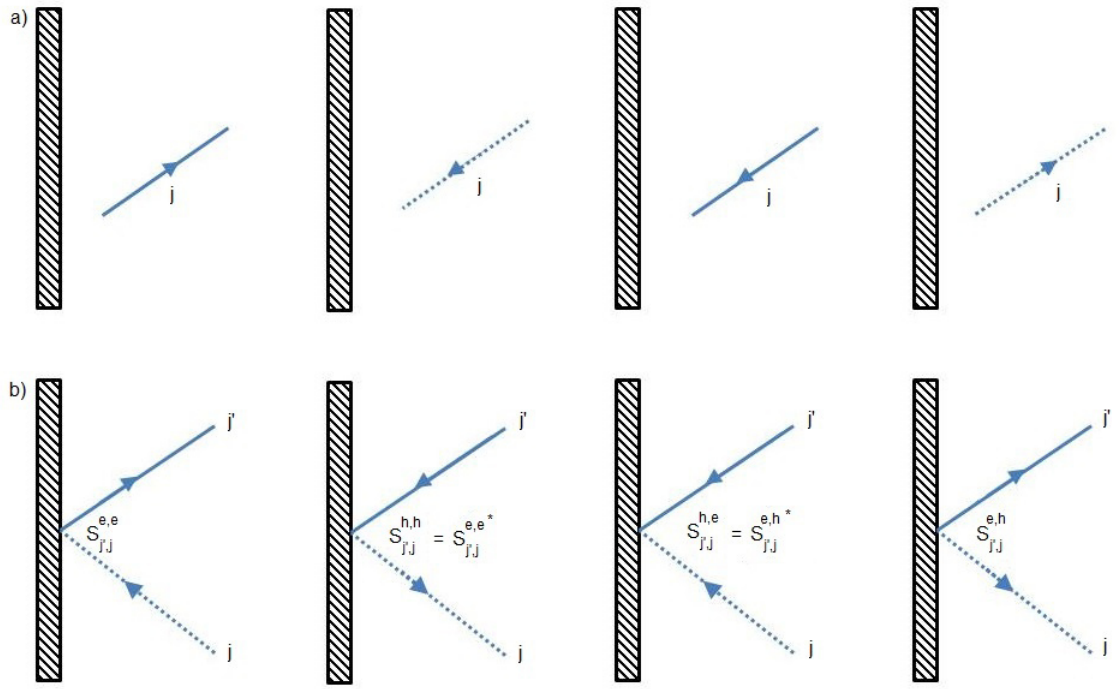

FIG. 8. Real space representation of the normal and anomalous Green's functions involving a) one chirality ($G_{(R,j);(R,j)}$, $G_{(L,j);(L,j)}$), b) two chiralities ($G_{(R,j');(L,j)}$, $F_{(R,j');(L,j)}$ and $\tilde{F}_{(R,j');(L,j)}$). First two diagrams of panel a) correspond to the propagation of a right or left Fermi point particle while the last two diagrams correspond to the propagation of a right or left Fermi points hole. Panel b) represent normal or Andreev reflection/transmission of a particle or of an hole at the junction.

$$G_{(L,j);(L,j')}(p, i\omega) = \frac{\delta_{j,j'}}{v_F p - i\omega} \tag{2.86}$$

It is useful to note that:

$$G_{(R,j);(R,j')}(p, i\omega) = -G^*_{(L,j);(L,j')}(p.i\omega) \tag{2.87}$$

Let us start from the Cooper pair channel a)

$$\begin{aligned}
\Pi^{(a)}_{j,j'} &= (g_{2;j,j'})^2 \int \frac{dQ}{2\pi} \int \frac{d\Omega}{2\pi} G_{(R,j);(R,j)}(Q, i\Omega) G_{(L,j');(L,j')}(-Q + p, -i\Omega + i\omega) \\
&= -(g_{2;j,j'})^2 \int \frac{dQ}{2\pi} \int \frac{d\Omega}{2\pi} \frac{1}{v_F Q + i\Omega} \cdot \frac{1}{v_F(-Q + p) - i(-\Omega + \omega)} \\
&= (g_{2;j,j'})^2 \int \frac{dQ}{2\pi} \int \frac{d\Omega}{2\pi} \frac{1}{\Omega - i v_F Q} \cdot \frac{1}{(\Omega - \omega) + i v_F (Q - p)}
\end{aligned}$$

(where $\omega \equiv \omega_1 + \omega_2$, $p \equiv p_1 + p_2$). Integrating in $d\Omega$ with the residues method, the two poles $\Omega_1 = +i v_F Q$ and $\Omega_2 = -i v_F (Q - p) + \omega$ have to be on different sides of the real axis to have a non zero integral. For $p > 0$ (for $p < 0$ the result is the same) such request is satisfied for $Q < 0$ and $p < Q < \Lambda/2$, where we have introduced the transfer cut-off Λ

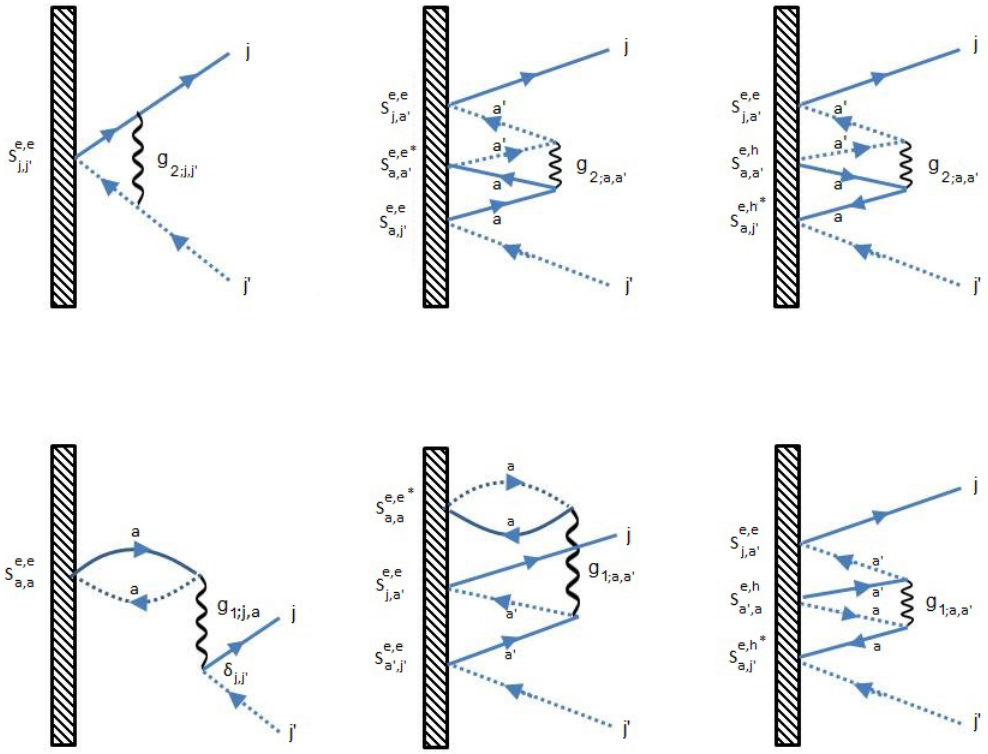

FIG. 9. Examples of first order contributions in real space to the RG equations of the scattering coefficient $S^{e,e}_{j,j'}$

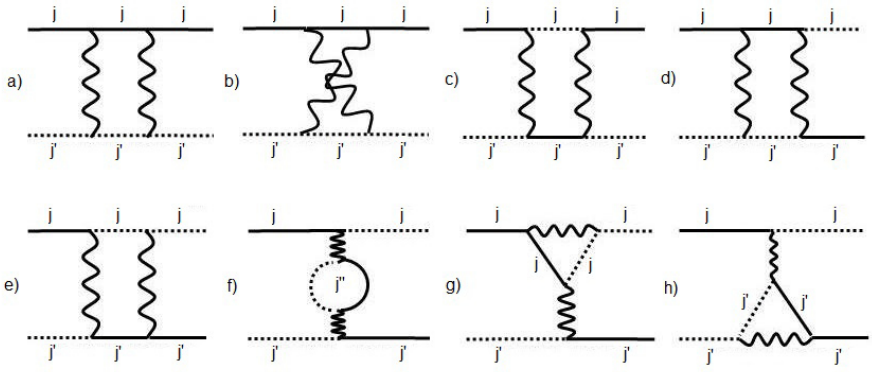

FIG. 10. One-loop processes that give a logarithmic contribution to the correction of the interaction constants. First three diagrams from first row contribute to the renormalization of $g_{2;j,j'}$ while last diagram of first row and second row contributes to the renormalization of $g_{1;j,j'}$. Diagrams a), c), d) and e) are the Cooper pair channel while diagrams b), f), g) and h) are the zero sound channel.

$$\Pi^{(a)}_{j,j'} = \frac{i\left(g_{2;j,j'}\right)^2}{2\pi}\left[\int_p^{\Lambda/2} dQ - \int_{-\Lambda/2}^{0} dQ\right]\frac{1}{2iv_FQ - iv_Fp - \omega}$$
$$\approx \frac{\left(g_{2;j,j'}\right)^2}{4v_F\pi}\ln\left[\frac{v_F^2\Lambda^2}{\omega^2 + v_F^2p^2}\right] + \dots \tag{2.88}$$

For the zero sound channel b)

$$\begin{aligned}\Pi^{(b)}_{j,j'} &= (g_{2;j,j'})^2 \int \frac{dQ}{2\pi}\int \frac{d\Omega}{2\pi} G_{(R,j);(R,j)}(Q,i\Omega)G_{(L,j');(L,j')}(Q+\bar{p},i\Omega+i\bar{\omega}) \\ &= -(g_{2;j,j'})^2 \int \frac{dQ}{2\pi}\int \frac{d\Omega}{2\pi} \frac{1}{v_F Q + i\Omega}\cdot\frac{1}{v_F(Q+\bar{p})-i(\Omega+\bar{\omega})} \\ &= -(g_{2;j,j'})^2 \int \frac{dQ}{2\pi}\int \frac{d\Omega}{2\pi} \frac{1}{\Omega - iv_F Q}\cdot\frac{1}{(\Omega+\bar{\omega})+iv_F(Q+\bar{p})} \\ &\approx -\frac{(g_{2;j,j'})^2}{4v_F\pi}\ln\left[\frac{v_F^2\Lambda^2}{\bar{\omega}^2+v_F^2\bar{p}^2}\right] \end{aligned} \tag{2.89}$$

(with $\bar{\omega}\equiv\omega_1-\omega_4$, $\bar{p}\equiv p_1-p_4$). For the channel c), making use of Eq. [2.87], we have

$$\begin{aligned}\Pi^{(c)}_{j,j'} &= (g_{1;j,j'})^2 \int \frac{dQ}{2\pi}\int \frac{d\Omega}{2\pi} G_{(L,j);(L,j)}(Q,i\Omega)G_{(R,j');(R,j')}(-Q+p,-i\Omega+i\omega) \\ &= (g_{1;j,j'})^2 \left[\int \frac{dQ}{2\pi}\int \frac{d\Omega}{2\pi} G_{(R,j');(R,j')}(Q,i\Omega)G_{(L,j);(L,j)}(-Q+p,-i\Omega+i\omega)\right]^* \\ &\approx \frac{(g_{1;j,j'})^2}{4v_F\pi}\ln\left[\frac{v_F^2\Lambda^2}{\omega^2+v_F^2p^2}\right] \end{aligned} \tag{2.90}$$

Channel d) it is the same as $\Pi^{(a)}_{j,j'}$ except for the different interaction strengths

$$\begin{aligned}\Pi^{(d)}_{j',j} &= (g_{2;j,j'}g_{1;j,j'}) \int \frac{dQ}{2\pi}\int \frac{d\Omega}{2\pi} G_{(R,j);(R,j)}(Q,i\Omega)G_{(L,j');(L,j')}(-Q+p,-i\Omega+i\omega) \\ &\approx \frac{(g_{2;j,j'}g_{1;j,j'})}{4v_F\pi}\ln\left[\frac{v_F^2\Lambda^2}{\omega^2+v_F^2p^2}\right] \end{aligned} \tag{2.91}$$

For channel e) we note that is the same as $\Pi^{(c)}_{j,j'}$ except for the interaction strengths

$$\begin{aligned}\Pi^{(e)}_{j',j} &= (g_{1;j,j'}g_{2;j,j'}) \int \frac{dQ}{2\pi}\int \frac{d\Omega}{2\pi} G_{(L,j);(L,j)}(Q,i\Omega)G_{(R,j');(R,j')}(-Q+p,-i\Omega+i\omega) \\ &\approx \frac{(g_{1;j,j'}g_{2;j,j'})}{4v_F\pi}\ln\left[\frac{v_F^2\Lambda^2}{\omega^2+v_F^2p^2}\right] \end{aligned} \tag{2.92}$$

The zero sound channel f) is an interesting one; the fermionic loop inside bring a minus sign and we have K of this diagrams (one for each wire index inside the loop). It is similar to $\Pi^{(b)}_{j,j'}$ and gives

$$\begin{aligned}\sum_{j"}\Pi^{(f)}_{j',j} &= -\left(\sum_{j"} g_{1;j,j"}g_{1;j',j"}\right)\int \frac{dQ}{2\pi}\int \frac{d\Omega}{2\pi} G_{(R,j");(R,j")}(Q,i\Omega)G_{(L,j");(L,j")}(Q-\bar{p},i\Omega-i\bar{\omega}) \\ &\approx \frac{\left(\sum_{j"} g_{1;j,j"}g_{1;j',j"}\right)}{4v_F\pi}\ln\left[\frac{v_F^2\Lambda^2}{\bar{\omega}^2+v_F^2\bar{p}^2}\right] \end{aligned} \tag{2.93}$$

Channel g) and h) are similar to $\Pi^{(f)}_{j,j'}$ without the minus sign and the sum over the wires

$$\begin{aligned}\Pi^{(g)}_{j',j} &= (g_{2;j,j}g_{1;j,j'}) \int \frac{dQ}{2\pi}\int \frac{d\Omega}{2\pi} G_{(R,j);(R,j)}(Q,i\Omega)G_{(L,j);(L,j)}(Q-\bar{p},i\Omega-i\bar{\omega}) \\ &\approx -\frac{(g_{2;j,j}g_{1;j,j'})}{4v_F\pi}\ln\left[\frac{v_F^2\Lambda^2}{\bar{\omega}^2+v_F^2\bar{p}^2}\right] \end{aligned} \tag{2.94}$$

and

$$\Pi^{(h)}_{j',j} = (g_{1;j,j'}g_{2;j',j'}) \int \frac{dQ}{2\pi} \int \frac{d\Omega}{2\pi} G_{(R,j');(R,j')}(Q, i\Omega) G_{(L,j');(L,j')}(Q-\bar{p}, i\Omega - i\bar{\omega})$$
$$\approx -\frac{(g_{1;j,j'}g_{2;j',j'})}{4v_F\pi} \ln\left[\frac{v_F^2\Lambda^2}{\bar{\omega}^2 + v_F^2\bar{p}^2}\right] \tag{2.95}$$

At this point, the sum of diagrams a), b) and c) form a new vertex $\Pi^{(2)}_{j,j'}$, while diagrams d), e), f), g) and h) form a new vertex $\Pi^{(1)}_{j',j}$

$$\begin{aligned} -\Pi^{(2)}_{j,j'} &= -g^{(2)}_{j,j'} + \Pi^{(a)}_{j,j'} + \Pi^{(b)}_{j,j'} + \Pi^{(c)}_{j,j'} \\ &= -g_{2;j,j'} + \frac{(g_{2;j,j'})^2}{4v_F\pi} \ln\left[\frac{v_F^2\Lambda^2}{\omega^2 + v_F^2p^2}\right] - \frac{(g_{2;j,j'})^2}{4v_F\pi} \ln\left[\frac{v_F^2\Lambda^2}{\bar{\omega}^2 + v_F^2\bar{p}^2}\right] + \frac{(g_{1;j,j'})^2}{4v_F\pi} \ln\left[\frac{v_F^2\Lambda^2}{\omega^2 + v_F^2p^2}\right] \\ &= -g_{2;j,j'} + \frac{(g_{2;j,j'})^2}{4v_F\pi} \ln\left[\frac{\bar{\omega}^2 + v_F^2\bar{p}^2}{\omega^2 + v_F^2p^2}\right] + \frac{(g_{1;j,j'})^2}{4v_F\pi} \ln\left[\frac{v_F^2\Lambda^2}{\omega^2 + v_F^2p^2}\right] \end{aligned} \tag{2.96}$$

$$\begin{aligned} -\Pi^{(1)}_{j',j} &= -g_{1;j,j'} + \Pi^{(d)}_{j',j} + \Pi^{(e)}_{j',j} + \sum_{j"} \Pi^{(f)}_{j',j} + \Pi^{(g)}_{j',j} + \Pi^{(h)}_{j',j} \\ &= -g^{(1)}_{j',j} + \frac{(g_{2;j,j'}g_{1;j,j'} + g_{1;j,j'}g_{2;j,j'})}{4v_F\pi} \ln\left[\frac{v_F^2\Lambda^2}{\omega^2 + v_F^2p^2}\right] + \frac{\left(\sum_{j"} g_{1;j,j"}g_{1;j',j"} - g_{2;j,j}g_{1;j,j'} - g_{1;j,j'}g_{2;j',j'}\right)}{4v_F\pi} \ln\left[\frac{v_F^2\Lambda^2}{\bar{\omega}^2 + v_F^2\bar{p}^2}\right] \\ &= -g^{(1)}_{j',j} + \frac{(g_{2;j,j'}g_{1;j,j'})}{2v_F\pi} \ln\left[\frac{v_F^2\Lambda^2}{\omega^2 + v_F^2p^2}\right] + \frac{\left(\sum_{j"} g_{1;j,j"}g_{1;j',j"} - g_{2;j,j}g_{1;j,j'} - g_{1;j,j'}g_{2;j',j'}\right)}{4v_F\pi} \ln\left[\frac{v_F^2\Lambda^2}{\bar{\omega}^2 + v_F^2\bar{p}^2}\right] \end{aligned} \tag{2.97}$$

In the renormalization group philosophy we ask the 1-loop corrected new vertex function to be cutoff independent. This is realized letting $g_{1;j,j'}$ and $g_{2;j,j'}$ to be energy dependent. That is, are valid the following differential equations:

$$\begin{aligned} \frac{\partial g_{2;j,j'}}{\partial\Lambda} &= \frac{\partial}{\partial\Lambda}\left[\Pi^{(a)}_{j,j'} + \Pi^{(b)}_{j,j'} + \Pi^{(c)}_{j,j'}\right] \\ &= \frac{2g_{2;j,j'}}{4v_F\pi} \frac{\partial g_{2;j,j'}}{\partial\Lambda} \ln\left[\frac{\bar{\omega}^2 + v_F^2\bar{p}^2}{\omega^2 + v_F^2p^2}\right] + \frac{1}{4v_F\pi} \frac{\partial\left(g_{1;j,j'}\right)^2}{\partial\Lambda} \ln\left[\frac{v_F^2\Lambda^2}{\omega^2 + v_F^2p^2}\right] + \frac{(g_{1;j,j'})^2}{4v_F\pi}\frac{2}{\Lambda} \end{aligned} \tag{2.98}$$

$$\begin{aligned} \frac{\partial g_{1;j,j'}}{\partial\Lambda} &= \frac{\partial}{\partial\Lambda}\left[\Pi^{(d)}_{j',j} + \Pi^{(e)}_{j',j} + \sum_{j"} \Pi^{(f)}_{j',j} + \Pi^{(g)}_{j',j} + \Pi^{(h)}_{j',j}\right] \\ &= \frac{1}{2v_F\pi} \frac{\partial\left(g_{2;j,j'}g_{1;j,j'}\right)}{\partial\Lambda} \ln\left[\frac{v_F^2\Lambda^2}{\omega^2 + v_F^2p^2}\right] + \frac{(g_{2;j,j'}g_{1;j,j'})}{2v_F\pi}\frac{2}{\Lambda} \\ &+ \frac{1}{4v_F\pi} \frac{\partial\left(\sum_{j"} g_{1;j,j"}g_{1;j',j"} - g_{2;j,j}g_{1;j,j'} - g_{1;j,j'}g_{2;j',j'}\right)}{\partial\Lambda} \ln\left[\frac{v_F^2\Lambda^2}{\bar{\omega}^2 + v_F^2\bar{p}^2}\right] \\ &+ \frac{\left(\sum_{j"} g_{1;j,j"}g_{1;j',j"} - g_{2;j,j}g_{1;j,j'} - g_{1;j,j'}g_{2;j',j'}\right)}{4v_F\pi}\frac{2}{\Lambda} \end{aligned} \tag{2.99}$$

At the second order in the interaction strengths these equations reduce to

$$\Lambda\frac{\partial g_{2;j,j'}}{\partial\Lambda} \approx \frac{(g_{1;j,j'})^2}{2v_F\pi}$$

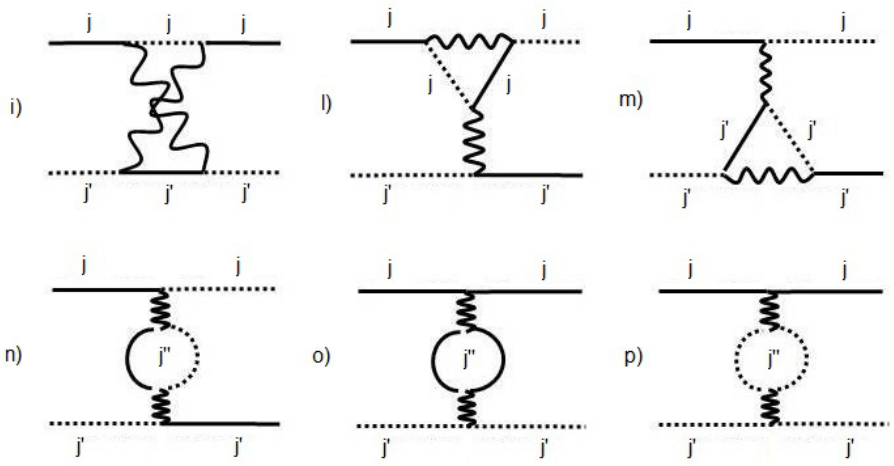

FIG. 11. Additional one-loop processes to the correction of the interaction constants. Diagrams i), l), m), n) involve an Umpklapp interaction and are only relevant at half filling. Diagrams o), p) are the not logarithmically divergent third channel diagrams.

$$\Lambda\frac{\partial g_{1;j,j'}}{\partial\Lambda}\approx\frac{2\left(g_{2;j,j'}g_{1;j,j'}\right)+\left(\sum_{j"}g_{1;j,j"}g_{1;j',j"}-g_{2;j,j}g_{1;j,j'}-g_{1;j,j'}g_{2;j',j'}\right)}{2v_F\pi}\tag{2.100}$$

Integrating from a given value D_0 such that $g_{1;j,j'}\left(D_0\right)=V_{j,j'}\left(2k_F\right)$ and $g_{2;j,j'}\left(D_0\right)=V_{j,j'}\left(0\right)$, to the energy scale E, we obtain the running coupling constants of the systems. Eqs. [2.100] are valid only if we assume not to be at half filling. Indeed, at half filling the Upklapp interaction term Eq. [2.56] cannot be discarded and contributes logarithmically to the renormalization of forward and backward scattering with the six zero sound diagrams i), l), m), n) of Fig. [11], all of them proportional to $\left(g_{3;j,j'}\right)^2$. Diagrams o) and p) of Fig. [11], called the third channel, are instead proportional to $g_{4;j,j'}g_{2:j,j'}$ and should always be taken into account due to the presence of the interaction term Eq. [2.53]. Luckily, it is easy to check that they give a non logarithmic correction and do not modify the RG equations for $g_{1;j,j'}$ and $g_{2;j,j'}$. In the particular cases of spinless electrons without inter-wire interaction the equations computed above reduces to

$$\begin{aligned}\Lambda\frac{\partial g_{j,2}}{\partial\Lambda}&=\frac{1}{2\pi v}(g_{j,1})^2\\ \Lambda\frac{\partial g_{j,1}}{\partial\Lambda}&=\frac{1}{2\pi v}(g_{j,1})^2\end{aligned}\tag{2.101}$$

From Eq. [2.101] follows that the linear combination $(g_{j,2}-g_{j,1})$, that appears also in Eq. [2.83] is scale invariant. It is not the case of spin-$\frac{1}{2}$ electrons, where the RG equations for the coupling constants reduce to

$$\begin{aligned}\Lambda\frac{\partial g_{j,2,\parallel}}{\partial\Lambda}&=\frac{1}{2\pi v}(g_{j,1,\parallel})^2\\ \Lambda\frac{\partial g_{j,2,\perp}}{\partial\Lambda}&=\frac{1}{2\pi v}(g_{j,1,\perp})^2\\ \Lambda\frac{\partial g_{j,1,\parallel}}{\partial\Lambda}&=\frac{1}{2\pi v}\left[(g_{j,1,\parallel})^2+(g_{j,1,\perp})^2\right]\\ \Lambda\frac{\partial g_{j,1,\perp}}{\partial\Lambda}&=\frac{1}{2\pi v}2g_{j,1,\perp}\left[g_{j,2,\perp}-g_{j,2,\parallel}+g_{j,1,\parallel}\right]\end{aligned}\tag{2.102}$$

II.4.3. Second order correction and sub leading contributions to the renormalization group equation for the scattering matrix

Solving the RG equation is equivalent in summing over an infinite class of diagrams in perturbation theory[78,80] proportional to $\left(g^{(i)}_{j,j'}\right)^n\left(\ln\frac{D}{D_0}\right)^n$. In the following we will show how the Matsubara formalism described in the last sec-

tions can be used to go beyond the leading-log correction including the sub leading terms of the form $\left(g^{(i)}_{j,j'}\right)^m \left(\ln \frac{D}{D_0}\right)^n$ with $m > n$ emerging starting from the second order correction. Being an example we will only consider forward scattering and assume that no Andreev-like processes are allowed at the boundary. For the second order of the Dyson's series we have

$$\delta G^{(2)}_{RL}(x,\tau,x') = +\frac{g^2}{2}\int_0^L dx_1 \int_0^\beta d\tau_1 \int_0^L dx_2 \int_0^\beta d\tau_2 \Big\langle T_\tau \psi_R(x,\tau) : \psi^\dagger_R(x_1,\tau_1)\psi_R(x_1,\tau_1) :: \psi^\dagger_L(x_1,\tau_1)\psi_L(x_1,\tau_1) : \\ : \psi^\dagger_R(x_2,\tau_2)\psi_R(x_2,\tau_2) :: \psi^\dagger_L(x_2,\tau_2)\psi_L(x_2,\tau_2) : \psi^\dagger_L(x',0)\Big\rangle \tag{2.103}$$

Using Wick's theorem, in space-frequency representation we have the following contributions

$$\begin{aligned}
\delta G^{(2)}_{RL}(x,x',i\omega) \approx \frac{g^2}{\beta^2}\int_0^L dx_1 \int_0^L dx_2 \sum_{\omega_1,\omega_2} \\
[&-G^{(0)}_{RR}(x,x_1,i\omega)\,G^{(0)}_{RL}(x_1,x',i\omega)\,G^{(0)}_{LR}(x_1,x_2,i\omega_1)\,G^{(0)}_{RL}(x_2,x_2,i\omega_2)\,G^{(0)}_{LL}(x_2,x_1,i\omega_1) \\
&-G^{(0)}_{RR}(x,x_1,i\omega)\,G^{(0)}_{RL}(x_1,x',i\omega)\,G^{(0)}_{LL}(x_1,x_2,i\omega_1)\,G^{(0)}_{RL}(x_2,x_1,i\omega_1)\,G^{(0)}_{LR}(x_2,x_2,i\omega_2) \\
&+G^{(0)}_{RR}(x,x_1,i\omega)\,G^{(0)}_{LL}(x_1,x',i\omega)\,G^{(0)}_{RR}(x_1,x_2,i\omega_1)\,G^{(0)}_{RL}(x_2,x_2,i\omega_2)\,G^{(0)}_{LL}(x_2,x_1,i\omega_1) \\
&+G^{(0)}_{RR}(x,x_1,i\omega)\,G^{(0)}_{LL}(x_1,x',i\omega)\,G^{(0)}_{RL}(x_1,x_2,i\omega_1)\,G^{(0)}_{RL}(x_2,x_1,i\omega_1)\,G^{(0)}_{LR}(x_2,x_2,i\omega_2) \\
&+G^{(0)}_{RR}(x,x_1,i\omega)\,G^{(0)}_{RL}(x_2,x',i\omega)\,G^{(0)}_{RL}(x_1,x_1,i\omega_1)\,G^{(0)}_{LL}(x_1,x_2,i\omega)\,G^{(0)}_{LR}(x_2,x_2,i\omega_2) \\
&-G^{(0)}_{RR}(x,x_1,i\omega)\,G^{(0)}_{RL}(x_2,x',i\omega)\,G^{(0)}_{RR}(x_1,x_2,i\omega-i\omega_1+i\omega_2)\,G^{(0)}_{LL}(x_1,x_2,i\omega_1)\,G^{(0)}_{LL}(x_2,x_1,i\omega_2) \\
&+G^{(0)}_{RR}(x,x_1,i\omega)\,G^{(0)}_{RL}(x_2,x',i\omega)\,G^{(0)}_{RL}(x_1,x_2,i\omega-i\omega_1+i\omega_2)\,G^{(0)}_{LR}(x_1,x_2,i\omega_1)\,G^{(0)}_{LL}(x_2,x_1,i\omega_2) \\
&+G^{(0)}_{RR}(x,x_1,i\omega)\,G^{(0)}_{LL}(x_2,x',i\omega)\,G^{(0)}_{RL}(x_1,x_1,i\omega_1)\,G^{(0)}_{LR}(x_1,x_2,i\omega)\,G^{(0)}_{RL}(x_2,x_2,i\omega_2) \\
&+G^{(0)}_{RR}(x,x_1,i\omega)\,G^{(0)}_{LL}(x_2,x',i\omega)\,G^{(0)}_{RR}(x_1,x_2,i\omega-i\omega_1+i\omega_2)\,G^{(0)}_{LL}(x_1,x_2,i\omega_1)\,G^{(0)}_{RL}(x_2,x_1,i\omega_2) \\
&-G^{(0)}_{RR}(x,x_1,i\omega)\,G^{(0)}_{LL}(x_2,x',i\omega)\,G^{(0)}_{RL}(x_1,x_2,i\omega-i\omega_1+i\omega_2)\,G^{(0)}_{LR}(x_1,x_2,i\omega_1)\,G^{(0)}_{RL}(x_2,x_1,i\omega_2) \\
&+G^{(0)}_{RL}(x,x_1,i\omega)\,G^{(0)}_{RL}(x_1,x',i\omega)\,G^{(0)}_{LR}(x_1,x_2,i\omega_1)\,G^{(0)}_{RL}(x_2,x_2,i\omega_2)\,G^{(0)}_{LR}(x_2,x_1,i\omega_1) \\
&+G^{(0)}_{RL}(x,x_1,i\omega)\,G^{(0)}_{RL}(x_1,x',i\omega)\,G^{(0)}_{LL}(x_1,x_2,i\omega_1)\,G^{(0)}_{RR}(x_2,x_1,i\omega_1)\,G^{(0)}_{LR}(x_2,x_2,i\omega_2) \\
&-G^{(0)}_{RL}(x,x_1,i\omega)\,G^{(0)}_{LL}(x_1,x',i\omega)\,G^{(0)}_{RR}(x_1,x_2,i\omega_1)\,G^{(0)}_{RL}(x_2,x_2,i\omega_2)\,G^{(0)}_{LR}(x_2,x_1,i\omega_1) \\
&-G^{(0)}_{RL}(x,x_1,i\omega)\,G^{(0)}_{LL}(x_1,x',i\omega)\,G^{(0)}_{RL}(x_1,x_2,i\omega_1)\,G^{(0)}_{RR}(x_2,x_1,i\omega_1)\,G^{(0)}_{LR}(x_2,x_2,i\omega_2) \\
&+G^{(0)}_{RL}(x,x_1,i\omega)\,G^{(0)}_{RL}(x_2,x',i\omega)\,G^{(0)}_{RR}(x_1,x_2,i\omega-i\omega_1+i\omega_2)\,G^{(0)}_{LL}(x_1,x_2,i\omega_1)\,G^{(0)}_{LR}(x_2,x_1,i\omega_2) \\
&+G^{(0)}_{RL}(x,x_1,i\omega)\,G^{(0)}_{RL}(x_2,x',i\omega)\,G^{(0)}_{RL}(x_1,x_2,i\omega)\,G^{(0)}_{LR}(x_1,x_1,i\omega_1)\,G^{(0)}_{LR}(x_2,x_2,i\omega_2) \\
&-G^{(0)}_{RL}(x,x_1,i\omega)\,G^{(0)}_{RL}(x_2,x',i\omega)\,G^{(0)}_{RL}(x_1,x_2,i\omega-i\omega_1+i\omega_2)\,G^{(0)}_{LR}(x_1,x_2,i\omega_1)\,G^{(0)}_{LR}(x_2,x_1,i\omega_2) \\
&+G^{(0)}_{RL}(x,x_1,i\omega)\,G^{(0)}_{LL}(x_2,x',i\omega)\,G^{(0)}_{RR}(x_1,x_2,i\omega)\,G^{(0)}_{LR}(x_1,x_1,i\omega_1)\,G^{(0)}_{RL}(x_2,x_2,i\omega_2) \\
&-G^{(0)}_{RL}(x,x_1,i\omega)\,G^{(0)}_{LL}(x_2,x',i\omega)\,G^{(0)}_{RR}(x_1,x_2,i\omega-i\omega_1+i\omega_2)\,G^{(0)}_{LL}(x_1,x_2,i\omega_1)\,G^{(0)}_{RR}(x_2,x_1,i\omega_2) \\
&+G^{(0)}_{RL}(x,x_1,i\omega)\,G^{(0)}_{LL}(x_2,x',i\omega)\,G^{(0)}_{RL}(x_1,x_2,i\omega-i\omega_1+i\omega_2)\,G^{(0)}_{LR}(x_1,x_2,i\omega_1)\,G^{(0)}_{RR}(x_2,x_1,i\omega_2)]
\end{aligned} \tag{2.104}$$

To each of this term correspond a real space diagrams like the ones depicted in Fig. [9] for the first order correction. We can identify leading-log terms, proportional to $g^2 \ln\left(\frac{D}{D_0}\right)^2$, corresponding to an iteration of the first order diagrams and that have already been taken into consideration at each order during the RG procedure. Furthermore we have non logarithmic contributions, that are small compared to the logarithmic divergent terms and finally sub leading terms proportional to $g^2 \ln\left(\frac{D}{D_0}\right)$ that are the ones we are searching for. A comparison with Eq. [2.71] give us the second order correction to the scattering matrix. The energy dependent case is computed in Appendix [II.9] while for the energy independent case, in presence of forward scattering only, the correction reduces to

$$\delta S^{(2)}_{j,j'} \approx \frac{\gamma}{16\pi^2 v^2}\frac{\delta D}{D}\Bigg[+g_{j,j'}g_{j,j'}S_{j,j'} - \sum_{a,a'} g_{j,j'}g_{a,a'}S_{j,a'}S_{a,j'}S^*_{a,a'} - \sum_{a,a'} g_{j,a'}g_{a,a'}S_{a,j'}S_{j,a'}S^*_{a,a'}$$
$$- \sum_{a,a'} g_{a,a'}g_{a,a'}S_{j,a'}S_{a,j'}S^*_{a,a'} + 2\sum_{a,a'}\sum_{b,b'} g_{a,a'}g_{b,b'}S_{j,a'}S_{b,j'}S_{a,b'}S^*_{a,a'}S^*_{b,b'}$$
$$+ \sum_{a,a'}\sum_{b,b'} g_{a,a'}g_{b,b'}S_{j,a'}S_{a,j'}S^*_{b,a'}S_{b,b'}S^*_{a,b'} - \sum_{a,a'} g_{a,a'}g_{a,j'}S_{j,a'}S^*_{a,a'}S_{a,j'}\Bigg]$$
$$+\frac{1}{16\pi^2 v^2}\frac{\delta D}{D}\Bigg[+\sum_{a,a'} g_{j,a'}g_{a,j'}S_{j,j'}S^*_{a,a'}S_{a,a'} - \sum_{a,a'}\sum_{b,b'} g_{a,a'}g_{b,b'}S_{j,a'}S_{b,j'}S_{a,b'}S^*_{b,a'}S^*_{a,b'}\Bigg] \tag{2.105}$$

(we have omitted the redundant electron/hole indices in the scattering matrix coefficients). In absence of inter-wire interaction (that is $g_{a,a'} = g_a\delta_{a,a'}$), we have

$$\delta S^{(2)}_{j,j'} \approx \frac{\gamma}{16\pi^2 v^2}\frac{\delta D}{D}\Bigg[+\delta_{j,j'}g_j g_j S_{j,j'} - \sum_a \delta_{j,j'}g_j g_a S_{j,a}S_{a,j'}S^*_{a,a} - g_j g_j S_{j,j'}S_{j,j}S^*_{j,j}$$
$$- \sum_a g_a g_a S_{j,a}S_{a,j'}S^*_{a,a} + 2\sum_{a,b} g_a g_b S_{j,a}S_{b,j'}S_{a,b}S^*_{a,a}S^*_{b,b}$$
$$+ \sum_{a,b} g_a g_b S_{j,a}S_{a,j'}S^*_{b,a}S_{b,b}S^*_{a,b} - g_{j'}g_{,j'}S_{j,j'}S^*_{j',,j'}S_{j',j'}\Bigg]$$
$$+\frac{1}{16\pi^2 v^2}\frac{\delta D}{D}\Bigg[+g_j g_{j'}S_{j,j'}S^*_{j',,j}S_{j',j} - \sum_{a,b} g_a g_b S_{j,a}S_{b,j'}S_{a,b}S^*_{b,a}S^*_{a,b}\Bigg] \tag{2.106}$$

If we assume the same interaction in all the wires (that is $g_a = g$), we are left with

$$\delta S^{(2)}_{j,j'} \approx \frac{\gamma g^2}{16\pi^2 v^2}\frac{\delta D}{D}\Bigg[\delta_{j,j'}S_{j,j'} - \sum_a \delta_{j,j'}S_{j,a}S_{a,j'}S^*_{a,a} - S_{j,j'}S_{j,j}S^*_{j,j} - S_{j,j'}S^*_{j',,j'}S_{j',j'}$$
$$- \sum_a S_{j,a}S_{a,j'}S^*_{a,a} + 2\sum_{a,b} S_{j,a}S_{b,j'}S_{a,b}S^*_{a,a}S^*_{b,b} + \sum_{a,b} S_{j,a}S_{a,j'}S^*_{b,a}S_{b,b}S^*_{a,b}\Bigg]$$
$$+\frac{g^2}{16\pi^2 v^2}\frac{\delta D}{D}\Bigg[S_{j,j'}S^*_{j',,j}S_{j',j} - \sum_{a,b} S_{j,a}S_{b,j'}S_{a,b}S^*_{b,a}S^*_{a,b}\Bigg] \tag{2.107}$$

It is easy to check that the second order correction to the scattering matrix reduces to zero in the following cases

$$\begin{aligned}
&2-wire\, S_N:\ S_{j,j}=1,\ S_{j,j+1}=0\\
&2-wire\, S_D:\ S_{j,j}=0,\ S_{j,j+1}=1\\
&3-wire\, S_N:\ S_{j,j}=1,\ S_{j,j\pm1}=0\\
&3-wire S_{\chi^\pm}: S_{j,j}=0,\ S_{j,j\mp1}=1,\ S_{j,j\pm1}=0\\
&3-wire\, S_M:\ S_{j,j}=-\frac{1}{3},\ S_{j,j\pm1}=\frac{2}{3}
\end{aligned} \tag{2.108}$$

that are the fixed point for two and three wires obtained through the first order correction but new non trivial and non universal fixed points depending from the interaction constants can emerge adding up first and second order contributions.

II.5. Luttinger liquid approach and splitting matrix implementation of the boundary conditions

In general, the effect of electron-electron interaction is threated using bosonization method. Bosonization is a mathematical procedure allowing for mapping a system of interacting Fermions in $1+1$ dimensions into a massless free Boson theory [see for example Ref. [13]]. In this section we introduce the procedure for a system of K spinless and spin-$\frac{1}{2}$ wires. The bulk Hamiltonian of Eq. [II.1] can be rewritten in bosonic coordinates introducing K bosonic fields $\Phi_j(x)$ described by the quadratic Hamiltonian

$$H_{Boso} = \frac{1}{2\pi}\sum_{j=1}^{K}\int_0^{\ell} dx \left[\frac{1}{v_j}\left(\partial_t \Phi_j(x)\right)^2 + v_j\left(\partial_x \Phi_j(x)\right)^2\right] \tag{2.109}$$

together with the corresponding dual fields $\Theta_j(x)$ related to the Φ-fields by the relation

$$\partial_t \Phi_j(x) = v_j \partial_x \Phi_j(x) \tag{2.110}$$

and satisfying the commutation relation

$$\left[\Phi_j(x), \partial_y \Theta_i(y)\right] = 2\pi i \delta(x-y)\,\delta_{j,i} \tag{2.111}$$

such that the bosonic Hamiltonian can also be written as

$$H_0 = \frac{1}{2\pi}\sum_{j=1}^{K} v_j \int_0^{\ell} dx \left[\left(\partial_x \Phi_j(x)\right)^2 + \left(\partial_x \Theta_j(x)\right)^2\right] \tag{2.112}$$

The relation between the fermionic and the bosonic fields is given by

$$\psi_{R/L,j}(x) = \eta_{R/L,j} e^{i\Phi_{R/L,j}(x)} \tag{2.113}$$

with the chiral bosonic fields defined as

$$\Phi_{R/L,j} = \Phi_j \pm \Theta_j \tag{2.114}$$

and $\eta_{R/L,j}$ real fermion Klein factors that ensure the right anticommutation relation between the fermionic operators in different wires. The total current and density operators

$$\begin{aligned} J_j &= J_{R,j} - J_{L,j} = v_j\left[:\psi^{\dagger}_{R,j}(x)\,\psi_{R,j}(x): - :\psi^{\dagger}_{L,j}(x)\,\psi_{L,j}(x):\right] \\ \rho &= \rho_R + \rho_L = \left[:\psi^{\dagger}_{R,j}(x)\,\psi_{R,j}(x): + :\psi^{\dagger}_{L,j}(x)\,\psi_{L,j}(x):\right] \end{aligned} \tag{2.115}$$

can be expressed in terms of the bosonic chiral fields as

$$\begin{aligned} J_{R/L,j} &= \pm v_j\,(1/2\pi)\,\partial_x \Phi_{R/L,j}(x) \\ \rho_{R/L,j} &= \pm\,(1/2\pi)\,\partial_x \Phi_{R/L,j}(x) \end{aligned} \tag{2.116}$$

In presence of an interaction given by Eqs. [2.53, 2.54, 2.55], with only inter-wire terms, that is $g_{k;j,j'} = \delta_{j,j'} g_{k;j}$, expressing the chiral fermionic fields in terms of the bosonic ones, we can observe that the term proportional to $g_{4;j}$ has the form

$$H_{g_4;j} = \sum_{X=L,R}\frac{g_{4;j}}{2}\int_0^{L} dx \left[\left(\rho_R\right)^2 + \left(\rho_L\right)^2\right]$$

$$= \sum_{X=L,R} \frac{g_{4;j}}{8\pi^2} \int_0^L dx \left[\left(\partial_x \Phi_j(x)\right)^2 + \left(\partial_x \Theta_j(x)\right)^2 \right] \tag{2.117}$$

and a comparison with the bulk Hamiltonian tell us that the only effect produced by it is a finite renormalization of the Fermi velocity

$$v_j^* = v_j + \frac{g_{4;j}}{4\pi} \tag{2.118}$$

The other two interaction terms instead mix the left and right sector as

$$\begin{aligned} H_{g_2+g_1} &= (g_{2;j} - g_{1;j}) \int_0^L dx \rho_R \rho_L \\ &= \frac{(g_{2;j} - g_{1;j})}{4\pi^2} \int_0^L dx \left(\partial_x \Phi_{R,j}(x)\right) \left(\partial_x \Phi_{L,j}(x)\right) \end{aligned} \tag{2.119}$$

Luckily, the full Hamiltonian is still quadratic in the bosonic Θ and Φ fields and it is given by

$$H = \frac{1}{2\pi} \sum_{j=1}^{K} u_j \int_0^L dx \left[g_j \left(\partial_x \Phi_j(x)\right)^2 + \frac{1}{g_j} \left(\partial_x \Theta_j(x)\right)^2 \right] \tag{2.120}$$

with the definitions

$$\begin{aligned} u_j g_j &= v_j \left(1 - \frac{g_{1;j} - g_{2;j}}{2\pi v_j}\right) \\ \frac{u_j}{g_j} &= v_j \left(1 + \frac{g_{1;j} - g_{2;j}}{2\pi v_j}\right) \end{aligned} \tag{2.121}$$

where $g_j = 1$ represent the non interacting case. Now it is easy to check that, in terms of the rescaled fields

$$\begin{aligned} \tilde{\Phi}_j(x) &= \sqrt{g_j} \Phi_j(x) \\ \tilde{\Theta}_j(x) &= \frac{1}{\sqrt{g_j}} \Theta_j(x) \end{aligned} \tag{2.122}$$

the non interacting Hamiltonian and the interacting one have the same form. At this point it is useful to define a new set of chiral fields

$$\tilde{\Phi}_{R/L,j} = \tilde{\Phi}_j \pm \tilde{\Theta}_j \tag{2.123}$$

that are related to the non interacting chiral fields by the Bogoliubov transformation

$$\begin{aligned} \Phi_{R,j} &= \frac{1}{2\sqrt{g_j}} \left\{ (1+g_j) \tilde{\Phi}_{R,j} + (1-g_j) \tilde{\Phi}_{L,j} \right\} \\ \Phi_{L,j} &= \frac{1}{2\sqrt{g_j}} \left\{ (1+g_j) \tilde{\Phi}_{L,j} + (1-g_j) \tilde{\Phi}_{R,j} \right\} \end{aligned} \tag{2.124}$$

and satisfying

$$\left[\tilde{\Phi}_{R/L,i}(x,t), \tilde{\Phi}_{R/L,j}(x',t) \right] = \pm i\pi sg(x-x') \delta_{ij} \tag{2.125}$$

The same procedure defined above for a spinless system can be extended in presence of spin-$\frac{1}{2}$ electrons. A junction of K spin-$\frac{1}{2}$ wires is described introducing $2K$ bosonic fields. The doubled number of fields, compared to the spinless case, is needed to take into account that each wire has now two channels ($\uparrow$ and $\downarrow$ channel). Accordingly with the spinless case, we label the bosonic fields as $\Phi_{j,\sigma}(x)$ and the dual fields as $\Theta_{j,\sigma}(x)$. In analogy with Eqs. [2.114, 2.116] we introduce the chiral spin-dependent currents and densities

$$\begin{aligned} J_{R/L,j,\sigma} &= \pm v_j \left(1/2\pi\right) \partial_x \Phi_{R/L,j,\sigma}(x) \\ \rho_{R/L,j,\sigma} &= \pm \left(1/2\pi\right) \partial_x \Phi_{R/L,j,\sigma}(x) \end{aligned} \tag{2.126}$$

However, it is more appropriate to work in terms of total (charge) current and density and spin current and density, defined as

$$\begin{aligned} J_{R/L,j,c(s)} &= J_{R/L,j,\uparrow} \pm J_{R/L,j,\downarrow} \\ \rho_{R/L,j,c(s)} &= \rho_{R/L,j,\uparrow} \pm \rho_{R/L,j,\downarrow} \end{aligned} \tag{2.127}$$

These quantities suggest to define the bosonic fields

$$\begin{aligned} \Phi_{R/L,j,c} &= \frac{1}{\sqrt{2}} \left(\Phi_{R/L,j,\uparrow} + \Phi_{R/L,j,\downarrow}\right) = \Phi_{j,c} \pm \Theta_{j,c} \\ \Phi_{R/L,j,s} &= \frac{1}{\sqrt{2}} \left(\Phi_{R/L,j,\uparrow} - \Phi_{R/L,j,\downarrow}\right) = \Phi_{j,s} \pm \Theta_{j,s} \end{aligned} \tag{2.128}$$

These linear combinations of the spin-dependent bosonic fields describe charge and spin plasmons respectively. In absence of interactions they are valid fundamental excitations like the original spin-$\uparrow$, spin-$\downarrow$ excitations (the same is true for any new excitation obtained through a canonical rotation of the spin-dependent bosonic fields). However, in presence of an intra-wire interaction, they correctly describe the spin-charge separation effect[81]. Indeed, due to the inter-channel interaction terms that allows electrons with different spin to interact each other inside each wire, they represent the correct degrees of freedom to use to map the interacting fermions Hamiltonian into an Hamiltonian for free bosons. Following Eq. [2.113], it is a straightforward to write the relation between fermionic and bosonic fields as

$$\begin{aligned} \psi_{R,\sigma,j}(x) &= \eta_{R,\sigma,j} e^{\frac{i}{2}\left[\Phi_{j,c}+\Theta_{j,c}+\sigma(\Phi_{j,s}+\Theta_{j,s})\right]} \\ \psi_{L,\sigma,j}(x) &= \eta_{L,\sigma,j} e^{\frac{i}{2}\left[\Phi_{j,c}-\Theta_{j,c}+\sigma(\Phi_{j,s}-\Theta_{j,s})\right]} \end{aligned} \tag{2.129}$$

Making use of these rules the bulk Hamiltonian for free fermions is mapped into a sum of two contribution. A term that rule over the charge sector

$$H_{0;B;c} = \frac{1}{4\pi} \int_0^L dx \sum_{j=1}^{K} \left[\frac{1}{v}(\partial_t \Phi_{c,j})^2 + v(\partial_x \Phi_{c,j})^2\right] \tag{2.130}$$

and a term that describe the spin sector

$$H_{0;B;s} = \frac{1}{4\pi} \int_0^L dx \sum_{j=1}^{K} \left[\frac{1}{v}(\partial_t \Phi_{s,j})^2 + v(\partial_x \Phi_{s,j})^2\right] \tag{2.131}$$

All the previous transformations lead to contributions to the system Hamiltonian that are quadratic in the bosonic fields. The interaction Hamiltonian shares this property, once one has set to zero the all the terms $\propto g_{j,1,\perp}$, in which case, on rewriting H_I in Eq. [2.10] in terms of the bosonic fields, one obtains $H_I = H_{\mathrm{int},1} + H_{\mathrm{int},2}$, with

$$H_{\mathrm{int},1} = \sum_{j=1}^{K} \frac{g_{j,1,\parallel} - g_{j,2,\parallel}}{16\pi^2} \int_0^L dx \left\{-(\partial_x \Theta_{j,c}(x))^2 - (\partial_x \Theta_{j,s}(x))^2 + (\partial_x \Phi_{j,c}(x))^2 + (\partial_x \Phi_{j,s}(x))^2\right\}$$

$$H_{\rm int,2} = \sum_{j=1}^{K} \frac{g_{j,2,\perp}}{16\pi^2} \int_0^L dx \, \{(\partial_x \Theta_{j,c}(x))^2 + (\partial_x \Phi_{j,s}(x))^2 - (\partial_x \Theta_{j,s}(x))^2 - (\partial_x \Phi_{j,c}(x))^2\} \tag{2.132}$$

On adding the terms in Eqs. [2.132] to the noninteracting Hamiltonian for the charge sector (Eq. [2.130]) plus the one for the spin sector (Eq. [2.131]), one eventually obtains a bosonic Hamiltonian H that is still quadratic, although with pertinently renormalized coefficients, given by

$$\begin{aligned} H = & \frac{1}{4\pi} \sum_{j=1}^{K} u_{j,c} \int_0^L dx \, \left\{ g_{j,c} (\partial_x \Phi_{j,c}(x))^2 + \frac{1}{g_{j,c}} (\partial_x \Theta_{j,c}(x))^2 \right\} \\ & + \frac{1}{4\pi} \sum_{j=1}^{K} u_{j,s} \int_0^L dx \, \left\{ g_{j,s} (\partial_x \Phi_{j,s}(x))^2 + \frac{1}{g_{j,s}} (\partial_x \Theta_{j,s}(x))^2 \right\} \end{aligned} \tag{2.133}$$

with

$$\begin{aligned} u_{j,c} g_{j,c} &= v \left[1 + \frac{g_{j,1,\parallel} - g_{j,2,\parallel} - g_{j,2,\perp}}{4\pi v} \right] \\ \frac{u_{j,c}}{g_{j,c}} &= v \left[1 - \frac{g_{j,1,\parallel} - g_{j,2,\parallel} - g_{j,2,\perp}}{4\pi v} \right] \\ u_{j,s} g_{j,s} &= v \left[1 + \frac{g_{j,1,\parallel} - g_{j,2,\parallel} + g_{j,2,\perp}}{4\pi v} \right] \\ \frac{u_{j,s}}{g_{j,s}} &= v \left[1 - \frac{g_{j,1,\parallel} - g_{j,2,\parallel} + g_{j,2,\perp}}{4\pi v} \right] \end{aligned} \tag{2.134}$$

When $g_{j,1,\perp} \neq 0$, one can employ the identities

$$\begin{aligned} \psi^\dagger_{R,\sigma,j}(x) \psi_{R,\bar{\sigma},j}(x) &\to e^{-i\sigma[\Phi_{j,s}(x) + \Theta_{j,s}(x)]} \\ \psi^\dagger_{L,\sigma,j}(x) \psi_{L,\bar{\sigma},j}(x) &\to e^{-i\sigma[\Phi_{j,s}(x) - \Theta_{j,s}(x)]} \end{aligned} \tag{2.135}$$

to express the total additional contribution to $H_{\rm int}$, $H_{\rm int,3}$, as

$$H_{\rm int,3} \sim \int_0^L dx \, \sum_{j=1}^{K} W_j \, \cos[2\Phi_{j,s}(x)] \tag{2.136}$$

with $W_j \propto g_{j,1,\perp}$. To lowest order, the renormalization group equation for W_j is

$$\frac{dW_j}{d\ell} = \left[2 - \frac{2}{g_{j,s}} \right] W_j \tag{2.137}$$

which tells us that the nonlinear interaction term $\propto g_{j,1,\perp}$ is irrelevant as long as $g_{j,s} < 1$ and, accordingly, even if $g_{j,1,\perp}$ has not been fine-tuned to 0.

Until now, we focused on the bulk, not considering the presence of the junction. This implies that we are working with double degree of freedom, keeping both Φ_j and Θ_j fields, in the spinless case, or both $\Phi_{j,c(s)}$ and $\Theta_{j,c(s)}$ fields, in the spinful case. To remove the redundant degree of freedom we have to impose the boundary conditions at $x = 0$. The standard approach, Refs. [23 and 29], consists in implementing the boundary conditions in terms of a splitting matrix that connect incoming and outgoing currents at the junction. In the spinless case it corresponds to set

$$J_{R,i} = \mathbb{M}_{ij} J_{L,j} \tag{2.138}$$

Making use of Eq. [2.116] we can switch this relation with a relation that connect incoming and outgoing field through

$$\Phi_{R,i} = \mathbb{M}_{ij}\Phi_{L,j} + C_i \tag{2.139}$$

In the following, we will discard the constant vector $\overrightarrow{C}$ as it play no role into the physical quantities like the conductance, the tunnel density of states or the correlation functions. This boundary condition can also be written for the Bogoliobov transformed chiral fields

$$\tilde{\Phi}_{R,i} = \tilde{\mathbb{M}}_{ij}\tilde{\Phi}_{L,j} + \tilde{C}_i \tag{2.140}$$

Assuming the same interaction in each wire, the matrices $\mathbb{M}$ and $\tilde{\mathbb{M}}$ are related by

$$\tilde{\mathbb{M}} = \frac{(1+g)\mathbb{M} - (1-g)\mathbb{I}}{(1+g)\mathbb{I} - (1-g)\mathbb{M}} \tag{2.141}$$

Let us note that if $\mathbb{M}$ is an involutory matrix, $\mathbb{M}^2 = \mathbb{I}$, then

$$\begin{aligned}
\tilde{\mathbb{M}} &= \frac{(1+g)\mathbb{M} - (1-g)\mathbb{I}}{(1+g)\mathbb{I} - (1-g)\mathbb{M}} \\
&= \frac{(1+g)\mathbb{M} - (1-g)\mathbb{M}\mathbb{M}}{(1+g)\mathbb{I} - (1-g)\mathbb{M}} \\
&= \frac{(1+g)\mathbb{I} - (1-g)\mathbb{M}}{(1+g)\mathbb{I} - (1-g)\mathbb{M}}\mathbb{M} \\
&= \mathbb{M}
\end{aligned} \tag{2.142}$$

In order for the incoming and outgoing fields to satisfy the right bosonic commutation relations, the splitting matrix must be real and belong to the orthogonal set

$$O(K) \equiv \left\{ \mathbb{M}_{K\times K} : \sum_k \mathbb{M}_{kj}\mathbb{M}_{ki} = \delta_{j,i} \ \wedge \ \sum_k \mathbb{M}_{jk}\mathbb{M}_{ik} = \delta_{j,i} \right\} \tag{2.143}$$

and, for a normal junction, must satisfy the current conservation law, $\sum_i J_i = 0$, that forces the splitting matrix to satisfy the following constraint

$$\sum_j \mathbb{M}_{ij} = 1 \tag{2.144}$$

that correspond to require that the splitting matrix belongs to the generalized doubly stochastic set, $D^{gen}_{stoc}(K)$ where the condition $\mathbb{M}_{ij} \in R^+$ is relaxed. Likewise, for a perfect superconducting junction, where the total electron density, $\sum_i \rho_i = 0$, must be zero at the junction, the current conservation constraint is replaced by

$$\sum_j \mathbb{M}_{ij} = -1 \tag{2.145}$$

It follows that, in the case of a superconducting junction, the splitting matrices that satisfy orthogonality and zero density at the boundary are simply related to the normal case by

$$\mathbb{M}_1^{sup} = -\mathbb{M}_1, \quad \mathbb{M}_2^{sup} = -\mathbb{M}_2 \tag{2.146}$$

A comparison with the scattering matrix approach described before, show us that the intersection between the boundary condition that can be studied through the bosonization approach ($\mathbb{M} \in O(K) \cap D^{gen}_{stoc}(K)$) and the boundary condition treated with the fermionic approach ($\mathbb{M}^{\mathbb{S}} \in U_{stot}(K)$) is given by the permutation set $P_{erm}(K)$ that contains

the only fixed points that can be studied simultaneously by fermionic and abelian bosonization approach. For $K = 2$ the only matrices that satisfy the orthogonal and current conservation constrain are given by

$$\mathbb{M}_1 = \begin{pmatrix} 1 & 0 \\ 0 & 1 \end{pmatrix}, \quad \mathbb{M}_2 = \begin{pmatrix} 0 & 1 \\ 1 & 0 \end{pmatrix} \tag{2.147}$$

They are the same obtained through the fermionic renormalization group approach and represent a disconnected or fully healed wire. For $K = 3$, it is possible to show that orthogonality and current conservation implies that the splitting matrix rows and columns are given by a cyclic permutation of three real number between $-1/3$ and 1 such that their sum and the sum of their squares is one. For a three wire junction we have two classes of splitting matrices, that satisfy such constraints, and both can be parametrized by a single parameter θ. We have:

$$\mathbb{M}_1 = \begin{pmatrix} a & b & c \\ c & a & b \\ b & c & a \end{pmatrix}, \quad \mathbb{M}_2 = \begin{pmatrix} b & a & c \\ a & c & b \\ c & b & a \end{pmatrix} \tag{2.148}$$

where:

$$a = \left[1 + 2cos\theta\right]/3 \tag{2.149}$$

$$b = \left[1 - cos\theta + \sqrt{3}sin\theta\right]/3 \tag{2.150}$$

$$c = \left[1 - cos\theta - \sqrt{3}sin\theta\right]/3 \tag{2.151}$$

In terms of the Bogoliubov transformed matrices:

$$\tilde{\mathbb{M}}_1 = \begin{pmatrix} \tilde{a} & \tilde{b} & \tilde{c} \\ \tilde{c} & \tilde{a} & \tilde{b} \\ \tilde{b} & \tilde{c} & \tilde{a} \end{pmatrix}, \quad \tilde{\mathbb{M}}_2 = \mathbb{M}_2 \tag{2.152}$$

due to the fact that $\mathbb{M}_2^2 = \mathbb{I}$ and where:

$$\tilde{a} = \frac{\left[3g^2 - 1 + (3g^2 + 1)cos\theta\right]}{3\left[1 + g^2 + (g^2 - 1)cos\theta\right]} \tag{2.153}$$

$$\tilde{b} = \frac{2\left[1 - cos\theta + \sqrt{3}gsin\theta\right]}{3\left[1 + g^2 + (g^2 - 1)cos\theta\right]} \tag{2.154}$$

$$\tilde{c} = \frac{2\left[1 - cos\theta - \sqrt{3}gsin\theta\right]}{3\left[1 + g^2 + (g^2 - 1)cos\theta\right]} \tag{2.155}$$

The $\mathbb{M}_1$ class ($det[\mathbb{M}_1] = 1$) represent the $\mathbb{Z}_3$ symmetric fixed points, while the $\mathbb{M}_2$ class ($det[\mathbb{M}_2] = -1$) breaks the $\mathbb{Z}_3$ symmetry. The $\mathbb{M}_1$ subclass with $b = c$ preserve the time reversal symmetry. For given values of θ we recover the permutation matrix depicted in Fig. [4], in particular

$$\begin{aligned} &\mathbb{M}_1\left(\theta = 0\right) = \mathbb{M}_N, \quad \mathbb{M}_1\left(\theta = \frac{2\pi}{3}\right) = \mathbb{M}_{\chi^-}, \quad \mathbb{M}_1\left(\theta = \frac{4\pi}{3}\right) = \mathbb{M}_{\chi^+}, \\ &\mathbb{M}_2\left(\theta = 0\right) = \mathbb{M}_{N_1}, \quad \mathbb{M}_2\left(\theta = \frac{4\pi}{3}\right) = \mathbb{M}_{N_2}, \quad \mathbb{M}_2\left(\theta = \frac{2\pi}{3}\right) = \mathbb{M}_{N_3} \end{aligned} \tag{2.156}$$

An interesting splitting matrix, not belonging to the permutation set, is obtained from the $\mathbb{M}_1$ class for $\theta = \pi$. It correspond to

$$\mathbb{M}_1\left(\theta = \pi\right) = \begin{pmatrix} -\frac{1}{3} & \frac{2}{3} & \frac{2}{3} \\ \frac{2}{3} & -\frac{1}{3} & \frac{2}{3} \\ \frac{2}{3} & \frac{2}{3} & -\frac{1}{3} \end{pmatrix} \tag{2.157}$$

and its coefficients can not be expressed as the modulus square of the coefficients of an unitary matrix. For this reason, the properties of this boundary condition, that is associated with the presence of multi particle Andreev-like boundary interactions at the junction[29], can not be studied within the standard FRG formalism. However, in the next Chapter we will develop an approach that, making use of both fermionic and bosonic coordinates, will allow to describe this boundary condition in terms of appropriate fermionic degrees of freedom. On the other side the unistochastic matrix

$$\mathbb{M} = \begin{pmatrix} \frac{1}{9} & \frac{4}{9} & \frac{4}{9} \\ \frac{4}{9} & \frac{1}{9} & \frac{4}{9} \\ \frac{4}{9} & \frac{4}{9} & \frac{1}{9} \end{pmatrix} \tag{2.158}$$

obtained from Eq. [2.82], is not orthogonal and represent an example of fixed point that can be studied with the FRG approach but is not accessible by abelian bosonization.

For $K > 3$, it is not straightaway to parametrize the splitting matrices set in terms of a finite amount of parameters such that the orthogonal and current (or charge) conservation low is ensured. However it can be done performing an appropriate change of basis. For $K = 3$, starting from the chiral bosonic fields, let us define the center of mass and relative fields through the change of basis

$$\begin{pmatrix} \tilde{\Phi}_{R/L,0} \\ \tilde{\Phi}_{R/L,I} \\ \tilde{\Phi}_{R/L,II} \end{pmatrix} = \begin{pmatrix} \frac{1}{\sqrt{3}} & \frac{1}{\sqrt{3}} & \frac{1}{\sqrt{3}} \\ \frac{1}{\sqrt{2}} & -\frac{1}{\sqrt{2}} & 0 \\ \frac{1}{\sqrt{6}} & \frac{1}{\sqrt{6}} & -\frac{2}{\sqrt{6}} \end{pmatrix} \begin{pmatrix} \tilde{\Phi}_{R/L,1} \\ \tilde{\Phi}_{R/L,2} \\ \tilde{\Phi}_{R/L,3} \end{pmatrix} = \tilde{\mathbb{B}} \begin{pmatrix} \tilde{\Phi}_{R/L,1} \\ \tilde{\Phi}_{R/L,2} \\ \tilde{\Phi}_{R/L,3} \end{pmatrix} \tag{2.159}$$

that means

$$\begin{pmatrix} \tilde{\Phi}_{R/L,1} \\ \tilde{\Phi}_{R/L,2} \\ \tilde{\Phi}_{R/L,3} \end{pmatrix} = \begin{pmatrix} \frac{1}{\sqrt{3}} & \frac{1}{\sqrt{2}} & \frac{1}{\sqrt{6}} \\ \frac{1}{\sqrt{3}} & -\frac{1}{\sqrt{2}} & \frac{1}{\sqrt{6}} \\ \frac{1}{\sqrt{3}} & 0 & -\frac{2}{\sqrt{6}} \end{pmatrix} \begin{pmatrix} \tilde{\Phi}_{R/L,0} \\ \tilde{\Phi}_{R/L,I} \\ \tilde{\Phi}_{R/L,II} \end{pmatrix} = \tilde{\mathbb{B}}^T \begin{pmatrix} \tilde{\Phi}_{R/L,0} \\ \tilde{\Phi}_{R/L,I} \\ \tilde{\Phi}_{R/L,II} \end{pmatrix} \tag{2.160}$$

The boundary conditions for the rotated basis is given by the transformation

$$\begin{pmatrix} \tilde{\Phi}_{R,0} \\ \tilde{\Phi}_{R,I} \\ \tilde{\Phi}_{R,II} \end{pmatrix} = \tilde{\mathbb{B}}\tilde{\mathbb{M}}\tilde{\mathbb{B}}^T \begin{pmatrix} \tilde{\Phi}_{L,0} \\ \tilde{\Phi}_{L,I} \\ \tilde{\Phi}_{L,II} \end{pmatrix} = \tilde{\mathbb{R}} \begin{pmatrix} \tilde{\Phi}_{L,0} \\ \tilde{\Phi}_{L,I} \\ \tilde{\Phi}_{L,II} \end{pmatrix} \tag{2.161}$$

The splitting matrix for the interacting rotated basis is then given by

$$\tilde{\mathbb{R}} = \tilde{\mathbb{B}}\tilde{\mathbb{M}}\tilde{\mathbb{B}}^T = \begin{cases} \begin{pmatrix} 1 & 0 & 0 \\ 0 & \frac{g^2-1+(1+g^2)cos\theta}{1+g^2+(g^2-1)cos\theta} & \frac{2gsin\theta}{1+g^2+(g^2-1)cos\theta} \\ 0 & -\frac{2gsin\theta}{1+g^2+(g^2-1)cos\theta} & \frac{g^2-1+(1+g^2)cos\theta}{1+g^2+(g^2-1)cos\theta} \end{pmatrix} = \begin{pmatrix} 1 & 0 \\ 0 & \tilde{\mathbb{R}}_{1,2x2} \end{pmatrix} & \tilde{\mathbb{M}}_1 \; class \\ \begin{pmatrix} 1 & 0 & 0 \\ 0 & \frac{1}{2}(cos\theta - \sqrt{3}sin\theta) & \frac{1}{2}(\sqrt{3}cos\theta + sin\theta) \\ 0 & \frac{1}{2}(\sqrt{3}cos\theta + sin\theta) & -\frac{1}{2}(cos\theta - \sqrt{3}sin\theta) \end{pmatrix} = \begin{pmatrix} 1 & 0 \\ 0 & \tilde{\mathbb{R}}_{2,2x2} \end{pmatrix} & \tilde{\mathbb{M}}_2 \; class \end{cases} \tag{2.162}$$

that reduces to

$$\mathbb{R} = \mathbb{B}\mathbb{M}\mathbb{B}^T = \begin{cases} \begin{pmatrix} 1 & 0 & 0 \\ 0 & cos\theta & -sin\theta \\ 0 & -sin\theta & cos\theta \end{pmatrix} = \begin{pmatrix} 1 & 0 \\ 0 & \mathbb{R}_{1,2x2} \end{pmatrix} & \mathbb{M}_1 \; class \\ \begin{pmatrix} 1 & 0 & 0 \\ 0 & \frac{1}{2}(cos\theta - \sqrt{3}sin\theta) & \frac{1}{2}(\sqrt{3}cos\theta + sin\theta) \\ 0 & \frac{1}{2}(\sqrt{3}cos\theta + sin\theta) & -\frac{1}{2}(cos\theta - \sqrt{3}sin\theta) \end{pmatrix} = \begin{pmatrix} 1 & 0 \\ 0 & \mathbb{R}_{2,2x2} \end{pmatrix} & \mathbb{M}_2 \; class \end{cases} \tag{2.163}$$

for the non interacting case. The first line and column simply reflect the fact that current is conserved (Neumann boundary condition on Φ_0, Dirichlet boundary condition on Θ_0 that is pinned). The superconducting junction splitting matrices are instead simply given again by minus these matrices (Neumann boundary condition on Θ_0, Dirichlet boundary condition on Φ_0 that is pinned).The 2×2 submatrices $\tilde{\mathbb{R}}$ are rotation matrices for the $\tilde{\mathbb{M}}_1$ class ($\tilde{\mathbb{R}}_{1,2x2} = \tilde{\mathbb{R}}^T_{1,2x2} = \mathbb{I}$, $det[\tilde{\mathbb{R}}_{1,2x2}] = 1$) and improper rotation matrices for the $\tilde{\mathbb{M}}_2$ class ($\tilde{\mathbb{R}}_{2,2x2} = \tilde{\mathbb{R}}^T_{2,2x2} = \mathbb{I}$, $det[\tilde{\mathbb{R}}_{2,2x2}] = -1$). It is easy to check that this connection between splitting matrices of order K and the proper and improper rotations of order $K-1$

$$\tilde{\mathbb{M}} = \tilde{\mathbb{B}}^T \tilde{\mathbb{R}} \tilde{\mathbb{B}}$$

is true at any order and give us an easy way to parametrize the splitting matrices provided a parametrization for the rotation matrices. A similar procedure is applied for a junction of spinful wires. Assuming that both total spin and charge are conserved at each scattering event at the junction, the boundary conditions ca be separately imposed to charge and spin bosonic fields. This is realized introducing two splitting matrices $\mathbb{M}_{c(s)}$

$$\Phi_{R,i;c(s)} = \mathbb{M}_{c(s);i,j} \Phi_{L,j;c(s)} + C_{i,c(s)} \tag{2.164}$$

The condition $\sum_i \mathbb{M}_{c(s);i,j} = \sum_j \mathbb{M}_{c(s);i,j} = 1$ becomes a conservation low for the charge and spin currents. Until now we have described how to implement boundary conditions within the abelian bosonization approach. The next step to build the flow diagrams of a physical system consist in the stability analysis of each boundary condition. This can be performed through the delayed evaluation of boundary condition (DEBC), developed by Ref. [82] and applied to junctions of two and three quantum wires in Refs. [29 and 30]. The basic idea behind the DEBC method is to delay the choice of the boundary condition until after we write the operators corresponding to the (multi)particle tunneling processes at the junction. The stable boundary condition is then imposed on the bosonic fields a posteriori, taking into account the scaling dimensions of the tunneling operators given the different choices of boundary conditions. In the next Chapter we will give an example of the method applying it to a junction of three spinful wires.

II.6. Appendix A: Matsubara imaginary-time Green's function technique

The properties of quantum mechanical systems are described by expectation values that, in general, can be written in terms of Green's functions. The method of Green's function is particularly effective for problem solved through perturbation theory, like the one we will treat in the following. A retarded Green's function, in terms of which physical quantities can be expressed, has the form

$$G^R_{A,B}(x,t;x',t') = i\Theta(t-t') \left\langle [A(x,t), B(x',t')]_{\pm} \right\rangle \tag{2.165}$$

where the anti-commutator, $[\,,\,]_+ = \{\,,\,\}$, is for fermions and the commutator, $[\,,\,]_- = [\,,\,]$, is for bosons operators. The operator are expressed in the Heisenberg representation as

$$A(x,t) = e^{iHt} A(x) e^{-iHt} \tag{2.166}$$

The average $\langle \cdots \rangle$ represent a thermal and quantum average given by

$$\langle \cdots \rangle = \frac{1}{Z} \sum_n \langle n | \cdots | n \rangle e^{-\beta E_n} \tag{2.167}$$

where $|n\rangle$ and E_n is a set of eigenstates and eigenvalues of the Hamiltonian, $\beta = 1/K_B T$ and

$$Z = \sum_n e^{-\beta E_n} \tag{2.168}$$

is the partition function. When the interaction Hamiltonian is time independent, the Green's function is invariant under time translation and then it does not depend on t and t' separately but only be their difference $t - t'$; in

this case is useful to move back and forth the space-time domain and the space-frequency domain through a Fourier transformation

$$G^R_{A,B}(x,x',t-t') = \frac{1}{2\pi}\int_{-\infty}^{+\infty} d\omega e^{-i\omega(t-t')} G^R_{A,B}(x,x',\omega)$$
$$G^R_{A,B}(x,x',\omega) = \int_{-\infty}^{+\infty} d(t-t')\, e^{i\omega(t-t')} G^R_{A,B}(x,x',t-t') \tag{2.169}$$

In order to simplify th computation it is convenient to make advantage of the Matsubara imaginary time formalism. We define the imaginary-time Matsubara Green's function as

$$G_{A,B}(x,\tau;x',\tau') = \langle T_\tau A(x,\tau), B(x',\tau')\rangle \tag{2.170}$$

where T_τ is the imaginary-time ordering operator

$$T_\tau A(x,\tau), B(x',\tau') = \begin{cases} A(x,\tau), B(x',\tau') & \tau > \tau' \\ \mp A(x,\tau), B(x',\tau') & \tau < \tau' \end{cases}$$

(with minus sign for fermions and plus sign for bosons) and τ and τ' real quantities $\in [0,\beta]$. In this formalism the time evolution is described by

$$A(x,\tau) = e^{\tau H} A(x) e^{-\tau H}$$
$$A^\dagger(x,\tau) = e^{\tau H} A^\dagger(x) e^{-\tau H} \tag{2.171}$$

Like the retarded real-time Green's function, the Matsubara Green's function, for a time independent Hamiltonian, depends only by the time difference

$$G_{A,B}(x,\tau;x',\tau') = G_{A,B}(x,x',\tau-\tau') \tag{2.172}$$

Furthermore it satisfy the anti-periodic (for fermions) or periodic (for bosons) condition of the form

$$G_{A,B}(x,x',\tau-\tau') = \mp G_{A,B}(x,x',\tau-\tau'+\beta) \tag{2.173}$$

This property ensure us that the Matsubara Green's function has period 2β and can be Fourier expanded on the interval $[-\beta,\beta]$

$$G_{A,B}(x,x',\tau-\tau') = \frac{1}{\beta}\sum_{n\in Z} e^{-i\Omega_n(\tau-\tau')} G_{A,B}(x,x',i\Omega_n)$$
$$G_{A,B}(x,x',i\Omega_n) = \frac{1}{2}\int_{-\beta}^{+\beta} d(\tau-\tau')\, e^{i\Omega_n(\tau-\tau')} G_{A,B}(x,x',\tau-\tau') \tag{2.174}$$

with $\Omega_n = n\pi/\beta$. Due to the (anti)-periodic condition we can write

$$G_{A,B}(x,x',i\Omega_n) = \frac{1}{2}\left[\int_{-\beta}^{0} d\omega e^{i\Omega_n(\tau-\tau')} G_{A,B}(x,x',\tau-\tau') + \int_{0}^{\beta} d\omega e^{i\Omega_n(\tau-\tau')} G_{A,B}(x,x',\tau-\tau')\right]$$

$$= \frac{\left[\mp\left(-1\right)^{n}+1\right]}{2}\int_{0}^{\beta} d\omega e^{i\Omega_{n}\left(\tau-\tau'\right)}G_{A,B}\left(x,x',\tau-\tau'\right)$$

where we used $e^{-i\Omega_n\beta}=(-1)^n$. For fermions and bosons respectively only odd and even values of n give non zero contribution to the Fourier series, so we can write the Fourier expansion as

$$G_{A,B}\left(x,x',\tau-\tau'\right)=\frac{1}{\beta}\sum_{\omega_n}e^{-i\omega_n\left(\tau-\tau'\right)}G_{A,B}\left(x,x',i\Omega_n\right)$$
$$G_{A,B}\left(x,x',i\omega_n\right)=\int_{0}^{\beta} d\left(\tau-\tau'\right)e^{i\omega_n\left(\tau-\tau'\right)}G_{A,B}\left(x,x',\tau-\tau'\right) \tag{2.175}$$

where we have defined the so called Matsubara frequencies

$$\omega_n=\begin{cases}\frac{(2n+1)\pi}{\beta} & fermions\\ \frac{2n\pi}{\beta} & bosons\end{cases} \tag{2.176}$$

It is worth to note that, in the zero temperature limit, $\beta\to\infty$, the discrete Matsubara frequencies become continuous.

The key ingredient of the Matsubara imaginary-time formalism is that it is possible to relate the retarded Green's functions and the Matsubara Green's functions through the analytic continuation procedure that consist in the replacing $i\omega_n\to\omega+i\eta$. Indeed, in the space-frequency domain, resorting to the Lehmann representation, we can write (respectively for fermions and bosons)

$$G_{A,B}\left(x,x',i\omega_n\right)=-\frac{1}{Z}\sum_{n,n'}\frac{\left\langle n\left|A\right|n'\right\rangle\left\langle n'\left|B\right|n\right\rangle}{i\omega_n+E_n-E_{n'}}\left(e^{-\beta E_n}-\left(\mp\right)e^{-\beta E_{n'}}\right)$$
$$G^{R}_{A,B}\left(x,x',\omega\right)=-\frac{1}{Z}\sum_{n,n'}\frac{\left\langle n\left|A\right|n'\right\rangle\left\langle n'\left|B\right|n\right\rangle}{\omega+E_n-E_{n'}+i\eta}\left(e^{-\beta E_n}-\left(\mp\right)e^{-\beta E_{n'}}\right) \tag{2.177}$$

from which it directly follows

$$G^{R}_{A,B}\left(x,x',\omega\right)=-iG_{A,B}\left(x,x',i\omega_n\to\omega+i\eta\right) \tag{2.178}$$

II.7. Appendix B: Normal and anomalous Green's functions

To compute the Green's function correction, the starting point are the left and right going fields of Eq. [2.3] that in the Schroedinger representation are

$$\psi_{R,j}\left(x\right)=\frac{1}{\sqrt{l}}\sum_{k}a_{R,j}\left(k\right)e^{ikx}$$
$$\psi_{L,j}\left(x\right)=\frac{1}{\sqrt{l}}\sum_{k}a_{L,j}\left(k\right)e^{-ikx} \tag{2.179}$$

with the right and left going modes related to each other through the scattering matrix S of Eq. [2.31]

$$a_{R,j}\left(k\right)=\sum_{j'=1}^{K}\left[S^{e,e}_{j,j'}\left(\epsilon_k\right)a_{L,j'}\left(k\right)+S^{e,h}_{j,j'}\left(\epsilon_k\right)a^{\dagger}_{L,j'}\left(-k\right)\right] \tag{2.180}$$

Annihilation and creating operators satisfy

$$\left\langle a_{L,j}^{\dagger}(k)\, a_{L,j'}(k')\right\rangle = \delta_{j,j'}\delta_{k,k'} f(\epsilon_k)$$
$$\left\langle a_{L,j}(k)\, a_{L,j'}^{\dagger}(k')\right\rangle = \delta_{j,j'}\delta_{k,k'}\left[1-f(\epsilon_k)\right] = \delta_{j,j'}\delta_{k,k'} f(-\epsilon) \tag{2.181}$$

where $f(\epsilon_k)$ is the fermi distribution function. Propagating at imaginary time τ, we obtain

$$\psi_{R,j}(x,\tau) = \frac{1}{\sqrt{l}}\sum_k a_{R,j}(k)\, e^{ikx-\epsilon_k\tau}$$
$$\psi_{L,j}(x,\tau) = \frac{1}{\sqrt{l}}\sum_k a_{L,j}(k)\, e^{-ikx-\epsilon_k\tau} \tag{2.182}$$

and

$$\psi_{R,j}^{\dagger}(x,\tau) = \frac{1}{\sqrt{l}}\sum_k a_{R,j}^{\dagger}(k)\, e^{-ikx+\epsilon_k\tau}$$
$$\psi_{L,j}^{\dagger}(x,\tau) = \frac{1}{\sqrt{l}}\sum_k a_{L,j}^{\dagger}(k)\, e^{+ikx+\epsilon_k\tau} \tag{2.183}$$

for the complex conjugate fields., with $\epsilon_k = vk$. From Eqs. (2.180, 2.181) we can compute the following expectation values involving different chiralities

$$\left\langle a_{L,j}^{\dagger}(k)\, a_{R,j'}(k')\right\rangle = \sum_i \left\langle a_{L,j}^{\dagger}(k)\left[S_{j',i}^{e,e}(\epsilon_k')\, a_{L,i}(k') + S_{j',i}^{e,h}(\epsilon_k')\, a_{L,i}^{\dagger}(-k')\right]\right\rangle$$
$$\left\langle a_{L,j}^{\dagger}(k)\left[S_{j',j}^{e,e}(\epsilon_k')\, a_{L,j}(k')\right]\right\rangle = S_{j',j}^{e,e}(\epsilon_k)\,\delta_{k,k'} f(\epsilon_k)$$
$$\left\langle a_{R,j}(k)\, a_{L,j'}^{\dagger}(k')\right\rangle = \sum_i \left\langle \left[S_{j,i}^{e,e}(\epsilon_k)\, a_{L,i}(k) + S_{j,i}^{e,h}(\epsilon_k)\, a_{L,i}^{\dagger}(-k)\right] a_{L,j'}^{\dagger}(k')\right\rangle$$
$$\left\langle \left[S_{j,j'}^{e,e}(\epsilon_k)\, a_{L,j'}(k)\right] a_{L,j'}^{\dagger}(k')\right\rangle = S_{j,j'}^{e,e}(\epsilon_k)\,\delta_{k,k'}\left[1-f(\epsilon_k)\right]$$
$$\left\langle a_{R,j}^{\dagger}(k)\, a_{L,j'}(k')\right\rangle = \sum_i \left\langle \left[S_{j,i}^{e,e*}(\epsilon_k)\, a_{L,i}^{\dagger}(k) + S_{j,i}^{e,h*}(\epsilon_k)\, a_{L,i}(-k)\right] a_{L,j'}(k')\right\rangle$$
$$\left\langle \left[S_{j,j'}^{e,e*}(\epsilon_k)\, a_{L,j'}^{\dagger}(k)\right] a_{L,j'}(k')\right\rangle = S_{j,j'}^{e,e*}(\epsilon_k)\,\delta_{k,k'} f(\epsilon_k)$$
$$\left\langle a_{L,j}(k)\, a_{R,j'}^{\dagger}(k')\right\rangle = \sum_i \left\langle a_{L,j}(k)\left[S_{j',i}^{e,e*}(\epsilon_k')\, a_{L,i}^{\dagger}(k') + S_{j',i}^{e,h*}(\epsilon_k')\, a_{L,i}(-k')\right]\right\rangle$$
$$\left\langle a_{L,j}(k)\left[S_{j',j}^{e,e*}(\epsilon_k')\, a_{L,j}^{\dagger}(k')\right]\right\rangle = S_{j',j}^{e,e*}(\epsilon_k)\,\delta_{k,k'}\left[1-f(\epsilon_k)\right]$$
$$\langle a_{L,j}(k)\, a_{R,j'}(k')\rangle = \sum_i \left\langle a_{L,j}(k)\left[S_{j',i}^{e,e}(\epsilon_k')\, a_{L,i}(k') + S_{j',i}^{e,h}(\epsilon_k')\, a_{L,i}^{\dagger}(-k')\right]\right\rangle$$
$$\left\langle a_{L,j}(k)\left[S_{j',j}^{e,h}(\epsilon_k')\, a_{L,j}^{\dagger}(-k')\right]\right\rangle = S_{j',j}^{e,h}(-\epsilon_k)\,\delta_{k,-k'}\left[1-f(\epsilon_k)\right]$$
$$\langle a_{R,j}(k)\, a_{L,j'}(k')\rangle = \sum_i \left\langle \left[S_{j,i}^{e,e}(\epsilon_k)\, a_{L,i}(k) + S_{j,i}^{e,h}(\epsilon_k)\, a_{L,i}^{\dagger}(-k)\right] a_{L,j'}(k')\right\rangle$$
$$\left\langle \left[S_{j,j'}^{e,h}(\epsilon_k)\, a_{L,j'}^{\dagger}(-k)\right] a_{L,j'}(k')\right\rangle = S_{j,j'}^{e,h}(\epsilon_k)\,\delta_{k,-k'} f(-\epsilon_k)$$
$$\left\langle a_{L,j}^{\dagger}(k)\, a_{R,j'}^{\dagger}(k')\right\rangle = \sum_i \left\langle a_{L,j}^{\dagger}(k)\left[S_{j',i}^{e,e*}(\epsilon_k')\, a_{L,i}^{\dagger}(k') + S_{j',i}^{e,h*}(\epsilon_k')\, a_{L,i}(-k')\right]\right\rangle$$
$$\left\langle a_{L,j}^{\dagger}(k)\left[S_{j',j}^{e,h*}(\epsilon_k')\, a_{L,j}(-k')\right]\right\rangle = S_{j',j}^{e,h*}(-\epsilon_k)\,\delta_{k,-k'} f(\epsilon_k)$$
$$\left\langle a_{R,j}^{\dagger}(k)\, a_{L,j'}^{\dagger}(k')\right\rangle = \sum_i \left\langle \left[S_{j,i}^{e,e*}(\epsilon_k)\, a_{L,i}^{\dagger}(k) + S_{j,i}^{e,h*}(\epsilon_k)\, a_{L,i}(-k)\right] a_{L,j'}^{\dagger}(k')\right\rangle$$

$$\left\langle \left[S^{e,h*}_{j,j'}\left(\epsilon_k\right) a_{L,j'}\left(-k\right)\right] a^{\dagger}_{L,j'}\left(k'\right)\right\rangle = S^{e,h*}_{j,j'}\left(\epsilon_k\right)\delta_{k,-k'}\left[1-f\left(-\epsilon_k\right)\right] \tag{2.184}$$

that will help us to compute the single particle Green's functions. Let us not that, due the presence of Andreev-like processes a the boundary, we have to compute not only the ordinary Green's function involving a creation and annihilation operator but also anomalous Green's functions that describe the annihilation or creation of two particles. In particular we have to compute

$$\begin{aligned}
G_{(X,j);(X',j')}\left(x,\tau;x',\tau'\right) &= \Theta\left(\tau-\tau'\right)\left\langle \psi_{X,j}\left(x,\tau\right)\psi^{\dagger}_{X',j'}\left(x',\tau'\right)\right\rangle - \Theta\left(\tau'-\tau\right)\left\langle \psi^{\dagger}_{X',j'}\left(x',\tau'\right)\psi_{X,j}\left(x,\tau\right)\right\rangle \\
F_{(X,j);(X',j')}\left(x,\tau;x',\tau'\right) &= \Theta\left(\tau-\tau'\right)\left\langle \psi_{X,j}\left(x,\tau\right)\psi_{X',j'}\left(x',\tau'\right)\right\rangle - \Theta\left(\tau'-\tau\right)\left\langle \psi_{X',j'}\left(x',\tau'\right)\psi_{X,j}\left(x,\tau\right)\right\rangle \\
\tilde{F}_{(X,j);(X',j')}\left(x,\tau;x',\tau'\right) &= \Theta\left(\tau-\tau'\right)\left\langle \psi^{\dagger}_{X,j}\left(x,\tau\right)\psi^{\dagger}_{X',j'}\left(x',\tau'\right)\right\rangle - \Theta\left(\tau'-\tau\right)\left\langle \psi^{\dagger}_{X',j'}\left(x',\tau'\right)\psi^{\dagger}_{X,j}\left(x,\tau\right)\right\rangle
\end{aligned} \tag{2.185}$$

In the Matsubara frequency-real space representation, using Eq. [2.175] (that holds also for the anomalous Green's functions), and

$$\left[e^{(i\omega_n-\epsilon)\beta}-1\right]\left[1-f\left(\epsilon\right)\right]=-1 \tag{2.186}$$

we have

$$\begin{aligned}
G_{(L,j);(L,j')}\left(x,x',i\omega_n\right) &= \frac{1}{l}\sum_k \frac{e^{-ik\left(x-x'\right)}}{\left(\epsilon_k-i\omega_n\right)}\delta_{j,j'} \\
G_{(R,j);(R,j')}\left(x,x',i\omega_n\right) &= \frac{1}{l}\sum_k \frac{e^{+ik\left(x-x'\right)}}{\left(\epsilon_k-i\omega_n\right)}\delta_{j,j'} \\
G_{(L,j);(R,j')}\left(x,x',i\omega_n\right) &= \frac{1}{l}\sum_k \frac{e^{-ik\left(x+x'\right)}}{\left(\epsilon_k-i\omega_n\right)}S^{e,e*}_{j',j}\left(\epsilon_k\right) \\
G_{(R,j);(L,j')}\left(x,x',i\omega_n\right) &= \frac{1}{l}\sum_k \frac{e^{+ik\left(x+x'\right)}}{\left(\epsilon_k-i\omega_n\right)}S^{e,e}_{j,j'}\left(\epsilon_k\right) \\
F_{(L,j);(L,j')}\left(x,x',i\omega_n\right) &= 0 \\
F_{(R,j);(R,j')}\left(x,x',i\omega_n\right) &= 0 \\
F_{(L,j);(R,j')}\left(x,x',i\omega_n\right) &= \frac{1}{l}\sum_k \frac{e^{-ik\left(x+x'\right)}}{\left(\epsilon_k-i\omega_n\right)}S^{e,h}_{j',j}\left(-\epsilon_k\right) \\
F_{(R,j);(L,j')}\left(x,x',i\omega_n\right) &= \frac{1}{l}\sum_k \frac{e^{+ik\left(x+x'\right)}}{\left(\epsilon_k-i\omega_n\right)}S^{e,h}_{j,j'}\left(\epsilon_k\right) \\
\tilde{F}_{(L,j);(L,j')}\left(x,x',i\omega_n\right) &= 0 \\
\tilde{F}_{(R,j);(R,j')}\left(x,x',i\omega_n\right) &= 0 \\
\tilde{F}_{(L,j);(R,j')}\left(x,x',i\omega_n\right) &= -\frac{1}{l}\sum_k \frac{e^{+ik\left(x+x'\right)}}{\left(\epsilon_k+i\omega_n\right)}S^{e,h*}_{j',j}\left(-\epsilon_k\right) \\
\tilde{F}_{(R,j);(L,j')}\left(x,x',i\omega_n\right) &= -\frac{1}{l}\sum_k \frac{e^{-ik\left(x+x'\right)}}{\left(\epsilon_k+i\omega_n\right)}S^{e,h*}_{j,j'}\left(\epsilon_k\right)
\end{aligned} \tag{2.187}$$

These are the normal and anomalous Green's functions in the space-frequency space used in the main text.

To simplify the notation we define the following quantities

$$\begin{aligned}
\varphi_{(L,j);(L,j')}\left(x,x',k\right) &= \delta_{j,j'}e^{-ik\left(x-x'\right)} \\
\varphi_{(R,j);(R,j')}\left(x,x',k\right) &= \delta_{j,j'}e^{+ik\left(x-x'\right)}
\end{aligned}$$

$$\varphi_{(L,j);(R,j')}(x,x',k) = S^{e,e*}_{j',j}(\epsilon_k)\, e^{-ik\left(x+x'\right)}$$
$$\varphi_{(R,j);(L,j')}(x,x',k) = S^{e,e}_{j,j'}(\epsilon_k)\, e^{+ik\left(x+x'\right)} \tag{2.188}$$

II.8. Appendix C: Linear response theory approach to the conductance tensor

In this appendix, we review the linear response theory approach to the derivation of the conductance tensor for a junction of quantum wires. Let $\mathcal{W}_j$ be the j-th wire connected to the junction ($j = 1, \ldots, K$). In order to implement linear response theory, we imagine to connect $\mathcal{W}_j$ to a reservoir $\mathcal{R}_j$, which can either be characterized by the same parameters as the wire to which it is connected, or not (a typical situation corresponds to $\mathcal{W}_j$ being an interacting one-dimensional quantum wire, described as a single Luttinger liquid, connected to a Fermi liquid reservoir[83]). For the sake of simplicity, we assume that the parameters characterizing both the wires and the reservoirs are all independent of j. In order to induce a current flow across the junction, we assume that each reservoir is characterized by an equilibrium distribution with chemical potential $\mu_j = eV_j$. This induces electric fields $\{\mathcal{E}_j(t)\}$ distributed in the various branches of the junction, which we account for by introducing a set of uniform vector potentials $\mathcal{A}_j(t)$, one for each wire, such that $\mathcal{E}_j(t) = -\partial_t \mathcal{A}_j(t)$. Letting $J_j(x)$ be the current operator for particles in wire-j and letting each wire to be of length ℓ, we may define the "source" Hamiltonian $H_{\rm Source}(t)$, describing the coupling to the applied electric fields, given by

$$H_{\rm Source}(t) = \sum_{j=1}^{K} \int_{\delta}^{\ell} dx \mathcal{A}_j(t) J_j(x) \tag{2.189}$$

Let us, now, denote with $J_{j;I}(x,t)$, $H_{{\rm Source};I}(t)$ the operators taken in the interaction representation with respect to the Hamiltonian without the source term. Within linear response theory, the current evaluated at point x of wire-j is therefore given by

$$I_j(x,t) = i \sum_{j'=1}^{K} \int_{-\infty}^{\infty} dt' \int_{\delta}^{\ell} dx' \mathcal{D}_{j,j'}(x,t;x',t') \mathcal{A}_{j'}(t') \tag{2.190}$$

with

$$\mathcal{D}_{j,j'}(x,t;x',t') = \theta(t-t') \langle [J_{j;I}(x,t), J_{j';I}(x',t')] \rangle \tag{2.191}$$

Equation [2.190] does generically apply to any situation, whether the wires are interacting, or not, and whether one uses a fermionic, or a bosonic representation for the Hamiltonian of the junction. An important remark, however, is that, in any case, the current must be consistently probed outside of the region across which the electric fields are applied, that is, in Eq. [2.190] one has always to assume that $x > \ell$. Another important formula is the Fourier-space counterpart of Eq. [2.190], that is

$$I_j(x,\omega) = -\frac{1}{\omega} \sum_{j'=1}^{K} \int_{\delta}^{\ell} dx' \mathcal{D}_{j,j'}(x,x';\omega) \mathcal{E}_{j'}(\omega) \tag{2.192}$$

with

$$I_j(x,\omega) = \int dt e^{i\omega t} I_j(x,t)$$
$$\mathcal{E}_{j'}(\omega) = \int dt e^{i\omega t} \mathcal{E}_{j'}(t)$$
$$\mathcal{D}_{j,j'}(x,x';\omega) = \int dt e^{i\omega t} \mathcal{D}_{j,j'}(x,t;x',0) \tag{2.193}$$

For a normal wire, the current operator in branch j is given by

$$J_j = ev \left\{ : \psi^{\dagger}_{R,j}(x) \psi_{R,j}(x) : - : \psi^{\dagger}_{L,j}(x) \psi_{L,j}(x) : \right\} \tag{2.194}$$

An important observation to make at this point is that, on connecting the wires to the reservoirs, we basically assume a continuity condition for the current operator at the interface. From the microscopical point of view, this appears

to be the "macroscopic" counterpart of the "smooth" crossover in the interaction strength in real space discussed in the microscopic lattice model considered in Ref. [41]. It would be also interesting to work out a macroscopic field-theoretical Hamiltonian describing a "sharp" interface in the microscopic model, but this goes beyond of the scope of this work. As specified above, in the following we assume current continuity at the interface, that is, a smooth crossover in the bulk interaction strength.

II.8.1. Conductance tensor in the non interacting case

In this section we compute the conductance tensor for a junction of quantum wires in absence of interaction. In this case, the $\mathcal{D}$-tensor, using imaginary time formalism, is given by

$$\begin{aligned}
&\mathcal{D}^{I}_{(0);j,j'}(x,x';i\Omega_n)\\
&=\frac{e^2v^2}{\beta}\sum_{\omega}\{-G^{(0)}_{(L,j);(L,j')}(x,x';i\omega+i\Omega_n)G^{(0)}_{(L,j');(L,j)}(x',x;i\omega)-G^{(0)}_{(R,j);(R,j')}(x,x';i\omega+i\Omega_n)G^{(0)}_{(R,j');(R,j)}(x',x;i\omega)\\
&+G^{(0)}_{(L,j);(R,j')}(x,x';i\omega+i\Omega_n)G^{(0)}_{(R,j');(L,j)}(x',x;i\omega)+G^{(0)}_{(R,j);(L,j')}(x,x';i\omega+i\Omega_n)G^{(0)}_{(L,j');(R,j)}(x',x;i\omega)\}
\end{aligned}\tag{2.195}$$

Making use of the Green's function of Appendix [II.7], for the unperturbed result on summing over ω, we obtain

$$\begin{aligned}
&\mathcal{D}^{I}_{(0);j,j'}(x,x';i\Omega_n)\\
&=\frac{e^2v^2}{\ell^2}\sum_{k_1,k_2}\sum_{X,X'=L,R}\frac{[f(\epsilon_1)f(-\epsilon_2)-f(\epsilon_2)f(-\epsilon_1)]}{i\Omega_n-\epsilon_1+\epsilon_2}\varphi_{(X,j);(X',j')}(x,x';k_1)\varphi_{(X',j');(X,j)}(x',x;k_2)
\end{aligned}\tag{2.196}$$

with the φ functions defined in Eqs. [4.38]. Therefore, returning to real times with the analytic continuation, we have

$$\begin{aligned}
&\mathcal{D}^{R}_{(0);j,j'}(x,x';\Omega)\\
&=-i\frac{e^2v^2}{\ell^2}\sum_{k_1,k_2}\sum_{X,X'=L,R}\frac{[f(\epsilon_1)f(-\epsilon_2)-f(\epsilon_2)f(-\epsilon_1)]}{\Omega+i\eta-\epsilon_1+\epsilon_2}\varphi_{(X,j);(X',j')}(x,x';k_1)\varphi_{(X',j');(X,j)}(x',x;k_2)\\
&\to -i\frac{e^2}{4\pi^2}\int d\epsilon_1 d\epsilon_2\sum_{X,X'=L,R}\frac{[f(\epsilon_1)f(-\epsilon_2)-f(\epsilon_2)f(-\epsilon_1)]}{\Omega+i\eta-\epsilon_1+\epsilon_2}\varphi_{(X,j);(X',j')}\left(x,x';\frac{\epsilon_1}{v}\right)\varphi_{(X',j');(X,j)}\left(x',x;\frac{\epsilon_2}{v}\right)
\end{aligned}\tag{2.197}$$

We are always assuming $x>x'$. Also, it easy to check that all the contributions from poles of the Fermi functions cancel with each other. Therefore, on pertinently closing the integration path in $d\epsilon_1$, we eventually obtain

$$\begin{aligned}
\mathcal{D}^{R}_{(0);j,j'}(x,x';\Omega)=-\frac{e^2}{2\pi}\int d\epsilon[f(\epsilon+\Omega)f(-\epsilon)-f(\epsilon)f(-\epsilon-\Omega)]\Bigg\{&\varphi_{(R,j);(R,j')}\left(x,x';\frac{\epsilon+\Omega}{v}\right)\varphi_{(R,j');(R,j)}\left(x',x;\frac{\epsilon}{v}\right)\\
-\varphi_{(R,j);(L,j')}\left(x,x';\frac{\epsilon+\Omega}{v}\right)&\varphi_{(L,j');(R,j)}\left(x',x;\frac{\epsilon}{v}\right)\Bigg\}
\end{aligned}\tag{2.198}$$

As $\Omega\to 0$, one obtains

$$\mathcal{D}^{R}_{(0);j,j'}(x,x';\Omega)\to\frac{e^2}{2\pi}\int d\epsilon\frac{\beta\Omega}{4\cosh^2\left(\frac{\beta\epsilon}{2}\right)}\{-\delta_{j,j'}+|S^{e,e}_{j,j'}(\epsilon)|^2\}\tag{2.199}$$

Therefore, the dc conductance tensor is given by

$$G_{j,j'}=\frac{\partial I_j}{\partial V_{j'}}=\frac{e^2}{2\pi}\int d\epsilon\frac{\beta}{4\cosh^2\left(\frac{\beta\epsilon}{2}\right)}\{\delta_{j,j'}-|S^{e,e}_{j,j'}(\epsilon)|^2\}\tag{2.200}$$

Eq. [2.192] remains valid also in the spinful case. The only difference is that the current and $\mathcal{D}$-tensor assume an explicit spin dependence. The $T\to 0$ limit dc-conductance tensor, assuming no spin-flip processes are allowed at the junction, becomes

$$G_{(j,\sigma);(j',\sigma')}=\frac{\partial I_{j,\sigma}}{\partial V_{j',\sigma}}=\delta_{\sigma,\sigma'}\frac{e^2}{2\pi}\left\{-|S^{e,e}_{j,j'}|^2+\delta_{j,j'}\right\}\tag{2.201}$$

It is then useful to introduce the charge- and the spin-conductance tensors G_c, G_s, respectively defined as

$$G_{c;(j,j')} = \sum_{\sigma,\sigma'} G_{(j,\sigma);(j',\sigma')} \quad , \quad G_{s;(j,j')} = \sum_{\sigma,\sigma'} \sigma\sigma' G_{(j,\sigma);(j',\sigma')} \tag{2.202}$$

which, from Eq. [2.201], implies

$$G_{c;(j,j')} = G_{s;(j,j')} = \frac{e^2}{\pi} \left\{ -|S^{e,e}_{j,j'}|^2 + \delta_{j,j'} \right\} \tag{2.203}$$

When a weak bulk interaction is added to the junction Hamiltonian we still use Eq. [2.200] in the spinless case and Eq. [2.203] for the charge- and the spin-conductance tensors by just replacing the "bare" S-matrix elements with the running ones, $S_{j,j'}(\Lambda)$ as discussed in Sec. [II.4].

II.9. Appendix D: First and second order scattering matrix corrections

II.9.1. First order correction

Let us start computing the first order of the Dyson's series for the normal Green's function

$$\delta G^{(1)}_{RL}(x,\tau,x') = +g \int_0^L dx_1 \int_0^\beta d\tau_1 \left\langle T_\tau \psi_R(x,\tau) : \psi^\dagger_R(x_1,\tau_1)\psi_R(x_1,\tau_1) :: \psi^\dagger_L(x_1,\tau_1)\psi_L(x_1,\tau_1) : \psi^\dagger_L(x',0) \right\rangle \tag{2.204}$$

Using Wick's theorem and considering that, due to the normal ordering within each chiral density operator, $G^{(0)}_{XX}(x_i,\tau_i,x_i,\tau_i) = 0$. We have

$$\begin{aligned}
&\delta G^{(1)}_{RL}(x,\tau,x') = +g \int_0^L dx_1 \int_0^\beta d\tau_1 \, [\\
&+G^{(0)}_{RR}(x,\tau,x_1,\tau_1) G^{(0)}_{RL}(x_1,\tau_1,x_1,\tau_1) G^{(0)}_{LL}(x_1,\tau_1,x',0) \\
&+G^{(0)}_{RL}(x,\tau,x_1,\tau_1) G^{(0)}_{LR}(x_1,\tau_1,x_1,\tau_1) G^{(0)}_{RL}(x_1,\tau_1,x',0) \\
&+G^{(0)}_{RL}(x,\tau,x_1,\tau_1) F^{(0)}_{RL}(x_1,\tau_1,x_1,\tau_1) \tilde{F}^{(0)}_{RL}(x_1,\tau_1,x',0) \\
&+F^{(0)}_{RL}(x,\tau,x_1,\tau_1) \tilde{F}^{(0)}_{RL}(x_1,\tau_1,x_1,\tau_1) G^{(0)}_{RL}(x_1,\tau_1,x',0) \\
&-F^{(0)}_{RL}(x,\tau,x_1,\tau_1) G^{(0)}_{RL}(x_1,\tau_1,x_1,\tau_1) \tilde{F}^{(0)}_{RL}(x_1,\tau_1,x',0)]
\end{aligned} \tag{2.205}$$

In Fourier space, integrating into the time variables to remove two over three ω_i sums, we obtain

$$\begin{aligned}
&\delta G^{(1)}_{RL}(x,x',i\omega) \approx +\frac{g}{\beta} \int_0^L dx_1 \sum_{\omega'} \, [\\
&+G^{(0)}_{RR}(x,x_1,i\omega) G^{(0)}_{RL}(x_1,x_1,i\omega') G^{(0)}_{LL}(x_1,x',i\omega) \\
&+G^{(0)}_{RL}(x,x_1,i\omega) G^{(0)}_{LR}(x_1,x_1,i\omega') G^{(0)}_{RL}(x_1,x',i\omega) \\
&+G^{(0)}_{RL}(x,x_1,i\omega) F^{(0)}_{RL}(x_1,x_1,i\omega') \tilde{F}^{(0)}_{RL}(x_1,x',i\omega) \\
&+F^{(0)}_{RL}(x,x_1,i\omega) \tilde{F}^{(0)}_{RL}(x_1,x_1,i\omega') G^{(0)}_{RL}(x_1,x',i\omega) \\
&-F^{(0)}_{RL}(x,x_1,i\omega) G^{(0)}_{RL}(x_1,x_1,i\omega') \tilde{F}^{(0)}_{RL}(x_1,x',i\omega)]
\end{aligned} \tag{2.206}$$

Substituting the full form of the Green's functions

$$\delta G^{(1)}_{RL}\left(x,x',i\omega\right)\approx+\frac{g}{\beta\left(2\pi\right)^{3}v^{3}}\int_{0}^{L}dx_{1}\sum_{\omega'}\int\prod_{i=1}^{3}d\epsilon_{i}\,[$$
$$+\frac{e^{+i\frac{\epsilon_1}{v}\left(x-x_1\right)}}{\left(\epsilon_1-i\omega\right)}\frac{e^{+i2\frac{\epsilon_2}{v}x_1}}{\left(\epsilon_2-i\omega'\right)}S^{e,e}\left(\epsilon_2\right)\frac{e^{-i\frac{\epsilon_3}{v}\left(x_1-x'\right)}}{\left(\epsilon_3-i\omega\right)}$$
$$+\frac{e^{+i\frac{\epsilon_1}{v}\left(x+x_1\right)}}{\left(\epsilon_1-i\omega\right)}S^{e,e}\left(\epsilon_1\right)\frac{e^{-i2\frac{\epsilon_2}{v}x_1}}{\left(\epsilon_2-i\omega'\right)}S^{e,e*}\left(\epsilon_2\right)\frac{e^{+i\frac{\epsilon_3}{v}\left(x_1+x'\right)}}{\left(\epsilon_3-i\omega\right)}S^{e,e}\left(\epsilon_3\right)$$
$$-\frac{e^{+i\frac{\epsilon_1}{v}\left(x+x_1\right)}}{\left(\epsilon_1-i\omega\right)}S^{e,e}\left(\epsilon_1\right)\frac{e^{+i2\frac{\epsilon_2}{v}x_1}}{\left(\epsilon_2-i\omega'\right)}S^{e,h}\left(\epsilon_2\right)\frac{e^{-i\frac{\epsilon_3}{v}\left(x_1+x'\right)}}{\left(\epsilon_3+i\omega\right)}S^{e,h*}\left(\epsilon_3\right)$$
$$-\frac{e^{+i\frac{\epsilon_1}{v}\left(x+x_1\right)}}{\left(\epsilon_1-i\omega\right)}S^{e,h}\left(\epsilon_1\right)\frac{e^{+i2\frac{\epsilon_2}{v}x_1}}{\left(\epsilon_2+i\omega'\right)}S^{e,h*}\left(-\epsilon_2\right)\frac{e^{+i\frac{\epsilon_3}{v}\left(x_1+x'\right)}}{\left(\epsilon_3-i\omega\right)}S^{e,e}\left(\epsilon_3\right)$$
$$+\frac{e^{+i\frac{\epsilon_1}{v}\left(x+x_1\right)}}{\left(\epsilon_1-i\omega\right)}S^{e,h}\left(\epsilon_1\right)\frac{e^{+i2\frac{\epsilon_2}{v}x_1}}{\left(\epsilon_2-i\omega'\right)}S^{e,e}\left(\epsilon_2\right)\frac{e^{-i\frac{\epsilon_3}{v}\left(x_1+x'\right)}}{\left(\epsilon_3+i\omega\right)}S^{e,h*}\left(\epsilon_3\right)]\tag{2.207}$$

and remembering that

$$x>x'>\{x_i\}>0\tag{2.208}$$

let us compute each contribution. We obtain

$$\delta G^{(1)}_{RL}\left(x,x',\omega\right)\approx+\frac{g}{\beta v^{3}}\Theta(\omega)e^{-\frac{\omega}{v}\left(x+x'\right)}\sum_{\omega'}\int_{0}^{L}dx_{1}$$
$$[-i\Theta\left(\omega'\right)S^{e,e}\left(i\omega'\right)e^{2\frac{x_1}{v}\left(\omega-\omega'\right)}$$
$$+i\Theta\left(-\omega'\right)S^{e,e}\left(i\omega\right)S^{e,e*}\left(i\omega'\right)S^{e,e}\left(i\omega\right)e^{2\frac{x_1}{v}\left(-\omega+\omega'\right)}$$
$$-i\Theta\left(\omega'\right)S^{e,e}\left(i\omega\right)S^{e,h}\left(i\omega'\right)S^{e,h*}\left(-i\omega\right)e^{-2\frac{x_1}{v}\left(\omega+\omega'\right)}$$
$$-i\Theta\left(\omega'\right)S^{e,h}\left(i\omega\right)S^{e,h*}\left(-i\omega'\right)S^{e,e}\left(i\omega\right)e^{-2\frac{x_1}{v}\left(\omega+\omega'\right)}$$
$$+i\Theta\left(\omega'\right)S^{e,h}\left(i\omega\right)S^{e,e}\left(i\omega'\right)S^{e,h*}\left(-i\omega\right)e^{-2\frac{x_1}{v}\left(\omega+\omega'\right)}]\tag{2.209}$$

If we make the comparison with the zeroth order Green's function

$$G^{(0)}_{R,L}\left(x,x',i\omega_n\right)=\frac{1}{l}\sum_{k}\frac{e^{+ik\left(x+x'\right)}}{\left(\epsilon_k-i\omega\right)}S^{e,e}\left(\epsilon_k\right)$$
$$\frac{1}{2\pi v}\int d\epsilon\frac{e^{+i\frac{\epsilon}{v}\left(x+x'\right)}}{\left(\epsilon-i\omega\right)}S^{e,e}\left(\epsilon\right)$$
$$\frac{i}{v}\Theta\left(\omega\right)S^{e,e}\left(i\omega\right)e^{-i\frac{\omega}{v}\left(x+x'\right)}\tag{2.210}$$

integrating in dx_1 exchanging the sum over ω' with an integral and letting the integral going from $-D$ to 0 we obtain

$$\delta S^{e,e}\left(i\omega\right)\approx+\frac{g}{2\left(2\pi\right)v}$$
$$[\ -\int_{-D}^{0}d\omega'S^{e,e}\left(-i\omega'\right)\frac{\left[e^{2\frac{L}{v}\left(\omega+\omega'\right)}-1\right]}{\left(\omega+\omega'\right)}$$

$$
\begin{aligned}
&-\int_{-D}^{0} d\omega' S^{e,e}\left(i\omega\right) S^{e,e*}\left(i\omega'\right) S^{e,e}\left(i\omega\right) \frac{\left[e^{2\frac{L}{v}\left(-\omega+\omega'\right)}-1\right]}{\left(\omega-\omega'\right)} \\
&+\int_{-D}^{0} d\omega' S^{e,e}\left(i\omega\right) S^{e,h}\left(-i\omega'\right) S^{e,h*}\left(-i\omega\right) \frac{\left[e^{-2\frac{L}{v}\left(\omega-\omega'\right)}-1\right]}{\left(\omega-\omega'\right)} \\
&+\int_{-D}^{0} d\omega' S^{e,h}\left(i\omega\right) S^{e,h*}\left(i\omega'\right) S^{e,e}\left(i\omega\right) \frac{\left[e^{-2\frac{L}{v}\left(\omega-\omega'\right)}-1\right]}{\left(\omega-\omega'\right)} \\
&-\int_{-D}^{0} d\omega' S^{e,h}\left(i\omega\right) S^{e,e}\left(-i\omega'\right) S^{e,h*}\left(-i\omega\right) \frac{\left[e^{-2\frac{L}{v}\left(\omega-\omega'\right)}-1\right]}{\left(\omega-\omega'\right)}]
\end{aligned} \tag{2.211}
$$

Let us analyse term by term the behaviour of the last equation under a change of the cut-off using the Leibniz rule

$$
\delta_D \int_{-D}^{0} d\omega_1 F\left(\omega_1\right) = F\left(-D\right)\delta D \tag{2.212}
$$

The first order correction to $S^{e,e}$ is

$$
\begin{aligned}
\delta S^{e,e}\left(i\omega\right) \approx & \frac{g}{2\left(2\pi\right)v}\frac{\delta D}{D} \\
& [\ -S^{e,e}\left(iD\right) \\
& \ +S^{e,e}\left(i\omega\right) S^{e,e*}\left(-iD\right) S^{e,e}\left(i\omega\right) \\
& \ -S^{e,e}\left(i\omega\right) S^{e,h}\left(iD\right) S^{e,h*}\left(-i\omega\right) \\
& \ -S^{e,h}\left(i\omega\right) S^{e,h*}\left(-iD\right) S^{e,e}\left(i\omega\right) \\
& \ +S^{e,h}\left(i\omega\right) S^{e,e}\left(iD\right) S^{e,h*}\left(-i\omega\right)]
\end{aligned} \tag{2.213}
$$

Let us restoring the wire indices, for the forward interaction, Eq. [2.54], through the replacement in Eq. [2.65] that means

$$
\begin{aligned}
\delta S^{e,e}_{j,j'}\left(i\omega\right) \approx & \frac{1}{2\left(2\pi\right)v}\frac{\delta D}{D} \\
& [\ -g_{2;j,j'} S^{e,e}_{j,j'}\left(iD\right) \\
& \ +\sum_{a,a'} g_{2;a,a'} S^{e,e}_{j,a'}\left(i\omega\right) S^{e,e*}_{a,a'}\left(-iD\right) S^{e,e}_{a,j'}\left(i\omega\right) \\
& \ -\sum_{a,a'} g_{2;a,a'} S^{e,e}_{j,a'}\left(i\omega\right) S^{e,h}_{a,a'}\left(iD\right) S^{e,h*}_{a,j'}\left(-i\omega\right) \\
& \ -\sum_{a,a'} g_{2;a,a'} S^{e,h}_{j,a'}\left(i\omega\right) S^{e,h*}_{a,a'}\left(-iD\right) S^{e,e}_{a,j'}\left(i\omega\right) \\
& \ +\sum_{a,a'} g_{2;a,a'} S^{e,h}_{j,a'}\left(i\omega\right) S^{e,e}_{a,a'}\left(iD\right) S^{e,h*}_{a,j'}\left(-i\omega\right)]
\end{aligned} \tag{2.214}
$$

while for the backscattering term, Eq. [2.55], we have to make the replacement in Eq. [2.66] that means

$$
\begin{aligned}
\delta S^{e,e}_{j,j'}\left(i\omega\right) \approx & \frac{1}{2\left(2\pi\right)v}\frac{\delta D}{D} \\
& [\ -\sum_{a} g_{1;j,a}\delta_{j,j'} S^{e,e}_{a,a}\left(iD\right)
\end{aligned}
$$

$$
\begin{aligned}
&+\sum_{a,a'} g_{1;a,a'} S^{e,e}_{j,a'}\left(i\omega\right) S^{e,e*}_{a,a}\left(-iD\right) S^{e,e}_{a',j'}\left(i\omega\right)\\
&-\sum_{a,a'} g_{1;a,a'} S^{e,e}_{j,a'}\left(i\omega\right) S^{e,h}_{a',a}\left(iD\right) S^{e,h*}_{a,j'}\left(-i\omega\right)\\
&-\sum_{a,a'} g_{1;a,a'} S^{e,h}_{j,a}\left(i\omega\right) S^{e,h*}_{a,a'}\left(-iD\right) S^{e,e}_{a',j'}\left(i\omega\right)\\
&+\sum_{a,a'} g_{1;a,a'} S^{e,h}_{j,a}\left(i\omega\right) S^{e,e}_{a',a'}\left(iD\right) S^{e,h*}_{a,j'}\left(-i\omega\right)] \qquad (2.215)
\end{aligned}
$$

Adding the two contributions we have the full first order correction to the normal elements of the scattering matrix. We are at half of the work; now, we have to repeat the full procedure for the anomalous Green's function, in order to obtain the RG equation for the Andreev scattering matrix elements.

For the first order of the Dyson's series, for the anomalous Green's function, we have

$$
\delta F^{(1)}_{RL}\left(x,\tau,x'\right) = +g\int_0^L dx_1 \int_0^\beta d\tau_1 \left\langle T_\tau \psi_R\left(x,\tau\right) : \psi^\dagger_R\left(x_1,\tau_1\right)\psi_R\left(x_1,\tau_1\right) :: \psi^\dagger_L\left(x_1,\tau_1\right)\psi_L\left(x_1,\tau_1\right) : \psi_L\left(x',0\right)\right\rangle \qquad (2.216)
$$

Using Wick's theorem

$$
\begin{aligned}
&\delta F^{(1)}_{RL}\left(x,\tau,x'\right) = +g\int_0^L dx_1 \int_0^\beta d\tau_1\,[\\
&+G^{(0)}_{RR}\left(x,\tau,x_1,\tau_1\right) F^{(0)}_{RL}\left(x_1,\tau_1,x_1,\tau_1\right) G^{(0)}_{LL}\left(x',0,x_1,\tau_1\right)\\
&+G^{(0)}_{RL}\left(x,\tau,x_1,\tau_1\right) G^{(0)}_{LR}\left(x_1,\tau_1,x_1,\tau_1\right) F^{(0)}_{RL}\left(x_1,\tau_1,x',0\right)\\
&-G^{(0)}_{RL}\left(x,\tau,x_1,\tau_1\right) F^{(0)}_{RL}\left(x_1,\tau_1,x_1,\tau_1\right) G^{(0)}_{LR}\left(x',0,x_1,\tau_1\right)\\
&+F^{(0)}_{RL}\left(x,\tau,x_1,\tau_1\right) \tilde{F}^{(0)}_{RL}\left(x_1,\tau_1,x_1,\tau_1\right) F^{(0)}_{RL}\left(x_1,\tau_1,x',0\right)\\
&+F^{(0)}_{RL}\left(x,\tau,x_1,\tau_1\right) G^{(0)}_{RL}\left(x_1,\tau_1,x_1,\tau_1\right) G^{(0)}_{LR}\left(x',0,x_1,\tau_1\right)] \qquad (2.217)
\end{aligned}
$$

In Fourier space, integrating into the time variables

$$
\begin{aligned}
&\delta F^{(1)}_{RL}\left(x,x',i\omega\right) \approx +\frac{g}{\beta}\int_0^L dx_1 \sum_{\omega'}\,[\\
&+G^{(0)}_{RR}\left(x,x_1,i\omega\right) F^{(0)}_{RL}\left(x_1,x_1,i\omega'\right) G^{(0)}_{LL}\left(x',x_1,-i\omega\right)\\
&+G^{(0)}_{RL}\left(x,x_1,i\omega\right) G^{(0)}_{LR}\left(x_1,x_1,i\omega'\right) F^{(0)}_{RL}\left(x_1,x',i\omega\right)\\
&-G^{(0)}_{RL}\left(x,x_1,i\omega\right) F^{(0)}_{RL}\left(x_1,x_1,i\omega'\right) G^{(0)}_{LR}\left(x',x_1,-i\omega\right)\\
&+F^{(0)}_{RL}\left(x,x_1,i\omega\right) \tilde{F}^{(0)}_{RL}\left(x_1,x_1,i\omega'\right) F^{(0)}_{RL}\left(x_1,x',i\omega\right)\\
&+F^{(0)}_{RL}\left(x,x_1,i\omega\right) G^{(0)}_{RL}\left(x_1,x_1,i\omega'\right) G^{(0)}_{LR}\left(x',x_1,-i\omega\right)] \qquad (2.218)
\end{aligned}
$$

Substituting the full form of the Green's functions

$$
\begin{aligned}
&\delta F^{(1)}_{RL}\left(x,x',i\omega\right) \approx +\frac{g}{\beta\left(2\pi\right)^3 v^3}\int_0^L dx_1 \sum_{\omega'}\int\prod_{i=1}^{3} d\epsilon_i\,[\\
&+\frac{e^{+i\frac{\epsilon_1}{v}\left(x-x_1\right)}}{\left(\epsilon_1-i\omega\right)}\frac{e^{+i2\frac{\epsilon_2}{v}x_1}}{\left(\epsilon_2-i\omega'\right)}S^{e,h}\left(\epsilon_2\right)\frac{e^{-i\frac{\epsilon_3}{v}\left(x'-x_1\right)}}{\left(\epsilon_3+i\omega\right)}\\
&+\frac{e^{+i\frac{\epsilon_1}{v}\left(x+x_1\right)}}{\left(\epsilon_1-i\omega\right)}S^{e,e}\left(\epsilon_1\right)\frac{e^{-i2\frac{\epsilon_2}{v}x_1}}{\left(\epsilon_2-i\omega'\right)}S^{e,e*}\left(\epsilon_2\right)\frac{e^{+i\frac{\epsilon_3}{v}\left(x_1+x'\right)}}{\left(\epsilon_3-i\omega\right)}S^{e,h}\left(\epsilon_3\right)
\end{aligned}
$$

$$
\begin{aligned}
&-\frac{e^{+i\frac{\epsilon_1}{v}(x+x_1)}}{(\epsilon_1-i\omega)}S^{e,e}(\epsilon_1)\frac{e^{+i2\frac{\epsilon_2}{v}x_1}}{(\epsilon_2-i\omega')}S^{e,h}(\epsilon_2)\frac{e^{-i\frac{\epsilon_3}{v}\left(x_1+x'\right)}}{(\epsilon_3+i\omega)}S^{e,e*}(\epsilon_3)\\
&-\frac{e^{+i\frac{\epsilon_1}{v}(x+x_1)}}{(\epsilon_1-i\omega)}S^{e,h}(\epsilon_1)\frac{e^{-i2\frac{\epsilon_2}{v}x_1}}{(\epsilon_2+i\omega')}S^{e,h*}(\epsilon_2)\frac{e^{+i\frac{\epsilon_3}{v}\left(x_1+x'\right)}}{(\epsilon_3-i\omega)}S^{e,h}(\epsilon_3)\\
&+\frac{e^{+i\frac{\epsilon_1}{v}(x+x_1)}}{(\epsilon_1-i\omega)}S^{e,h}(\epsilon_1)\frac{e^{+i2\frac{\epsilon_2}{v}x_1}}{(\epsilon_2-i\omega')}S^{e,e}(\epsilon_2)\frac{e^{-i\frac{\epsilon_3}{v}\left(x_1+x'\right)}}{(\epsilon_3+i\omega)}S^{e,e*}(\epsilon_3)]
\end{aligned}
\tag{2.219}
$$

Let us compute contribution by contribution. We are left with

$$
\begin{aligned}
&\delta F^{(1)}_{RL}(x,x',\omega)\approx+\frac{g}{\beta v^3}\Theta(\omega)e^{-\frac{\omega}{v}\left(x+x'\right)}\sum_{\omega'}\int_0^L dx_1\\
&[+i\Theta(\omega')S^{e,h}(i\omega')e^{2\frac{x_1}{v}\left(\omega-\omega'\right)}\\
&+i\Theta(-\omega')S^{e,e}(i\omega)S^{e,e*}(i\omega')S^{e,h}(i\omega)e^{2\frac{x_1}{v}\left(-\omega+\omega'\right)}\\
&-i\Theta(\omega')S^{e,e}(i\omega)S^{e,h}(i\omega')S^{e,e*}(-i\omega)e^{-2\frac{x_1}{v}\left(\omega+\omega'\right)}\\
&-i\Theta(\omega')S^{e,h}(i\omega)S^{e,h*}(-i\omega')S^{e,h}(i\omega)e^{-2\frac{x_1}{v}\left(\omega+\omega'\right)}\\
&+i\Theta(\omega')S^{e,h}(i\omega)S^{e,e}(i\omega')S^{e,e*}(-i\omega)e^{-2\frac{x_1}{v}\left(\omega+\omega'\right)}]
\end{aligned}
\tag{2.220}
$$

The comparison with the zeroth order Green's function

$$
\begin{aligned}
F^{(0)}_{R,L}(x,x',i\omega_n)=&\frac{1}{l}\sum_k\frac{e^{+ik\left(x+x'\right)}}{(\epsilon_k-i\omega)}S^{e,h}(\epsilon_k)\\
&\frac{1}{2\pi v}\int d\epsilon\frac{e^{+i\frac{\epsilon}{v}\left(x+x'\right)}}{(\epsilon-i\omega)}S^{e,h}(\epsilon)\\
&\frac{i}{v}\Theta(\omega)S^{e,h}(i\omega)e^{-\frac{\omega}{v}\left(x+x'\right)}
\end{aligned}
\tag{2.221}
$$

brings us to

$$
\begin{aligned}
\delta S^{e,h}(i\omega)\approx&+\frac{g}{2(2\pi)v}\\
&[+\int_{-D}^0 d\omega' S^{e,h}(-i\omega')\frac{\left[e^{2\frac{L}{v}\left(\omega+\omega'\right)}-1\right]}{(\omega+\omega')}\\
&-\int_{-D}^0 d\omega' S^{e,e}(i\omega)S^{e,e*}(i\omega')S^{e,h}(i\omega)\frac{\left[e^{2\frac{L}{v}\left(-\omega+\omega'\right)}-1\right]}{(\omega-\omega')}\\
&+\int_{-D}^0 d\omega' S^{e,e}(i\omega)S^{e,h}(-i\omega')S^{e,e*}(-i\omega)\frac{\left[e^{-2\frac{L}{v}\left(\omega-\omega'\right)}-1\right]}{(\omega-\omega')}\\
&+\int_{-D}^0 d\omega' S^{e,h}(i\omega)S^{e,h*}(i\omega')S^{e,h}(i\omega)\frac{\left[e^{-2\frac{L}{v}\left(\omega-\omega'\right)}-1\right]}{(\omega-\omega')}\\
&-\int_{-D}^0 d\omega' S^{e,h}(i\omega)S^{e,e}(-i\omega')S^{e,e*}(-i\omega)\frac{\left[e^{-2\frac{L}{v}\left(\omega-\omega'\right)}-1\right]}{(\omega-\omega')}]
\end{aligned}
\tag{2.222}
$$

Let us analyse term by term the behaviour of the last equation under a change of the cut-off applying the variation rule

$$\begin{aligned}\delta S^{e,h}\left(i\omega\right) \approx & \frac{g}{2\left(2\pi\right)v}\frac{\delta D}{D}\\ & \left[\begin{array}{l} +S^{e,h}\left(iD\right)\\ +S^{e,e}\left(i\omega\right)S^{e,e*}\left(-iD\right)S^{e,h}\left(i\omega\right)\\ -S^{e,e}\left(i\omega\right)S^{e,h}\left(iD\right)S^{e,e*}\left(-i\omega\right)\\ -S^{e,h}\left(i\omega\right)S^{e,h*}\left(-iD\right)S^{e,h}\left(i\omega\right)\\ +S^{e,h}\left(i\omega\right)S^{e,e}\left(iD\right)S^{e,e*}\left(-i\omega\right)\end{array}\right] \end{aligned} \tag{2.223}$$

Let us restoring the wire indices, for the forward interaction, Eq. [2.54], making the replacement in Eq. [2.65], we have

$$\begin{aligned}\delta S_{j,j'}^{e,h}\left(i\omega\right) \approx & \frac{1}{2\left(2\pi\right)v}\frac{\delta D}{D}\\ & \left[\begin{array}{l} +g_{2;j,j'}S_{j,j'}^{e,h}\left(iD\right)\\ +\sum\limits_{a,a'}g_{2;a,a'}S_{j,a'}^{e,e}\left(i\omega\right)S_{a,a'}^{e,e*}\left(-iD\right)S_{a,j'}^{e,h}\left(i\omega\right)\\ -\sum\limits_{a,a'}g_{2;a,a'}S_{j,a'}^{e,e}\left(i\omega\right)S_{a,a'}^{e,h}\left(iD\right)S_{a,j'}^{e,e*}\left(-i\omega\right)\\ -\sum\limits_{a,a'}g_{2;a,a'}S_{j,a'}^{e,h}\left(i\omega\right)S_{a,a'}^{e,h*}\left(-iD\right)S_{a,j'}^{e,h}\left(i\omega\right)\\ +\sum\limits_{a,a'}g_{2;a,a'}S_{j,a'}^{e,h}\left(i\omega\right)S_{a,a'}^{e,e}\left(iD\right)S_{a,j'}^{e,e*}\left(-i\omega\right)\end{array}\right] \end{aligned} \tag{2.224}$$

while for the backscattering term, Eq. [2.55], with the replacement in Eq. [2.66], we have

$$\begin{aligned}\delta S_{j,j'}^{e,h}\left(i\omega\right) \approx & -\frac{1}{2\left(2\pi\right)v}\frac{\delta D}{D}\\ & \left[\begin{array}{l} +g_{1;j',j}S_{j',j}^{e,h}\left(iD\right)\\ +\sum\limits_{a,a'}g_{1;a,a'}S_{j,a'}^{e,e}\left(i\omega\right)S_{a,a}^{e,e*}\left(-iD\right)S_{a',j'}^{e,h}\left(i\omega\right)\\ -\sum\limits_{a,a'}g_{1;a,a'}S_{j,a'}^{e,e}\left(i\omega\right)S_{a',a}^{e,h}\left(iD\right)S_{a,j'}^{e,e*}\left(-i\omega\right)\\ -\sum\limits_{a,a'}g_{1;a,a'}S_{j,a}^{e,h}\left(i\omega\right)S_{a,a'}^{e,h*}\left(-iD\right)S_{a',j'}^{e,h}\left(i\omega\right)\\ +\sum\limits_{a,a'}g_{1;a,a'}S_{j,a}^{e,h}\left(i\omega\right)S_{a',a'}^{e,e}\left(iD\right)S_{a,j'}^{e,e*}\left(-i\omega\right)\end{array}\right] \end{aligned} \tag{2.225}$$

Adding the two contributions we have the full first order correction to the Andreev elements of the scattering matrix. At this point putting together Eqs. [2.214,2.215,2.224,2.225] and back-rotating to real frequencies we obtain the first order correction used in the main text.

II.9.2. Second order correction

In this section we will compute one by one all the second order contributions the scattering matrix for a normal junction. Starting from the second order of the Dyson's series we have

$$\delta G_{RL}^{(2)}\left(x,\tau,x'\right) = +\frac{g^2}{2}\int_0^L dx_1\int_0^\beta d\tau_1\int_0^L dx_2\int_0^\beta d\tau_2\left\langle T_\tau\psi_R\left(x,\tau\right):\psi_R^\dagger\left(x_1,\tau_1\right)\psi_R\left(x_1,\tau_1\right)::\psi_L^\dagger\left(x_1,\tau_1\right)\psi_L\left(x_1,\tau_1\right):\right.$$

$$: \psi_R^{\dagger}(x_2,\tau_2)\,\psi_R(x_2,\tau_2) :: \psi_L^{\dagger}(x_2,\tau_2)\,\psi_L(x_2,\tau_2) : \psi_L^{\dagger}(x',0)\Big\rangle \tag{2.226}$$

that using the Wick's theorem and ignoring for the moment that, due to the normal ordering within each chiral density operator, $G^{(0)}_{XX}(x_i,\tau_i,x_i,\tau_i)=0$

$$\delta G^{(2)}_{RL}(x,\tau,x') \approx \frac{g^2}{2}\int_0^L dx_1\int_0^\beta d\tau_1\int_0^L dx_2\int_0^\beta d\tau_2$$
$$\begin{vmatrix} G^{(0)}_{RL}(x,\tau,x',0) & G^{(0)}_{RR}(x,\tau,x_1,\tau_1) & G^{(0)}_{RL}(x,\tau,x_1,\tau_1) & G^{(0)}_{RR}(x,\tau,x_2,\tau_2) & G^{(0)}_{RL}(x,\tau,x_2,\tau_2)\\ G^{(0)}_{RL}(x_1,\tau_1,x',0) & G^{(0)}_{RR}(x_1,\tau_1,x_1,\tau_1) & G^{(0)}_{RL}(x_1,\tau_1,x_1,\tau_1) & G^{(0)}_{RR}(x_1,\tau_1,x_2,\tau_2) & G^{(0)}_{RL}(x_1,\tau_1,x_2,\tau_2)\\ G^{(0)}_{LL}(x_1,\tau_1,x',0) & G^{(0)}_{LR}(x_1,\tau_1,x_1,\tau_1) & G^{(0)}_{LL}(x_1,\tau_1,x_1,\tau_1) & G^{(0)}_{LR}(x_1,\tau_1,x_2,\tau_2) & G^{(0)}_{LL}(x_1,\tau_1,x_2,\tau_2)\\ G^{(0)}_{RL}(x_2,\tau_2,x',0) & G^{(0)}_{RR}(x_2,\tau_2,x_1,\tau_1) & G^{(0)}_{RL}(x_2,\tau_2,x_1,\tau_1) & G^{(0)}_{RR}(x_2,\tau_2,x_2,\tau_2) & G^{(0)}_{RL}(x_2,\tau_2,x_2,\tau_2)\\ G^{(0)}_{LL}(x_2,\tau_2,x',0) & G^{(0)}_{LR}(x_2,\tau_2,x_1,\tau_1) & G^{(0)}_{LL}(x_2,\tau_2,x_1,\tau_1) & G^{(0)}_{LR}(x_2,\tau_2,x_2,\tau_2) & G^{(0)}_{LL}(x_2,\tau_2,x_2,\tau_2)\end{vmatrix}_{connected} \tag{2.227}$$

we have $5!=120$ terms within the determinant whence we have to remove the disconnected diagrams. This means that we can remove all the 4! terms contained in

$$G^{(0)}_{RL}(x,\tau,x',0)\begin{vmatrix} G^{(0)}_{RR}(x_1,\tau_1,x_1,\tau_1) & G^{(0)}_{RL}(x_1,\tau_1,x_1,\tau_1) & G^{(0)}_{RR}(x_1,\tau_1,x_2,\tau_2) & G^{(0)}_{RL}(x_1,\tau_1,x_2,\tau_2)\\ G^{(0)}_{LR}(x_1,\tau_1,x_1,\tau_1) & G^{(0)}_{LL}(x_1,\tau_1,x_1,\tau_1) & G^{(0)}_{LR}(x_1,\tau_1,x_2,\tau_2) & G^{(0)}_{LL}(x_1,\tau_1,x_2,\tau_2)\\ G^{(0)}_{RR}(x_2,\tau_2,x_1,\tau_1) & G^{(0)}_{RL}(x_2,\tau_2,x_1,\tau_1) & G^{(0)}_{RR}(x_2,\tau_2,x_2,\tau_2) & G^{(0)}_{RL}(x_2,\tau_2,x_2,\tau_2)\\ G^{(0)}_{LR}(x_2,\tau_2,x_1,\tau_1) & G^{(0)}_{LL}(x_2,\tau_2,x_1,\tau_1) & G^{(0)}_{LR}(x_2,\tau_2,x_2,\tau_2) & G^{(0)}_{LL}(x_2,\tau_2,x_2,\tau_2)\end{vmatrix} \tag{2.228}$$

because it is easy to see that they are completely disconnected. So we are left with $4\times 4!=96$ terms, some of them still corresponding to disconnected diagrams. Let us expand the determinant

$$\begin{vmatrix} 0 & G^{(0)}_{RR}(x,\tau,x_1,\tau_1) & G^{(0)}_{RL}(x,\tau,x_1,\tau_1) & G^{(0)}_{RR}(x,\tau,x_2,\tau_2) & G^{(0)}_{RL}(x,\tau,x_2,\tau_2)\\ G^{(0)}_{RL}(x_1,\tau_1,x',0) & G^{(0)}_{RR}(x_1,\tau_1,x_1,\tau_1) & G^{(0)}_{RL}(x_1,\tau_1,x_1,\tau_1) & G^{(0)}_{RR}(x_1,\tau_1,x_2,\tau_2) & G^{(0)}_{RL}(x_1,\tau_1,x_2,\tau_2)\\ G^{(0)}_{LL}(x_1,\tau_1,x',0) & G^{(0)}_{LR}(x_1,\tau_1,x_1,\tau_1) & G^{(0)}_{LL}(x_1,\tau_1,x_1,\tau_1) & G^{(0)}_{LR}(x_1,\tau_1,x_2,\tau_2) & G^{(0)}_{LL}(x_1,\tau_1,x_2,\tau_2)\\ G^{(0)}_{RL}(x_2,\tau_2,x',0) & G^{(0)}_{RR}(x_2,\tau_2,x_1,\tau_1) & G^{(0)}_{RL}(x_2,\tau_2,x_1,\tau_1) & G^{(0)}_{RR}(x_2,\tau_2,x_2,\tau_2) & G^{(0)}_{RL}(x_2,\tau_2,x_2,\tau_2)\\ G^{(0)}_{LL}(x_2,\tau_2,x',0) & G^{(0)}_{LR}(x_2,\tau_2,x_1,\tau_1) & G^{(0)}_{LL}(x_2,\tau_2,x_1,\tau_1) & G^{(0)}_{LR}(x_2,\tau_2,x_2,\tau_2) & G^{(0)}_{LL}(x_2,\tau_2,x_2,\tau_2)\end{vmatrix}_{connected}$$
$$= -G^{(0)}_{RR}(x,\tau,x_1,\tau_1)\begin{vmatrix} G^{(0)}_{RL}(x_1,\tau_1,x',0) & G^{(0)}_{RL}(x_1,\tau_1,x_1,\tau_1) & G^{(0)}_{RR}(x_1,\tau_1,x_2,\tau_2) & G^{(0)}_{RL}(x_1,\tau_1,x_2,\tau_2)\\ G^{(0)}_{LL}(x_1,\tau_1,x',0) & G^{(0)}_{LL}(x_1,\tau_1,x_1,\tau_1) & G^{(0)}_{LR}(x_1,\tau_1,x_2,\tau_2) & G^{(0)}_{LL}(x_1,\tau_1,x_2,\tau_2)\\ G^{(0)}_{RL}(x_2,\tau_2,x',0) & G^{(0)}_{RL}(x_2,\tau_2,x_1,\tau_1) & G^{(0)}_{RR}(x_2,\tau_2,x_2,\tau_2) & G^{(0)}_{RL}(x_2,\tau_2,x_2,\tau_2)\\ G^{(0)}_{LL}(x_2,\tau_2,x',0) & G^{(0)}_{LL}(x_2,\tau_2,x_1,\tau_1) & G^{(0)}_{LR}(x_2,\tau_2,x_2,\tau_2) & G^{(0)}_{LL}(x_2,\tau_2,x_2,\tau_2)\end{vmatrix}_{connected}$$
$$+G^{(0)}_{RL}(x,\tau,x_1,\tau_1)\begin{vmatrix} G^{(0)}_{RL}(x_1,\tau_1,x',0) & G^{(0)}_{RR}(x_1,\tau_1,x_1,\tau_1) & G^{(0)}_{RR}(x_1,\tau_1,x_2,\tau_2) & G^{(0)}_{RL}(x_1,\tau_1,x_2,\tau_2)\\ G^{(0)}_{LL}(x_1,\tau_1,x',0) & G^{(0)}_{LR}(x_1,\tau_1,x_1,\tau_1) & G^{(0)}_{LR}(x_1,\tau_1,x_2,\tau_2) & G^{(0)}_{LL}(x_1,\tau_1,x_2,\tau_2)\\ G^{(0)}_{RL}(x_2,\tau_2,x',0) & G^{(0)}_{RR}(x_2,\tau_2,x_1,\tau_1) & G^{(0)}_{RR}(x_2,\tau_2,x_2,\tau_2) & G^{(0)}_{RL}(x_2,\tau_2,x_2,\tau_2)\\ G^{(0)}_{LL}(x_2,\tau_2,x',0) & G^{(0)}_{LR}(x_2,\tau_2,x_1,\tau_1) & G^{(0)}_{LR}(x_2,\tau_2,x_2,\tau_2) & G^{(0)}_{LL}(x_2,\tau_2,x_2,\tau_2)\end{vmatrix}_{connected}$$
$$-G^{(0)}_{RR}(x,\tau,x_2,\tau_2)\begin{vmatrix} G^{(0)}_{RL}(x_1,\tau_1,x',0) & G^{(0)}_{RR}(x_1,\tau_1,x_1,\tau_1) & G^{(0)}_{RL}(x_1,\tau_1,x_1,\tau_1) & G^{(0)}_{RL}(x_1,\tau_1,x_2,\tau_2)\\ G^{(0)}_{LL}(x_1,\tau_1,x',0) & G^{(0)}_{LR}(x_1,\tau_1,x_1,\tau_1) & G^{(0)}_{LL}(x_1,\tau_1,x_1,\tau_1) & G^{(0)}_{LL}(x_1,\tau_1,x_2,\tau_2)\\ G^{(0)}_{RL}(x_2,\tau_2,x',0) & G^{(0)}_{RR}(x_2,\tau_2,x_1,\tau_1) & G^{(0)}_{RL}(x_2,\tau_2,x_1,\tau_1) & G^{(0)}_{RL}(x_2,\tau_2,x_2,\tau_2)\\ G^{(0)}_{LL}(x_2,\tau_2,x',0) & G^{(0)}_{LR}(x_2,\tau_2,x_1,\tau_1) & G^{(0)}_{LL}(x_2,\tau_2,x_1,\tau_1) & G^{(0)}_{LL}(x_2,\tau_2,x_2,\tau_2)\end{vmatrix}_{connected}$$
$$+G^{(0)}_{RL}(x,\tau,x_2,\tau_2)\begin{vmatrix} G^{(0)}_{RL}(x_1,\tau_1,x',0) & G^{(0)}_{RR}(x_1,\tau_1,x_1,\tau_1) & G^{(0)}_{RL}(x_1,\tau_1,x_1,\tau_1) & G^{(0)}_{RR}(x_1,\tau_1,x_2,\tau_2)\\ G^{(0)}_{LL}(x_1,\tau_1,x',0) & G^{(0)}_{LR}(x_1,\tau_1,x_1,\tau_1) & G^{(0)}_{LL}(x_1,\tau_1,x_1,\tau_1) & G^{(0)}_{LR}(x_1,\tau_1,x_2,\tau_2)\\ G^{(0)}_{RL}(x_2,\tau_2,x',0) & G^{(0)}_{RR}(x_2,\tau_2,x_1,\tau_1) & G^{(0)}_{RL}(x_2,\tau_2,x_1,\tau_1) & G^{(0)}_{RR}(x_2,\tau_2,x_2,\tau_2)\\ G^{(0)}_{LL}(x_2,\tau_2,x',0) & G^{(0)}_{LR}(x_2,\tau_2,x_1,\tau_1) & G^{(0)}_{LL}(x_2,\tau_2,x_1,\tau_1) & G^{(0)}_{LR}(x_2,\tau_2,x_2,\tau_2)\end{vmatrix}_{connected} \tag{2.229}$$

At this point let us note that if we rename the dummy index $(x_1,\tau_1)\rightleftharpoons(x_2,\tau_2)$, first and third line are the same at less than an even number of exchanges of rows or columns and the same happens for the second and fourth line. So that we are left with only 48 terms. The determinant is now

$$
\begin{vmatrix}
0 & G^{(0)}_{RR}(x,\tau,x_1,\tau_1) & G^{(0)}_{RL}(x,\tau,x_1,\tau_1) & G^{(0)}_{RR}(x,\tau,x_2,\tau_2) & G^{(0)}_{RL}(x,\tau,x_2,\tau_2) \\
G^{(0)}_{RL}(x_1,\tau_1,x',0) & G^{(0)}_{RR}(x_1,\tau_1,x_1,\tau_1) & G^{(0)}_{RL}(x_1,\tau_1,x_1,\tau_1) & G^{(0)}_{RR}(x_1,\tau_1,x_2,\tau_2) & G^{(0)}_{RL}(x_1,\tau_1,x_2,\tau_2) \\
G^{(0)}_{LL}(x_1,\tau_1,x',0) & G^{(0)}_{LR}(x_1,\tau_1,x_1,\tau_1) & G^{(0)}_{LL}(x_1,\tau_1,x_1,\tau_1) & G^{(0)}_{LR}(x_1,\tau_1,x_2,\tau_2) & G^{(0)}_{LL}(x_1,\tau_1,x_2,\tau_2) \\
G^{(0)}_{RL}(x_2,\tau_2,x',0) & G^{(0)}_{RR}(x_2,\tau_2,x_1,\tau_1) & G^{(0)}_{RL}(x_2,\tau_2,x_1,\tau_1) & G^{(0)}_{RR}(x_2,\tau_2,x_2,\tau_2) & G^{(0)}_{RL}(x_2,\tau_2,x_2,\tau_2) \\
G^{(0)}_{LL}(x_2,\tau_2,x',0) & G^{(0)}_{LR}(x_2,\tau_2,x_1,\tau_1) & G^{(0)}_{LL}(x_2,\tau_2,x_1,\tau_1) & G^{(0)}_{LR}(x_2,\tau_2,x_2,\tau_2) & G^{(0)}_{LL}(x_2,\tau_2,x_2,\tau_2)
\end{vmatrix}_{connected}
$$

$$
= -2G^{(0)}_{RR}(x,\tau,x_1,\tau_1)
\begin{vmatrix}
G^{(0)}_{RL}(x_1,\tau_1,x',0) & G^{(0)}_{RL}(x_1,\tau_1,x_1,\tau_1) & G^{(0)}_{RR}(x_1,\tau_1,x_2,\tau_2) & G^{(0)}_{RL}(x_1,\tau_1,x_2,\tau_2) \\
G^{(0)}_{LL}(x_1,\tau_1,x',0) & G^{(0)}_{LL}(x_1,\tau_1,x_1,\tau_1) & G^{(0)}_{LR}(x_1,\tau_1,x_2,\tau_2) & G^{(0)}_{LL}(x_1,\tau_1,x_2,\tau_2) \\
G^{(0)}_{RL}(x_2,\tau_2,x',0) & G^{(0)}_{RL}(x_2,\tau_2,x_1,\tau_1) & G^{(0)}_{RR}(x_2,\tau_2,x_2,\tau_2) & G^{(0)}_{RL}(x_2,\tau_2,x_2,\tau_2) \\
G^{(0)}_{LL}(x_2,\tau_2,x',0) & G^{(0)}_{LL}(x_2,\tau_2,x_1,\tau_1) & G^{(0)}_{LR}(x_2,\tau_2,x_2,\tau_2) & G^{(0)}_{LL}(x_2,\tau_2,x_2,\tau_2)
\end{vmatrix}_{connected}
$$

$$
+2G^{(0)}_{RL}(x,\tau,x_1,\tau_1)
\begin{vmatrix}
G^{(0)}_{RL}(x_1,\tau_1,x',0) & G^{(0)}_{RR}(x_1,\tau_1,x_1,\tau_1) & G^{(0)}_{RR}(x_1,\tau_1,x_2,\tau_2) & G^{(0)}_{RL}(x_1,\tau_1,x_2,\tau_2) \\
G^{(0)}_{LL}(x_1,\tau_1,x',0) & G^{(0)}_{LR}(x_1,\tau_1,x_1,\tau_1) & G^{(0)}_{LR}(x_1,\tau_1,x_2,\tau_2) & G^{(0)}_{LL}(x_1,\tau_1,x_2,\tau_2) \\
G^{(0)}_{RL}(x_2,\tau_2,x',0) & G^{(0)}_{RR}(x_2,\tau_2,x_1,\tau_1) & G^{(0)}_{RR}(x_2,\tau_2,x_2,\tau_2) & G^{(0)}_{RL}(x_2,\tau_2,x_2,\tau_2) \\
G^{(0)}_{LL}(x_2,\tau_2,x',0) & G^{(0)}_{LR}(x_2,\tau_2,x_1,\tau_1) & G^{(0)}_{LR}(x_2,\tau_2,x_2,\tau_2) & G^{(0)}_{LL}(x_2,\tau_2,x_2,\tau_2)
\end{vmatrix}_{connected}
\tag{2.230}
$$

Using now that contraction at the same position with the same chiral indices are zero and removing disconnected diagrams, we are left with

$$
\delta G^{(2)}_{RL}(x,\tau,x') = +\frac{g^2}{2}\int_0^L dx_1 \int_0^\beta d\tau_1 \int_0^L dx_2 \int_0^\beta d\tau_2 \left\langle T_\tau \psi_R(x,\tau) : \psi^\dagger_R(x_1,\tau_1)\psi_R(x_1,\tau_1) :: \psi^\dagger_L(x_1,\tau_1)\psi_L(x_1,\tau_1) : \right.
$$

$$
\left. : \psi^\dagger_R(x_2,\tau_2)\psi_R(x_2,\tau_2) :: \psi^\dagger_L(x_2,\tau_2)\psi_L(x_2,\tau_2) : \psi^\dagger_L(x',0) \right\rangle
$$

$$
= g^2 \int_0^L dx_1 \int_0^\beta d\tau_1 \int_0^L dx_2 \int_0^\beta d\tau_2 \, [
$$

$$
\begin{aligned}
&-G^{(0)}_{RR}(x,\tau,x_1,\tau_1)\,G^{(0)}_{RL}(x_1,\tau_1,x',0)\,G^{(0)}_{LR}(x_1,\tau_1,x_2,\tau_2)\,G^{(0)}_{RL}(x_2,\tau_2,x_2,\tau_2)\,G^{(0)}_{LL}(x_2,\tau_2,x_1,\tau_1) \\
&-G^{(0)}_{RR}(x,\tau,x_1,\tau_1)\,G^{(0)}_{RL}(x_1,\tau_1,x',0)\,G^{(0)}_{LL}(x_1,\tau_1,x_2,\tau_2)\,G^{(0)}_{RL}(x_2,\tau_2,x_1,\tau_1)\,G^{(0)}_{LR}(x_2,\tau_2,x_2,\tau_2) \\
&+G^{(0)}_{RR}(x,\tau,x_1,\tau_1)\,G^{(0)}_{LL}(x_1,\tau_1,x',0)\,G^{(0)}_{RR}(x_1,\tau_1,x_2,\tau_2)\,G^{(0)}_{RL}(x_2,\tau_2,x_2,\tau_2)\,G^{(0)}_{LL}(x_2,\tau_2,x_1,\tau_1) \\
&+G^{(0)}_{RR}(x,\tau,x_1,\tau_1)\,G^{(0)}_{LL}(x_1,\tau_1,x',0)\,G^{(0)}_{RL}(x_1,\tau_1,x_2,\tau_2)\,G^{(0)}_{RL}(x_2,\tau_2,x_1,\tau_1)\,G^{(0)}_{LR}(x_2,\tau_2,x_2,\tau_2) \\
&+G^{(0)}_{RR}(x,\tau,x_1,\tau_1)\,G^{(0)}_{RL}(x_2,\tau_2,x',0)\,G^{(0)}_{RL}(x_1,\tau_1,x_1,\tau_1)\,G^{(0)}_{LL}(x_1,\tau_1,x_2,\tau_2)\,G^{(0)}_{LR}(x_2,\tau_2,x_2,\tau_2) \\
&-G^{(0)}_{RR}(x,\tau,x_1,\tau_1)\,G^{(0)}_{RL}(x_2,\tau_2,x',0)\,G^{(0)}_{RR}(x_1,\tau_1,x_2,\tau_2)\,G^{(0)}_{LL}(x_1,\tau_1,x_2,\tau_2)\,G^{(0)}_{LL}(x_2,\tau_2,x_1,\tau_1) \\
&+G^{(0)}_{RR}(x,\tau,x_1,\tau_1)\,G^{(0)}_{RL}(x_2,\tau_2,x',0)\,G^{(0)}_{RL}(x_1,\tau_1,x_2,\tau_2)\,G^{(0)}_{LR}(x_1,\tau_1,x_2,\tau_2)\,G^{(0)}_{LL}(x_2,\tau_2,x_1,\tau_1) \\
&+G^{(0)}_{RR}(x,\tau,x_1,\tau_1)\,G^{(0)}_{LL}(x_2,\tau_2,x',0)\,G^{(0)}_{RL}(x_1,\tau_1,x_1,\tau_1)\,G^{(0)}_{LR}(x_1,\tau_1,x_2,\tau_2)\,G^{(0)}_{RL}(x_2,\tau_2,x_2,\tau_2) \\
&+G^{(0)}_{RR}(x,\tau,x_1,\tau_1)\,G^{(0)}_{LL}(x_2,\tau_2,x',0)\,G^{(0)}_{RR}(x_1,\tau_1,x_2,\tau_2)\,G^{(0)}_{LL}(x_1,\tau_1,x_2,\tau_2)\,G^{(0)}_{RL}(x_2,\tau_2,x_1,\tau_1) \\
&-G^{(0)}_{RR}(x,\tau,x_1,\tau_1)\,G^{(0)}_{LL}(x_2,\tau_2,x',0)\,G^{(0)}_{RL}(x_1,\tau_1,x_2,\tau_2)\,G^{(0)}_{LR}(x_1,\tau_1,x_2,\tau_2)\,G^{(0)}_{RL}(x_2,\tau_2,x_1,\tau_1) \\
&+G^{(0)}_{RL}(x,\tau,x_1,\tau_1)\,G^{(0)}_{RL}(x_1,\tau_1,x',0)\,G^{(0)}_{LR}(x_1,\tau_1,x_2,\tau_2)\,G^{(0)}_{RL}(x_2,\tau_2,x_2,\tau_2)\,G^{(0)}_{LR}(x_2,\tau_2,x_1,\tau_1) \\
&+G^{(0)}_{RL}(x,\tau,x_1,\tau_1)\,G^{(0)}_{RL}(x_1,\tau_1,x',0)\,G^{(0)}_{LL}(x_1,\tau_1,x_2,\tau_2)\,G^{(0)}_{RR}(x_2,\tau_2,x_1,\tau_1)\,G^{(0)}_{LR}(x_2,\tau_2,x_2,\tau_2) \\
&-G^{(0)}_{RL}(x,\tau,x_1,\tau_1)\,G^{(0)}_{LL}(x_1,\tau_1,x',0)\,G^{(0)}_{RR}(x_1,\tau_1,x_2,\tau_2)\,G^{(0)}_{RL}(x_2,\tau_2,x_2,\tau_2)\,G^{(0)}_{LR}(x_2,\tau_2,x_1,\tau_1) \\
&-G^{(0)}_{RL}(x,\tau,x_1,\tau_1)\,G^{(0)}_{LL}(x_1,\tau_1,x',0)\,G^{(0)}_{RL}(x_1,\tau_1,x_2,\tau_2)\,G^{(0)}_{RR}(x_2,\tau_2,x_1,\tau_1)\,G^{(0)}_{LR}(x_2,\tau_2,x_2,\tau_2) \\
&+G^{(0)}_{RL}(x,\tau,x_1,\tau_1)\,G^{(0)}_{RL}(x_2,\tau_2,x',0)\,G^{(0)}_{RR}(x_1,\tau_1,x_2,\tau_2)\,G^{(0)}_{LL}(x_1,\tau_1,x_2,\tau_2)\,G^{(0)}_{LR}(x_2,\tau_2,x_1,\tau_1) \\
&+G^{(0)}_{RL}(x,\tau,x_1,\tau_1)\,G^{(0)}_{RL}(x_2,\tau_2,x',0)\,G^{(0)}_{RL}(x_1,\tau_1,x_2,\tau_2)\,G^{(0)}_{LR}(x_1,\tau_1,x_1,\tau_1)\,G^{(0)}_{LR}(x_2,\tau_2,x_2,\tau_2) \\
&-G^{(0)}_{RL}(x,\tau,x_1,\tau_1)\,G^{(0)}_{RL}(x_2,\tau_2,x',0)\,G^{(0)}_{RL}(x_1,\tau_1,x_2,\tau_2)\,G^{(0)}_{LR}(x_1,\tau_1,x_2,\tau_2)\,G^{(0)}_{LR}(x_2,\tau_2,x_1,\tau_1) \\
&+G^{(0)}_{RL}(x,\tau,x_1,\tau_1)\,G^{(0)}_{LL}(x_2,\tau_2,x',0)\,G^{(0)}_{RR}(x_1,\tau_1,x_2,\tau_2)\,G^{(0)}_{LR}(x_1,\tau_1,x_1,\tau_1)\,G^{(0)}_{RL}(x_2,\tau_2,x_2,\tau_2)
\end{aligned}
$$

$$-G^{(0)}_{RL}(x,\tau,x_1,\tau_1)\,G^{(0)}_{LL}(x_2,\tau_2,x',0)\,G^{(0)}_{RR}(x_1,\tau_1,x_2,\tau_2)\,G^{(0)}_{LL}(x_1,\tau_1,x_2,\tau_2)\,G^{(0)}_{RR}(x_2,\tau_2,x_1,\tau_1)$$
$$+G^{(0)}_{RL}(x,\tau,x_1,\tau_1)\,G^{(0)}_{LL}(x_2,\tau_2,x',0)\,G^{(0)}_{RL}(x_1,\tau_1,x_2,\tau_2)\,G^{(0)}_{LR}(x_1,\tau_1,x_2,\tau_2)\,G^{(0)}_{RR}(x_2,\tau_2,x_1,\tau_1) \quad (2.231)$$

for a total of 20 terms. In Fourier space and integrating into the time variables to remove three over five ω_i sums, we obtain

$$\begin{aligned}
\delta G^{(2)}_{RL}(x,x',i\omega) \approx \frac{g^2}{\beta^2}\int_0^L dx_1\int_0^L dx_2 \sum_{\omega_1,\omega_2}\\
[&-G^{(0)}_{RR}(x,x_1,i\omega)\,G^{(0)}_{RL}(x_1,x',i\omega)\,G^{(0)}_{LR}(x_1,x_2,i\omega_1)\,G^{(0)}_{RL}(x_2,x_2,i\omega_2)\,G^{(0)}_{LL}(x_2,x_1,i\omega_1)\\
&-G^{(0)}_{RR}(x,x_1,i\omega)\,G^{(0)}_{RL}(x_1,x',i\omega)\,G^{(0)}_{LL}(x_1,x_2,i\omega_1)\,G^{(0)}_{RL}(x_2,x_1,i\omega_1)\,G^{(0)}_{LR}(x_2,x_2,i\omega_2)\\
&+G^{(0)}_{RR}(x,x_1,i\omega)\,G^{(0)}_{LL}(x_1,x',i\omega)\,G^{(0)}_{RR}(x_1,x_2,i\omega_1)\,G^{(0)}_{RL}(x_2,x_2,i\omega_2)\,G^{(0)}_{LL}(x_2,x_1,i\omega_1)\\
&+G^{(0)}_{RR}(x,x_1,i\omega)\,G^{(0)}_{LL}(x_1,x',i\omega)\,G^{(0)}_{RL}(x_1,x_2,i\omega_1)\,G^{(0)}_{RL}(x_2,x_1,i\omega_1)\,G^{(0)}_{LR}(x_2,x_2,i\omega_2)\\
&+G^{(0)}_{RR}(x,x_1,i\omega)\,G^{(0)}_{RL}(x_2,x',i\omega)\,G^{(0)}_{RL}(x_1,x_1,i\omega_1)\,G^{(0)}_{LL}(x_1,x_2,i\omega)\,G^{(0)}_{LR}(x_2,x_2,i\omega_2)\\
&-G^{(0)}_{RR}(x,x_1,i\omega)\,G^{(0)}_{RL}(x_2,x',i\omega)\,G^{(0)}_{RR}(x_1,x_2,i\omega-i\omega_1+i\omega_2)\,G^{(0)}_{LL}(x_1,x_2,i\omega_1)\,G^{(0)}_{LL}(x_2,x_1,i\omega_2)\\
&+G^{(0)}_{RR}(x,x_1,i\omega)\,G^{(0)}_{RL}(x_2,x',i\omega)\,G^{(0)}_{RL}(x_1,x_2,i\omega-i\omega_1+i\omega_2)\,G^{(0)}_{LR}(x_1,x_2,i\omega_1)\,G^{(0)}_{LL}(x_2,x_1,i\omega_2)\\
&+G^{(0)}_{RR}(x,x_1,i\omega)\,G^{(0)}_{LL}(x_2,x',i\omega)\,G^{(0)}_{RL}(x_1,x_1,i\omega_1)\,G^{(0)}_{LR}(x_1,x_2,i\omega)\,G^{(0)}_{RL}(x_2,x_2,i\omega_2)\\
&+G^{(0)}_{RR}(x,x_1,i\omega)\,G^{(0)}_{LL}(x_2,x',i\omega)\,G^{(0)}_{RR}(x_1,x_2,i\omega-i\omega_1+i\omega_2)\,G^{(0)}_{LL}(x_1,x_2,i\omega_1)\,G^{(0)}_{RL}(x_2,x_1,i\omega_2)\\
&-G^{(0)}_{RR}(x,x_1,i\omega)\,G^{(0)}_{LL}(x_2,x',i\omega)\,G^{(0)}_{RL}(x_1,x_2,i\omega-i\omega_1+i\omega_2)\,G^{(0)}_{LR}(x_1,x_2,i\omega_1)\,G^{(0)}_{RL}(x_2,x_1,i\omega_2)\\
&+G^{(0)}_{RL}(x,x_1,i\omega)\,G^{(0)}_{RL}(x_1,x',i\omega)\,G^{(0)}_{LR}(x_1,x_2,i\omega_1)\,G^{(0)}_{RL}(x_2,x_2,i\omega_2)\,G^{(0)}_{LR}(x_2,x_1,i\omega_1)\\
&+G^{(0)}_{RL}(x,x_1,i\omega)\,G^{(0)}_{RL}(x_1,x',i\omega)\,G^{(0)}_{LL}(x_1,x_2,i\omega_1)\,G^{(0)}_{RR}(x_2,x_1,i\omega_1)\,G^{(0)}_{LR}(x_2,x_2,i\omega_2)\\
&-G^{(0)}_{RL}(x,x_1,i\omega)\,G^{(0)}_{LL}(x_1,x',i\omega)\,G^{(0)}_{RR}(x_1,x_2,i\omega_1)\,G^{(0)}_{RL}(x_2,x_2,i\omega_2)\,G^{(0)}_{LR}(x_2,x_1,i\omega_1)\\
&-G^{(0)}_{RL}(x,x_1,i\omega)\,G^{(0)}_{LL}(x_1,x',i\omega)\,G^{(0)}_{RL}(x_1,x_2,i\omega_1)\,G^{(0)}_{RR}(x_2,x_1,i\omega_1)\,G^{(0)}_{LR}(x_2,x_2,i\omega_2)\\
&+G^{(0)}_{RL}(x,x_1,i\omega)\,G^{(0)}_{RL}(x_2,x',i\omega)\,G^{(0)}_{RR}(x_1,x_2,i\omega-i\omega_1+i\omega_2)\,G^{(0)}_{LL}(x_1,x_2,i\omega_1)\,G^{(0)}_{LR}(x_2,x_1,i\omega_2)\\
&+G^{(0)}_{RL}(x,x_1,i\omega)\,G^{(0)}_{RL}(x_2,x',i\omega)\,G^{(0)}_{RL}(x_1,x_2,i\omega)\,G^{(0)}_{LR}(x_1,x_1,i\omega_1)\,G^{(0)}_{LR}(x_2,x_2,i\omega_2)\\
&-G^{(0)}_{RL}(x,x_1,i\omega)\,G^{(0)}_{RL}(x_2,x',i\omega)\,G^{(0)}_{RL}(x_1,x_2,i\omega-i\omega_1+i\omega_2)\,G^{(0)}_{LR}(x_1,x_2,i\omega_1)\,G^{(0)}_{LR}(x_2,x_1,i\omega_2)\\
&+G^{(0)}_{RL}(x,x_1,i\omega)\,G^{(0)}_{LL}(x_2,x',i\omega)\,G^{(0)}_{RR}(x_1,x_2,i\omega)\,G^{(0)}_{LR}(x_1,x_1,i\omega_1)\,G^{(0)}_{RL}(x_2,x_2,i\omega_2)\\
&-G^{(0)}_{RL}(x,x_1,i\omega)\,G^{(0)}_{LL}(x_2,x',i\omega)\,G^{(0)}_{RR}(x_1,x_2,i\omega-i\omega_1+i\omega_2)\,G^{(0)}_{LL}(x_1,x_2,i\omega_1)\,G^{(0)}_{RR}(x_2,x_1,i\omega_2)\\
&+G^{(0)}_{RL}(x,x_1,i\omega)\,G^{(0)}_{LL}(x_2,x',i\omega)\,G^{(0)}_{RL}(x_1,x_2,i\omega-i\omega_1+i\omega_2)\,G^{(0)}_{LR}(x_1,x_2,i\omega_1)\,G^{(0)}_{RR}(x_2,x_1,i\omega_2)] \quad (2.232)
\end{aligned}$$

As done for the first order we have to compute each contribution. We have

$$\begin{aligned}
\delta G^{(2)}_{RL}(x,x',i\omega) \approx \frac{g^2}{\beta^2 v^5}\sum_{\omega_1,\omega_2}\int_0^L dx_1\int_0^L dx_2\Theta(\omega)e^{-\frac{\omega}{v}(x+x')}\\
[&-i\Theta(-\omega_1)\,\Theta(\omega_2)\,\Theta(x_2-x_1)\,S(i\omega)\,S^*(i\omega_1)\,S(i\omega_2)\,e^{2\frac{x_1}{v}0}e^{2\frac{x_2}{v}(\omega_1-\omega_2)}\\
&+i\Theta(\omega_1)\,\Theta(-\omega_2)\,\Theta(x_2-x_1)\,S(i\omega)\,S(i\omega_1)\,S^*(i\omega_2)\,e^{2\frac{x_1}{v}0}e^{2\frac{x_2}{v}(\omega_2-\omega_1)}\\
&+i\Theta(\omega_1)\,\Theta(\omega_2)\,\Theta(x_1-x_2)\,S(i\omega_2)\,e^{2\frac{x_1}{v}(\omega-\omega_1)}e^{2\frac{x_2}{v}(\omega_1-\omega_2)}\\
&+i\Theta(-\omega_1)\,\Theta(\omega_2)\,\Theta(x_2-x_1)\,S(i\omega_2)\,e^{2\frac{x_1}{v}(\omega-\omega_1)}e^{2\frac{x_2}{v}(\omega_1-\omega_2)}\\
&-i\Theta(\omega_1)\,\Theta(-\omega_2)\,S(i\omega_1)\,S(i\omega_1)\,S^*(i\omega_2)\,e^{2\frac{x_1}{v}(\omega-\omega_1)}e^{2\frac{x_2}{v}(\omega_2-\omega_1)}\\
&-i\Theta(\omega_1)\,\Theta(-\omega_2)\,\Theta(x_2-x_1)\,S(i\omega)\,S(i\omega_1)\,S^*(i\omega_2)\,e^{2\frac{x_1}{v}(\omega-\omega_1)}e^{2\frac{x_2}{v}(\omega_2-\omega)}\\
&+i\Theta(-\omega_1)\,\Theta(\omega_2)\,\Theta(x_1-x_2)\,S(i\omega)\,e^{2\frac{x_1}{v}(\omega_1-\omega_2)}e^{2\frac{x_2}{v}(\omega_2-\omega_1)}\\
&-i\Theta(\omega_1)\,\Theta(-\omega_2)\,\Theta(\omega_1-\omega-\omega_2)\,\Theta(x_2-x_1)\,S(i\omega)\,e^{2\frac{x_1}{v}(\omega_1-\omega_2)}e^{2\frac{x_2}{v}(\omega_2-\omega_1)}
\end{aligned}$$

$$
\begin{aligned}
&-i\Theta\left(-\omega_1\right)\Theta\left(\omega_2\right)\Theta\left(x_1-x_2\right)S\left(i\omega\right)S\left(i\omega-i\omega_1+i\omega_2\right)S^*\left(i\omega_1\right)e^{2\frac{x_1}{v}\left(\omega_1-\omega_2\right)}e^{2\frac{x_2}{v}\left(\omega_1-\omega\right)}\\
&+i\Theta\left(-\omega_1\right)\Theta\left(-\omega_2\right)\Theta\left(\omega-\omega_1+\omega_2\right)\Theta\left(x_2-x_1\right)S\left(i\omega\right)S\left(i\omega-i\omega_1+i\omega_2\right)S^*\left(i\omega_1\right)e^{2\frac{x_1}{v}\left(\omega_1-\omega_2\right)}e^{2\frac{x_2}{v}\left(\omega_1-\omega\right)}\\
&+0\\
&-i\Theta\left(-\omega_1\right)\Theta\left(\omega_2\right)\Theta\left(x_1-x_2\right)S\left(i\omega_2\right)e^{2\frac{x_1}{v}\left(\omega_1-\omega_2\right)}e^{2\frac{x_2}{v}\left(\omega-\omega_1\right)}\\
&-i\Theta\left(\omega_2\right)\Theta\left(\omega_1-\omega-\omega_2\right)\Theta\left(x_2-x_1\right)S\left(i\omega_2\right)e^{2\frac{x_1}{v}\left(\omega_1-\omega_2\right)}e^{2\frac{x_2}{v}\left(\omega-\omega_1\right)}\\
&+i\Theta\left(-\omega_1\right)\Theta\left(\omega_2\right)S\left(i\omega-i\omega_1+i\omega_2\right)S^*\left(i\omega_1\right)S\left(i\omega_2\right)e^{2\frac{x_1}{v}\left(\omega_1-\omega_2\right)}e^{2\frac{x_2}{v}\left(\omega_1-\omega_2\right)}\\
&+i\Theta\left(-\omega_1\right)\Theta\left(\omega_2\right)S\left(i\omega\right)S\left(i\omega\right)S^*\left(i\omega_1\right)S\left(i\omega_2\right)S^*\left(i\omega_1\right)e^{2\frac{x_1}{v}\left(\omega_1-\omega\right)}e^{2\frac{x_2}{v}\left(\omega_1-\omega_2\right)}\\
&-i\Theta\left(\omega_1\right)\Theta\left(-\omega_2\right)\Theta\left(x_2-x_1\right)S\left(i\omega\right)S\left(i\omega\right)S^*\left(i\omega_2\right)e^{2\frac{x_1}{v}\left(\omega_1-\omega\right)}e^{2\frac{x_2}{v}\left(\omega_2-\omega_1\right)}\\
&-i\Theta\left(-\omega_1\right)\Theta\left(-\omega_2\right)\Theta\left(x_1-x_2\right)S\left(i\omega\right)S\left(i\omega\right)S^*\left(i\omega_2\right)e^{2\frac{x_1}{v}\left(\omega_1-\omega\right)}e^{2\frac{x_2}{v}\left(\omega_2-\omega_1\right)}\\
&-i\Theta\left(-\omega_1\right)\Theta\left(\omega_2\right)\Theta\left(x_2-x_1\right)S\left(i\omega\right)S\left(i\omega_2\right)S^*\left(i\omega_1\right)e^{2\frac{x_1}{v}0}e^{2\frac{x_2}{v}\left(\omega_1-\omega_2\right)}\\
&+i\Theta\left(\omega_1\right)\Theta\left(-\omega_2\right)\Theta\left(x_2-x_1\right)S\left(i\omega\right)S\left(i\omega_1\right)S^*\left(i\omega_2\right)e^{2\frac{x_1}{v}0}e^{2\frac{x_2}{v}\left(\omega_2-\omega_1\right)}\\
&+i\Theta\left(-\omega_1\right)\Theta\left(-\omega_2\right)\Theta\left(\omega-\omega_1+\omega_2\right)\Theta\left(x_1-x_2\right)S\left(i\omega\right)S\left(i\omega\right)S^*\left(i\omega_2\right)e^{2\frac{x_1}{v}\left(\omega_1-\omega\right)}e^{2\frac{x_2}{v}\left(\omega_2-\omega_1\right)}\\
&+i\Theta\left(\omega_1\right)\Theta\left(-\omega_2\right)\Theta\left(\omega_1-\omega-\omega_2\right)\Theta\left(x_2-x_1\right)S\left(i\omega\right)S\left(i\omega\right)S^*\left(i\omega_2\right)e^{2\frac{x_1}{v}\left(\omega_1-\omega\right)}e^{2\frac{x_2}{v}\left(\omega_2-\omega_1\right)}\\
&+i\Theta\left(-\omega_1\right)\Theta\left(-\omega_2\right)S\left(i\omega\right)S\left(i\omega\right)S\left(i\omega\right)S^*\left(i\omega_1\right)S^*\left(i\omega_2\right)e^{2\frac{x_1}{v}\left(\omega_1-\omega\right)}e^{2\frac{x_2}{v}\left(\omega_2-\omega\right)}\\
&-i\Theta\left(-\omega_1\right)\Theta\left(-\omega_2\right)\Theta\left(\omega-\omega_1+\omega_2\right)S\left(i\omega\right)S\left(i\omega\right)S\left(i\omega-i\omega_1+i\omega_2\right)S^*\left(i\omega_1\right)S^*\left(i\omega_2\right)e^{2\frac{x_1}{v}\left(\omega_1-\omega\right)}e^{2\frac{x_2}{v}\left(\omega_1-\omega\right)}\\
&-i\Theta\left(-\omega_1\right)\Theta\left(\omega_2\right)\Theta\left(x_1-x_2\right)S\left(i\omega\right)S^*\left(i\omega_1\right)S\left(i\omega_2\right)e^{2\frac{x_1}{v}\left(\omega_1-\omega\right)}e^{2\frac{x_2}{v}\left(\omega-\omega_2\right)}\\
&-i\Theta\left(-\omega_1\right)\Theta\left(-\omega_2\right)\Theta\left(\omega-\omega_1+\omega_2\right)\Theta\left(x_1-x_2\right)S\left(i\omega\right)e^{2\frac{x_1}{v}\left(\omega_1-\omega\right)}e^{2\frac{x_2}{v}\left(\omega-\omega_1\right)}\\
&+i\Theta\left(\omega_2\right)\Theta\left(\omega_1-\omega-\omega_2\right)\Theta\left(x_2-x_1\right)S\left(i\omega\right)e^{2\frac{x_1}{v}\left(\omega_1-\omega\right)}e^{2\frac{x_2}{v}\left(\omega-\omega_1\right)}\\
&-i\Theta\left(-\omega_1\right)\Theta\left(\omega_2\right)\Theta\left(\omega-\omega_1+\omega_2\right)\Theta\left(x_2-x_1\right)S\left(i\omega\right)S\left(i\omega-i\omega_1+i\omega_2\right)S^*\left(i\omega_1\right)e^{2\frac{x_1}{v}\left(\omega_1-\omega\right)}e^{2\frac{x_2}{v}\left(\omega_1-\omega_2\right)}\\
&+i\Theta\left(-\omega_1\right)\Theta\left(-\omega_2\right)\Theta\left(\omega-\omega_1+\omega_2\right)\Theta\left(x_1-x_2\right)S\left(i\omega\right)S\left(i\omega-i\omega_1+i\omega_2\right)S^*\left(i\omega_1\right)e^{2\frac{x_1}{v}\left(\omega_1-\omega\right)}e^{2\frac{x_2}{v}\left(\omega_1-\omega_2\right)}]
\end{aligned}
\tag{2.233}
$$

Now we can note that first and second line are equal and opposite, 11th line is zero, fourth and 12th lines are equal and opposite, 18th and 14th are equal and opposite. Comparing with Eq. [2.71] we are left with

$$
\begin{aligned}
&\delta S^{(2)}\left(i\omega\right)=\frac{g^2}{\beta^2v^4}\\
&[+\sum_{\omega_1}^{>0}\sum_{\omega_2}^{>0}S\left(i\omega_2\right)\int_0^L dx_2e^{2\frac{x_2}{v}\left(\omega_1-\omega_2\right)}\int_{x_2}^L dx_1e^{2\frac{x_1}{v}\left(\omega-\omega_1\right)}\\
&-\sum_{\omega_1}^{>0}\sum_{\omega_2}^{<0}S\left(i\omega_1\right)S\left(i\omega_1\right)S^*\left(i\omega_2\right)\int_0^L dx_1e^{2\frac{x_1}{v}\left(\omega-\omega_1\right)}\int_0^L dx_2e^{2\frac{x_2}{v}\left(\omega_2-\omega_1\right)}\\
&-\sum_{\omega_1}^{>0}\sum_{\omega_2}^{<0}S\left(i\omega\right)S\left(i\omega_1\right)S^*\left(i\omega_2\right)\int_0^L dx_1e^{2\frac{x_1}{v}\left(\omega-\omega_1\right)}\int_{x_1}^L dx_2e^{2\frac{x_2}{v}\left(\omega_2-\omega\right)}\\
&+\sum_{\omega_1}^{<0}\sum_{\omega_2}^{>0}S\left(i\omega\right)\int_0^L dx_2e^{2\frac{x_2}{v}\left(\omega_2-\omega_1\right)}\int_{x_2}^L dx_1e^{2\frac{x_1}{v}\left(\omega_1-\omega_2\right)}\\
&-\sum_{\omega_1}^{>0}\sum_{\omega_2}^{<0}\Theta\left(\omega_1-\omega-\omega_2\right)S\left(i\omega\right)\int_0^L dx_1e^{2\frac{x_1}{v}\left(\omega_1-\omega_2\right)}\int_{x_1}^L dx_2e^{2\frac{x_2}{v}\left(\omega_2-\omega_1\right)}\\
&-\sum_{\omega_1}^{<0}\sum_{\omega_2}^{>0}S\left(i\omega\right)S\left(i\omega-i\omega_1+i\omega_2\right)S^*\left(i\omega_1\right)\int_0^L dx_2e^{2\frac{x_2}{v}\left(\omega_1-\omega\right)}\int_{x_2}^L dx_1e^{2\frac{x_1}{v}\left(\omega_1-\omega_2\right)}
\end{aligned}
$$

$$
\begin{aligned}
&+\sum_{\omega_1}^{<0}\sum_{\omega_2}^{<0}\Theta\left(\omega-\omega_1+\omega_2\right)S\left(i\omega\right)S\left(i\omega-i\omega_1+i\omega_2\right)S^{*}\left(i\omega_1\right)\int_0^L dx_1 e^{2\frac{x_1}{v}\left(\omega_1-\omega_2\right)}\int_{x_1}^L dx_2 e^{2\frac{x_2}{v}\left(\omega_1-\omega\right)}\\
&-\sum_{\omega_1}^{<0}\sum_{\omega_2}^{>0}\Theta\left(\omega_1-\omega-\omega_2\right)S\left(i\omega_2\right)\int_0^L dx_1 e^{2\frac{x_1}{v}\left(\omega_1-\omega_2\right)}\int_{x_1}^L dx_2 e^{2\frac{x_2}{v}\left(\omega-\omega_1\right)}\\
&+\sum_{\omega_1}^{<0}\sum_{\omega_2}^{>0}S\left(i\omega-i\omega_1+i\omega_2\right)S^{*}\left(i\omega_1\right)S\left(i\omega_2\right)\int_0^L dx_1 e^{2\frac{x_1}{v}\left(\omega_1-\omega_2\right)}\int_0^L dx_2 e^{2\frac{x_2}{v}\left(\omega_1-\omega_2\right)}\\
&+\sum_{\omega_1}^{<0}\sum_{\omega_2}^{>0}S\left(i\omega\right)S\left(i\omega\right)S^{*}\left(i\omega_1\right)S\left(i\omega_2\right)S^{*}\left(i\omega_1\right)\int_0^L dx_1 e^{2\frac{x_1}{v}\left(\omega_1-\omega\right)}\int_0^L dx_2 e^{2\frac{x_2}{v}\left(\omega_1-\omega_2\right)}\\
&-\sum_{\omega_1}^{>0}\sum_{\omega_2}^{<0}S\left(i\omega\right)S\left(i\omega\right)S^{*}\left(i\omega_2\right)\int_0^L dx_1 e^{2\frac{x_1}{v}\left(\omega_1-\omega\right)}\int_{x_1}^L dx_2 e^{2\frac{x_2}{v}\left(\omega_2-\omega_1\right)}\\
&-\sum_{\omega_1}^{<0}\sum_{\omega_2}^{<0}S\left(i\omega\right)S\left(i\omega\right)S^{*}\left(i\omega_2\right)\int_0^L dx_2 e^{2\frac{x_2}{v}\left(\omega_2-\omega_1\right)}\int_{x_2}^L dx_1 e^{2\frac{x_1}{v}\left(\omega_1-\omega\right)}\\
&+\sum_{\omega_1}^{<0}\sum_{\omega_2}^{<0}\Theta\left(\omega-\omega_1+\omega_2\right)S\left(i\omega\right)S\left(i\omega\right)S^{*}\left(i\omega_2\right)\int_0^L dx_2 e^{2\frac{x_2}{v}\left(\omega_2-\omega_1\right)}\int_{x_2}^L dx_1 e^{2\frac{x_1}{v}\left(\omega_1-\omega\right)}\\
&+\sum_{\omega_1}^{>0}\sum_{\omega_2}^{<0}\Theta\left(\omega_1-\omega-\omega_2\right)S\left(i\omega\right)S\left(i\omega\right)S^{*}\left(i\omega_2\right)\int_0^L dx_1 e^{2\frac{x_1}{v}\left(\omega_1-\omega\right)}\int_0^L dx_2 e^{2\frac{x_2}{v}\left(\omega_2-\omega_1\right)}\\
&+\sum_{\omega_1}^{<0}\sum_{\omega_2}^{<0}S\left(i\omega\right)S\left(i\omega\right)S\left(i\omega\right)S^{*}\left(i\omega_1\right)S^{*}\left(i\omega_2\right)\int_0^L dx_1 e^{2\frac{x_1}{v}\left(\omega_1-\omega\right)}\int_0^L dx_2 e^{2\frac{x_2}{v}\left(\omega_2-\omega\right)}\\
&-\sum_{\omega_1}^{<0}\sum_{\omega_2}^{<0}\Theta\left(\omega-\omega_1+\omega_2\right)S\left(i\omega\right)S\left(i\omega\right)S\left(i\omega-i\omega_1+i\omega_2\right)S^{*}\left(i\omega_1\right)S^{*}\left(i\omega_2\right)\int_0^L dx_1 e^{2\frac{x_1}{v}\left(\omega_1-\omega\right)}\int_0^L dx_2 e^{2\frac{x_2}{v}\left(\omega_1-\omega\right)}\\
&-\sum_{\omega_1}^{<0}\sum_{\omega_2}^{>0}S\left(i\omega\right)S^{*}\left(i\omega_1\right)S\left(i\omega_2\right)\int_0^L dx_2 e^{2\frac{x_2}{v}\left(\omega-\omega_2\right)}\int_{x_2}^L dx_1 e^{2\frac{x_1}{v}\left(\omega_1-\omega\right)}\\
&-\sum_{\omega_1}^{<0}\sum_{\omega_2}^{<0}\Theta\left(\omega-\omega_1+\omega_2\right)S\left(i\omega\right)\int_0^L dx_2 e^{2\frac{x_2}{v}\left(\omega-\omega_1\right)}\int_{x_2}^L dx_1 e^{2\frac{x_1}{v}\left(\omega_1-\omega\right)}\\
&+\sum_{\omega_1}^{>0}\sum_{\omega_2}^{<0}\Theta\left(\omega_1-\omega-\omega_2\right)S\left(i\omega\right)\int_0^L dx_1 e^{2\frac{x_1}{v}\left(\omega_1-\omega\right)}\int_{x_1}^L dx_2 e^{2\frac{x_2}{v}\left(\omega-\omega_1\right)}\\
&-\sum_{\omega_1}^{<0}\sum_{\omega_2}^{>0}\Theta\left(\omega-\omega_1+\omega_2\right)S\left(i\omega\right)S\left(i\omega-i\omega_1+i\omega_2\right)S^{*}\left(i\omega_1\right)\int_0^L dx_1 e^{2\frac{x_1}{v}\left(\omega_1-\omega\right)}\int_{x_1}^L dx_2 e^{2\frac{x_2}{v}\left(\omega_1-\omega_2\right)}\\
&+\sum_{\omega_1}^{<0}\sum_{\omega_2}^{<0}\Theta\left(\omega-\omega_1+\omega_2\right)S\left(i\omega\right)S\left(i\omega-i\omega_1+i\omega_2\right)S^{*}\left(i\omega_1\right)\int_0^L dx_2 e^{2\frac{x_2}{v}\left(\omega_1-\omega_2\right)}\int_{x_2}^L dx_1 e^{2\frac{x_1}{v}\left(\omega_1-\omega\right)}]
\end{aligned}
\tag{2.234}
$$

Integrating in dx_1 and dx_2, introducing the wire indices for the forward scattering, exchanging the sum over ω_i with an integral and letting the integral going from $-D$ to 0 we have that

$$\delta S^{(2)}_{j,j'}\left(i\omega\right)=\sum_{a,a'}\sum_{b,b'}\frac{g_{a,a'}g_{b,b'}}{4\left(2\pi\right)^{2}v^{2}}$$

$$[+\int_{-D}^{0}d\omega_1\int_{-D}^{0}d\omega_2\delta_{j,a}\delta_{a',j'}\delta_{a,b}S_{b,b'}\left(-i\omega_2\right)\delta_{b',a'}\frac{1}{\left(\omega+\omega_1\right)}$$

$$\left[\frac{1}{\left(\omega_2-\omega_1\right)}\left(e^{\frac{2L}{v}\left(\omega+\omega_2\right)}-e^{\frac{2L}{v}\left(\omega+\omega_1\right)}\right)-\frac{1}{\left(\omega+\omega_2\right)}\left(e^{\frac{2L}{v}\left(\omega+\omega_2\right)}-1\right)\right]$$

$$-\int_{-D}^{0}d\omega_1\int_{-D}^{0}d\omega_2\delta_{j,a}\delta_{a',j'}S_{a,b'}\left(-i\omega_1\right)S_{b,a'}\left(-i\omega_1\right)S^{*}_{b,b'}\left(i\omega_2\right)$$

$$\frac{1}{\left(\omega+\omega_1\right)\left(\omega_2+\omega_1\right)}\left[e^{\frac{2L}{v}\left(\omega+\omega_2+2\omega_1\right)}-e^{\frac{2L}{v}\left(\omega+\omega_1\right)}-e^{\frac{2L}{v}\left(\omega_2+\omega_1\right)}+1\right]$$

$$-\int_{-D}^{0}d\omega_1\int_{-D}^{0}d\omega_2\delta_{j,a}S_{b,j'}\left(i\omega\right)S_{a,a'}\left(-i\omega_1\right)\delta_{a',b'}S^{*}_{b,b'}\left(i\omega_2\right)\frac{1}{\left(\omega_2-\omega\right)}$$

$$\left[\frac{1}{\left(\omega+\omega_1\right)}\left(e^{\frac{2L}{v}\left(\omega_2+\omega_1\right)}-e^{\frac{2L}{v}\left(\omega_2-\omega\right)}\right)-\frac{1}{\left(\omega_2+\omega_1\right)}\left(e^{\frac{2L}{v}\left(\omega_2+\omega_1\right)}-1\right)\right]$$

$$+\int_{-D}^{0}d\omega_1\int_{-D}^{0}d\omega_2\delta_{j,a}S_{b,j'}\left(i\omega\right)\delta_{a,b}\delta_{a',b'}\delta_{b',a'}\frac{1}{\left(\omega_1+\omega_2\right)}\left[\frac{1}{\left(\omega_2+\omega_1\right)}\left(e^{\frac{2L}{v}\left(\omega_1+\omega_2\right)}-1\right)-\frac{2L}{v}\right]$$

$$-\int_{-D}^{0}d\omega_1\int_{-D}^{0}d\omega_2\Theta\left(-\omega_1-\omega-\omega_2\right)\delta_{j,a}S_{b,j'}\left(i\omega\right)\delta_{a,b}\delta_{a',b'}\delta_{b',a'}\frac{1}{\left(\omega_2+\omega_1\right)}$$

$$\left[\frac{1}{\left(\omega_1+\omega_2\right)}\left(e^{\frac{2L}{v}\left(\omega_2+\omega_1\right)}-1\right)-\frac{2L}{v}\right]$$

$$-\int_{-D}^{0}d\omega_1\int_{-D}^{0}d\omega_2\delta_{j,a}S_{b,j'}\left(i\omega\right)S_{a,b'}\left(i\omega-i\omega_1-i\omega_2\right)S^{*}_{b,a'}\left(i\omega_1\right)\delta_{b',a'}\frac{1}{\left(\omega_1+\omega_2\right)}$$

$$\left[\frac{1}{\left(\omega_1-\omega\right)}\left(e^{\frac{2L}{v}\left(2\omega_1-\omega+\omega_2\right)}-e^{\frac{2L}{v}\left(\omega_1+\omega_2\right)}\right)-\frac{1}{\left(2\omega_1-\omega+\omega_2\right)}\left(e^{\frac{2L}{v}\left(2\omega_1-\omega+\omega_2\right)}-1\right)\right]$$

$$+\int_{-D}^{0}d\omega_1\int_{-D}^{0}d\omega_2\Theta\left(\omega-\omega_1+\omega_2\right)\delta_{j,a}S_{b,j'}\left(i\omega\right)S_{a,b'}\left(i\omega-i\omega_1+i\omega_2\right)S^{*}_{b,a'}\left(i\omega_1\right)\delta_{b',a'}$$

$$\frac{1}{\left(\omega_1-\omega\right)}\left[\frac{1}{\left(\omega_1-\omega_2\right)}\left(e^{\frac{2L}{v}\left(2\omega_1-\omega-\omega_2\right)}-e^{\frac{2L}{v}\left(\omega_1-\omega\right)}\right)-\frac{1}{\left(2\omega_1-\omega-\omega_2\right)}\left(e^{\frac{2L}{v}\left(2\omega_1-\omega-\omega_2\right)}-1\right)\right]$$

$$-\int_{-D}^{D}d\omega_1\int_{-D}^{0}d\omega_2\Theta\left(\omega_1-\omega+\omega_2\right)\delta_{j,a}\delta_{b'j'}\delta_{a,b}\delta_{a',b'}S_{b,a'}\left(-i\omega_2\right)\frac{1}{\left(\omega-\omega_1\right)}$$

$$\left[\frac{1}{\left(\omega_1+\omega_2\right)}\left(e^{\frac{2L}{v}\left(\omega+\omega_2\right)}-e^{\frac{2L}{v}\left(\omega-\omega_1\right)}\right)-\frac{1}{\left(\omega+\omega_2\right)}\left(e^{\frac{2L}{v}\left(\omega+\omega_2\right)}-1\right)\right]$$

$$+\int_{-D}^{0}d\omega_1\int_{-D}^{0}d\omega_2\delta_{j,a}\delta_{b',j'}S_{a,b'}\left(i\omega-i\omega_1-i\omega_2\right)S^{*}_{b,a'}\left(i\omega_1\right)S_{b,a'}\left(-i\omega_2\right)$$

$$\frac{1}{\left(\omega_1+\omega_2\right)\left(\omega_1+\omega_2\right)}\left[e^{\frac{2L}{v}\left(2\omega_1+2\omega_2\right)}-2e^{\frac{2L}{v}\left(\omega_1+\omega_2\right)}+1\right]$$

$$+\int_{-D}^{0}d\omega_1\int_{-D}^{0}d\omega_2 S_{j,a'}\left(i\omega\right)S_{a,j'}\left(i\omega\right)S^{*}_{b,a'}\left(i\omega_1\right)S_{b,b'}\left(-i\omega_2\right)S^{*}_{a,b'}\left(i\omega_1\right)$$
$$\frac{1}{\left(\omega_1+\omega_2\right)\left(\omega_1-\omega\right)}\left[e^{\frac{2L}{v}\left(2\omega_1+\omega_2-\omega\right)}-e^{\frac{2L}{v}\left(\omega_1+\omega_2\right)}-e^{\frac{2L}{v}\left(\omega_1-\omega\right)}+1\right]$$
$$-\int_{-D}^{0}d\omega_1\int_{-D}^{0}d\omega_2 S_{j,a'}\left(i\omega\right)S_{a,j'}\left(i\omega\right)\delta_{a',b'}\delta_{b,a}S^{*}_{b,b'}\left(i\omega_2\right)\frac{1}{\left(\omega_2+\omega_1\right)}$$
$$\left[\frac{1}{\left(\omega_1+\omega\right)}\left(e^{\frac{2L}{v}\left(\omega_2+\omega_1\right)}-e^{\frac{2L}{v}\left(\omega_2-\omega\right)}\right)-\frac{1}{\left(\omega_2-\omega\right)}\left(e^{\frac{2L}{v}\left(\omega_2-\omega\right)}-1\right)\right]$$
$$-\int_{-D}^{0}d\omega_1\int_{-D}^{0}d\omega_2 S_{j,a'}\left(i\omega\right)S_{a,j'}\left(i\omega\right)\delta_{a',b'}\delta_{b,a}S^{*}_{b,b'}\left(i\omega_2\right)\frac{1}{\left(\omega_1-\omega\right)}$$
$$\left[\frac{1}{\left(\omega_2-\omega_1\right)}\left(e^{\frac{2L}{v}\left(\omega_2-\omega\right)}-e^{\frac{2L}{v}\left(\omega_1-\omega\right)}\right)-\frac{1}{\left(\omega_2-\omega\right)}\left(e^{\frac{2L}{v}\left(\omega_2-\omega\right)}-1\right)\right]$$
$$+\int_{-D}^{0}d\omega_1\int_{-D}^{0}d\omega_2\Theta\left(\omega-\omega_1+\omega_2\right)S_{j,a'}\left(i\omega\right)S_{b,j'}\left(i\omega\right)\delta_{a,b}\delta_{a',b'}S^{*}_{a,b'}\left(i\omega_2\right)\frac{1}{\left(\omega_1-\omega\right)}$$
$$\left[\frac{1}{\left(\omega_2-\omega_1\right)}\left(e^{\frac{2L}{v}\left(\omega_2-\omega\right)}-e^{\frac{2L}{v}\left(\omega_1-\omega\right)}\right)-\frac{1}{\left(\omega_2-\omega\right)}\left(e^{\frac{2L}{v}\left(\omega_2-\omega\right)}-1\right)\right]$$
$$+\int_{-D}^{0}d\omega_1\int_{-D}^{0}d\omega_2\Theta\left(-\omega_1-\omega-\omega_2\right)S_{j,a'}\left(i\omega\right)S_{b,j'}\left(i\omega\right)\delta_{a,b}\delta_{a',b'}S^{*}_{a,b'}\left(i\omega_2\right)\frac{1}{\left(\omega_2+\omega_1\right)}$$
$$\left[\frac{1}{\left(\omega_1+\omega\right)}\left(e^{\frac{2L}{v}\left(\omega_2+\omega_1\right)}-e^{\frac{2L}{v}\left(\omega_2-\omega\right)}\right)-\frac{1}{\left(\omega_2-\omega\right)}\left(e^{\frac{2L}{v}\left(\omega_2-\omega\right)}-1\right)\right]$$
$$+\int_{-D}^{0}d\omega_1\int_{-D}^{0}d\omega_2 S_{j,a'}\left(i\omega\right)S_{b,j'}\left(i\omega\right)S_{a,b'}\left(i\omega\right)S^{*}_{a,a'}\left(i\omega_1\right)S^{*}_{b,b'}\left(i\omega_2\right)\frac{1}{\left(\omega_1-\omega\right)\left(\omega_2-\omega\right)}$$
$$\left[e^{\frac{2L}{v}\left(\omega_1+\omega_2-2\omega\right)}-e^{\frac{2L}{v}\left(\omega_1-\omega\right)}-e^{\frac{2L}{v}\left(\omega_2-\omega\right)}+1\right]$$
$$-\int_{-D}^{0}d\omega_1\int_{-D}^{0}d\omega_2\Theta\left(\omega-\omega_1+\omega_2\right)S_{j,a'}\left(i\omega\right)S_{b,j'}\left(i\omega\right)S_{a,b'}\left(i\omega-i\omega_1+i\omega_2\right)S^{*}_{b,a'}\left(i\omega_1\right)S^{*}_{a,b'}\left(i\omega_2\right)$$
$$\frac{1}{\left(\omega_1-\omega\right)\left(\omega_1-\omega\right)}\left[e^{\frac{2L}{v}\left(2\omega_1-2\omega\right)}-2e^{\frac{2L}{v}\left(\omega_1-\omega\right)}+1\right]$$
$$-\int_{-D}^{0}d\omega_1\int_{-D}^{0}d\omega_2 S_{j,a'}\left(i\omega\right)\delta_{b',j'}\delta_{a,b}S^{*}_{a,a'}\left(i\omega_1\right)S_{b,b'}\left(-i\omega_2\right)\frac{1}{\left(\omega_1-\omega\right)}$$
$$\left[\frac{1}{\left(\omega+\omega_2\right)}\left(e^{\frac{2L}{v}\left(\omega_1+\omega_2\right)}-e^{\frac{2L}{v}\left(\omega_1-\omega\right)}\right)-\frac{1}{\left(\omega_1+\omega_2\right)}\left(e^{\frac{2L}{v}\left(\omega_1+\omega_2\right)}-1\right)\right]$$
$$-\int_{-D}^{0}d\omega_1\int_{-D}^{0}d\omega_2\Theta\left(\omega-\omega_1+\omega_2\right)S_{j,a'}\left(i\omega\right)\delta_{b',j'}\delta_{a,b}\delta_{a',b'}\delta_{b,a}\frac{1}{\left(\omega_1-\omega\right)}\left[\frac{1}{\left(\omega-\omega_1\right)}\left(1-e^{\frac{2L}{v}\left(\omega_1-\omega\right)}\right)-\frac{2L}{v}\right]$$
$$+\int_{-D}^{D}d\omega_1\int_{-D}^{0}d\omega_2\Theta\left(\omega_1-\omega+\omega_2\right)S_{j,a'}\left(i\omega\right)\delta_{b',j'}\delta_{a,b}\delta_{a',b'}\delta_{b,a}\frac{1}{\left(\omega-\omega_1\right)}\left[\frac{1}{\left(\omega_1-\omega\right)}\left(1-e^{\frac{2L}{v}\left(\omega-\omega_1\right)}\right)-\frac{2L}{v}\right]$$
$$-\int_{-D}^{0}d\omega_1\int_{-D}^{0}d\omega_2\Theta\left(\omega-\omega_1-\omega_2\right)S_{j,a'}\left(i\omega\right)\delta_{b',j'}S_{a,b'}\left(i\omega-i\omega_1-i\omega_2\right)S^{*}_{b,a'}\left(i\omega_1\right)\delta_{b,a}$$

$$\frac{1}{(\omega_1+\omega_2)}\left[\frac{1}{(\omega_1-\omega)}\left(e^{\frac{2L}{v}(2\omega_1+\omega_2-\omega)}-e^{\frac{2L}{v}(\omega_1+\omega_2)}\right)-\frac{1}{(2\omega_1+\omega_2-\omega)}\left(e^{\frac{2L}{v}(2\omega_1+\omega_2-\omega)}-1\right)\right]$$
$$+\int_{-D}^{0}d\omega_1\int_{-D}^{0}d\omega_2\Theta\left(\omega-\omega_1+\omega_2\right)S_{j,a'}\left(i\omega\right)\delta_{b',j'}S_{a,b'}\left(i\omega-i\omega_1+i\omega_2\right)S^{*}_{b,a'}\left(i\omega_1\right)\delta_{b,a}$$
$$\frac{1}{(\omega_1-\omega)}\left[\frac{1}{(\omega_1-\omega_2)}\left(e^{\frac{2L}{v}(2\omega_1-\omega_2-\omega)}-e^{\frac{2L}{v}(\omega_1-\omega)}\right)-\frac{1}{(2\omega_1-\omega_2-\omega)}\left(e^{\frac{2L}{v}(2\omega_1-\omega_2-\omega)}-1\right)\right]]$$

At this point we apply the generalized Leibniz rule

$$\delta_D\int_{-D}^{0}d\omega_1\int_{-D}^{0}d\omega_2F\left(\omega_1,\omega_2\right)=\int_{-D}^{0}d\omega_1F\left(\omega_1,-D\right)\delta D+\int_{-D}^{0}d\omega_2F\left(-D,\omega_2\right)\delta D \tag{2.235}$$

term by term. Let us start from 1st+8th lines, after some manipulations we obtain

$$\delta_{1st}+\delta_{8th}\approx\frac{g_{j,j'}g_{j,j'}}{16\pi^2v^2}S_{j,j'}\left(iD\right)\frac{\delta D}{D}\left[\mathrm{Ei}\left(\frac{2L}{v}\omega\right)-\ln\left(\omega\right)+\ln\left(D\right)\right] \tag{2.236}$$

Using the Puiseux series of Ei(z)

$$Ei\left(z\right)=\gamma+\ln\left|z\right|+\sum_{n=1}^{\infty}\frac{z^n}{n\cdot n!} \tag{2.237}$$

where $\gamma\approx0,57721...$ is the Euler-Mascheroni constant, we are left with

$$\delta_{1st}+\delta_{8th}\approx\frac{g_{j,j'}g_{j,j'}}{16\pi^2v^2}S_{j,j'}\left(iD\right)\left[\gamma+...\right]\frac{\delta D}{D} \tag{2.238}$$

where ... stands for non sub leading corrections. Next terms is

$$\begin{aligned}\delta_{2nd}=&\frac{\sum_{a,a'}g_{j,j'}g_{a,a'}}{16\pi^2v^2}\delta D\\&[-\int_{-D}^{0}d\omega_1\frac{S_{j,a'}\left(-i\omega_1\right)S_{a,j'}\left(-i\omega_1\right)S^{*}_{a,a'}\left(-iD\right)}{\left(\omega+\omega_1\right)\left(\omega_1-D\right)}\left[e^{\frac{2L}{v}(2\omega_1-D)}-e^{\frac{2L}{v}(\omega+\omega_1)}-e^{\frac{2L}{v}(\omega_1-D)}+1\right]\\&+\int_{-D}^{0}d\omega_2\frac{S_{j,a'}\left(iD\right)S_{a,j'}\left(iD\right)S^{*}_{a,a'}\left(i\omega_2\right)}{D\left(\omega_2-D\right)}\left[e^{\frac{2L}{v}(\omega_2-2D)}-e^{-\frac{2L}{v}D}-e^{\frac{2L}{v}(\omega_2-D)}+1\right]]\end{aligned} \tag{2.239}$$

It can not be further simplified without an explicit form for the scattering matrix. Instead, forgetting about the energy dependence of the scattering matrix we can solve the integrals to obtain

$$\delta_{2nd}\approx-\frac{\sum_{a,a'}g_{j,j'}g_{a,a'}}{16\pi^2v^2}S_{j,a'}S_{a,j'}S^{*}_{a,a'}\left[\gamma+...\right]\frac{\delta D}{D} \tag{2.240}$$

Next one is

$$\begin{aligned}\delta_{3rd}=&\frac{\sum_{a,a'}g_{j,a'}g_{a,a'}}{16\pi^2v^2}\delta D\\&[\int_{-D}^{0}d\omega_1\frac{S_{a,j'}\left(i\omega\right)S_{j,a'}\left(-i\omega_1\right)S^{*}_{a,a'}\left(-iD\right)}{D}\left[\frac{1}{(\omega+\omega_1)}\left(e^{\frac{2L}{v}(\omega_1-D)}-e^{-\frac{2L}{v}D}\right)-\frac{1}{(\omega_1-D)}\left(e^{\frac{2L}{v}(\omega_1-D)}-1\right)\right]\end{aligned}$$

$$-\int_{-D}^{0} d\omega_2 \frac{S_{a,j'}\left(i\omega\right) S_{j,a'}\left(iD\right) S^{*}_{a,a'}\left(i\omega_2\right)}{\left(\omega_2-\omega\right)} \left[\frac{1}{D}\left(e^{\frac{2L}{v}\left(\omega_2-\omega\right)}-e^{\frac{2L}{v}\left(\omega_2-D\right)}\right)-\frac{1}{\left(\omega_2-D\right)}\left(e^{\frac{2L}{v}\left(\omega_2-D\right)}-1\right)\right]] \quad (2.241)$$

In the energy independent case it reduces to

$$\delta_{3rd} \approx -\frac{\sum_{a,a'} g_{j,a'} g_{a,a'}}{16\pi^2 v^2} S_{a,j'} S_{j,a'} S^{*}_{a,a'} \left[\gamma + \ln\left(\frac{2L}{v}\right) + ...\right] \frac{\delta D}{D} \quad (2.242)$$

Proceeding, we have

$$\begin{aligned}\delta_{4th} &= \frac{\sum_a g_{j,a} g_{j,a}}{16\pi^2 v^2} 2\delta D[+\int_{-D}^{0} d\omega_1 S_{j,j'}\left(i\omega\right) \frac{1}{\left(\omega_1-D\right)} \left[\frac{1}{\left(\omega_1-D\right)}\left(e^{\frac{2L}{v}\left(\omega_1-D\right)}-1\right)-\frac{2L}{v}\right]] \\ &\approx -\frac{\sum_a g_{j,a} g_{j,a}}{16\pi^2 v^2} S_{j,j'}\left(i\omega\right) \frac{\delta D}{D} + ... \end{aligned} \quad (2.243)$$

and

$$\begin{aligned}\delta_{5th} &= \frac{\sum_a g_{j,a} g_{j,a}}{16\pi^2 v^2} \delta D \\ &\quad [-2\int_{-D}^{0} d\omega_1 \Theta\left(-\omega_1-\omega+D\right) S_{j,j'}\left(i\omega\right) \frac{1}{\left(\omega_1-D\right)} \left[\frac{1}{\left(\omega_1-D\right)}\left(e^{\frac{2L}{v}\left(\omega_1-D\right)}-1\right)-\frac{2L}{v}\right]] \\ &\approx \frac{\sum_a g_{j,a} g_{j,a}}{16\pi^2 v^2} S_{j,j'}\left(i\omega\right) \frac{\delta D}{D} + ... \end{aligned} \quad (2.244)$$

The following term is

$$\begin{aligned}\delta_{6th} &= \frac{\sum_{a,a'} g_{j,a'} g_{a,a'}}{16\pi^2 v^2} \delta D \\ &\quad [-\int_{-D}^{0} d\omega_1 \frac{S_{a,j'}\left(i\omega\right) S_{j,a'}\left(i\omega - i\omega_1 + iD\right) S^{*}_{a,a'}\left(i\omega_1\right)}{\left(\omega_1-D\right)} \\ &\quad \left[\frac{1}{\left(\omega_1-\omega\right)}\left(e^{\frac{2L}{v}\left(2\omega_1-D\right)}-e^{\frac{2L}{v}\left(\omega_1-D\right)}\right)-\frac{1}{\left(2\omega_1-D\right)}\left(e^{\frac{2L}{v}\left(2\omega_1-D\right)}-1\right)\right] \\ &\quad +\int_{-D}^{0} d\omega_2 \frac{S_{a,j'}\left(i\omega\right) S_{j,a'}\left(i\omega + iD - i\omega_2\right) S^{*}_{a,a'}\left(-iD\right)}{\left(\omega_2-D\right)} \\ &\quad \left[\frac{1}{D}\left(e^{\frac{2L}{v}\left(-2D+\omega_2\right)}-e^{\frac{2L}{v}\left(-D+\omega_2\right)}\right)-\frac{1}{\left(2D-\omega_2\right)}\left(e^{\frac{2L}{v}\left(-2D+\omega_2\right)}-1\right)\right]] \end{aligned} \quad (2.245)$$

Forgetting about the energy dependence of the scattering matrix and solving the integrals

$$\delta_{6th} = \frac{\sum_{a,a'} g_{j,a'} g_{a,a'}}{16\pi^2 v^2} S_{a,j'} S_{j,a'} S^{*}_{a,a'} \left[...\right] \frac{\delta D}{D} \quad (2.246)$$

We observe no linear contribution in $\ln D$. Then we have

$$\delta_{7th} \approx \frac{\sum_{a,a'} g_{j,a'} g_{a,a'}}{16\pi^2 v^2} \delta D$$

$$[+\int_{-D}^{0} d\omega_2 S_{a,j'}\left(i\omega\right) S_{j,a'}\left(i\omega+iD+i\omega_2\right) S^*_{a,a'}\left(-iD\right)$$
$$\frac{1}{D}\left[\frac{1}{\left(D+\omega_2\right)}\left(e^{\frac{2L}{v}\left(-2D-\omega_2\right)}-e^{-\frac{2L}{v}D}\right)-\frac{1}{\left(2D+\omega_2\right)}\left(e^{\frac{2L}{v}\left(-2D-\omega_2\right)}-1\right)\right]] \tag{2.247}$$

that in the energy independent case reduces to

$$\delta_{7th}=\frac{\sum_{a,a'} g_{j,a'}g_{a,a'}}{16\pi^2v^2}S_{a,j'}S_{j,a'}S^*_{a,a'}\left[...\right]\frac{\delta D}{D} \tag{2.248}$$

Again, no linear contribution in $\ln D$. The successive is

$$\delta_{9th}=\frac{\sum_{a,a'} g_{j,a'}g_{a,j'}}{16\pi^2v^2}\delta D$$
$$[+\int_{-D}^{0} d\omega_1\left[S_{j,j'}\left(i\omega-i\omega_1+iD\right)S^*_{a,a'}\left(i\omega_1\right)S_{a,a'}\left(iD\right)+S_{j,j'}\left(i\omega+iD-i\omega_1\right)S^*_{a,a'}\left(-iD\right)S_{a,a'}\left(-i\omega_1\right)\right]$$
$$\frac{1}{\left(\omega_1-D\right)\left(\omega_1-D\right)}\left[e^{\frac{2L}{v}\left(2\omega_1-2D\right)}-2e^{\frac{2L}{v}\left(\omega_1-D\right)}+1\right] \tag{2.249}$$

Forgetting about the energy dependence of the scattering matrix and solving the integral

$$\delta_{9th}=+2\frac{\sum_{a,a'} g_{j,a'}g_{a,j'}}{16\pi^2v^2}S_{j,j'}S^*_{a,a'}S_{a,a'}\left[\frac{1}{2}+...\right]\frac{\delta D}{D} \tag{2.250}$$

Next

$$\delta_{10th}=\frac{\sum_{a,a'}\sum_{b,b'} g_{a,a'}g_{b,b'}}{16\pi^2v^2}\delta D$$
$$[+\int_{-D}^{0} d\omega_1 S_{j,a'}\left(i\omega\right)S_{a,j'}\left(i\omega\right)S^*_{b,a'}\left(i\omega_1\right)S_{b,b'}\left(iD\right)S^*_{a,b'}\left(i\omega_1\right)$$
$$\frac{1}{\left(\omega_1-D\right)\left(\omega_1-\omega\right)}\left[e^{\frac{2L}{v}\left(2\omega_1-D\right)}-e^{\frac{2L}{v}\left(\omega_1-D\right)}-e^{\frac{2L}{v}\left(\omega_1-\omega\right)}+1\right]$$
$$-\int_{-D}^{0} d\omega_2 S_{j,a'}\left(i\omega\right)S_{a,j'}\left(i\omega\right)S^*_{b,a'}\left(-iD\right)S_{b,b'}\left(-i\omega_2\right)S^*_{a,b'}\left(-iD\right)$$
$$\frac{1}{\left(\omega_2-D\right)D}\left[e^{\frac{2L}{v}\left(-2D+\omega_2\right)}-e^{\frac{2L}{v}\left(-D+\omega_2\right)}-e^{-\frac{2L}{v}D}+1\right]] \tag{2.251}$$

with no energy dependence it is

$$\delta_{10th}=+\frac{\sum_{a,a'}\sum_{b,b'} g_{a,a'}g_{b,b'}}{16\pi^2v^2}S_{j,a'}S_{a,j'}S^*_{b,a'}S_{b,b'}S^*_{a,b'}\left[\gamma+\ln\left(\frac{2L}{v}\right)+...\right]\frac{\delta D}{D} \tag{2.252}$$

Next one is

$$\delta_{11th}\approx\frac{\sum_{a,a'} g_{a,a'}g_{a,a'}}{16\pi^2v^2}\delta D$$
$$[+\int_{-D}^{0} d\omega_2\frac{S_{j,a'}\left(i\omega\right)S_{a,j'}\left(i\omega\right)S^*_{a,a'}\left(i\omega_2\right)}{\left(\omega_2-D\right)}$$

$$\left[\frac{1}{D}\left(e^{\frac{2L}{v}(\omega_2-D)}-e^{\frac{2L}{v}(\omega_2-\omega)}\right)+\frac{1}{(\omega_2-\omega)}\left(e^{\frac{2L}{v}(\omega_2-\omega)}-1\right)\right]] \tag{2.253}$$

Forgetting about the energy dependence of the scattering matrix and solving the integral

$$\delta_{11th}=-\frac{\sum_{a,a'}g_{a,a'}g_{a,a'}}{16\pi^2v^2}S_{j,a'}S_{a,j'}S^*_{a,a'}\left[\gamma+...\right]\frac{\delta D}{D} \tag{2.254}$$

Likewise

$$\begin{aligned}\delta_{12th}\approx&\frac{\sum_{a,a'}g_{a,a'}g_{a,a'}}{16\pi^2v^2}\delta D\\&[-\frac{S_{j,a'}\left(i\omega\right)S_{a,j'}\left(i\omega\right)S^*_{a,a'}\left(-iD\right)}{D}\left[\gamma+\ln\left(\frac{2L}{v}\right)+...\right]\\&+\int_{-D}^{0}d\omega_2\frac{S_{j,a'}\left(i\omega\right)S_{a,j'}\left(i\omega\right)S^*_{a,a'}\left(i\omega_2\right)}{D}\\&\left[\frac{1}{(\omega_2+D)}\left(e^{\frac{2L}{v}(\omega_2-\omega)}-e^{-\frac{2L}{v}D}\right)-\frac{1}{(\omega_2-\omega)}\left(e^{\frac{2L}{v}(\omega_2-\omega)}-1\right)\right]]\end{aligned} \tag{2.255}$$

that can be reduced to

$$\delta_{12th}=-2\frac{\sum_{a,a'}g_{a,a'}g_{a,a'}}{16\pi^2v^2}S_{j,a'}S_{a,j'}S^*_{a,a'}\left[\gamma+...\right]\frac{\delta D}{D} \tag{2.256}$$

Next one is

$$\begin{aligned}\delta_{13th}\approx&\frac{\sum_{a,a'}g_{a,a'}g_{a,a'}}{16\pi^2v^2}\delta D\\&[+\int_{-D}^{0}d\omega_2\frac{S_{j,a'}\left(i\omega\right)S_{a,j'}\left(i\omega\right)S^*_{a,a'}\left(i\omega_2\right)}{(D+\omega)}\\&\left[\frac{1}{(\omega_2-\omega)}\left(e^{\frac{2L}{v}(\omega_2-\omega)}-1\right)-\frac{1}{(\omega_2+D)}\left(e^{\frac{2L}{v}(\omega_2-\omega)}-e^{-\frac{2L}{v}D}\right)\right]]\end{aligned} \tag{2.257}$$

that implies

$$\delta_{13th}=\frac{\sum_{a,a'}g_{a,a'}g_{a,a'}}{16\pi^2v^2}S_{j,a'}S_{a,j'}S^*_{a,a'}\left[\gamma+\ln\left(\frac{2L}{v}\right)+...\right]\frac{\delta D}{D} \tag{2.258}$$

The following is

$$\begin{aligned}\delta_{14th}\approx[+&\int_{-D}^{0}d\omega_2\frac{S_{j,a'}\left(i\omega\right)S_{a,j'}\left(i\omega\right)S^*_{a,a'}\left(i\omega_2\right)}{(\omega_2-D)}\\&\left[\frac{1}{D}\left(e^{\frac{2L}{v}(\omega_2-\omega)}-e^{\frac{2L}{v}(\omega_2-D)}\right)-\frac{1}{(\omega_2-\omega)}\left(e^{\frac{2L}{v}(\omega_2-\omega)}-1\right)\right]]\end{aligned} \tag{2.259}$$

such that

$$\delta_{14th}=\frac{\sum_{a,a'}g_{a,a'}g_{a,a'}}{16\pi^2v^2}S_{j,a'}S_{a,j'}S^*_{a,a'}\left[\gamma+...\right]\frac{\delta D}{D} \tag{2.260}$$

The sixteenth is

$$\delta_{15th} \approx \frac{\sum_{a,a'}\sum_{b,b'} g_{a,a'}g_{b,b'}}{16\pi^2 v^2}\delta D$$
$$[+\int_{-D}^{0} d\omega_1 \frac{\left[S_{j,a'}\left(i\omega\right)S_{b,j'}\left(i\omega\right)S_{a,b'}\left(i\omega\right)S^*_{a,a'}\left(i\omega_1\right)S^*_{b,b'}\left(-iD\right)+S_{j,a'}\left(i\omega\right)S_{b,j'}\left(i\omega\right)S_{a,b'}\left(i\omega\right)S^*_{a,a'}\left(-iD\right)S^*_{b,b'}\left(i\omega_1\right)\right]}{\left(\omega-\omega_1\right)D}$$
$$\left[e^{\frac{2L}{v}(\omega_1-D)}-e^{\frac{2L}{v}(\omega_1-\omega)}-e^{-\frac{2L}{v}D}+1\right]]$$

Forgetting about the energy dependence it becomes

$$\delta_{15th} = 2\frac{\sum_{a,a'}\sum_{b,b'} g_{a,a'}g_{b,b'}}{16\pi^2 v^2}S_{j,a'}S_{b,j'}S_{a,b'}S^*_{a,a'}S^*_{b,b'}\left[\gamma+...\right]\frac{\delta D}{D} \tag{2.261}$$

Next is

$$\delta_{16th} \approx \frac{\sum_{a,a'}\sum_{b,b'} g_{a,a'}g_{b,b'}}{16\pi^2 v^2}\delta D$$
$$[-\int_{-D}^{0} d\omega_2 S_{j,a'}\left(i\omega\right)S_{b,j'}\left(i\omega\right)S_{a,b'}\left(i\omega+iD+i\omega_2\right)S^*_{b,a'}\left(-iD\right)S^*_{a,b'}\left(i\omega_2\right)\frac{1}{D}] \tag{2.262}$$

and

$$\delta_{16th} = \frac{\sum_{a,a'}\sum_{b,b'} g_{a,a'}g_{b,b'}}{16\pi^2 v^2}S_{j,a'}S_{b,j'}S_{a,b'}S^*_{b,a'}S^*_{a,b'}\left[-1+...\right]\frac{\delta D}{D} \tag{2.263}$$

The following is

$$\delta_{17th} = \frac{\sum_{a,a'} g_{a,a'}g_{a,j'}}{16\pi^2 v^2}\delta D$$
$$[-\int_{-D}^{0} d\omega_1 \frac{S_{j,a'}\left(i\omega\right)S^*_{a,a'}\left(i\omega_1\right)S_{a,j'}\left(iD\right)}{\left(\omega_1-\omega\right)}$$
$$\left[\frac{1}{\left(\omega-D\right)}\left(e^{\frac{2L}{v}(\omega_1-D)}-e^{\frac{2L}{v}(\omega_1-\omega)}\right)-\frac{1}{\left(\omega_1-D\right)}\left(e^{\frac{2L}{v}(\omega_1-D)}-1\right)\right]$$
$$[+\int_{-D}^{0} d\omega_2 \frac{S_{j,a'}\left(i\omega\right)S^*_{a,a'}\left(-iD\right)S_{a,j'}\left(-i\omega_2\right)}{D}$$
$$\left[\frac{1}{\left(\omega+\omega_2\right)}\left(e^{\frac{2L}{v}(\omega_2-D)}-e^{-\frac{2L}{v}D}\right)-\frac{1}{\left(\omega_2-D\right)}\left(e^{\frac{2L}{v}(\omega_2-D)}-1\right)\right]] \tag{2.264}$$

such that

$$\delta_{17th} = -\frac{\sum_{a,a'} g_{a,a'}g_{a,j'}}{16\pi^2 v^2}S_{j,a'}S^*_{a,a'}S_{a,j'}\left[\gamma+...\right]\frac{\delta D}{D} \tag{2.265}$$

We have then

$$\delta_{18th} \approx \frac{\sum_{a} g_{a,j'}g_{a,j'}}{16\pi^2 v^2}\delta D[\int_{-D}^{0} d\omega_2 \frac{S_{j,j'}\left(i\omega\right)}{\left(D+\omega\right)}\left[\frac{1}{\left(\omega+D\right)}\left(1-e^{\frac{2L}{v}(-D-\omega)}\right)-\frac{2L}{v}\right]]$$

$$\approx \frac{\sum_a g_{a,j'} g_{a,j'}}{16\pi^2 v^2} \frac{\delta D}{D} S_{j,j'}\left(i\omega\right)\left[1-\frac{2LD}{v}\right] \tag{2.266}$$

and

$$\begin{aligned}\delta_{19th} &\approx \frac{\sum_a g_{a,j'} g_{a,j'}}{16\pi^2 v^2}\delta D\left[+\int_{-D}^{0} d\omega_2 \frac{S_{j,j'}\left(i\omega\right)}{D}\left[\frac{1}{D}\left(e^{\frac{2L}{v}(\omega-D)}-1\right)+\frac{2L}{v}\right]\right] \\ &\approx \frac{\sum_a g_{a,j'} g_{a,j'}}{16\pi^2 v^2}\frac{\delta D}{D} S_{j,j'}\left(i\omega\right)\left[\frac{2LD}{v}-1\right]\end{aligned} \tag{2.267}$$

Finally

$$\begin{aligned}\delta_{20th} = &\frac{\sum_{a,a'} g_{a,a'} g_{a,j'}}{16\pi^2 v^2}\delta D \\ &[-\int_{-D}^{0} d\omega_1 S_{j,a'}\left(i\omega\right) S_{a,j'}\left(i\omega - i\omega_1 + iD\right) S^*_{a,a'}\left(i\omega_1\right) \\ &\frac{1}{(\omega_1 - D)}\left[\frac{1}{(\omega_1-\omega)}\left(e^{\frac{2L}{v}(2\omega_1 - D)} - e^{\frac{2L}{v}(\omega_1 - D)}\right) - \frac{1}{(2\omega_1 - D)}\left(e^{\frac{2L}{v}(2\omega_1 - D)} - 1\right)\right] \\ &+\int_{-D}^{0} d\omega_2 S_{j,a'}\left(i\omega\right) S_{a,j'}\left(i\omega + iD - i\omega_2\right) S^*_{a,a'}\left(-iD\right) \\ &\frac{1}{(\omega_2 - D)}\left[\frac{1}{D}\left(e^{\frac{2L}{v}(-2D+\omega_2)} - e^{\frac{2L}{v}(-D+\omega_2)}\right) - \frac{1}{(2D-\omega_2)}\left(e^{\frac{2L}{v}(-2D+\omega_2)} - 1\right)\right]]\end{aligned} \tag{2.268}$$

that in the energy independent case gives no linear contribution in $\ln D$

$$\delta_{20th} = \frac{\sum_{a,a'} g_{a,a'} g_{a,j'}}{16\pi^2 v^2} S_{j,a'} S_{a,j'} S^*_{a,a'}\left[...\right]\frac{\delta D}{D} \tag{2.269}$$

like

$$\begin{aligned}\delta_{21th} \approx &\frac{\sum_{a,a'} g_{a,a'} g_{a,j'}}{16\pi^2 v^2}\delta D \\ &[+\int_{-D}^{0} d\omega_2 \Theta\left(\omega + D + \omega_2\right) S_{j,a'}\left(i\omega\right) S_{a,j'}\left(i\omega + iD + i\omega_2\right) S^*_{a,a'}\left(-iD\right) \\ &\frac{1}{D}\left[\frac{1}{(D+\omega_2)}\left(e^{\frac{2L}{v}(-2D-\omega_2)} - e^{-\frac{2L}{v}D}\right) - \frac{1}{(2D+\omega_2)}\left(e^{\frac{2L}{v}(-2D-\omega_2)} - 1\right)\right]]\end{aligned} \tag{2.270}$$

that is indeed

$$\delta_{21th} = \frac{\sum_{a,a'} g_{a,a'} g_{a,j'}}{16\pi^2 v^2} S_{j,a'} S_{a,j'} S^*_{a,a'}\left[...\right]\frac{\delta D}{D} \tag{2.271}$$

Adding together all the term computed above in both the energy dependent and independent cases gives the second order correction of the scattering matrix used in the main text.

III. DUAL FERMIONIC VARIABLES AND RENORMALIZATION GROUP APPROACH TO JUNCTIONS OF STRONGLY INTERACTING QUANTUM WIRES

Quite a three pipe problem.
Arthur Conan Doyle

In this Chapter, to overcome all the limitation of the fermionic and bosonic approaches we study a junction of spinful interacting QWs by making a combined use of bosonization and fermionization, that is, we go back and forth from fermionic to bosonic coordinates, and vice versa, to build "dual-fermion" representations of the junction in strongly interacting regimes. In resorting from a bosonic to a fermionic problem, our approach is reminiscent of the refermionization scheme used in Ref. [84] to discuss the large-distance behavior of the classical sine-Gordon model at the commensurate-incommensurate phase transition. Specifically, in Ref. [84] the refermionization allows for singling out at criticality the low-energy two-fermion excitations from the one-fermion ones and to prove that the latter ones keep gapped along the phase transitions and do not contribute to the large-distance scaling of the correlations. At variance, in our case it is the second of a two-step process, that ends up again into a fermionic "dual fermionic" model for the strongly-interacting system. The guideline to construct the appropriate novel fermionic degrees of freedom is to eventually rewrite the relevant boundary interactions as bilinear functionals of the fermionic fields. Specifically, moving from the original fermionic coordinates to the TLL-bosonic description of the junction, we are able to warp from the weakly interacting regime to different strongly interacting regimes. Therefore, at appropriate values of the interaction-dependent Luttinger parameters, we move back from the bosonic- to pertinent dual-fermionic coordinates, chosen so that the relevant boundary interactions are bilinear functionals of the fermionic fields. Our mapping between dual coordinates is actually preliminary to the implementation of the RG-approach.

The RG-approach formulated in fermionic coordinates, such as FRG, suffers of the limitation that it requires that relevant scattering processes at the junction are fully encoded in terms of a single-particle S-matrix. While this is certainly the case at weak bulk interaction, a strong attractive interaction in either charge-, or spin-channel (or in both) is known to stabilize phases (RG attractive fixed points) at which two-particle scattering is the most relevant process at the junction[25–29]. Just because of the way it is formulated, the FRG-approach fails to describe many-particle scattering processes, even after improvements of the technique that allow to circumvent the constraint of having a small bulk interaction[52–54]. Resorting to the appropriate dual-fermion basis allows us to describe within the FRG-approach also fixed points stabilized by many-particle scattering processes, as well as fixed points whose properties have not been mapped out within the TLL-framework in terms of a rotation matrix such as, for instance, the mysterious-fixed point in the three-wire junction of spinless quantum wires studied in Ref. [29] and its counterpart in the junction of spinful quantum wires. Moreover, in computing the conductance tensor along the RG-trajectories connecting fixed points of the phase diagram, we show how our approach, while being consistent with the TLL-approach in the range of parameters where both of them apply, on the other hand allows for complementing the results of Refs. [25–27, and 30] about the two-wire and the three-wire junction, with a number of additional results about the topology of their phase diagram and their conductance properties.

III.1. Dual Fermionic variables and renormalization group approach to the calculation of the conductance at a junction of two spinful interacting quantum wires

To introduce and check the validity of our approach, in this section we discuss a junction of two interacting spinful quantum wires. This appears to be quite an appropriate place to test our technique: indeed, the two-wire junction has widely been studied in the past, both within the bosonization approach[25–27], and by means of standard RG techniques for a weak bulk interaction[37–40]. The two-wire junction of spinful quantum wires is described by the ($K = 2$) Hamiltonian $H = H_B + H_I$ of Eqs. [2.9, 2.10]
For a weak bulk interaction, the most relevant contribution to H_B is given by a linear combination of the operators $B_{(j,j'),\sigma,(X,Y)}(0)$, defined as

$$B_{(j,j'),\sigma,(X,X')}(0) = \psi^{\dagger}_{X,j,\sigma}(0)\psi_{X',j',\sigma}(0) \tag{3.1}$$

with $X, X' = L, R$. Assuming equivalence between the two wires and a spin-symmetric and spin-conserving boundary interaction, H_B can be generically written as

$$H_B = \sum_{X,X'=L,R} \sum_{\sigma} \{[\tau_{X,X'} B_{(1,2),\sigma,(X,X')}(0) + \text{h.c.}] + \sum_{j=1,2} \mu_{X,X'} B_{(j,j),\sigma,(X,X')}(0)\} \tag{3.2}$$

In addition to the contributions reported in Eq. [3.2], terms that are quadratic (or of higher order) in the B's can in principle arise along RG-procedure, even if they are not present in the "bare" Hamiltonian. For instance, the simplest higher-order boundary interaction terms consistent with spin conservation at the junction, $H_{2,0}$ and $H_{0,2}$, are given by[25–27]

$$\begin{aligned} H_{2,0} &= V_{2,0} \sum_{X,X'=R,L} \{B_{(X,X'),\uparrow,(1,2)}(0) B_{(X',X),\downarrow,(1,2)}(0) + \text{h.c.}\} \\ H_{0,2} &= V_{0,2} \sum_{X,X'=R,L} \{B_{(X,X'),\uparrow,(1,2)}(0) B_{(X',X),\downarrow,(2,1)}(0) + \text{h.c.}\} \end{aligned} \tag{3.3}$$

III.1.1. The weakly interacting regime

As it can be shown using the bosonization approach, for a weak bulk interaction, higher-order operators such as those in Eqs. [3.3] are highly irrelevant operators and, accordingly they are typically ignored and one uses for H_B the formula in Eq. [3.2]. Physically, this means that the relevant scattering processes at the junction consist only of one single particle/hole scattered into one single particle/hole, such as those drawn in Fig. [12], panel a. These processes are fully described by the single-particle S-matrix, for which the renormalization group equations can be fully recovered using the technique we review in Sec. [II.4]. The symmetry requirements listed above imply that the single-particle S-matrix takes the block-diagonal form

$$S_{(j,\sigma);(j',\sigma')}(k) = \delta_{\sigma,\sigma'} S_{j,j'}(k) \tag{3.4}$$

with the $S(k)$-matrix being given by

$$S(k) = \begin{bmatrix} r_k & t_k \\ t_k & r_k \end{bmatrix} \tag{3.5}$$

and r_k and t_k respectively corresponding to the amplitude for the particle to be backscattered in the same wire, or transmitted into the other wire. In the following we will pose no particular constraints on the r_k's and the t_k's, except that, near the Fermi points, they are quite flat functions of k, without displaying particular features, such as a resonant behavior: accordingly, we assume that the amplitudes are all computed at the Fermi level and drop the $_k$ label (this is a specific case of the general assumptions on the behavior of the S-matrix elements near by the Fermi surface that we make in Sec. [II.4]). To write the RG-equations for the S-matrix elements, one needs the F matrix which, in this specific case, is given by Eq. [2.84] and has the form

$$F = \frac{1}{2} \begin{bmatrix} \beta r & 0 & 0 & 0 \\ 0 & \beta r & 0 & 0 \\ 0 & 0 & \beta r & 0 \\ 0 & 0 & 0 & \beta r \end{bmatrix} \tag{3.6}$$

with $\beta = \frac{1}{2\pi v} \left(-g_{1\parallel} - g_{1\perp} + g_{2\parallel}\right)$. Taking into account the symmetries of the S- and of the F-matrix, the RG-equations for the amplitudes r, t are obtained in the form

$$\begin{aligned} \frac{dr}{d\ell} &= \frac{\beta}{2} \left(r - r\,|r|^2 - r^* t^2\right) = \beta r\,|t|^2 \\ \frac{dt}{d\ell} &= -\beta t\,|r|^2 = -\beta (t - t\,|t|^2) \end{aligned} \tag{3.7}$$

Equations [3.7] must be supplemented with the RG-equation for the running strength β, which is given by

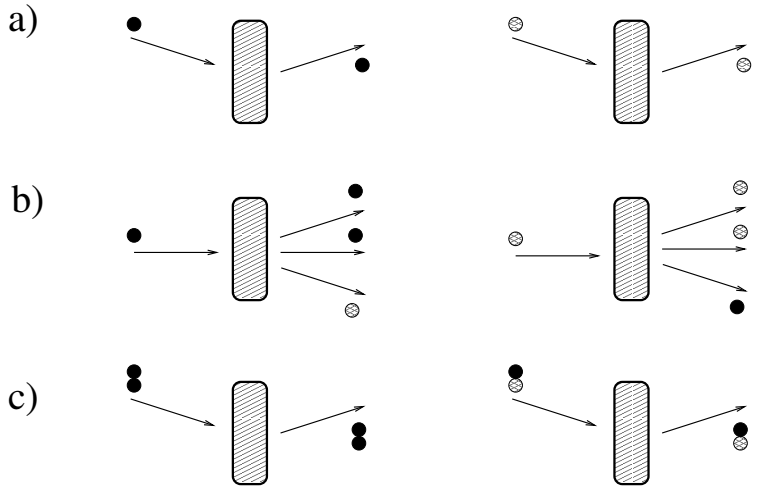

FIG. 12. Sketch of possible scattering processes at a two-wire junction (note that incoming particles from wire j can either be scattered into the same wire, or into a different wire):
(a) Single-particle/single-hole scattering processes. These are determined by $H_{\rm tun}$ in Eq. [3.2] and are fully described in terms of a single-particle S-matrix;
(b) Many-body scattering processes in which one particle/one hole is scattered into two particles and one hole/two holes and one particle. These processes can be induced by boundary interaction Hamiltonians such as those in Eq. [3.3] and their proliferation requires resorting to a bosonic Luttinger-liquid description of the junction;
(c) Scattering processes for a particle-particle and for a particle-hole pair. These are again determined by the Hamiltonians in Eq. [3.3] and are the only allowed processes in the presence of a strong repulsive (attractive) interaction in the spin (charge) channel, and vice versa. On pertinently defining new fermionic coordinates, they can still be described in terms of a "single-pair" S-matrix.

$$\frac{d\beta}{d\ell} = \frac{1}{(2\pi v)^2}\{(g_{1,\perp})^2 + 2g_{1,\perp}\left(g_{2,\perp} - g_{2,\parallel} + g_{1,\parallel}\right)\} \tag{3.8}$$

(See Eqs. [2.57] for the definition of the bulk interaction strengths $g_{j,1(2),\perp}, g_{j,1(2),\parallel}$: here we drop the wire index j as the interaction strengths are assumed to be the same in each wire.) Equations [3.7], together with Eq. [3.8] and Eqs. [2.102] for the running interaction strengths, constitute a closed set of equations, whose solution yields the scaling functions $r(D), t(D)$. From the explicit formulas for the running scattering amplitudes, one may readily compute the charge- and the spin-conductance tensors, using the formulas derived in Appendix [II.8]. As a result, due to the symmetries of the S-matrix, the charge- and the spin-conductance tensor are equal to each other and both given by

$$G_c(D) = G_s(D) = G(D)\begin{bmatrix} 1 & -1 \\ -1 & 1 \end{bmatrix} \tag{3.9}$$

with $G(D) = \frac{e^2}{\pi}|t(D)|^2$. An explicit analytical formula can be provided for $G(D)$ in some simple cases such as, for instance, if $g_{1\perp}$ is fine-tuned to 0. In this case, as it arises from Eq. [3.8], β keeps constant along the RG-trajectories and, therefore, one may exactly integrate Eqs. [3.7] for $r(D)$ and $t(D)$. One obtains

$$G(D) = \frac{e^2}{\pi}\,\frac{T_0\,|D/D_0|^{2\beta}}{R_0 + T_0\,|D/D_0|^{2\beta}} \tag{3.10}$$

with $T_0 = 1 - R_0 = |t_0|^2$ and r_0, t_0 corresponding to the "bare" scattering amplitudes in Eq. [3.5]. Another case in which an explicit analytical solution can be provided corresponds to having $g_{1\perp} = g_{1\parallel} = g_1$ and $g_{2\perp} = g_{2\parallel} = g_2$. In this case, the set of Eqs. [2.102] collapse onto a set of two equations for $g_1(D), g_2(D)$ which can be readily integrated, yielding the running interaction strengths

$$g_1(D) = \frac{g_1}{1 + \frac{g_1}{\pi v}\ln\frac{D_0}{D}}$$

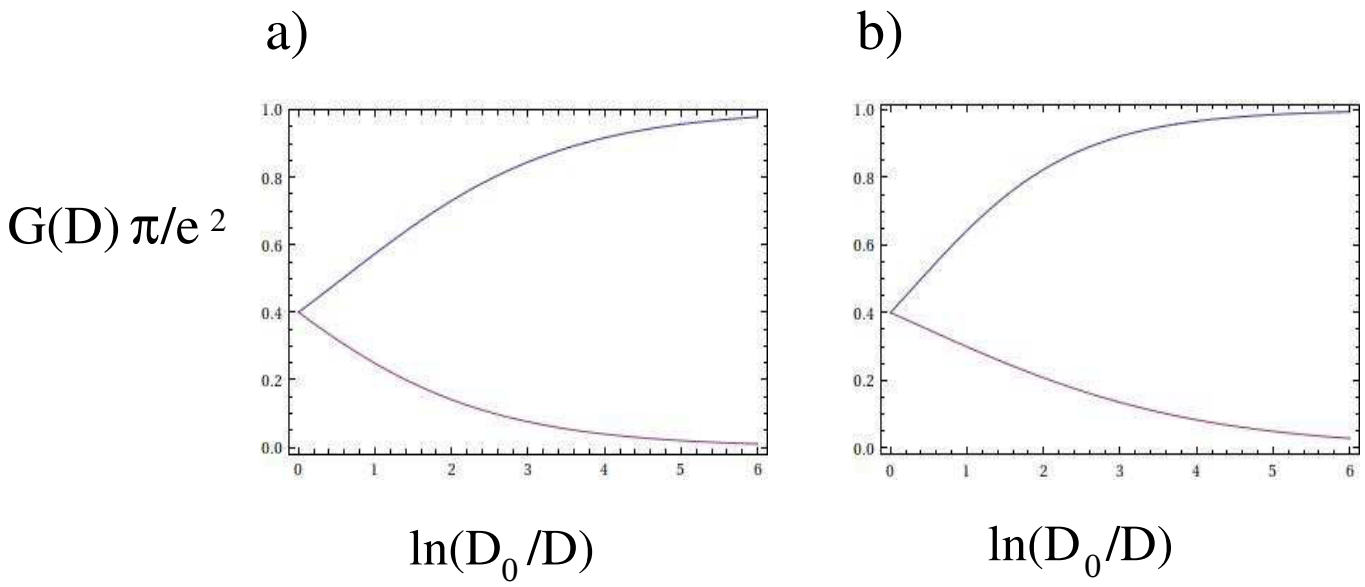

FIG. 13. (a) Plot of $G(D)$ *vs.* $\ln(D_0/D)$ as from Eq. [3.10] for $T_0 = 1 - R_0 = 0.4$, $\beta = 0.35$ (purple curve - corresponding to an effectively repulsive interaction), and $\beta = -0.35$ (blue curve - corresponding to an effectively attractive interaction), with $T_0 = |t_0|^2, R_0 = |r_0|^2$;
(b) Plot of $G(D)$ *vs.* $\ln(D_0/D)$ as given in Eq. [3.12] for $T_0 = 1 - R_0 = 0.4$, $g_1/(2\pi v) = 0.2$, $\gamma = 0.36$ (purple curve - corresponding to an effectively repulsive interaction), and $\beta = -0.36$ (blue curve - corresponding to an effectively attractive interaction).

$$g_2(D) = g_2 - \frac{g_1}{2} + \frac{1}{2}\frac{g_1}{1 + \frac{g_1}{\pi v}\ln\frac{D_0}{D}} \tag{3.11}$$

and $\beta(D) = [g_2(D) - 2g_1(D)]/(2\pi v)$. Once $\beta(D)$ is known, Eqs. [3.7] can be integrated, yielding

$$G(D) = \frac{e^2}{\pi}\left[\frac{T_0\left[1 + \frac{g_1}{\pi v}\ln\left|\frac{D_0}{D}\right|\right]^{3/2}|D/D_0|^{2\gamma}}{R_0 + T_0\left[1 + \frac{g_1}{\pi v}\ln\left|\frac{D_0}{D}\right|\right]^{3/2}|D/D_0|^{2\gamma}}\right] \tag{3.12}$$

with $\gamma = \left(-\frac{g_1}{2} + g_2\right)/(2\pi v)$, $T_0 = |t_0|^2, R_0 = |r_0|^2$. As an example of typical scaling plots for $G(D)$ in the simple cases discussed before, in Fig. [13] we plot $G(D)\pi/e^2$ *vs.* $\ln(D_0/D)$, as from Eq. [3.10] (panel (a)) and from Eq. [3.12] (panel (b)), with the values of the parameters reported in the caption. Consistently with the results obtained within Luttinger liquid framework[25–27], $G(D)\pi/e^2$ either flows to 0 for an effectively repulsive interaction ($\beta, \gamma > 0$), or to 2 (the maximum value allowed by unitarity), for an effectively attractive interaction ($\beta, \gamma < 0$). For general values of the interaction strengths, the equations have to be numerically integrated. In Fig. [14], we provide some examples of scaling of $G(D)$ *vs.* $\ln(D_0/D)$ in the general case. It is important to stress[39] that, due to the nontrivial renormalization group flow of the interaction strengths, the flow of $G(D)$ can be a nonmonotonic function of D for some specific values of the interaction strengths. It would be interesting to check such a feature in a real life two-wire junction: remarkably, this prediction is only obtained within the FRG-approach, in which it is possible to account for the flow of the running interaction strengths, as well.
The possibility of mapping out the full crossover of the conductance as a function of the scale D is possibly the most important feature of the FRG approach.

III.1.2. The strongly interacting regimes

Yet, since, as we discuss to some extent in Sec. [II.4], the validity of the FRG technique is grounded on the assumption that all the relevant scattering processes at the junction are described by the single-particle S-matrix[37–40], it breaks down when attempting to recover the full crossover of the conductance towards fixed points where multi-particle scattering is the most relevant process at the junction, such as the strongly coupled fixed point stabilized by either $H_{2,0}$ or $H_{0,2}$ in Eq. [3.3][25–27]. Technically, what happens is that, as soon as boundary operators such as $H_{2,0}$

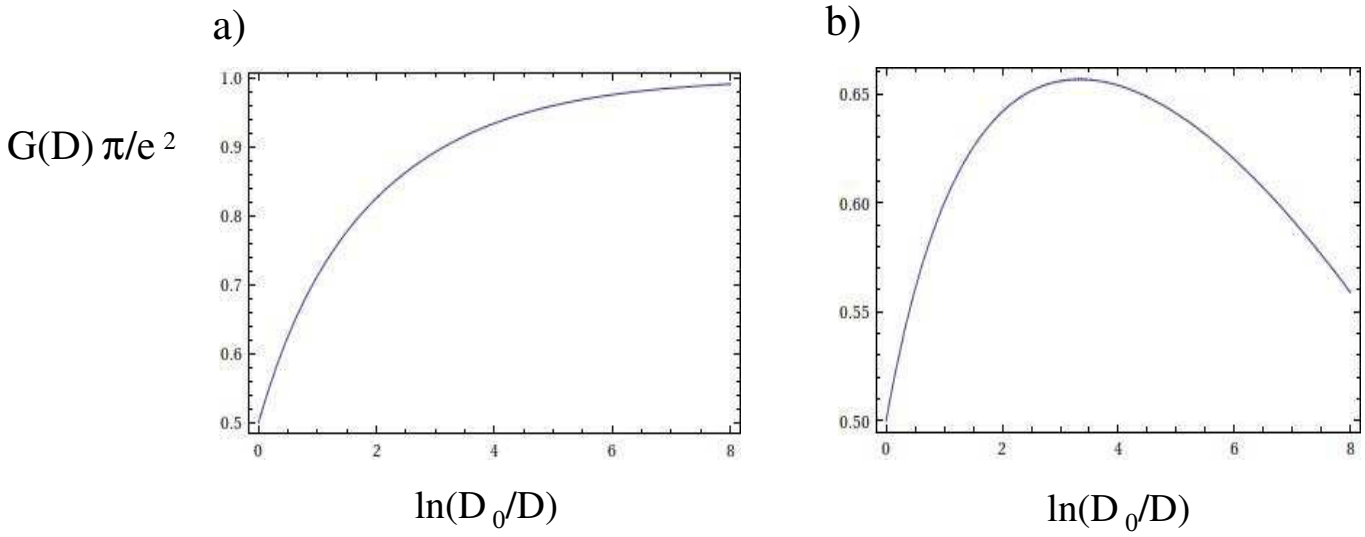

FIG. 14. (a) Plot of $G(D)$ *vs.* $\ln(D_0/D)$, obtained by numerically integrating Eqs. [3.7,3.8,2.102] for $g_{1,\parallel}(D_0)/(2\pi v) = g_{1,\perp}(D_0)/(2\pi v) = g_{2,\perp}(D_0)/(2\pi v) = 0.3$, $g_{2,\parallel}(D_0)/(2\pi v) = 0$, $R_0 = T_0 = 0.5$;
(b) Same as in panel (a), but with $g_{2,\parallel}(0)/(2\pi v) = 0.3$, as well.

or $H_{0,2}$ become relevant, the proliferation of low-energy many-body scattering processes such as the one we sketch in Fig. [12], panel b, invalidates the single-particle S-matrix description of the junction dynamics. Nevertheless, some many-body scattering processes can be strongly limited by having, for instance, a strong repulsive interaction among particles with the same spin and a strong attractive interaction among particles with the same charge. In the bosonic framework, this corresponds to having values of the Luttinger parameters in Eqs. [2.134] such that $g_c \geq 2, g_s \ll 1$. Indeed, in this limit on one hand, the strong spin repulsive interaction forbids the single-particle processes described by H_B in Eq. [3.2] (at small values of the boundary coupling strengths $\tau_{X,X'}, \mu_{X,X'}$ this can be readily seen from the explicit result for the scaling dimension of H_B computed within the bosonization approach, which is $x_{B,weak} = 1 - \frac{1}{2g_c} - \frac{1}{2g_s}$, which becomes $\gg 1$, corresponding to a largely irrelevant operator). On the other hand, one expects that the strong charge attraction stabilizes tunneling of composite objects carrying zero spin, such as two-particle pairs, as the one depicted at the left-hand panel of Fig. [12], panel c. As a consequence, due to the fact that these are again one-into-one scattering processes, one expects that it is possible to choose the effective low-energy degrees of freedom of the system to resort to a single-particle S-matrix in the new coordinates. In fact, this is the idea behind the dual fermion approach we are going to discuss next. When resorting to dual fermion coordinates, an important issue is related to whether the vacuum states at a fixed particle number[85] for the original and the dual-fermions are the same. In fact, while dual fermion formalism only captures composite excitations e.g. two-particle states in the $g_c \sim 2, g_s \ll 1$-regime, at such values of the parameters, these states are the only ones that at low energy are effectively able to tunnel across the junction (that is, the only ones whose tunneling is described by a non-irrelevant operator). So, as long as one is only concerned about states relevant for low-energy tunneling across the junction (that is, states relevant for the calculation of the dc-conductance tensor of the junction), one can effectively assume that the fixed-particle number vacuum states are the same in terms of the new (dual) and of the old fermions. The definition of the dual fermion operators strongly depends on the boundary conditions of the various fields at the junction. Accordingly, in the following we define different dual fermion operators in different regimes of values of the boundary interaction, and eventually show that, whenever two different sets of dual coordinates apply to the same region, they yield the same results, as they are expected to.

Let us begin with the weak boundary interaction regime. Referring to the bosonization formulas of Sec. [II.5], this corresponds to assuming Neumann (Dirichlet) boundary conditions for all the Φ (Θ)-fields in Sec. [II.5] and, in addition, to equating the Klein factors so that $\eta_{R,\sigma,j} = \eta_{R,\sigma,j}, \forall \sigma, j$. In this limit, one may respectively rewrite $H_{0,2}$ and $H_{2,0}$ in bosonic coordinates as

$$\begin{aligned} H_{2,0} &= v_{2,0} \cos[\Phi_{1,c}(0) - \Phi_{2,c}(0)] \\ H_{0,2} &= v_{0,2} \cos[\Phi_{1,s}(0) - \Phi_{2,s}(0)] \end{aligned} \tag{3.13}$$

with $v_{2,0} \propto V_{2,0}, v_{0,2} \propto V_{0,2}$. The scaling dimensions of the operators in Eqs. [3.13] are respectively given by $x_{2,0} = 2/g_c, x_{0,2} = 2/g_s$. Thus, in the regime of a strongly attractive interaction in the charge (spin)-channel and

strongly repulsive interaction in the spin (charge)-channel, $H_{2,0}$ ($H_{0,2}$) may become the most relevant boundary operator at weak boundary coupling. The strategy of our dual fermion approach consists in defining a novel set of fermionic fields, in terms of which the operators in Eqs. [3.13] are realized as bilinears, similar to the B-operators in Eq. [3.1]. To be specific, let us introduce the center-of-mass and the relative fields in the charge- and in the spin-sector, respectively given by

$$\begin{aligned}\Phi_{c(s)}(x) &= \frac{1}{\sqrt{2}}[\Phi_{1,c(s)}(x) + \Phi_{2,c(s)}(x)] \\ \Theta_{c(s)}(x) &= \frac{1}{\sqrt{2}}[\Theta_{1,c(s)}(x) + \Theta_{2,c(s)}(x)]\end{aligned} \tag{3.14}$$

and

$$\begin{aligned}\varphi_{c(s)}(x) &= \frac{1}{\sqrt{2}}[\Phi_{1,c(s)}(x) - \Phi_{2,c(s)}(x)] \\ \vartheta_{c(s)}(x) &= \frac{1}{\sqrt{2}}[\Theta_{1,c(s)}(x) - \Theta_{2,c(s)}(x)]\end{aligned} \tag{3.15}$$

Next, let us perform the canonical transformation to a new set of bosonic fields, defined as

$$\begin{bmatrix} \bar{\Phi}_{c(s)}(x) \\ \bar{\Theta}_{c(s)}(x) \\ \bar{\varphi}_{c(s)}(x) \\ \bar{\vartheta}_{c(s)}(x) \end{bmatrix} = \begin{bmatrix} \sqrt{2} & 0 & 0 & 0 \\ 0 & \frac{1}{\sqrt{2}} & 0 & 0 \\ 0 & 0 & \sqrt{2} & 0 \\ 0 & 0 & 0 & \frac{1}{\sqrt{2}} \end{bmatrix} \begin{bmatrix} \Phi_{c(s)}(x) \\ \Theta_{c(s)}(x) \\ \varphi_{c(s)}(x) \\ \vartheta_{c(s)}(x) \end{bmatrix} \tag{3.16}$$

It is worth stressing that the transformation in Eqs. [3.16] relate to each other bosonic operators at a given position in real space. Since the correspondence rules between the bosonic and the (original or dual) fermionic fields, summarized in Sec. [II.5], are local in real space, as well, one concludes that, written in terms of dual fermionic coordinates, the boundary interaction Hamiltonian H_B is still local and that the dynamics far from the junction can be fully encoded within dual fermion scattering states. Now, assuming $g_s \ll 1$, $g_c = 2 + \delta g_c$, with $|\delta g_c| \ll 1$, we see that $g_s \ll 1$ makes $H_{0,2}$ strongly irrelevant. This fully suppresses spin transport across the junction and, therefore, we may just focus onto charge transport, ruled by $H_{2,0}$. In fact, it appears that single-spinful particle-tunneling processes are already suppressed against two-particle pair tunneling processes as soon as $g_s < 2/3$. As conservation of spin symmetry implies $g_s = 1$, in order to realize the condition above one may, for instance, think of two coupled spinless interacting one-dimensional electronic systems (which could possibly realized as semiconducting quantum wires in the presence of spin-orbit and Zeeman interactions), with a mismatch in the Fermi momenta that prevents the interaction from opening a gap in the fermion spectrum. The two channels can, therefore, be regarded as the two opposite spin polarization, although without any symmetry implying $g_s = 1$. To rewrite this latter operator as a bilinear functional of fermionic operators, we define the spinless chiral fermionic fields $\chi_{R,j}(x), \chi_{L,j}(x)$ as

$$\begin{aligned}\chi_{R,j}(x) &= \eta_{R,j}\ e^{\frac{i}{2}[\bar{\Phi}_c(x) - (-1)^j \bar{\varphi}_c(x) + \bar{\Theta}_c(x) - (-1)^j \bar{\vartheta}_c(x)]} \\ \chi_{L,j}(x) &= \eta_{L,j}\ e^{\frac{i}{2}[\bar{\Phi}_c(x) + (-1)^j \bar{\varphi}_c(x) + \bar{\Theta}_c(x) + (-1)^j \bar{\vartheta}_c(x)]}\end{aligned} \tag{3.17}$$

with $j = 1, 2$ and with $\eta_{R,j}, \eta_{L,j}$ being real fermionic Klein factors. "Inverting" the bosonization procedure outlined in Sec. [II.5] into a pertinent re-fermionization to spinless fermions, we find that the bulk Hamiltonian for the χ-fermions is given by

$$\begin{aligned}H_{\rm c;bulk} &= -iu \sum_{j=1,2} \int_0^L dx\ \{\chi^\dagger_{R,j}(x)\partial_x \chi_{R,j}(x) - \chi^\dagger_{L,j}(x)\partial_x \chi_{L,j}(x)\} \\ &\quad - \tfrac{u\pi\delta g_c}{2} \sum_{j=1,2} \int_0^L dx\ :\chi^\dagger_{R,j}(x)\chi_{R,j}(x)::\chi^\dagger_{L,j}(x)\chi_{L,j}(x):\end{aligned} \tag{3.18}$$

with the velocity $u \propto v$. The $\chi_{L/R,j}$-fields are the appropriate degrees of freedom to describe pair scattering at the junction in terms of a single-particle S-matrix. In order to prove that it is so, we note that $H_{2,0}$ can be regarded as

the bosonic expression for the boundary weak coupling limit of a tunnel Hamiltonian for the spinless fermions, $H_{\rm c,tun}$, given by

$$H_{\rm c,tun} = v_{2,0}\{\chi_1^\dagger(0)\chi_2(0) + \chi_2^\dagger(0)\chi_1(0)\} \tag{3.19}$$

with $\chi_j(0) = \chi_{R,j}(0) + \chi_{L,j}(0)$. While the strong spin repulsion sets the spin conductance tensor to 0, the charge conductance can nevertheless be different from zero, due to zero-spin pair-tunneling across the junction. Once the RG-flow for the S-matrix elements describing χ-fermion scattering at the junction has been derived as we did before, using the formulas we report in Appendix [II.8] and the expression of the charge current operator in wire j in terms of the dual fermionic fields:

$$J_{c,j}(x) = eu\sqrt{2}\,\{:\chi_{R,j}^\dagger(x)\chi_{R,j}(x): - :\chi_{L,j}^\dagger(x)\chi_{L,j}(x):\} \tag{3.20}$$

we obtain that the charge conductance tensor scales according to

$$G_c(D) = \begin{bmatrix} \frac{e^2}{\pi} - G(D) & G(D) \\ G(D) & \frac{e^2}{\pi} - G(D) \end{bmatrix} \tag{3.21}$$

with

$$G(D) = \frac{e^2}{\pi}\,\left[\frac{T_0|D/D_0|^{-\frac{\delta g_c}{2}}}{R_0 + T_0|D/D_0|^{-\frac{\delta g_c}{2}}}\right] \tag{3.22}$$

and the bare reflection and transmission coefficients respectively given by

$$\begin{aligned} R_0 &= \left|\frac{u^2 - v_{2,0}^2}{u^2 + v_{2,0}^2}\right|^2 \\ T_0 &= \left|\frac{2uv_{2,0}}{u^2 + v_{2,0}^2}\right|^2 \end{aligned} \tag{3.23}$$

In Fig. [15], we plot $G(D)$ versus $\ln(D_0/D)$ in two paradigmatic cases, respectively corresponding to $\delta g_c > 0$ and to $\delta g_c < 0$. To our knowledge, this is the first example of a full scaling plot of the conductance for a junction of strongly interacting one-dimensional quantum wires. While, on one hand, this shows the effectiveness of our approach in describing the crossover of the conductance towards the spin-insulating charge-conducting fixed point, on the other hand, one has also to prove the consistency of an effective theory strongly relying on the weak boundary coupling assumption with an RG-flow taking the system all the way down to the perfectly charge-conducting fixed point, corresponding to the strongly interacting limit of the boundary interaction[25–27]. When $\delta g_c > 0$, the relevance of $H_{2,0}$ drives the system towards the strongly boundary interaction limit in the charge channel, corresponding to pinning $\varphi_c(0)$ and, accordingly, to imposing Neumann boundary conditions on $\vartheta_c(0)$. Since $\Phi_c(0)$ does not appear in the boundary interaction, one assumes that it still obeys Neumann boundary conditions and, accordingly, that $\Theta_c(0)$ is pinned at a constant value. We now prove that these boundary conditions are recovered by taking the strongly coupled limit of $H_{\rm c,tun}$ in Eq. [3.19] and using the refermionization rules in Eqs. [3.17]. Indeed, on making the strong-coupling assumption, $\left|\frac{v_{2,0}}{u}\right| \gg 1$, as from Eqs. [3.23], one obtains $R_0 \to 0, T_0 \to 1$, that is, the boundary conditions correspond to perfect transmission from wire-1 to wire-2, and vice versa. In terms of the dual fermionic fields, this corresponds to the conditions

$$\begin{aligned} \chi_{R,2}(x) &= e^{i\lambda}\,\chi_{L,1}(-x) \\ \chi_{R,1}(x) &= e^{-i\lambda}\,\chi_{L,2}(-x) \end{aligned} \tag{3.24}$$

with λ being some nonuniversal phase. From Eqs. [3.17], one sees that Eqs. [3.24] imply Dirichlet boundary conditions at $x = 0$ for both $\bar\varphi_c(x)$ and $\bar\Theta_c(x)$, with the dual fields $\bar\vartheta_c(x), \bar\Phi_c(x)$ obeying Neumann boundary conditions. This is exactly the same result one would obtain working in bosonic variables by sending to ∞ the interaction strength $v_{2,0}$ in Eq. [3.13]. Due to the strong repulsion in the spin channel, such a fixed point corresponds to perfect transmission

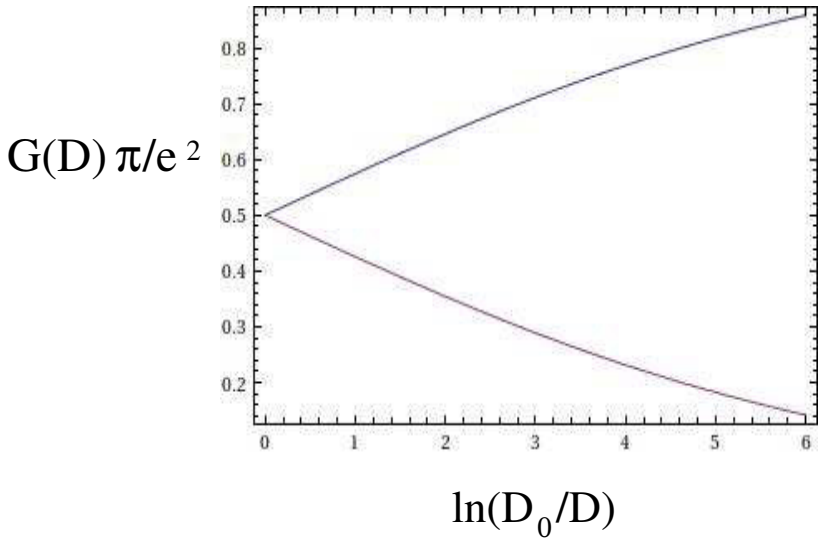

FIG. 15. Plot of $G_c(D)$ *vs.* $\ln(D_0/D)$ as from Eq. [3.22] for $T_0 = R_0 = 0.5$ and for δg_c respectively equal to 0.6 (blue curve) and to -0.6 (purple curve).

in the charge channel, but perfect reflection in the spin channel, that is, it must be identified with the non-symmetric charge-conducting spin-insulating phase of Refs. [25–27]. To conclude the consistency check, we note that, on alledging for additional backscattering contributions to $H_{c,tun}$ of the generic form $\mu_1 \chi^\dagger_{R,1}(0)\chi^\dagger_{R,1}(0) + \mu_2 \chi^\dagger_{L,1}(0)\chi^\dagger_{L,}(0)$ (which play no role at weak coupling) and using again Eqs. [3.24], one obtains the bosonic operators

$$\tilde{H}_{\rm c,tun} \sim \mu \cos\left[\bar{\vartheta}_c(0)\right] \tag{3.25}$$

with μ being some nonuniversal constant. Equation [3.25] corresponds to the bosonic version of the leading boundary perturbation at the non-symmetric charge-conducting spin-insulating fixed point[25–27].

Our approach also allows for analyzing the complementary situation in which $g_c \ll 1$ and $g_s \sim 2$. In this case, one expects that the strong repulsion in the charge channel and the strong attraction in the spin channel stabilize single-pair tunneling processes at the junction such as those sketched at the right-hand panel of Fig. [12], panel c, that is, tunneling of particle-hole pairs, with total spin 1. Again, for $g_s = 2$, the S-matrix describes single-particle into single-particle scattering processes, once it is written in the appropriate basis. To select the pertinent degrees of freedom, we therefore repeat the refermionization procedure in Eq. [3.17], by just exchanging the charge- and the spin-sector with each other. Of course, charge- and spin-conductance are exchanged with each other, compared to the previous situation and, accordingly, the flow will be towards the charge-insulating spin-conducting fixed point of Refs. [25–27]. An important remark, however, concerns the effects of a possible residual interaction, which, as we did before, can be in principle introduced for accounting for g_s slightly different from 2. Indeed, a term in the "residual" bulk interaction Hamiltonian such as the one $\propto g_{j,1,\perp}$ in Eq. [2.10], once expressed in terms of the fermionic fields in Eqs. [3.17] would take the form

$$H_\delta = \sum_{j=1}^{2} m_j \int dx \, \{\chi^\dagger_{R,j}(x)\chi_{L,j}(x) + \chi^\dagger_{L,j}(x)\chi_{R,j}(x)\} \tag{3.26}$$

with $m_j \propto g_{j,1,\perp}$, which would open a bulk gap in the single-χ fermion spectrum, thus making the whole system behave as a bulk spin insulator. Therefore, in order to recover the correct physics of the charge-insulating spin-conducting fixed point, we must assume that all the $g_{j,1,\perp}$ are tuned to zero, which is typically the case when resorting to the bosonic approach to spinful electrons[25–27].

As we have just shown, resorting to pertinent dual-fermion operators allows for mapping out the full crossover with the appropriate energy scale of the charge and/or spin conductance of a junction in region of values of the interaction parameters in which one is typically forbidden to use the standard weak-coupling formulation of either FRG, or fRG. In the following, we apply our technique to the spinful three-wire junction studied using the bosonization approach in Ref. [30], and will recover the full crossover of the conductance tensor in regions typically not accessible in the bosonic formalism.

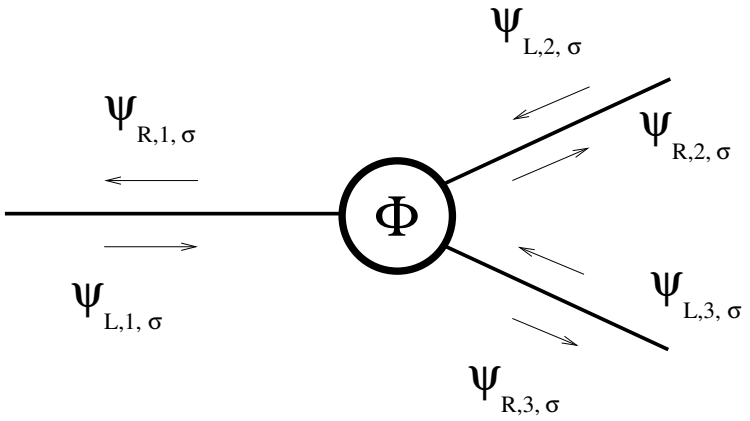

FIG. 16. Sketch of a three-wire junction of spinful quantum wires pierced by a magnetic flux Φ.

III.2. Dual Fermionic variables and renormalization group approach to the calculation of the conductance at a junction of three spinful interacting quantum wires

We now consider a three-spinful-wire junction, such as the one we sketch in Fig. [16]. Resorting to the appropriate fermionic variables, we generalize to strongly interacting regions the weak-coupling FRG-approach. As a result, we map out the full dependence of the conductance tensor on the low-energy running cutoff scale even in strongly-interacting regions of the parameter space. Eventually, we discuss the consistency of our results about the phase diagram of the junction with those obtained in Ref. [30], particularly showing how our technique can be used to recover informations that typically cannot be derived within the bosonization approach used there. Consistently with Ref. [30], in the following, we make the simplifying assumption that, in the weakly interacting regime, the bulk interaction is purely intra-wire and is the same in all the three wires. In fact, while this assumption is already expected to yields quite a rich phase diagram[30], in principle our approach can be readily generalized to cases of different bulk interactions in different wires, such as the one considered in Ref. [31].

III.2.1. The weakly interacting regime

For a weak boundary interaction, assuming total spin conservation at the junction, the most relevant boundary interaction Hamiltonian is a combination of the bilinear operators in Eq. [3.1]. The relevant scattering processes at the junction are all encoded in the single-particle S-matrix elements, $S_{(j,\sigma),(j',\sigma')}(k)$. Because of spin conservation, the S-matrix is diagonal in the spin index, that is, $S_{(j,\sigma),(j',\sigma')}(k) = \delta_{\sigma,\sigma'} S_{j,j'}(k)$. Assuming also that the boundary Hamiltonian is symmetric under exchanging the wires with each other, the 3×3 matrix $S(k)$ takes the form

$$S = \begin{bmatrix} r & \bar{t} & t \\ t & r & \bar{t} \\ \bar{t} & t & r \end{bmatrix} \tag{3.27}$$

(Note that, in Eq. [3.27] we assume that all the amplitudes are computed at the Fermi level and accordingly drop the index k from the S-matrix elements. This is consistent with the discussion of Sec. [II.4], where we assume that, close to the Fermi level, the scattering amplitudes are smooth functions of k.) It is worth mentioning that, in writing Eq. [3.27], we allowed for time-reversal symmetry breaking as a consequence, for instance, of a magnetic flux ϕ piercing the centre of the junction (see Fig. [16]). This implies that, in general, the scattering amplitude t from wire j to wire $j+1$ is different from the one from wire j to wire $j-1$ ($\bar{t}$). From Eq. [3.27] one therefore finds that the F-matrix elements in Eq. [2.84] are given by $F_{j,j'} = \frac{\beta}{2} r \delta_{j,j'}$, with again $\beta = \frac{1}{2\pi v}\left[-g_{1\parallel} - g_{1\perp} + g_{2\parallel}\right]$. On applying the FRG formalism of Sec. [II.4], one readily obtains the RG-equations for the independent S-matrix elements, given by

$$\begin{aligned} \frac{dr}{d\ell} &= \frac{\beta}{2}\left[r - |r|^2 r - 2t\bar{t}r^*\right] \\ \frac{dt}{d\ell} &= -\frac{\beta}{2}\left[2t\,|r|^2 + \bar{t}^2 r^*\right] \end{aligned}$$

$$\frac{d\bar{t}}{d\ell} = -\frac{\beta}{2}\left[2\bar{t}\,|r|^2 + t^2 r^*\right] \tag{3.28}$$

which, again, must be supplemented with the RG-equations for the running coupling strengths, Eqs. [2.102,3.8]. Since, as a consequence of spin conservation in scattering processes at the junction, the S-matrix is diagonal in the spin indices, the charge- and spin-conductance tensors are equal to each other at the fixed points, as well as along the RG-trajectories obtained integrating Eqs. [3.28]. In particular, using the formalism of Appendix [II.8], one obtains

$$G_{c,s}(D) = \frac{e^2}{\pi}\begin{bmatrix} -R(D)+1 & -\bar{T}(D) & -T(D) \\ -T(D) & -R(D)+1 & -\bar{T}(D) \\ -\bar{T}(D) & -T(D) & -R(D)+1 \end{bmatrix} \tag{3.29}$$

with $R(D) = |r(D)|^2, T(D) = |t(D)|^2$, and $\bar{T}(D) = |\bar{t}(D)|^2$. The RG-flow of the scattering coefficients $T(D), \bar{T}(D)$ is recovered by solving the set of differential equations

$$\begin{aligned} \frac{dT}{d\ell} &= -\frac{\beta}{2}\left[\left(5T - \bar{T}\right)\left(1 - T - \bar{T}\right) - T\bar{T}\right] \\ \frac{d\bar{T}}{d\ell} &= -\frac{\beta}{2}\left[\left(5\bar{T} - T\right)\left(1 - T - \bar{T}\right) - T\bar{T}\right] \end{aligned} \tag{3.30}$$

which are derived from Eqs. [3.28] by taking into account the unitarity constraint $T(D) + \bar{T}(D) + R(D) = 1$. The fixed points of the boundary phase diagram are, therefore, determined by setting to zero the terms at the right-hand side of Eqs. [3.30]. From Eq. [3.29] one may therefore recover the corresponding charge- and the spin-conductance tensors. Borrowing the labels used in Ref. [30], we obtain the following fixed points:

- *The $[N_c, N_s]$ ("disconnected") fixed point*

  This fixed point corresponds to having $R = 1$ and $T = \bar{T} = 0$ which, according to Eq. [3.29], yields

$$G_c = G_s = \frac{e^2}{\pi}\begin{bmatrix} 0 & 0 & 0 \\ 0 & 0 & 0 \\ 0 & 0 & 0 \end{bmatrix} \tag{3.31}$$

  as it is appropriate for a disconnected junction.

- *The χ_{++} fixed point*

  This corresponds to $R = \bar{T} = 0$, $T = 1$, which yields

$$|S_{j,j'}|^2 = \begin{bmatrix} 0 & 0 & 1 \\ 1 & 0 & 0 \\ 0 & 1 & 0 \end{bmatrix} \tag{3.32}$$

  and, accordingly

$$G_c = G_s = \frac{e^2}{\pi}\begin{bmatrix} 1 & 0 & -1 \\ -1 & 1 & 0 \\ 0 & -1 & 1 \end{bmatrix} \tag{3.33}$$

- *The χ_{--} fixed point*

  This corresponds to $R = T = 0$, $\bar{T} = 1$, which yields

$$|S_{j,j'}|^2 = \begin{bmatrix} 0 & 1 & 0 \\ 0 & 0 & 1 \\ 1 & 0 & 0 \end{bmatrix} \tag{3.34}$$

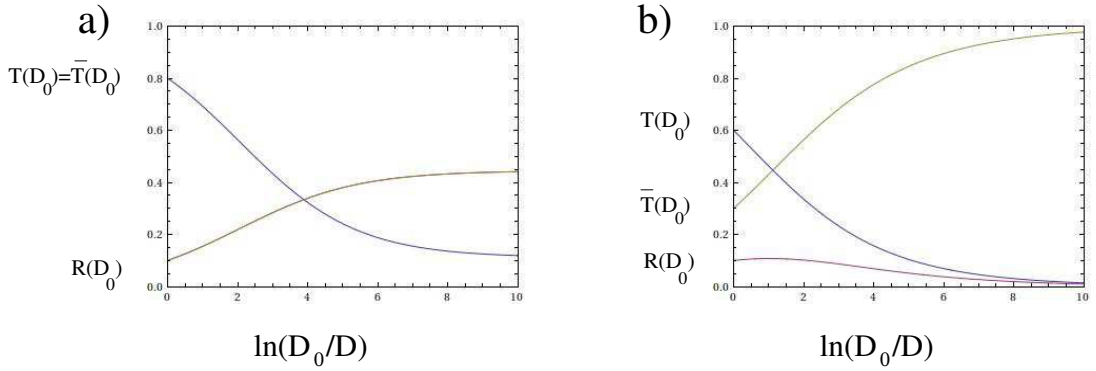

FIG. 17. Renormalization group flow of the scattering coefficients for a three-wire junction for $g_{1,\perp} = 0$, β constant and equal to -0.3, and different choices of the initial values of the scattering coefficients:
(a) Renormalization group flow corresponding to $T(D_0) = \bar{T}(D_0) = 0.1$, $R(D_0) = 0.8$. The curves corresponding to $T(D)$ and to $\bar{T}(D)$ *vs* $\ln(D_0/D)$ collapse onto the single red curve of the graph, while the flow of $R(D)$ *vs* $\ln(D_0/D)$ is described by the blue curve. As D_0/D grows, the scattering coefficients flow towards the asymptotic values corresponding to the M-fixed point;
(b) Renormalization group flow corresponding to $T(D_0) = 0.1, \bar{T}(D_0) = 0.3, R(D_0) = 0.6$. As D_0/D grows, the scattering coefficients flow towards the asymptotic values corresponding to the χ_{--}-fixed point.

and, accordingly

$$G_c = G_s = \frac{e^2}{\pi} \begin{bmatrix} 1 & -1 & 0 \\ 0 & 1 & -1 \\ -1 & 0 & 1 \end{bmatrix} \tag{3.35}$$

- *The M fixed point*

  This corresponds to $T = \bar{T} = \frac{4}{9}$, $R = \frac{1}{9}$ and has to be identified with the symmetric[39], or with the Griffith[86] fixed point of a junction of three interacting wires. One obtains

$$|S_{j,j'}|^2 = \begin{bmatrix} \frac{1}{9} & \frac{4}{9} & \frac{4}{9} \\ \frac{4}{9} & \frac{1}{9} & \frac{4}{9} \\ \frac{4}{9} & \frac{4}{9} & \frac{1}{9} \end{bmatrix} \tag{3.36}$$

  and, accordingly

$$G_c = G_s = \frac{e^2}{\pi} \begin{bmatrix} \frac{8}{9} & -\frac{4}{9} & -\frac{4}{9} \\ -\frac{4}{9} & \frac{8}{9} & -\frac{4}{9} \\ -\frac{4}{9} & -\frac{4}{9} & \frac{8}{9} \end{bmatrix} \tag{3.37}$$

$\chi_{\pm\pm}$ must clearly be identified with the "chiral" fixed points of Ref. [30], where time-reversal symmetry breaking is maximum, both in the charge and in the spin sector. Along the RG-trajectories connecting two fixed points, the conductance flow is determined by Eq. [3.29]. The topology and the direction of the RG-trajectories depend on both β and on the bare values of the S-matrix elements. β scales with ℓ as determined by Eqs. [2.102,3.8], which makes it necessary to resort to a full numerical integration approach. A set of simplified situations can be realized, however, where β keeps constant along RG-trajectories. For instance, if $g_{1,\perp}(D_0) = 0$, Eq. [3.8] implies that β is constant. In this case, from Eqs. [3.30] one readily sees that, if $\beta > 0$, the boundary flow is towards the NN-fixed point. At variance, if $\beta < 0$ and $T(D_0) > (<)\bar{T}(D_0)$, the boundary flow is towards the χ_{++} (χ_{--})-fixed point. As an example of possible RG-trajectories that may be realized in this specific case, in Fig. [17] we plot $T(D)$ and $\bar{T}(D)$ for β constant and negative, while we draw similar plots in Fig. [18] for constant and positive β and in Fig. [19] for non-constant β (see the captions for details).
All the analysis we have done so far applies to a junction of three spinful quantum wires for weak bulk interaction. We now employ the dual-fermion approach to generalize the FRG-technique to regimes corresponding to strong bulk interactions either in the charge-, or in the spin-channel (or in both of them). See Appendix [III.4] for a detailed list of relevant boundary operators for different values of the interaction constants.

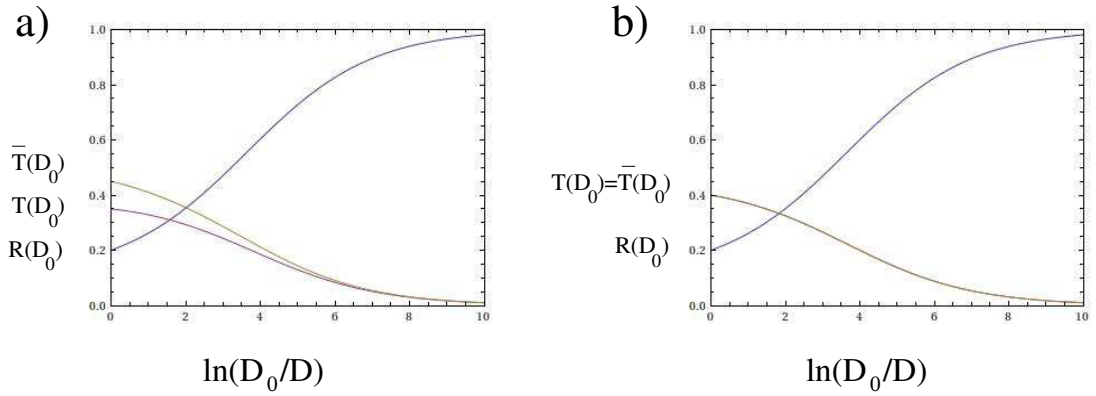

FIG. 18. Renormalization group flow of the scattering coefficients for a three-wire junction for $g_{1,\perp} = 0$, β constant and equal to 0.3, and different choices of the initial values of the scattering coefficients:
(a) Renormalization group flow corresponding to $T(D_0) = 0.35, \bar{T}(D_0) = 0.45, R(D_0) = 0.2$;
(b) Renormalization group flow corresponding to $T(D_0) = \bar{T}(D_0) = 0.4, R(D_0) = 0.2$. As D_0/D grows, in both cases the scattering coefficients flow towards the NN-fixed point.

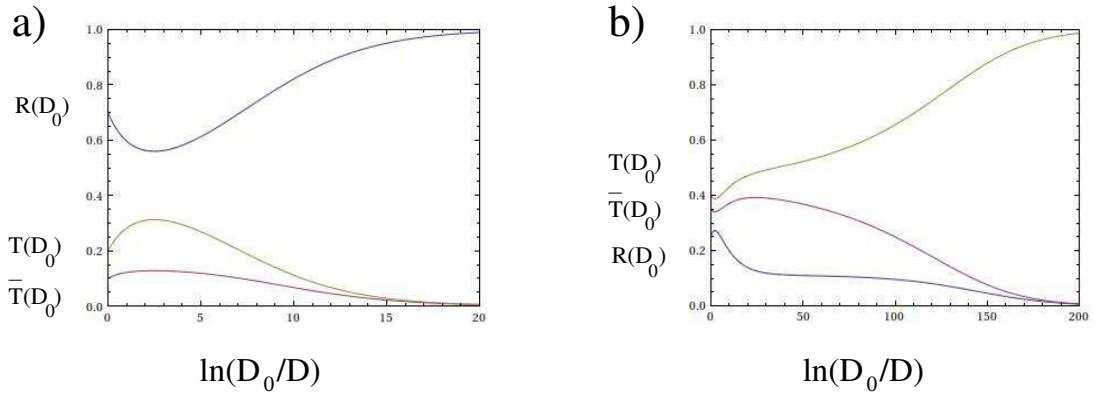

FIG. 19. Renormalization group flow of the scattering coefficients for a three-wire junction for non-constant β:
(a) Renormalization group flow corresponding to $T(D_0) = 0.2, \bar{T}(D_0) = 0.1, R(D_0) = 0.4$ and to $g_{1,\parallel}(D_0)/(2\pi v) = g_{1,\perp}(D_0)/(2\pi v) = g_{2,\parallel}(D_0)/(2\pi v) = g_{1,\perp}(D_0)/(2\pi v) = 0.4$. For these values of the bare parameters the junction is attracted by the disconnected fixed point ($R \to 1$ while $T, \bar{T} \to 0$);
(b) Renormalization group flow corresponding to $T(D_0) = 0.4, \bar{T}(D_0) = 0.35, R(D_0) = 0.25$ and to $g_{1,\parallel}(D_0)/(2\pi v) = 0.3, g_{1,\perp}(D_0)/(2\pi v) = -0.2, g_{2,\parallel}(D_0)/(2\pi v) = g_{1,\perp}(D_0)/(2\pi v) = 0.2$. For these values of the bare parameters the junction is attracted by the χ_{++}-fixed point.

III.2.2. Fermionic analysis of the strongly interacting regime at $g_c \sim g_s \sim 3$

A first regime to which our dual-fermion approach can be successfully applied corresponds to a strong attractive interaction, both in the charge and in the spin channels. In particular, we assume $g_c \sim g_s \sim 3$. According to the phase diagram derived in Ref. [30] within the bosonization approach, in this range of values of the Luttinger parameters one expects to find a fixed point where paired electron tunneling and Andreev reflection are the dominant scattering processes at the junction and, in addition, two fixed points with maximally broken time-reversal symmetry, to be identified with the χ_{++} and the χ_{--}-fixed points discussed in the previous subsection. To apply the FRG-approach to this part of the phase diagram, we have to define the appropriate dual fermion coordinates. To do so, let us set $g_c = g_s = 3$. We therefore note that, though, in general, the charge- and spin-velocities u_c and u_s can be different from each other, one may easily make them equal by a pertinent rescaling of the real-space coordinate in the charge- and in the spin-sector of the bosonic Hamiltonian in Eq. [2.133]. As the rescaling does not affect the boundary interaction (which is localized at $x = 0$), in the following, without loss of generality, we will assume $u_c = u_s \equiv u$. In choosing the appropriate dual fermion coordinates, we use the criterion of mapping the fixed point we recover in the strongly interacting limit one-to-one onto those of the phase diagram in the weakly interacting regime. Referring to the bosonization formulas of Sec. [II.5], we define the dual bosonic fields $\tilde{\Phi}_{c(s),j}(x), \tilde{\Theta}_{c(s),j}(x)$ in terms of those in

Eqs. [2.130,2.131] as

$$\begin{bmatrix} \tilde{\Phi}_{c(s),1}(x) \\ \tilde{\Phi}_{c(s),2}(x) \\ \tilde{\Phi}_{c(s),3}(x) \\ \tilde{\Theta}_{c(s),1}(x) \\ \tilde{\Theta}_{c(s),2}(x) \\ \tilde{\Theta}_{c(s),3}(x) \end{bmatrix} = \begin{bmatrix} \frac{1}{\sqrt{3}} & \frac{1}{\sqrt{3}} & \frac{1}{\sqrt{3}} & 0 & \frac{1}{3} & -\frac{1}{3} \\ \frac{1}{\sqrt{3}} & \frac{1}{\sqrt{3}} & \frac{1}{\sqrt{3}} & -\frac{1}{3} & 0 & \frac{1}{3} \\ \frac{1}{\sqrt{3}} & \frac{1}{\sqrt{3}} & \frac{1}{\sqrt{3}} & \frac{1}{3} & -\frac{1}{3} & 0 \\ 0 & -1 & 1 & \frac{1}{3\sqrt{3}} & \frac{1}{3\sqrt{3}} & \frac{1}{3\sqrt{3}} \\ 1 & 0 & -1 & \frac{1}{3\sqrt{3}} & \frac{1}{3\sqrt{3}} & \frac{1}{3\sqrt{3}} \\ -1 & 1 & 0 & \frac{1}{3\sqrt{3}} & \frac{1}{3\sqrt{3}} & \frac{1}{3\sqrt{3}} \end{bmatrix} \begin{bmatrix} \Phi_{c(s),1}(x) \\ \Phi_{c(s),2}(x) \\ \Phi_{c(s),3}(x) \\ \Theta_{c(s),1}(x) \\ \Theta_{c(s),2}(x) \\ \Theta_{c(s),3}(x) \end{bmatrix} \tag{3.38}$$

Consistently with Eqs. [2.129], we therefore define the dual fermionic fields as

$$\begin{aligned} \tilde{\psi}_{R,\sigma,j}(x) &= \eta_{R,\sigma,j} e^{\frac{i}{2}[\tilde{\Phi}_{j,c}(x)+\tilde{\Theta}_{j,c}(x)+\sigma(\tilde{\Phi}_{j,s}(x)+\tilde{\Theta}_{j,s}(x))]} \\ \tilde{\psi}_{L,\sigma,j}(x) &= \eta_{L,\sigma,j} e^{\frac{i}{2}[\tilde{\Phi}_{j,c}(x)-\tilde{\Theta}_{j,c}(x)+\sigma(\tilde{\Phi}_{j,s}(x)-\tilde{\Theta}_{j,s}(x))]} \end{aligned} \tag{3.39}$$

Using Eq. [3.38] one sees that, when expressed in terms of the $\tilde{\Phi}$ and of the $\tilde{\Theta}$-fields, the bulk Hamiltonian in Eq. [2.133] reduces back to the one with $g_c = g_s = 1$, which, when expressed in terms of the fermionic fields defined in Eqs. [3.39], corresponds to the free Hamiltonian $H_{0,F}$, given by

$$H_{0,F} = -iu \sum_{j=1}^{3} \sum_{\sigma} \int_0^L dx \, \left\{ \tilde{\psi}^{\dagger}_{R,j,\sigma}(x) \partial_x \tilde{\psi}_{R,j,\sigma}(x) - \tilde{\psi}^{\dagger}_{L,j,\sigma}(x) \partial_x \tilde{\psi}_{L,j,\sigma}(x) \right\} \tag{3.40}$$

Equation [3.40] is the striking result of our technique of introducing dual fermion operators: it is a free-fermion Hamiltonian which describes a system that is strongly interacting in the original coordinates. Based upon the dual fermion fields in Eqs. [3.39] one may therefore introduce dual boundary operators analogous to those defined in Eq. [3.1], namely, one may set

$$\tilde{B}_{(j,j'),\sigma,(X,X')}(0) = \tilde{\psi}^{\dagger}_{X,j,\sigma}(0) \tilde{\psi}_{X',j',\sigma}(0) \tag{3.41}$$

and assume that the boundary interaction is realized as a linear combination of the operators in Eq. [3.41] and/or of products of two of them. In the absence of additional bulk interaction involving the dual fermion fields, or in the weakly interacting regime, the most relevant boundary interaction term is realized as a linear combination of the $\tilde{B}$-operators only. Therefore, the physically relevant processes at the junction are all encoded within the single-particle S-matrix elements in the basis of the dual fields, $\tilde{S}_{(j,\sigma);(j',\sigma')}$. A nontrivial flow for the $\tilde{S}$-matrix elements is induced by a nonzero bulk interaction in the dual-fermion theory, that is, by having $g_{c(s)} = 3 + \delta g_{c(s)}$, with $|\delta g_{c(s)}|/g_{c(s)} \ll 1$. The dual interaction Hamiltonian, $\tilde{H}_{\rm int}$ can be readily recovered using Eqs. [3.38,3.39]. The result is

$$\tilde{H}_{\rm int} = \sum_{j=1}^{3} \sum_{\sigma,\sigma'} g_{j;(\sigma,\sigma')} \int_0^L dx \, \tilde{\rho}_{R,j,\sigma}(x) \tilde{\rho}_{L,j,\sigma'}(x) + \sum_{j \neq j'=1}^{3} \sum_{\sigma,\sigma'} g_{(j,j');(\sigma,\sigma')} \int_0^L dx \, \tilde{\rho}_{R,j,\sigma}(x) \tilde{\rho}_{L,j',\sigma'}(x) \tag{3.42}$$

with $\tilde{\rho}_{R(L),j,\sigma}(x) =: \tilde{\psi}^{\dagger}_{R(L),j,\sigma}(x) \tilde{\psi}_{R(L),j,\sigma}(x) :$, and

$$\begin{aligned} g_{j;(\sigma,\sigma')} &= \frac{2\pi u(\delta g_c + \delta g_s)}{9} \delta_{\sigma,\sigma'} + \frac{2\pi u(\delta g_c - \delta g_s)}{9} \delta_{\sigma,\bar{\sigma}'} \\ g_{(j,j');(\sigma,\sigma')} &= -\frac{8\pi u(\delta g_c + \delta g_s)}{9} \delta_{\sigma,\sigma'} - \frac{8\pi u(\delta g_c - \delta g_s)}{9} \delta_{\sigma,\bar{\sigma}'} \end{aligned} \tag{3.43}$$

plus terms that do not renormalize the scattering amplitudes. $\tilde{H}_{\rm int}$ takes the form of the generalized bulk Hamiltonian in Eq. [2.10]. Given the corresponding F-matrix elements reported in Eq. [2.76], one may derive the RG-equations in the case in which the spin is conserved at a scattering process at the junction, which implies $\tilde{S}_{(j,\sigma);(j',\sigma')} = \delta_{\sigma,\sigma'} \tilde{S}_{j,j'}$, and the boundary interaction is symmetric under a cyclic permutation of the three wires, that is, the $\tilde{S}_{j,j'}$-matrix elements are given by

$$\tilde{S} = \begin{bmatrix} \tilde{r} & \tilde{\bar{t}} & \tilde{t} \\ \tilde{t} & \tilde{r} & \tilde{\bar{t}} \\ \tilde{\bar{t}} & \tilde{t} & \tilde{r} \end{bmatrix} \tag{3.44}$$

Summing over both the inter-wire and the intra-wire processes allowed by the bulk interaction, one obtains

$$\begin{aligned} \frac{d\tilde{r}}{d\ell} &= \left(\frac{\gamma-\alpha}{2}\right)\{\tilde{r} - |\tilde{r}|^2\tilde{r} - 2\tilde{\bar{t}}\tilde{t}\tilde{r}^*\} \\ \frac{d\tilde{t}}{d\ell} &= -\left(\frac{\gamma-\alpha}{2}\right)\{2\tilde{t}|\tilde{r}|^2 + (\tilde{\bar{t}})^2\tilde{r}^*\} \\ \frac{d\tilde{\bar{t}}}{d\ell} &= -\left(\frac{\gamma-\alpha}{2}\right)\{2\tilde{\bar{t}}|\tilde{r}|^2 + (\tilde{t})^2\tilde{r}^*\} \end{aligned} \tag{3.45}$$

with $\alpha = g_{(j,j');(\sigma,\sigma)}/(2\pi u), \gamma = g_{j;(\sigma,\sigma)}/(2\pi u)$. Equations [3.45] are equal with Eqs. [3.28] in the weakly interacting case, provided one substitutes the (running) parameter β in Eqs. [3.28] with the (constant) parameter $\gamma - \alpha$. As a result, the RG-flow of the $\tilde{S}$-matrix elements is the same as the one obtained for the S-matrix elements. Nevertheless, due to the nonlinear correspondence between the original and the dual fermionic fields, the result for the conductance at corresponding points of the phase diagram is completely different. To discuss this point, let us write the current operators at fixed spin polarization, $J_{j,\sigma}(x)$, in terms of the dual fermionic fields as

$$J_{j,\sigma}(x) = eu \sum_{X=L,R} \{\tilde{\rho}_{X,j-1,\sigma}(x) - \tilde{\rho}_{X,j+1,\sigma}(x)\} \tag{3.46}$$

with $j + 3 \equiv j$. Using Eq. [3.46], the $\mathcal{D}$-tensor

$$\mathcal{D}_{(j,\sigma),(j',\sigma')}(x,x';\omega) = \delta_{\sigma,\sigma'}\mathcal{D}_{j,j'}(x,x';\omega) \tag{3.47}$$

has the form

$$\begin{aligned} \mathcal{D}_{j,j'}(x,x';\omega) = \frac{e^2}{2\pi} \int dE\, f(E)[f(-E-\omega) - f(-E+\omega)] \\ \times \Big\{ 2e^{i\frac{\omega}{u}(x-x')}\delta_{j,j'} + e^{i\frac{\omega}{u}(x+x')}[|\tilde{S}_{j-1,j'-1}|^2 + |\tilde{S}_{j+1,j'+1}|^2] \\ - \; e^{i\frac{\omega}{u}(x-x')}[\delta_{j-1,j'+1} + \delta_{j+1,j'-1}] - e^{i\frac{\omega}{u}(x+x')}[|\tilde{S}_{j-1,j'+1}|^2 + |\tilde{S}_{j+1,j'-1}|^2] \Big\} \end{aligned} \tag{3.48}$$

Following the approach developed in Chap. [II] one therefore readily derives the dc conductance tensor, which is given by

$$G_{(j,\sigma);(j',\sigma')} = \delta_{\sigma,\sigma'}G_{j,j'} \tag{3.49}$$

with

$$\begin{aligned} G_{j,j'} = \frac{e^2}{2\pi} \Big\{ 2\delta_{j,j'} + |\tilde{S}_{j+1,j'+1}|^2 + |\tilde{S}_{j-1,j'-1}|^2 \\ - \; \Big[\delta_{j+1,j'-1} + \delta_{j-1,j'+1} + |\tilde{S}_{j-1,j'+1}|^2 + |\tilde{S}_{j+1,j'-1}|^2\Big] \Big\} \end{aligned} \tag{3.50}$$

One eventually obtains the spin and conductance tensors

$$G_c(D) = G_s(D) = G_0 - \frac{3e^2}{2\pi}\,\Gamma(D) \tag{3.51}$$

with

$$G_0 = \frac{e^2}{\pi}\begin{bmatrix} 4 & -2 & -2 \\ -2 & 4 & -2 \\ -2 & -2 & 4 \end{bmatrix} \quad , \quad \Gamma(D) = \begin{bmatrix} (\tilde{T}(D)+\tilde{\tilde{T}}(D)) & -\tilde{\tilde{T}}(D) & -\tilde{T}(D) \\ -\tilde{T}(D) & (\tilde{T}(D)+\tilde{\tilde{T}}(D)) & -\tilde{\tilde{T}}(D) \\ -\tilde{\tilde{T}}(D) & -\tilde{T}(D) & (\tilde{T}(D)+\tilde{\tilde{T}}(D)) \end{bmatrix} \tag{3.52}$$

and $\tilde{T}(D) = |\tilde{t}(D)|^2, \tilde{\tilde{T}}(D) = |\tilde{\tilde{t}}(D)|^2$. The RG-flow of $\tilde{T}(D)$ and of $\tilde{\tilde{T}}(D)$ is determined by Eqs. [3.30], with β replaced by $\gamma-\alpha \propto \delta g_c+\delta g_s$. As a result, for $\delta g_c+\delta g_s > 0$ the stable fixed point is the "dual" disconnected fixed point, which we dub $[\tilde{N}_c, \tilde{N}_s]$, as, in bosonic coordinates, it corresponds to imposing Neumann boundary conditions on all the $\tilde{\Phi}_{j,c(s)}(x)$-fields at $x = 0$. From Eqs. [3.51,3.52] one therefore finds that the corresponding charge- and spin-conductance tensors are given by $G_c = G_s = G_0$. This is absolutely consistent with the result provided in Ref. [30] for $g_c = g_s = 3$. Indeed, from Eqs. [3.38,3.39] one sees that, resorting back to the original bosonic fields, the $[\tilde{N}_c, \tilde{N}_s]$-fixed points corresponds to the $[D_c, D_s]$-fixed point of Ref. [30], with Dirichlet boundary conditions imposed on the relative fields $\varphi_{1,c(s)}(x) = \frac{1}{\sqrt{2}}[\Phi_{1,c(s)}(x) - \Phi_{2,c(s)}(x)]$ and $\varphi_{2,c(s)}(x) = \frac{1}{\sqrt{6}}[\Phi_{1,c(s)}(x) + \Phi_{2,c(s)}(x) - 2\Phi_{3,c(s)}(x)]$, where the charge- and the spin-conductance tensors for $g_c = g_s = 3$ are equal to each other and both equal to G_0. To double-check the consistency between our dual-fermion FRG-formalism and the bosonization approach, we note that, at the $[\tilde{N}_c, \tilde{N}_s]$-fixed point, a generic linear combination of the boundary operators in Eq. [3.41] can be expressed, in the original bosonic degrees of freedom, as a linear combination of the operators $O_{j,\sigma}(0) = \eta_{L,2,\sigma}\eta_{L,1,\sigma}\, e^{-\frac{i}{2}[\Theta_{j+1,c}(0)+\Theta_{j,c}(0)]-\frac{i\sigma}{2}[\Theta_{j+1,s}(0)+\Theta_{j,s}(0)]}$ and of their Hermitean conjugates, which is the result obtained in Ref. [30] by means of a pertinent application of the delayed evaluation of boundary conditions (DEBC)-technique[28,29].

When $\delta g_c + \delta g_s < 0$, the $[\tilde{N}_c, \tilde{N}_s]$-fixed point becomes unstable. As in the weakly interacting case, we see that, if $\tilde{T}(D_0) \neq \tilde{\tilde{T}}(D_0)$, the junction flows towards either one of the "dual-chiral" fixed points, $\tilde{\chi}_{++}, \tilde{\chi}_{--}$, with the crossover of the conductance tensors with the scale being given by Eq. [3.51]. In particular, if $\tilde{T}(D_0) > \tilde{\tilde{T}}(D_0)$, the flow is towards the infrared stable $\tilde{\chi}_{++}$-fixed point. This corresponds to $\tilde{R} = \tilde{\tilde{T}} = 0, \tilde{T} = 1$. From Eq. [3.51], one therefore obtains that the fixed point conductances are given by

$$G_c = G_s = \frac{e^2}{\pi}\begin{bmatrix} 1 & -2 & 1 \\ 1 & 1 & -2 \\ -2 & 1 & 1 \end{bmatrix} \equiv \frac{e^2}{\pi} Q_\chi^+ \tag{3.53}$$

By consistency, one would expect that the $\tilde{\chi}_{++}$ fixed point should be identified with the χ_{++} fixed point emerging from the weak interaction calculation of the previous section. However, in order to compare the conductances obtained in Eq. [3.53] with those of Eq. [3.33] one has to take into account that formula for the conductance tensor derived within dual-fermion approach applies to a junction connected to reservoirs with $g_c = g_s = 3$. Therefore, to make the comparison, one has to trade Eq. [3.53] for a formula for the conductance tensors of a junction connected to reservoirs with $g_c = g_s = 1$, $G_{c;wl}, G_{s;wl}$. As pointed out in[28,29,83], this can be done by means of pertinent generalizations of Eq. [2.7] of Refs. [28 and 29], that is,

$$[G^{-1}]_{c(s);(j,j')} = [G^{-1}]_{c(s);wl;(j,j')} + G^{-1}_{\mathrm{in},c(s)}\delta_{j,j'} \tag{3.54}$$

with the interface charge (spin) conductance $G_{\mathrm{in},c(s)} = \frac{2g_{c(s)}}{g_{c(s)}-1}\frac{e^2}{\pi}$ (see Fig. [20] for a sketch of the junction connected to reservoirs with generic values of the Luttinger parameter g_L).
The result is

$$G_{c;wl} = G_{s;wl} = \frac{e^2}{\pi}\, Q_\chi^+ \left\{ I + \frac{Q_\chi^+}{3} \right\}^{-1} = \frac{e^2}{\pi}\begin{bmatrix} 1 & 0 & -1 \\ -1 & 1 & 0 \\ 0 & -1 & 1 \end{bmatrix} \tag{3.55}$$

that is, the same result as in Eq. [3.33]. Similarly, one can prove that the chiral $\tilde{\chi}_{--}$-fixed point, towards which the RG-trajectories flow if $\tilde{T}(D_0) < \tilde{\tilde{T}}(D_0)$, has to be identified with the χ_{--}-fixed point of Sec. III.2.1.

When $\tilde{T}(D_0) = \tilde{\tilde{T}}(D_0)$, the RG-trajectories flow towards a nontrivial fixed point, which we dub $\tilde{M}$, by analogy to the M-fixed point we found in Sec. III.2.1. Such a fixed point corresponds to $\tilde{R} = 1/9, \tilde{T} = \tilde{\tilde{T}} = 4/9$. Therefore, from Eq. [3.51], one finds that the fixed point conductance tensors are given by

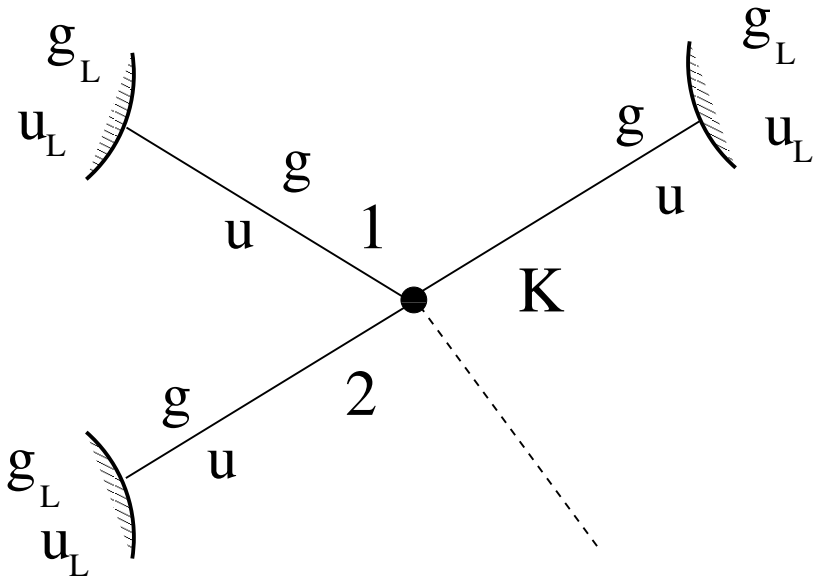

FIG. 20. Sketch of a connected junction of K wires with parameters g, u connected to reservoirs with parameters g_L, u_L.

$$G_c = G_s = \frac{e^2}{\pi} \begin{bmatrix} \frac{4}{3} & -\frac{2}{3} & -\frac{2}{3} \\ -\frac{2}{3} & \frac{4}{3} & -\frac{2}{3} \\ -\frac{2}{3} & -\frac{2}{3} & \frac{4}{3} \end{bmatrix} \equiv \frac{e^2}{\pi} Q_\chi^M \tag{3.56}$$

Performing the same transformation as in Eq. [3.55], one eventually finds

$$G_{c;wl} = G_{s;wl} = \frac{e^2}{\pi} Q_\chi^M \left\{ I + \frac{Q_\chi^M}{3} \right\}^{-1} = \frac{e^2}{\pi} \begin{bmatrix} \frac{4}{5} & -\frac{2}{5} & -\frac{2}{5} \\ -\frac{2}{5} & \frac{4}{5} & -\frac{2}{5} \\ -\frac{2}{5} & -\frac{2}{5} & \frac{4}{5} \end{bmatrix} \tag{3.57}$$

On comparing Eq. [3.57] with Eq. [3.37] we now see that, at odds with what happens with the chiral fixed points, the M and the $\tilde{M}$-fixed points cannot be identified with each other. While we are still lacking a clear explanation for this different behavior at different fixed points, we suspect that this shows that, while the conductance at χ_{++} as well as the χ_{--}-fixed points are in a sense universal, that is, independent of the Luttinger parameters (provided one pertinently takes into account the corrections due to different Luttinger parameters for the reservoirs), the conductance at the M-fixed point does depend explicitly on the Luttinger parameters. This would definitely not be surprising, as such a feature would be shared by a similar fixed point such as, for instance, the nontrivial fixed point at a junction between a topological superconductor and two interacting one-dimensional electronic systems[61]. In any case, we believe that this issue calls for a deeper investigation, which will possibly be the subject of a forthcoming work.

As so far we mainly concentrated around the "diagonal" in Luttinger parameter plane, that is, at $g_c \sim g_s$, we are now going to complement our analysis by discussing the regime with $g_c \sim 3, g_s \sim 1$, together with the complementary one, $g_c \sim 1, g_s \sim 3$.

III.2.3. Fermionic analysis of the strongly interacting regime for $g_c \sim 3, g_s \sim 1$ and $g_c \sim 1, g_s \sim 3$

We now discuss the "asymmetric" regime $g_c \sim 3, g_s \sim 1$. In order to recover the whole procedure, we again note that it is always possible to separately rescale the real-space coordinate in the bosonic Hamiltonian in Eq. [2.133], so to make the charge- and the spin-plasmon velocities to be both equal to u. Therefore, to actually define the dual fermion coordinates, let us assume $g_c = 3, g_s = 1$. Due to the absence of bulk interaction in the spin sector, we have no need to transform the $\Phi_{s,j}, \Theta_{s,j}$-fields. At variance, we do trade the fields $\Phi_{c,j}, \Theta_{c,j}$ for the fields $\tilde{\Phi}_{c,j}, \tilde{\Theta}_{c,j}$ defined in Eq. [3.38]. Accordingly, we consistently define the dual fermionic fields as

$$\chi_{R,\sigma,j}(x) = \eta_{R,\sigma,j} e^{\frac{i}{2}[\tilde{\Phi}_{j,c}(x) + \tilde{\Theta}_{j,c}(x) + \sigma(\Phi_{j,s}(x) + \Theta_{j,s}(x))]}$$

$$\chi_{L,\sigma,j}(x) = \eta_{L,\sigma,j} e^{\frac{i}{2}[\tilde{\Phi}_{j,c}(x) - \tilde{\Theta}_{j,c}(x) + \sigma(\Phi_{j,s}(x) - \Theta_{j,s}(x))]} \tag{3.58}$$

Again, one sees that, when expressed in terms of the dual fermion operators in Eqs. [3.58], the bulk Hamiltonian in Eq. [2.133] reduces back to the free fermionic Hamiltonian, given by

$$H_{0,F;\chi} = -iu \sum_{j=1}^{3} \sum_{\sigma} \int_0^L dx \, \left\{ \chi^{\dagger}_{R,j,\sigma}(x) \partial_x \chi_{R,j,\sigma}(x) - \chi^{\dagger}_{L,j,\sigma}(x) \partial_x \chi_{L,j,\sigma}(x) \right\} \tag{3.59}$$

Having defined the dual fermion operators, we now assume that the leading boundary perturbation is realized as a linear combination of the dual boundary operators defined as

$$\tilde{B}_{\chi;(j,j'),\sigma,(X,X')}(0) = \chi^{\dagger}_{X,j,\sigma}(0) \chi_{X',j',\sigma}(0) \tag{3.60}$$

and/or of products of two of them. Just as we have done before, we also assume that the most relevant scattering processes at the junction are fully described by means of the single-particle S-matrix elements in the basis of the χ-fields, $S_{\chi;(j,\sigma);(j',\sigma')}$. Slightly displacing (g_c, g_s) from (3,1), that is, setting $g_c = 3 + \delta g_c, g_s = 1 + \delta g_s$, with $|\delta g_c|/3, |\delta g_s| \ll 1$, gives rise to an effective interaction Hamiltonian $H_{\chi;\mathrm{int}}$, which takes exactly the same form as $\tilde{H}_{\mathrm{int}}$ in Eq. [3.42], and is given by

$$H_{\chi;\mathrm{int}} = \sum_{j=1}^{3} \sum_{\sigma,\sigma'} g_{\chi;j;(\sigma,\sigma')} \int_0^L dx \, \rho_{\chi;R,j,\sigma}(x) \rho_{\chi;L,j,\sigma'}(x) + \sum_{j \neq j'=1}^{3} \sum_{\sigma,\sigma'} g_{\chi;(j,j');(\sigma,\sigma')} \int_0^L dx \, \rho_{\chi;R,j,\sigma}(x) \rho_{\chi;L,j',\sigma'}(x) \tag{3.61}$$

with $\rho_{\chi;R(L),j,\sigma}(x) =: \chi^{\dagger}_{R(L),j,\sigma}(x) \chi_{R(L),j,\sigma}(x) :$, and

$$\begin{aligned} g_{\chi;j;(\sigma,\sigma')} &= \frac{8\pi u(\delta g_c - 3\delta g_s)}{9} \delta_{\sigma,\sigma'} + \frac{8\pi u(\delta g_c + 3\delta g_s)}{9} \delta_{\sigma,\bar{\sigma}'} \\ g_{\chi;(j,j');(\sigma,\sigma')} &= -\frac{4\pi u(\delta g_c - 3\delta g_s)}{9} \delta_{\sigma,\sigma'} - \frac{4\pi u(\delta g_c + 3\delta g_s)}{9} \delta_{\sigma,\bar{\sigma}'} \end{aligned} \tag{3.62}$$

plus terms that do not renormalize the scattering amplitudes. Making the assumption that the spin is conserved at a scattering process at the junction, we again obtain that $S_{\chi;(j,\sigma);(j',\sigma')} = \delta_{\sigma,\sigma'} S_{\chi;(j,j')}$, with, for a boundary interaction symmetric under a cyclic permutation of the three wires, the S_{χ}-matrix being given by

$$S_{\chi} = \begin{bmatrix} r_{\chi} & \bar{t}_{\chi} & t_{\chi} \\ t_{\chi} & r_{\chi} & \bar{t}_{\chi} \\ \bar{t}_{\chi} & t_{\chi} & r_{\chi} \end{bmatrix} \tag{3.63}$$

The RG-equations for the running S_{χ}-matrix elements are derived in perfect analogy with Eq. [3.45]. The result is exactly the same, except that now $\gamma - \alpha \propto \delta g_c - 3\delta g_s$. In order to trace out the correspondence between the fixed point of the boundary phase diagram for the dual-fermion scattering amplitudes and those of the phase diagram for the original fermion amplitudes, we now discuss the behavior of the charge- and of the spin-conductance tensor along the RG-trajectories. To do so, we note that, due to the fact that the spin sector of the theory is left unchanged, when resorting to the dual coordinates, the spin-conductance tensor, when expressed in terms of the scattering coefficients at the junction, takes the same form as in the noninteracting case, given in Eq. [3.29]. As variance, the charge-conductance tensor depends on the scattering coefficients as given in Eq. [3.52]. As a result, one obtains

$$G_c(D) = G_0 - \frac{3e^2}{2\pi} \Gamma_{\chi}(D) \quad , \quad G_s(D) = \frac{e^2}{\pi} \begin{bmatrix} -R_{\chi}(D) + 1 & -\bar{T}_{\chi}(D) & -T_{\chi}(D) \\ -T_{\chi}(D) & -R_{\chi}(D) + 1 & -\bar{T}_{\chi}(D) \\ -\bar{T}_{\chi}(D) & -T_{\chi}(D) & -R_{\chi}(D) + 1 \end{bmatrix} \tag{3.64}$$

with $R_{\chi}(D) = |r_{\chi}(D)|^2, T_{\chi}(D) = |t_{\chi}(D)|^2, \bar{T}_{\chi}(D) = |\bar{t}_{\chi}(D)|^2$. We are, now, in the position of mapping out the whole phase diagram of the spinful junction for $g_c \sim 3, g_s \sim 1$, including the fixed point manifold, and of tracing out the correspondence between the fixed points given in terms of the dual fermion amplitudes, and the described in terms of

the original fermionic coordinates[30]. First of all, we note that, when $\delta g_c - 3\delta g_s > 0$, the system is attracted towards the "dual disconnected" fixed point $[N_{\chi,c}, N_{\chi,s}]$, characterized by the scattering coefficients $R_\chi = 1, T_\chi = \bar{T}_\chi = 0$. At such a fixed point, one obtains $G_c = G_0, G_s = 0$, which enables us to identify $[N_{\chi,c}, N_{\chi,s}]$ with the $[D_c, N_s]$-fixed point in the phase diagram of Ref. [30], that is, with a spin-insulating fixed point where the most relevant process at the junction is pair-correlated Andreev reflection in each wire. At variance, when $\delta g_c - 3\delta g_s < 0$, the junction flows towards one among the dual χ_{++}, χ_{--}, or M-fixed points. In particular, from Eqs. [3.64], one sees that, at the dual χ_{++}-fixed point, G_c is given by Eq. [3.53], while G_s takes the form provided in Eq. [3.33]. After the correction of Eq. [3.55], one eventually finds that G_c and G_s are equal to each other, and both equal to the fixed-point conductance at the χ_{++}-fixed point in the original coordinates. Thus, we are eventually led to identify the dual χ_{++}-fixed point with the analogous one, realized in the original coordinates. A similar argument leads to the identification of the dual χ_{--}-fixed point with the analogous one, realized in the original coordinates. As for what concerns the dual M-fixed point, after correcting the charge-conductance tensor as in Eq. [3.57], one finds that, at such a fixed point,

$$G_{c;wl} = \frac{e^2}{\pi} \begin{bmatrix} \frac{4}{5} & -\frac{2}{5} & -\frac{2}{5} \\ -\frac{2}{5} & \frac{4}{5} & -\frac{2}{5} \\ -\frac{2}{5} & -\frac{2}{5} & \frac{4}{5} \end{bmatrix} \quad , \quad G_{s;wl} = G_s = \frac{e^2}{\pi} \begin{bmatrix} \frac{8}{9} & -\frac{4}{9} & -\frac{4}{9} \\ -\frac{4}{9} & \frac{8}{9} & -\frac{4}{9} \\ -\frac{4}{9} & -\frac{4}{9} & \frac{8}{9} \end{bmatrix} \tag{3.65}$$

Putting together Eqs. [3.65,3.57,3.37] we again see that M-like fixed points are not mapped onto each other, not even after the correction of Eq. [3.57]. This is again consistent with our previous hypothesis, namely, that the conductance at the M-fixed point does depend explicitly on the Luttinger parameters and, therefore, it is different in the various cases we discussed before.

Before concluding this subsection, we point out that the same analysis we just performed in the case $g_c \sim 3, g_s \sim 1$ does apply equally well to the complementary situation $g_c \sim 1, g_s \sim 3$, provided one swaps charge- and spin-operators (and conductances) with each other.

Putting together all the results we obtained using the FRG-approach, one may infer the global topology of the phase diagram of a spinful three-wire junction and compare the results with those obtained within the bosonization approach. This will be the subject of the next subsection.

III.2.4. Global topology of the phase diagram from fermionic renormalization group approach

Following Ref. [30], we discuss the main features of the phase diagram of the three-wire junction within various regions in the $g_c - g_s$ plane. Let us start from the "quasisymmetric" region $g_c \sim g_s$. From the results of Sec. III.2.1 we see that, setting $g_c = 1 + \delta g_c, g_s = 1 + \delta g_s$, as long as $\delta g_c + \delta g_s < 0$ (corresponding to $\frac{1}{2g_c} + \frac{1}{2g_s} < 1$), the system flows towards the disconnected $[N_c, N_s]$-fixed point. At variance, for $\delta g_c + \delta g_s > 0$ (that is, for $\frac{1}{2g_c} + \frac{1}{2g_s} > 1$), as soon as scattering processes from wire j to wires $j \pm 1$ take place at different rates (i.e., $T \neq \bar{T}$), the RG-trajectories flow towards either one of the χ_{++} or χ_{--}-fixed points. While this is basically consistent with the region of the phase diagram derived in[30] corresponding to $g_c \sim g_s \sim 1$, in addition, when $T = \bar{T}$, we found that the system flows towards a symmetric fixed point, which we dubbed M, with peculiar, g_c, g_s-dependent transport properties. Within the FRG-approach we were able to map out the full crossover of the charge- and spin-conductance tensor between any two of the fixed points listed above, with some paradigmatic examples shown in the figures of Sec. III.2.1. Keeping within the quasisymmetric region, in Sec. III.2.2 we show that, setting $g_c = 3 + \delta g_c, g_s = 3 + \delta g_s$, for $\delta g_c + \delta g_s > 0$ (that is, for $g_c + g_s > 6$), the stable RG-fixed point corresponds to the $[D_c, D_s]$-fixed point of Ref. [30] while, as soon as $\delta g_c + \delta g_s < 0$ (that is, for $g_c + g_s < 6$), the system flows towards either one of the χ_{++} or χ_{--} fixed points in the non-symmetric case, or towards an "M-like" fixed point in the symmetric case. As discussed above, while, at both the χ_{++} and the χ_{--}-fixed points the conductance tensors for the junction not connected to the leads are the same, regardless of the value of the Luttinger parameters, at variance, at the M-fixed point they do depend on g_c and g_s and, in this sense, they appear to be "nonuniversal". Over all, the results we obtained across the region $g_c \sim g_s$ are consistent with a phase diagram where the $[N_c, N_s]$ and the $[D_c, D_s]$-fixed points are respectively stable for $\frac{1}{2g_c} + \frac{1}{2g_s} < 1$ and for $g_c + g_s > 6$, while, at intermediate values of the Luttinger parameters, depending on the bare values of the scattering coefficients at the junction, one out of the (universal) chiral χ_{++}, χ_{--}-fixed points or the (nonuniversal) M-fixed point becomes stable. This results already complements the phase diagram of Ref. [30] by introducing the M-fixed point, which has necessarily to be there, in order to separate the phases corresponding to χ_{++} and to χ_{--} from each other. To push our analysis outside of the $g_c \sim g_s$-region, we discussed the nonsymmetric case $g_c \sim 3, g_s \sim 1$. In this case, we found that the manifold of fixed points consists of the $[D_c, N_s]$ asymmetric fixed point, at which the junction is characterized by perfect pair-correlated Andreev reflection in each wire, while it is perfectly insulating in the spin sector, the chiral χ_{++}, χ_{--}-fixed points and, again, an M-like fixed point. Also

in this region our results appear on one hand to be consistent with the phase diagram of Ref. [30], on the other hand to complement it with singling out the M-like fixed point. The complementary regime $g_c \sim 1, g_s \sim 3$ can be straightforwardly recovered from the previous discussion by just swapping charge and spin with each other. Aside from recovering the global phase diagram of the junction, our technique allows for generalizing to strongly-interacting regimes the main advantage of using fermionic, rather than bosonic coordinates, that is, the possibility mapping out the crossover of the conductance between fixed points in the phase diagram.

III.3. Discussion and conclusions

In the Chapter, we generalize the RG approach to junctions of strongly-interacting QWs. In order to do so, we make a combined use of both the fermionic and the bosonic approaches to interacting electronic systems in one dimension, which enables us to build pertinent nonlocal transformation between the original fermion fields and dual-fermion operators, so that, a theory that is strongly interacting in terms of the former ones, maps onto a weakly interacting one, in terms of the latter ones. On combining the dual-fermion approach with the FRG-technique, we are able to produce new and interesting results, already for the well-known two wire junction. When applied to a Z_3-symmetric three-wire junction, our technique first of all allows for recovering fundamental informations concerning the topology of the global phase diagram, as well as all the fixed points accessible to the junction in various regions of the parameter space. While, in this respect, our approach looks like a useful means to complement the bosonization approach to conductance properties of junctions of quantum wires, where it appears extremely useful and, in a sense, rather unique, is in providing the full crossover of the conductance tensors between any two fixed points connected by an RG-trajectory. The crossover in the conductance properties can be experimentally mapped out by monitoring the transport properties of the junction as a function of a running reference scale, such as the temperature, or the effective system size. While the standard FRG approach just yields crossover curves at weak bulk interaction in the quantum wires[37–40], as stated above, our approach extends such a virtue of the fermionic approach to regions at strong values of the bulk electronic interaction in the wires.

By resorting to the appropriate dual fermionic degrees of freedom, our approach allows for describing in terms of effectively one-particle S-matrix elements correlated pair scattering and/or Andreev reflection, in regions of values of the interaction parameters where they correspond to the most relevant scattering processes at the junction. This allows for envisaging, within our technique, fixed points such as the $[D_c, D_s]$, or the $[D_c, N_s]$ one. In fact, due to basic assumption of the standard FRG-approach that all the relevant processes at the junction are encoded in the single-particle S-matrix elements, fixed points such as those listed before are typically not expected to be recovered without resorting to the appropriate dual fermion coordinates, not even after relaxing the weak bulk interaction constraint[53].

While, for simplicity, here we restrict ourselves to the case of a symmetric junction and of a spin-conserving boundary interaction at the junction, our approach can be readily generalized to a non-symmetric junction characterized, for instance, by different Luttinger parameters in different wires[31], and/or by a non-spin-conserving boundary interaction. Also, a generalization of our approach to a junction involving ordinary[51], or topological superconductors[61,64] is likely to allow for describing the full crossover of the conductance in a single junction, as well as of the equilibrium (Josephson) current in a SNS-junction thus generalizing, in this latter case, the results obtained Refs. [87–89] to an SNS-junction with an interacting central region.

III.4. Appendix A: Bosonization analysis of the three-wire junction

In this Appendix, following the approach of Ref. [30], we start our analysis with of all the leadingmost boundary interaction operators at the three-wire junction. In fact, the phase diagram of the three-wire junction is much richer than the one of the two-wire junction[27]. In analogy to what we have done for the two-wire junction, the boundary Hamiltonian for the three-wire junction is a linear combination of the bilinear operators in Eq. [3.1] and contain terms corresponding to inter-wire single-particle tunneling, as well as to intra-wire single-particle backscattering. That is

$$H_{tun}^{single} = -\left(\sum_j \sum_\sigma \Gamma_{j,j-1}^\sigma \psi_{\sigma,j}^\dagger(0)\psi_{\sigma,j-1}(0) + h.c.\right) - \left(\sum_j \sum_\sigma \mu_j^\sigma \psi_{R,\sigma,j}^\dagger(0)\psi_{L,\sigma,j}(0) + h.c.\right) \tag{3.66}$$

with $\Gamma_{j,j-1}^\sigma$ being complex tunneling amplitudes. In addition to the operators appearing in Eq.[3.66], additional composite operators, corresponding to two-particle scattering processes at the junction, may arise and potentially become relevant, for a pertinent choice of the bulk interaction parameters of the system. At the various fixed points

appearing in the boundary phase diagram of the three-wire junction, all these operators must be supplemented with the pertinent boundary conditions on the various bosonic fields describing charge and spin degrees of freedom, within a pertinent implementation of the DEBC method developed in Ref. [82]. In order to resort to DEBC method, it is appropriate to resort to the center of mass and relative fields, $\Phi_{c(s)}(x), \varphi_{1,c(s)}(x), \varphi_{2,c(s)}$ and $\Theta_{c(s)}, \vartheta_{1,c(s)}, \theta_{2,c(s)}$, defined as

$$\begin{aligned}
\Phi_{c(s)}(x) &= \frac{1}{\sqrt{3}}\left(\Phi_{1,c(s)}(x) + \Phi_{2,c(s)}(x) + \Phi_{3,c(s)}(x)\right) \\
\varphi_{1,c(s)} &= \frac{1}{\sqrt{2}}\left(\Phi_{1,c(s)}(x) - \Phi_{2,c(s)}(x)\right) \\
\varphi_{2,c(s)}(x) &= \frac{1}{\sqrt{6}}\left(\Phi_{1,c(s)}(x) + \Phi_{2,c(s)}(x) - 2\Phi_{3,c(s)}(x)\right) \\
\Theta_{c(s)}(x) &= \frac{1}{\sqrt{3}}\left(\Theta_{1,c(s)}(x) + \Theta_{2,c(s)}(x) + \Theta_{3,c(s)}(x)\right) \\
\vartheta_{1,c(s)}(x) &= \frac{1}{\sqrt{2}}(x)\left(\Theta_{1,c(s)(x)} - \Theta_{2,c(s)}(x)\right) \\
\vartheta_{2,c(s)}(x) &= \frac{1}{\sqrt{6}}\left(\Theta_{1,c(s)}(x) + \Theta_{2,c(s)}(x) - 2\Theta_{3,c(s)}(x)\right)
\end{aligned} \tag{3.67}$$

Remarkably, the continuity equation for the charge and the spin current at the junction implies

$$\partial_x \Phi_c(0) = \partial_x \Phi_s(0) = 0 \tag{3.68}$$

which implies that both $\Theta_c(0)$ and $\Theta_s(0)$ are pinned at any point of the phase diagram. Keeping in mind Eq. [3.68] as an over-all condition, we now proceed to consider the set of fixed point at which the fermionic renormalization group approach can be effectively applied.

III.4.1. Allowed boundary interaction terms at three-wire junction

In this part of the Appendix, we list all the allowed boundary interaction terms at a three-wire junction. In particular, after working out their expressions in fermionic coordinates, we resort to the corresponding bosonized operators, by pertinently using the bosonization rules for fermionic fields encoded in Eqs. [2.129]. For a spinful three-wire junction, the derivation of the leadingmost boundary interaction terms, which can drive the junction towards any of the allowed infrared stable fixed points, has been performed in Ref. [30]. In order to simplify the notation both in this subsection and in the following one, when listing the various boundary interaction terms, it is useful to define the operators $S^{\pm}_{j,\sigma;(X,Y)}$, with $X, Y = L, R$, respectively given by

$$\begin{aligned}
S^{+}_{j,\sigma;(X,Y)}(x) &= \psi^{\dagger}_{X,\sigma,j+1}(x)\psi_{Y,\sigma,j}(x) \\
S^{-}_{j,\sigma;(X,Y)}(x) &= \psi^{\dagger}_{X,\sigma,j-1}(x)\psi_{Y,\sigma,j}(x)
\end{aligned} \tag{3.69}$$

The quadratic Hamiltonian in Eq. [3.66], describing boundary tunneling plus backscattering at a three-wire junction, can be fully expressed as a linear combination of the operators in Eq. [3.69], together with the corresponding Hermitean conjugate. As it happens at the two-wire junction, additional multi-particle boundary interactions can arise as combinations of single particle processes and their Hermitian conjugates. Following the analysis of[30], in the following we will mainly focus onto the most relevant ones, namely, the two-particle processes, which can become the leading operators at some nontrivial fixed point of the phase diagram. In the following, after providing the bosonized version of the various operators in Eqs. [3.69], we will list the additional two-particle boundary interaction terms that can arise at the junction, together with their corresponding bosonized expressions. Starting with the one-particle operators, we may single out the following terms

- **Tunneling in the + cycle**

$$S^{+}_{j,\sigma}(0) = \psi^{\dagger}_{R,\sigma,j+1}(0)\psi_{L,\sigma,j}(0) \to \eta_{R,\sigma,j+1}\eta_{L,\sigma,j}$$

$$\times\, e^{-\frac{i}{2}[\Phi_{j+1,c}(0)+\Theta_{j+1,c}(0)+\sigma(\Phi_{j+1,s}(0)+\Theta_{j+1,s}(0))]} e^{\frac{i}{2}[\Phi_{j,c}(0)-\Theta_{j,c}(0)+\sigma(\Phi_{j,s}(0)-\Theta_{j,s}(0))]} \tag{3.70}$$

- **Tunneling in the − cycle**

$$\begin{aligned} S^{-}_{j,\sigma}(0) &= \psi^{\dagger}_{R,\sigma,j-1}(0)\psi_{L,\sigma,j}(0) \to \eta_{R,\sigma,j-1}\eta_{L,\sigma,j} \\ &\times\, e^{-\frac{i}{2}[\Phi_{j-1,c}(0)+\Theta_{j-1,c}(0)+\sigma(\Phi_{j-1,s}(0)+\Theta_{j-1,s}(0))]} e^{\frac{i}{2}[\Phi_{j,c}(0)-\Theta_{j,c}(0)+\sigma(\Phi_{j,s}(0)-\Theta_{j,s}(0))]} \end{aligned} \tag{3.71}$$

- **Backscattering**

$$\begin{aligned} S^{B}_{j,\sigma}(0) &= \psi^{\dagger}_{R,\sigma,j}(0)\psi_{L,\sigma,j}(0) \to \eta_{R,\sigma,j}\eta_{L,\sigma,j} \\ &\times\, e^{-\frac{i}{2}[\Phi_{j,c}(0)+\Theta_{j,c}(0)+\sigma(\Phi_{j,s}(0)+\Theta_{j,s}(0))]} e^{\frac{i}{2}[\Phi_{j,c}(0)-\Theta_{j,c}(0)+\sigma(\Phi_{j,s}(0)-\Theta_{j,s}(0))]} \end{aligned} \tag{3.72}$$

- **LL-combinations**

$$\begin{aligned} S^{L}_{j,\sigma}(0) &= \psi^{\dagger}_{L,\sigma,j+1}(0)\psi_{L,\sigma,j}(0) \to \eta_{L,\sigma,j+1}\eta_{L,\sigma,j} \\ &\times\, e^{-\frac{i}{2}[\Phi_{j+1,c}(0)-\Theta_{j+1,c}(0)+\sigma(\Phi_{j+1,s}(0)-\Theta_{j+1,s}(0))]} e^{\frac{i}{2}[\Phi_{j,c}(0)-\Theta_{j,c}(0)+\sigma(\Phi_{j,s}(0)-\Theta_{j,s}(0))]} \end{aligned} \tag{3.73}$$

- **RR-combinations**

$$\begin{aligned} S^{R}_{j,\sigma}(0) &= \psi^{\dagger}_{R,\sigma,j+1}(0)\psi_{R,\sigma,j}(0) \to \eta_{R,\sigma,j+1}\eta_{R,\sigma,j} \\ &\times\, e^{-\frac{i}{2}[\Phi_{j+1,c}(0)+\Theta_{j+1,c}(0)+\sigma(\Phi_{j+1,s}(0)+\Theta_{j+1,s}(0))]} e^{\frac{i}{2}[\Phi_{j,c}(0)+\Theta_{j,c}(0)+\sigma(\Phi_{j,s}(0)+\Theta_{j,s}(0))]} \end{aligned} \tag{3.74}$$

together with their Hermitean conjugates.

Let us, now, extend the above list by including all the two-particle operators that can become relevant at some nontrivial fixed point of the phase diagram of the spinful three-wire junction. The allowed terms (together with the corresponding bosonized expressions) are given by

- **Pair Tunneling in + cycle**

$$\begin{aligned} PT^{+}_{j} &= S^{+}_{j,\uparrow;(R,L)}(0)S^{+}_{j,\downarrow;(R,L)}(0) \to \eta_{R,j+1,\uparrow}\eta_{L,j,\uparrow}\ \eta_{R,j+1,\downarrow}\eta_{L,j,\downarrow} \\ &\times\, e^{-\frac{i}{2}[\Phi_{j+1,c}(0)+\Theta_{j+1,c}(0)+\Phi_{j+1,s}(0)+\Theta_{j+1,s}(0)]} e^{\frac{i}{2}[\Phi_{j,c}(0)-\Theta_{j,c}(0)+\Phi_{j,s}(0)-\Theta_{j,s}(0)]} \\ &\times\, e^{-\frac{i}{2}[\Phi_{j+1,c}(0)+\Theta_{j+1,c}(0)-\Phi_{j+1,s}(0)-\Theta_{j+1,s}(0)]} e^{\frac{i}{2}[\Phi_{j,c}(0)-\Theta_{j,c}(0)-\Phi_{j,s}(0)+\Theta_{j,s}(0)]} \end{aligned} \tag{3.75}$$

- **Pair Tunneling in − cycle**

$$\begin{aligned} PT^{-}_{j+1} &= S^{-}_{j+1,\uparrow;(R,L)}(0)S^{-}_{j+1,\downarrow;(R,L)}(0) \to \eta_{R,j,\uparrow}\eta_{L,j+1,\uparrow}\ \eta_{R,j,\downarrow}\eta_{L,j+1,\downarrow} \\ &\times\, e^{-\frac{i}{2}[\Phi_{j,c}(0)+\Theta_{j,c}(0)+\Phi_{j,s}(0)+\Theta_{j,s}(0)]} e^{\frac{i}{2}[\Phi_{j+1,c}(0)-\Theta_{j+1,c}(0)+\Phi_{j+1,s}(0)-\Theta_{j+1,s}(0)]} \\ &\times\, e^{-\frac{i}{2}[\Phi_{j,c}(0)+\Theta_{j,c}(0)-\Phi_{j,s}(0)-\Theta_{j,s}(0)]} e^{\frac{i}{2}[\Phi_{j+1,c}(0)-\Theta_{j+1,c}(0)-\Phi_{j+1,s}(0)+\Theta_{j+1,s}(0)]} \end{aligned} \tag{3.76}$$

- **Pair Tunneling in LL-RR combinations with net spin**

$$\begin{aligned} PTS^{L,R}_{j,\sigma} &= S^{+}_{j,\sigma;(L,L)}(0)S^{-}_{j,\sigma;(R,R)}(0) \rightarrow \eta_{L,j+1,\sigma}\eta_{L,j,\sigma}\eta_{R,j+1,\sigma}\eta_{R,j,\sigma} \\ &\times e^{-\frac{i}{2}[\Phi_{j+1,c}(0)-\Theta_{j+1,c}(0)+\sigma(\Phi_{j+1,s}(0)-\Theta_{j+1,s}(0))]}e^{\frac{i}{2}[\Phi_{j,c}(0)-\Theta_{j,c}(0)+\sigma(\Phi_{j,s}(0)-\Theta_{j,s}(0))]} \\ &\times e^{-\frac{i}{2}[\Phi_{j+1,c}(0)+\Theta_{j+1,c}(0)+\sigma(\Phi_{j+1,s}(0)+\Theta_{j+1,s}(0))]}e^{\frac{i}{2}[\Phi_{j,c}(0)+\Theta_{j+1,c}(0)+\sigma(\Phi_{j+1,s}(0)+\Theta_{j+1,s}(0))]} \end{aligned} \tag{3.77}$$

- **Pair Tunneling in LL-RR combinations without net spin**

$$\begin{aligned} PT^{L,R}_{j,\sigma} &= S^{+}_{j,\sigma;(L,L)}(0)S^{-}_{j,-\sigma;(R,R)}(0) \rightarrow \eta_{L,j+1,\sigma}\eta_{L,j,\sigma}\eta_{R,j+1,-\sigma}\eta_{R,j,-\sigma} \\ &\times e^{-\frac{i}{2}[\Phi_{j+1,c}(0)-\Theta_{j+1,c}(0)+\sigma(\Phi_{j+1,s}(0)-\Theta_{j+1,s}(0))]}e^{\frac{i}{2}[\Phi_{j,c}(0)-\Theta_{j,c}(0)+\sigma(\Phi_{j,s}(0)-\Theta_{j,s}(0))]} \\ &\times e^{-\frac{i}{2}[\Phi_{j+1,c}(0)+\Theta_{j+1,c}(0)-\sigma(\Phi_{j+1,s}(0)+\Theta_{j+1,s}(0))]}e^{\frac{i}{2}[\Phi_{j,c}(0)+\Theta_{j+1,c}(0)-\sigma(\Phi_{j+1,s}(0)+\Theta_{j+1,s}(0))]} \end{aligned} \tag{3.78}$$

- **Intra-wire pair backscattering**

$$\begin{aligned} PB_{j} &= S^{B}_{j,\uparrow}(0)S^{B}_{j,\downarrow}(0) \rightarrow \eta_{R,\uparrow,j}\eta_{L,\uparrow,j}\eta_{R,\downarrow,j}\eta_{L,\downarrow,j} \\ &\times e^{-\frac{i}{2}[\Phi_{j,c}(0)+\Theta_{j,c}(0)+\Phi_{j,s}(0)+\Theta_{j,s}(0)]}e^{\frac{i}{2}[\Phi_{j,c}(0)-\Theta_{j,c}(0)+\Phi_{j,s}(0)-\Theta_{j,s}(0)]} \\ &\times e^{-\frac{i}{2}[\Phi_{j,c}(0)+\Theta_{j,c}(0)-\Phi_{j,s}(0)-\Theta_{j,s}(0)]}e^{\frac{i}{2}[\Phi_{j,c}(0)-\Theta_{j,c}(0)-\Phi_{j,s}(0)+\Theta_{j,s}(0)]} \end{aligned} \tag{3.79}$$

- **Inter-wire pair backscattering with net spin**

$$\begin{aligned} PBS_{j,j+1,\sigma} &= S^{B}_{j,\sigma}(0)S^{B}_{j+1,\sigma}(0) \rightarrow \eta_{R,\sigma,j}\eta_{L,\sigma,j}\eta_{R,\sigma,j+1}\eta_{L,\sigma,j+1} \\ &\times e^{-\frac{i}{2}[\Phi_{j,c}(0)+\Theta_{j,c}(0)+\sigma(\Phi_{j,s}(0)+\Theta_{j,s}(0))]}e^{\frac{i}{2}[\Phi_{j,c}(0)-\Theta_{j,c}(0)+\sigma(\Phi_{j,s}(0)-\Theta_{j,s}(0))]} \\ &\times e^{-\frac{i}{2}[\Phi_{j+1,c}(0)+\Theta_{j+1,c}(0)+\sigma(\Phi_{j+1,s}(0)+\Theta_{j+1,s}(0))]}e^{\frac{i}{2}[\Phi_{j+1,c}(0)-\Theta_{j+1,c}(0)+\sigma(\Phi_{j+1,s}(0)-\Theta_{j+1,s}(0))]} \end{aligned} \tag{3.80}$$

- **Inter-wire pair backscattering without net spin**

$$\begin{aligned} PB_{j,j+1,\sigma} &= S^{B}_{j,\sigma}(0)S^{B}_{j+1,-\sigma}(0) \rightarrow \eta_{R,\sigma,j}\eta_{L,\sigma,j}\eta_{R,-\sigma,j+1}\eta_{L,-\sigma,j+1} \\ &\times e^{-\frac{i}{2}[\Phi_{j,c}(0)+\Theta_{j,c}(0)+\sigma(\Phi_{j,s}(0)+\Theta_{j,s}(0))]}e^{\frac{i}{2}[\Phi_{j,c}(0)-\Theta_{j,c}(0)+\sigma(\Phi_{j,s}(0)-\Theta_{j,s}(0))]} \\ &\times e^{-\frac{i}{2}[\Phi_{j+1,c}(0)+\Theta_{j+1,c}(0)-\sigma(\Phi_{j+1,s}(0)+\Theta_{j+1,s}(0))]}e^{\frac{i}{2}[\Phi_{j+1,c}(0)-\Theta_{j+1,c}(0)-\sigma(\Phi_{j+1,s}(0)-\Theta_{j+1,s}(0))]} \end{aligned} \tag{3.81}$$

- **Pair Exchange processes**

$$\begin{aligned} PE_{j,\sigma} &= S^{+}_{j,\sigma;(R,L)}(0)S^{-}_{j+1,-\sigma;(R,L)}(0) \rightarrow \eta_{R,\sigma,j+1}\eta_{L,\sigma,j}\eta_{R,-\sigma,j}\eta_{L,-\sigma,j+1} \\ &\times e^{-\frac{i}{2}[\Phi_{j+1,c}(0)+\Theta_{j+1,c}(0)+\sigma(\Phi_{j+1,s}(0)+\Theta_{j+1,s}(0))]}e^{\frac{i}{2}[\Phi_{j,c}(0)-\Theta_{j,c}(0)+\sigma(\Phi_{j,s}(0)-\Theta_{j,s}(0))]} \\ &\times e^{-\frac{i}{2}[\Phi_{j,c}(0)+\Theta_{j,c}(0)-\sigma(\Phi_{j,s}(0)+\Theta_{j,s}(0))]}e^{\frac{i}{2}[\Phi_{j+1,c}(0)-\Theta_{j+1,c}(0)-\sigma(\Phi_{j+1,s}(0)-\Theta_{j+1,s}(0))]} \end{aligned} \tag{3.82}$$

- **Particle Hole Pair Tunneling in + cycle**

$$\begin{aligned} PH^{+}_{j} &= S^{+}_{j,\uparrow;(R,L)}(0)[S^{-}_{j,\downarrow;(R,L)}(0)]^{\dagger} \rightarrow \eta_{R,\uparrow,j+1}\eta_{L,\uparrow,j}\eta_{L,\downarrow,j}\eta_{R,\downarrow,j+1} \\ &\times e^{-\frac{i}{2}[\Phi_{j+1,c}(0)+\Theta_{j+1,c}(0)+\Phi_{j+1,s}(0)+\Theta_{j+1,s}(0)]}e^{\frac{i}{2}[\Phi_{j,c}(0)-\Theta_{j,c}(0)+\Phi_{j,s}(0)-\Theta_{j,s}(0)]} \\ &\times e^{-\frac{i}{2}[\Phi_{j,c}(0)-\Theta_{j,c}(0)-\Phi_{j,s}(0)+\Theta_{j,s}(0)]}e^{\frac{i}{2}[\Phi_{j+1,c}(0)+\Theta_{j+1,c}(0)-\Phi_{j+1,s}(0)-\Theta_{j+1,s}(0)]} \end{aligned} \tag{3.83}$$

- **Particle Hole Pair Tunneling in − cycle**

$$\begin{aligned} PH_j^- = S^-_{j+1,\uparrow;(R,L)}(0)[S^-_{j+1,\downarrow;(R,L)}(0)]^\dagger \rightarrow \eta_{R,\uparrow,j}\eta_{L,\uparrow,j+1}\eta_{L,\downarrow,j+1}\eta_{R,\downarrow,j} \\ \times e^{-\frac{i}{2}[\Phi_{j,c}(0)+\Theta_{j,c}(0)+\Phi_{j,s}(0)+\Theta_{j,s}(0)]}e^{\frac{i}{2}[\Phi_{j+1,c}(0)-\Theta_{j+1,c}(0)+\Phi_{j+1,s}(0)-\Theta_{j+1,s}(0)]} \\ \times e^{-\frac{i}{2}[\Phi_{j+1,c}(0)-\Theta_{j+1,c}(0)-\Phi_{j+1,s}(0)+\Theta_{j+1,s}(0)]}e^{\frac{i}{2}[\Phi_{j,c}(0)+\Theta_{j,c}(0)-\Phi_{j,s}(0)-\Theta_{j,s}(0)]} \end{aligned} \tag{3.84}$$

- **Particle Hole Exchange processes**

$$\begin{aligned} PHE_{j,\sigma} = S^+_{j,\sigma;(R,L)}(0)[S^-_{j+1,-\sigma;(R,L)}(0)]^\dagger \rightarrow \eta_{R,\sigma,j+1}\eta_{L,\sigma,j}\eta_{L,-\sigma,j+1}\eta_{R,-\sigma,j} \\ \times e^{-\frac{i}{2}[\Phi_{j+1,c}(0)+\Theta_{j+1,c}(0)+\sigma(\Phi_{j,s}(0)+\Theta_{j,s}(0))]}e^{\frac{i}{2}[\Phi_{j,c}(0)-\Theta_{j,c}(0)+\sigma(\Phi_{j,s}(0)-\Theta_{j,s}(0))]} \\ \times e^{-\frac{i}{2}[\Phi_{j+1,c}(0)-\Theta_{j+1,c}(0)-\sigma(\Phi_{j+1,s}(0)+\Theta_{j+1,s}(0))]}e^{\frac{i}{2}[\Phi_{j,c}(0)+\Theta_{j,c}(0)-\sigma(\Phi_{j,s}(0)-\Theta_{j,s}(0))]} \end{aligned} \tag{3.85}$$

together with all the corresponding Hermitean conjugate operators.

In the following, we use all the expressions listed above to derive the relevant boundary operators allowed at each fixed point, by means of a systematic application of the DEBC method.

III.4.2. The weakly coupled fixed point

As stated in Eq. [3.68], the boundary conditions obeyed by the center-of-mass fields, both in the charge- and in the spin-sector, are uniquely set by charge- and spin-continuity equations. As a result, flowing between fixed points in the boundary phase diagram of the three-wire junction can only determine a change in the boundary conditions obeyed by the relative fields $\varphi_{j,c(s)}(x), \vartheta_{j,c(s)}(x)$, at $x = 0$. Among all possible boundary fixed point, the simplemost one corresponds to a "disconnected" junction, characterized by the fact that all the φ-fields obey Neumann boundary conditions at $x = 0$, that is,

$$\partial_x \varphi_{j,c}(0) = \partial_x \varphi_{j,s}(0) = 0 \tag{3.86}$$

Accordingly, from now on we will denote the disconnected fixed point as $[N_c, N_s]$. Consistently with Eq. [3.86], one obtains that all the fields $\vartheta_{1(2),c(s)}(x)$ are "pinned" at $x = 0$. At a three-wire spinful junction, we find that, at the $[N_c, N_s]$-fixed point, the most relevant allowed boundary operators are the ones listed in the table below, together with the corresponding scaling dimension

Operators	Bosonized Form	Scaling dimension Δ
$S^+_{1,\sigma}(0), [S^-_{2,\sigma}]^\dagger(0), S^L_{1,\sigma}(0), S^R_{1,\sigma}(0)$	$\eta_{L,2,\sigma}\eta_{L,1,\sigma}e^{-\frac{i}{2}\left[-\frac{2}{\sqrt{2}}\varphi_{1,c}(0)\right]}e^{-\frac{i}{2}\sigma\left[-\frac{2}{\sqrt{2}}\varphi_{1,s}(0)\right]}$	$\Delta_S^{NN} = \frac{1}{2g_c} + \frac{1}{2g_s}$
$S^+_{2,\sigma}(0), [S^-_{3,\sigma}]^\dagger(0), S^L_{2,\sigma}(0), S^R_{2,\sigma}(0)$	$\eta_{L,3,\sigma}\eta_{L,2,\sigma}e^{-\frac{i}{2}\left[\frac{1}{\sqrt{2}}\varphi_{1,c}(0)-\frac{3}{\sqrt{6}}\varphi_{2,c}(0)\right]}e^{-\frac{i}{2}\sigma\left[\frac{1}{\sqrt{2}}\varphi_{1,s}(0)-\frac{3}{\sqrt{6}}\varphi_{2,s}(0)\right]}$	
$S^+_{3,\sigma}(0), [S^-_{1,\sigma}]^\dagger(0), S^L_{3,\sigma}(0), S^R_{3,\sigma}(0)$	$\eta_{L,1,\sigma}\eta_{L,3,\sigma}e^{-\frac{i}{2}\left[\frac{1}{\sqrt{2}}\varphi_{1,c}(0)+\frac{3}{\sqrt{6}}\varphi_{2,c}(0)\right]}e^{-\frac{i}{2}\sigma\left[\frac{1}{\sqrt{2}}\varphi_{1,s}(0)+\frac{3}{\sqrt{6}}\varphi_{2,s}(0)\right]}$	
$PT_1^+, PT_2^{-\dagger}, PHE_{1,\sigma}, PT^{LR}_{1,\sigma}$	$\eta_{L,2,\uparrow}\eta_{L,1,\uparrow}\eta_{L,2,\downarrow}\eta_{L,1,\downarrow}e^{-\frac{i}{2}\left[-\frac{4}{\sqrt{2}}\varphi_{1,c}(0)\right]}$	$\Delta_{PT}^{NN} = \frac{2}{g_c}$
$PT_2^+, PT_3^{-\dagger}, PHE_{2,\sigma}, PT^{LR}_{2,\sigma}$	$\eta_{L,3,\uparrow}\eta_{L,2,\uparrow}\eta_{L,3,\downarrow}\eta_{L,2,\downarrow}e^{-\frac{i}{2}\left[\frac{2}{\sqrt{2}}\varphi_{1,c}(0)-\frac{6}{\sqrt{6}}\varphi_{2,c}(0)\right]}$	
$PT_3^+, PT_1^{-\dagger}, PHE_{3,\sigma}, PT^{LR}_{3,\sigma}$	$\eta_{L,1,\uparrow}\eta_{L,3,\uparrow}\eta_{L,1,\downarrow}\eta_{L,3,\downarrow}e^{-\frac{i}{2}\left[\frac{2}{\sqrt{2}}\varphi_{1,c}(0)+\frac{6}{\sqrt{6}}\varphi_{2,c}(0)\right]}$	
$PE_{1,\uparrow}, PE^\dagger_{1,\downarrow}$	$\eta_{L,2,\uparrow}\eta_{L,1,\uparrow}\eta_{L,2,\downarrow}\eta_{L,1,\downarrow}e^{-\frac{i}{2}\left[-\frac{4}{\sqrt{2}}\varphi_{1,s}(0)\right]}$	$\Delta_{PE}^{NN} = \frac{2}{g_s}$
$PE_{2,\uparrow}, PE^\dagger_{2,\downarrow}$	$\eta_{L,3,\uparrow}\eta_{L,2,\uparrow}\eta_{L,3,\downarrow}\eta_{L,2,\downarrow}e^{-\frac{i}{2}\left[\frac{2}{\sqrt{2}}\varphi_{1,s}(0)-\frac{6}{\sqrt{6}}\varphi_{2,s}(0)\right]}$	
$PE_{3,\uparrow}, PE^\dagger_{3,\downarrow}$	$\eta_{L,1,\uparrow}\eta_{L,3,\uparrow}\eta_{L,1,\downarrow}\eta_{L,3,\downarrow}e^{-\frac{i}{2}\left[\frac{2}{\sqrt{2}}\varphi_{1,s}(0)+\frac{6}{\sqrt{6}}\varphi_{2,s}(0)\right]}$	

plus the corresponding Hermitean conjugates (note that, in constructing the table above, we have employed the condition on the Klein factors $\eta_{R,j,\sigma} = \eta_{L,j,\sigma}$, valid at the $[N_c, N_s]$-fixed point $\forall j, \sigma$. The table above suggests us for which values of the Luttinger interaction parameter it is appropriate to use the fermionic renormalization group approach. Clearly, the simplest possible option is the noninteracting case, namely, $g_c = g_s = 1$. In this case, one recovers a junction of three noninteracting quantum wires. All the allowed boundary interaction terms at the $[N_c, N_s]$-fixed point are irrelevant, except the "tunneling ones", that is $S^+_{j,\sigma}(0)$, all the operators that collapse onto the set of the ones above, as from the table, together with their Hermitean conjugate. Thus, the generic boundary interaction, for such values of the Luttinger parameters, is simply given by

$$H_{B;(NN);(1,1)} = \sum_{j=1}^{3} \tau_j S^+_{j,\sigma}(0) + \text{h.c.} \tag{3.87}$$

On adding a weak interaction, either in the charge-, or in the spin-channel (or in both of them), allows for treating the problem within standard fermionic renormalization group approach.

III.4.3. The $[D_c, D_s]$-fixed point

We now consider the fixed point corresponding to a "fully healed" junction, that is, the one with Dirichlet boundary conditions on all the relative fields $\varphi_{1(2),c}(0), \varphi_{1(2),s}(0)$. Henceforth, we dub such a fixed point $[D_c, D_s]$. At the $[D_c, D_s]$-fixed point, the allowed boundary operators may be again recovered by a straightforward application of DEBC-technique. Taking into account that Dirichlet-like boundary conditions in the bosonic fields correspond to relations among the fermionic fields of the form $\psi_{R,\sigma,j}(0) \propto \psi^\dagger_{L,\sigma,j}(0)$, which implies $\eta_{R,\sigma,j} = \eta_{L,\sigma,j}$, the leading boundary operators can be collected in the following table

Operators	Bosonic Form	Scaling dimension Δ
$S^+_{1,\sigma}(0), S^-_{2,\sigma}(0)$	$\eta_{L,\sigma,2}\eta_{L,\sigma,1} e^{-\frac{i}{2}\left[\frac{2}{\sqrt{6}}\vartheta_{2,c}(0)\right]} e^{-\frac{i}{2}\sigma\left[\frac{2}{\sqrt{6}}\vartheta_{2,s}(0)\right]}$	$\Delta^{DD}_S = \frac{1}{6}(g_c + g_s)$
$S^+_{2,\sigma}(0), S^-_{3,\sigma}(0)$	$\eta_{L,\sigma,2}\eta_{L,\sigma,3} e^{-\frac{i}{2}\left[-\frac{1}{\sqrt{2}}\vartheta_{1,c}(0)-\frac{1}{\sqrt{6}}\vartheta_{2,c}(0)\right]} e^{-\frac{i}{2}\sigma\left[-\frac{1}{\sqrt{2}}\vartheta_{1,s}(0)-\frac{1}{\sqrt{6}}\vartheta_{2,s}(0)\right]}$	
$S^+_{3,\sigma}(0), S^-_{1,\sigma}(0)$	$\eta_{L,\sigma,3}\eta_{L,\sigma,1} e^{-\frac{i}{2}\left[\frac{1}{\sqrt{2}}\vartheta_{1,c}(0)-\frac{1}{\sqrt{6}}\vartheta_{2,c}(0)\right]} e^{-\frac{i}{2}\sigma\left[\frac{1}{\sqrt{2}}\vartheta_{1,s}(0)-\frac{1}{\sqrt{6}}\vartheta_{2,s}(0)\right]}$	
$PT^+_1, PT^-_2, PE_{1,\sigma}$	$\eta_{L,2,\uparrow}\eta_{L,2,\downarrow}\eta_{L,1,\uparrow}\eta_{L,1,\downarrow} e^{-\frac{i}{2}\left[\frac{4}{\sqrt{6}}\vartheta_{2,c}(0)\right]}$	$\Delta^{DD}_{PT} = \frac{2}{3}g_c$
$PT^+_2, PT^-_3, PE_{2,\sigma}$	$\eta_{L,3,\uparrow}\eta_{L,3,\downarrow}\eta_{L,2,\uparrow}\eta_{L,2,\downarrow} e^{-\frac{i}{2}\left[-\frac{2}{\sqrt{2}}\vartheta_{1,c}(0)-\frac{2}{\sqrt{6}}\vartheta_{2,c}(0)\right]}$	
$PT^+_3, PT^-_1, PE_{3,\sigma},$	$\eta_{L,1,\uparrow}\eta_{L,1,\downarrow}\eta_{L,3,\uparrow}\eta_{L,3,\downarrow} e^{-\frac{i}{2}\left[\frac{2}{\sqrt{2}}\vartheta_{1,c}(0)-\frac{2}{\sqrt{6}}\vartheta_{2,c}(0)\right]}$	
$PH^+_1, PH^-_2, PHE_{1,\uparrow}, PHE^\dagger_{1,\downarrow}$	$\eta_{L,2,\uparrow}\eta_{L,2,\downarrow}\eta_{L,1,\uparrow}\eta_{L,1,\downarrow} e^{-\frac{i}{2}\left[\frac{4}{\sqrt{6}}\vartheta_{2,s}(0)\right]}$	$\Delta^{DD}_{PH} = \frac{2}{3}g_s$
$PH^+_2, PH^-_3, PHE_{2,\sigma}, PHE^\dagger_{2,\downarrow}$	$\eta_{L,3,\uparrow}\eta_{L,3,\downarrow}\eta_{L,2,\uparrow}\eta_{L,2,\downarrow} e^{-\frac{i}{2}\left[-\frac{2}{\sqrt{2}}\vartheta_{1,s}(0)-\frac{2}{\sqrt{6}}\vartheta_{2,s}(0)\right]}$	
$PH^+_3, PH^-_1, PHE_{3,\sigma}, PHE^\dagger_{3,\downarrow}$	$\eta_{L,1,\uparrow}\eta_{L,1,\downarrow}\eta_{L,3,\uparrow}\eta_{L,3,\downarrow} e^{-\frac{i}{2}\left[\frac{2}{\sqrt{2}}\vartheta_{1,s}(0)-\frac{2}{\sqrt{6}}\vartheta_{2,s}(0)\right]}$	

together with the corresponding Hermitean conjugates. At the $[D_c, D_s]$-fixed point, an effective refermionization can be done for $g_c \sim g_s \sim 3$, as realized in the main text. Indeed, for values of the Luttinger parameters as such, the leadingmost boundary operators are the tunneling term at the first lines of the table before.

III.4.4. The $[D_c, N_s]$-fixed point

The $[D_c, N_s]$-fixed point has been predicted in the phase diagram of Ref.[30] as corresponding to Dirichlet boundary conditions on the relative fields $\varphi_{j,c}(x)$ at $x = 0$, and Neumann boundary conditions on $\varphi_{j,s}(x)$ at x = 0. Again, one may succesfully employ the DEBC-method to work out the leadingmost boundary operators at such a fixed point, which we list in the following table, together with the corresponding scaling dimensions

Operators	Bosonic Form	Scaling dimension Δ
$S^{+}_{1,\sigma}(0), S^{-}_{2,-\sigma}(0)$	$\eta_{L,\sigma,2}\eta_{L,\sigma,1}e^{-\frac{i}{2}\left[\frac{2}{\sqrt{6}}\vartheta_{2,c}(0)\right]}e^{-\frac{i}{2}\sigma\left[-\frac{2}{\sqrt{2}}\varphi_{1,s}(0)\right]}$	$\Delta^{DN}_{S}=\frac{g_c}{6}+\frac{1}{2g_s}$
$S^{+}_{2,\sigma}(0), S^{-}_{3,-\sigma}(0)$	$\eta_{L,\sigma,3}\eta_{L,\sigma,2}e^{-\frac{i}{2}\left[-\frac{1}{\sqrt{2}}\vartheta_{1,c}(0)-\frac{1}{\sqrt{6}}\vartheta_{2,c}(0)\right]}e^{-\frac{i}{2}\sigma\left[\frac{1}{\sqrt{2}}\varphi_{1,s}(0)-\frac{3}{\sqrt{6}}\varphi_{2,s}(0)\right]}$	
$S^{+}_{3,\sigma}(0), S^{-}_{1,-\sigma}(0)$	$\eta_{L,\sigma,1}\eta_{L,\sigma,3}e^{-\frac{i}{2}\left[\frac{1}{\sqrt{2}}\vartheta_{1,c}(0)-\frac{1}{\sqrt{6}}\vartheta_{2,c}(0)\right]}e^{-\frac{i}{2}\sigma\left[\frac{1}{\sqrt{2}}\varphi_{1,s}(0)+\frac{3}{\sqrt{6}}\phi_{2,s}(0)\right]}$	
$S^{B}_{1,\sigma}(0), PT^{++\dagger}_{2}, PT^{-\dagger}_{3}, PB^{\dagger}_{23,\sigma}, PBS^{\dagger}_{23,\sigma}$	$\propto e^{-\frac{i}{2}\left[\frac{2}{\sqrt{2}}\vartheta_{1,c}(0)+\frac{2}{\sqrt{6}}\vartheta_{2,c}(0)\right]}$	$\Delta^{DN}_{B}=\frac{2}{3}g_c$
$S^{B}_{2,\sigma}(0), PT^{++\dagger}_{3}, PT^{-\dagger}_{1}, PB^{\dagger}_{31,\sigma}, PBS^{\dagger}_{31,\sigma}$	$\propto e^{-\frac{i}{2}\left[-\frac{2}{\sqrt{2}}\vartheta_{1,c}(0)+\frac{2}{\sqrt{6}}\vartheta_{2,c}(0)\right]}$	
$S^{B}_{3,\sigma}(0), PT^{++\dagger}_{1}, PT^{-\dagger}_{2}, PB^{\dagger}_{12,\sigma}, PBS^{\dagger}_{12,\sigma}$	$\propto e^{-\frac{i}{2}\left[-\frac{4}{\sqrt{6}}\vartheta_{2,c}(0)\right]}$	
$PTS^{LR}_{1\uparrow}, PTS^{LR}_{1\downarrow}, PH^{+}_{1}, PH^{-\dagger}_{2}$	$\propto e^{-\frac{i}{2}\left[-\frac{4}{\sqrt{2}}\varphi_{1,s}(0)\right]}$	$\Delta^{DN}_{PTS}=\frac{2}{g_s}$
$PTS^{LR}_{2\uparrow}, PTS^{LR}_{2\downarrow}, PH^{+}_{2}, PH^{-\dagger}_{3}$	$\propto e^{-\frac{i}{2}\left[\frac{2}{\sqrt{2}}\varphi_{1,s}(0)-\frac{6}{\sqrt{6}}\varphi_{2,s}(0)\right]}$	
$PTS^{LR}_{3\uparrow}, PTS^{LR}_{3\downarrow}, PH^{+}_{3}, PH^{-\dagger}_{1}$	$\propto e^{-\frac{i}{2}\left[\frac{2}{\sqrt{2}}\varphi_{1,s}(0)+\frac{6}{\sqrt{6}}\varphi_{2,s}(0)\right]}$	

together with the corresponding Hermitean conjugates. Note that we have not specified the functional of Klein factors appearing in front of the bosonized vertex in any of the operators in the table above but the tunneling ones. In fact, in the region of values of bulk parameters in which refermionization can be effectively implemented, that is, $g_c \sim 3, g_s \sim 1$, the tunneling operators are the leadingmost ones. Yet, before refermionizing it is important to point out that, in general, due to the large difference between g_c and g_s, one expects that the plasmon velocities in the charge- and in the spin-sector are, in general, quite different from each other. Nevertheless, this does not spoil the whole procedure. In fact, as we are dealing with fields defined onto half-lines ranging from $x = 0$ to $x \to \infty$, one may always separately rescale the spatial coordinates in the charge-Hamiltonian.

III.4.5. The $[N_c, D_s]$-fixed point

The $[N_c, D_s]$-fixed point has been predicted as symmetric to the $[D_c, N_s]$-one upon swapping charge- and spin-sectors with each other. After discussing the refermionization near by the $[D_c, N_s]$-fixed point, the one near by the $[D_c, N_s]$-one can be simply recovered by symmetry, just swapping charge and spin with each other. Accordingly, one readily obtains that the table of allowed boundary interaction at this fixed point is given by

Operators	Bosonic Form	Scaling dimension Δ
$S^{+}_{1,\sigma}(0)$	$\eta_{L,2,\sigma}\eta_{L,1,\sigma}e^{-\frac{i}{2}\left[-\frac{2}{\sqrt{2}}\varphi_{1,c}(0)\right]}e^{-\frac{i}{2}\sigma\left[\frac{2}{\sqrt{6}}\vartheta_{2,s}(0)\right]}$	$\Delta^{ND}_{S}=\frac{1}{2g_c}+\frac{g_s}{6}$
$S^{+}_{2,\sigma}(0)$	$\eta_{L,3,\sigma}\eta_{L,2,\sigma}e^{-\frac{i}{2}\left[\frac{1}{\sqrt{2}}\varphi_{1,c}(0)-\frac{3}{\sqrt{6}}\varphi_{2,c}(0)\right]}e^{-\frac{i}{2}\sigma\left[-\frac{1}{\sqrt{2}}\vartheta_{1,s}(0)-\frac{1}{\sqrt{6}}\vartheta_{2,s}(0)\right]}$	
$S^{+}_{3,\sigma}(0)$	$\eta_{L,1,\sigma}\eta_{L,3,\sigma}e^{-\frac{i}{2}\left[\frac{1}{\sqrt{2}}\varphi_{1,c}(0)+\frac{3}{\sqrt{6}}\varphi_{2,c}(0)\right]}e^{-\frac{i}{2}\sigma\left[\frac{1}{\sqrt{2}}\theta^{s}_{1}-\frac{1}{\sqrt{6}}\theta^{s}_{2}\right]}$	
$S^{B}_{1,\uparrow}(0)$	$\propto e^{-\frac{i}{2}\left[\frac{2}{\sqrt{2}}\vartheta_{1,s}(0)+\frac{2}{\sqrt{6}}\vartheta_{2,s}(0)\right]}$	$\Delta^{ND}_{B}=\frac{2}{3}g_s$
$S^{B}_{2,\uparrow}(0)$	$\propto e^{-\frac{i}{2}\left[-\frac{2}{\sqrt{2}}\vartheta_{1,s}(0)+\frac{2}{\sqrt{6}}\vartheta_{2,s}(0)\right]}$	
$S^{B}_{3,\uparrow}(0)$	$\propto e^{-\frac{i}{2}\left[-\frac{4}{\sqrt{6}}\vartheta_{2,s}(0)\right]}$	
$PTS^{LR}_{1\uparrow}$	$\propto e^{-\frac{i}{2}\left[-\frac{4}{\sqrt{2}}\varphi_{1,c}(0)\right]}$	$\Delta^{ND}_{PTS}=\frac{2}{g_c}$
$PTS^{LR}_{2\uparrow}$	$\propto e^{-\frac{i}{2}\left[\frac{2}{\sqrt{2}}\varphi_{1,c}(0)-\frac{6}{\sqrt{6}}\varphi_{2,c}(0)\right]}$	
$PTS^{LR}_{3\uparrow}$	$\propto e^{-\frac{i}{2}\left[\frac{2}{\sqrt{2}}\varphi_{1,c}(0)+\frac{6}{\sqrt{6}}\varphi_{2,c}(0)\right]}$	

plus, of course, the corresponding Hermitean conjugates. By symmetry, one readily infers that, in this case, refermionization will be effective for $g_c \sim 1, g_s \sim 3$.

III.4.6. The chiral fixed points $[\chi^{\pm}_{c}, \chi^{\pm}_{s}]$

The "clockwise" and the "counterclockwise"-chiral fixed points, respectively denoted with $[\chi^{+}_{c}, \chi^{+}_{s}]$ and $[\chi^{-}_{c}, \chi^{-}_{s}]$ in the following, correspond to respectively pinning the $S^{+}_{j,\sigma}$- and the $S^{-}_{j,\sigma}$-boundary operators. Pinning the $S^{+}_{j,\sigma}$'s

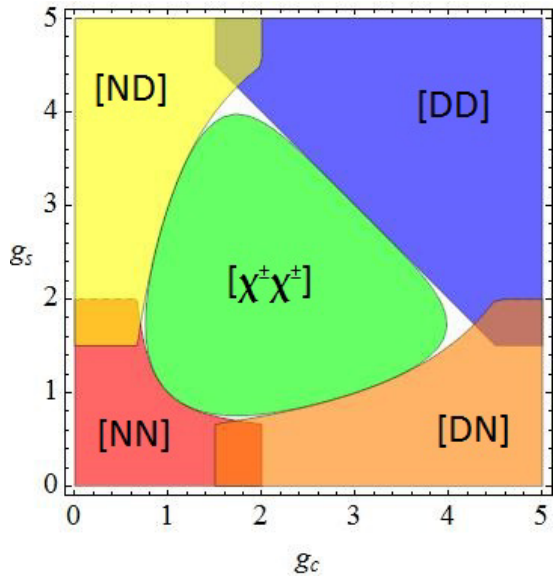

FIG. 21. Phase diagram predicted by the DEBC method, as proposed by Ref. [30]

is equivalent to imposing Dirichlet boundary conditions on $\frac{1}{\sqrt{6}}\vartheta_{2,c(s)}(0) - \frac{1}{\sqrt{2}}\varphi_{1,c(s)}(0)$ as well as on $\frac{1}{\sqrt{2}}\vartheta_{1,c(s)}(0) + \frac{3}{\sqrt{6}}\varphi_{2,c(s)}(0)$. This leads to the following table for the leading allowed boundary operators at the $[\chi_c^+, \chi_s^+]$-fixed point

Operators	Bosonic Form	Scaling dimension Δ
$S^-_{1,\sigma}(0), S^{B\dagger}_{1,\sigma}(0), S^L_{1,\sigma}(0), S^R_{2,\sigma}(0), PTS^{LR\dagger}_{3,\sigma}, PBS_{31,\sigma}, PE_{3,-\sigma}, PHE^\dagger_{3,-\sigma}$	$\eta_{L,\sigma,3}\eta_{L,\sigma,1}e^{-\frac{i}{2}\left[\frac{2}{\sqrt{2}}\vartheta_{1,c}(0)-\frac{2}{\sqrt{6}}\vartheta_{2,c}(0)\right]}e^{-\frac{i}{2}\sigma\left[\frac{2}{\sqrt{2}}\vartheta_{1,s}(0)-\frac{2}{\sqrt{6}}\vartheta_{2,s}(0)\right]}$	$\Delta_S^{\chi\chi} = \frac{2g_c}{3+g_c^2} + \frac{2g_s}{3+g_s^2}$
$S^-_{2,\sigma}(0), S^{B\dagger}_{2,\sigma}(0), S^L_{2,\sigma}(0), S^R_{3,\sigma}(0), PTS^{LR\dagger}_{1,\sigma}, PBS_{12,\sigma}, PE_{1,-\sigma}, PHE^\dagger_{1,-\sigma}$	$\eta_{L,\sigma,1}\eta_{L,\sigma,2}e^{-\frac{i}{2}\left[\frac{4}{\sqrt{6}}\vartheta_{2,c}(0)\right]}e^{-\frac{i}{2}\sigma\left[\frac{4}{\sqrt{6}}\vartheta_{2,s}(0)\right]}$	
$S^-_{3,\sigma}(0), S^{B\dagger}_{3,\sigma}(0), S^L_{3,\sigma}(0), S^R_{1,\sigma}(0), PTS^{LR\dagger}_{2,\sigma}, PBS_{23,\sigma}, PE_{2,-\sigma}, PHE^\dagger_{2,-\sigma}$	$\eta_{L,\sigma,2}\eta_{L,\sigma,3}e^{-\frac{i}{2}\left[-\frac{2}{\sqrt{2}}\vartheta_{1,c}(0)-\frac{2}{\sqrt{6}}\vartheta_{2,c}(0)\right]}e^{-\frac{i}{2}\sigma\left[-\frac{2}{\sqrt{2}}\vartheta_{1,s}(0)-\frac{2}{\sqrt{6}}\vartheta_{2,s}(0)\right]}$	

plus the corresponding Hermitean conjugates. As for what concerns the $[\chi_c^-, \chi_s^-]$-fixed point, similar observations apply, except that the fields to be pinned now are given by $\frac{1}{\sqrt{6}}\vartheta_{2,c(s)}(0) + \frac{1}{\sqrt{2}}\varphi_{1,c(s)}(0)$ and $\frac{1}{\sqrt{2}}\vartheta_{1,c(s)}(0) - \frac{3}{\sqrt{6}}\varphi_{2,c(s)}(0)$. This leads to a collapse of the leadingmost allowed boundary operators onto the three ones listed in the table below

Operators	Bosonic Form	Scaling dimension Δ
$S^+_{1,\sigma}(0)$	$\eta_{L,\sigma,1}\eta_{L,\sigma,2}e^{-\frac{i}{2}\left[\frac{4}{\sqrt{6}}\vartheta_{2,c}(0)\right]}e^{-\frac{i}{2}\sigma\left[\frac{4}{\sqrt{6}}\vartheta_{2,s}(0)\right]}$	$\Delta_S^{\chi\chi} = \frac{2g_c}{3+g_c^2} + \frac{2g_s}{3+g_s^2}$
$S^+_{2,\sigma}(0)$	$\eta_{L,\sigma,2}\eta_{L,\sigma,3}e^{-\frac{i}{2}\left[-\frac{2}{\sqrt{2}}\vartheta_{1,c}(0)-\frac{2}{\sqrt{6}}\vartheta_{2,c}(0)\right]}e^{-\frac{i}{2}\sigma\left[-\frac{2}{\sqrt{2}}\vartheta_{1,s}(0)-\frac{2}{\sqrt{6}}\vartheta_{2,s}(0)\right]}$	
$S^+_{3,\sigma}(0)$	$\eta_{L,\sigma,3}\eta_{L,\sigma,1}e^{-\frac{i}{2}\left[\frac{2}{\sqrt{2}}\vartheta_{1,c}(0)-\frac{2}{\sqrt{6}}\vartheta_{2,c}(0)\right]}e^{-\frac{i}{2}\sigma\left[\frac{2}{\sqrt{2}}\vartheta_{1,s}(0)-\frac{2}{\sqrt{6}}\vartheta_{2,s}(0)\right]}$	

again together with the corresponding Hermitean conjugates. The $[\chi_c^\pm, \chi_s^\pm]$-fixed points can be accessed from either the $[N_c, N_s]$, or from the $[D_c, D_s]$ fixed point, in the presence of a small time-reversal breaking magnetic flux pearcing the junction[30]. The bosonization analysis we performed in this Appendix allows to list and classify, according to their scaling dimension, the allowed boundary operators at any fixed point of the phase diagram (see Fig. [21] for the proposed phase diagram obtained within the DEBC method). This paves the way to the systematic implementation of the refermionization procedure of both the bulk and the (leadingmost) boundary Hamiltonians.

IV. TUNNELING SPECTROSCOPY OF MAJORANA-KONDO DEVICES

What I tell you three times is true.
Lewis Carroll

Majorana bound states have become of major interest in condensed matter physics,[90–98] due to potential applications as building blocks in fault-tolerant quantum computing[99] and the possibility to engineer such topological states using conventional s-wave superconductors and spin-orbit coupling.[100–102] Information in these states is encoded non-locally, with the long-range entanglement providing a mechanism for electron teleportation[103].

Recently, it has been realized that the topologically protected ground-state subspace formed by several Majorana bound states can act as a non-local quantum impurity, which when subjected to strong charging effects and coupled to conduction electrons can give rise to a *topological Kondo effect*.[56] Here a stable non-Fermi liquid behavior is obtained, reminiscent of the multichannel Kondo effect but robust against perturbations. In Ref. [104] the full crossover was studied using numerical renormalization group. The situation with an arbitrary number of leads of interacting electrons was studied in Refs. [105 and 106], where in addition an interaction-induced intermediate-coupling unstable fixed point was discovered. The topological protection of this novel Kondo effect opens new possibilities for the experimental observation of multi-channel Kondo impurity dynamics.[107,108] Additional physical effects can be observed when including a Josephson coupling to the mesoscopic island hosting the Majorana bound states; phase fluctuations then cause a non-trivial interplay between topological Kondo and resonant Andreev reflection processes, giving a continuous manifold of stable non-Fermi liquid states.[109] With N wires each connected to one Majorana on the island, the symmetry group of this topological Kondo effect is $\mathrm{SO}_1(N)$, previously encountered also for a junction of Ising chains,[110] unlike that of Ref. [56] which is $\mathrm{SO}_2(N)$.

The observable predictions regarding the topological Kondo effect have so far been focused on charge transport through the system[56,105–107,109,111] or measurements of the occupation of pairs of Majorana zero modes, analogous to magnetization.[107] In this Chapter, we show that the local density of states (LDOS) of the lead electrons close to the island provide a clear signature of the topological Kondo effect of Béri and Cooper,[56] directly measurable with a scanning tunneling microscope (STM). In particular, we show that the LDOS close to the island follows the power law $\rho(\omega) \sim \omega^{\frac{1}{Ng}+\frac{N-1}{N}g-1}$ as a function of energy $\omega \to 0$, where g is the Luttinger liquid parameter for the electron-electron interaction strength with $g = 1$ for non-interacting leads and $g < 1$ for repulsive interactions. Hence for realistic values $1/(N-1) < g < 1$, we have a diverging LDOS in the zero-bias limit close to the junction.

In contrast to the usual picture of a power-law vanishing of the low-energy LDOS in a Luttinger liquid with or without boundary/impurity,[26,85,112–114] an interaction-induced divergence is in fact a rather generic feature of Luttinger-liquid wire junctions,[70] and Luttinger-liquid junctions with a superconductor, with[64] or without[115,116] Majorana bound states. The key feature of the $\mathrm{SO}_2(N)$ topological Kondo effect of Ref. [56] is that the power law governing the divergence depends on the number N of leads participating in the effect, making adjustable gate voltages a route to observe this signature. This N dependence of the LDOS is however absent in the $\mathrm{SO}_1(N)$ topological Kondo effect of Ref. [109], where we find the zero-energy divergence $\rho(\omega) \sim \omega^{g-1}$ for all fixed points within the non-Fermi liquid manifold, which is the same power law as that encountered for perfect Andreev reflection at a single Luttinger-liquid junction with a Majorana fermion[64].

IV.1. Model

IV.1.1. Device setup

We consider the setup where the topological Kondo effect can take place[56], namely a mesoscopic s-wave superconducting island hosting a set of N_{tot} localized Majorana bound states, of which $N \geq 3$ are tunnel-coupled to normal leads of conduction electrons. This setup is sketched in Fig. [22]. Experimentally, this can be achieved by depositing $N_{\mathrm{tot}}/2$ nanowires with strong spin-orbit coupling, e.g. InSb or InAs, subjected to a magnetic field, on top of a floating mesoscopic superconducting island; this creates N_{tot} Majorana bound states, one at each end of the wire parts that are on top of the superconductor.[90–98] With proper gating, N of these N_{tot} Majoranas are tunnel coupled to the N normal parts of the nanowires, which then act as leads. We will also consider a generalized setup, where the island is Josephson coupled to a bulk s-wave superconductor.[109]

The full Hamiltonian of the system under consideration is hence given by $H = H_{\mathrm{leads}} + H_{\mathrm{island}} + H_t$.

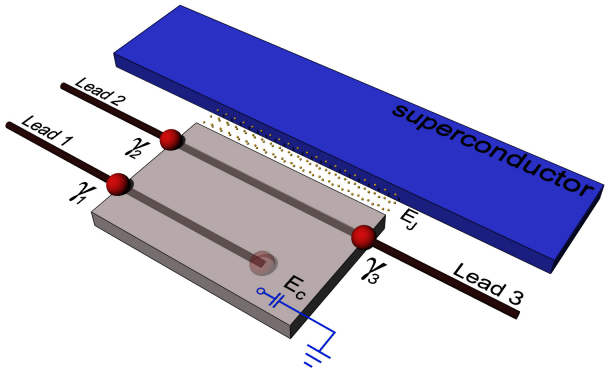

FIG. 22. Schematic setup for a Majorana device hosting the topological Kondo effect. Spin-orbit coupled semiconductor nanowires (two in the figure) are deposited on top of an ordinary superconducing island (grey box) with charging energy E_C. In a magnetic field, Majorana bound states γ_i (red dots) are formed at the ends of the wire parts coupled to the superconductor (dark grey). Gate voltages create tunnel barriers between N Majorana fermions and the N normal leads (in the figure, $N = 3$). This leads to an $SO_2(N)$ topological Kondo effect at low temperature.[56] When Josephson coupling the superconducting island to an additional bulk superconductor (blue), the system will, in the limit of large Josephson energy E_J, give an $SO_1(N)$ topological Kondo effect which becomes tunable by the lead-Majorana couplings.[109]

The normal leads of effectively spinless electrons are described by the Hamiltonian

$$H_{\text{leads}} = -\mathrm{i}v_F \sum_{j=1}^{N} \int_0^\infty \mathrm{d}x \ \left[\psi_{j,R}^\dagger \partial_x \psi_{j,R} - \psi_{j,L}^\dagger \partial_x \psi_{j,L}\right], \tag{4.1}$$

with fermionic fields $\psi_j(x)$ for each lead j, consisting of outgoing (R) and incoming (L) components (i.e. right and left movers). We assume all leads are identical. At $x = 0$, we have the boundary condition $\psi_{j,R}(0) = \psi_{j,L}(0) \equiv \psi_j(0)$ for disconnected leads. However, here the lead electrons are coupled to the localized Majorana modes on the island. These are described by operators γ_j obeying $\gamma_j^\dagger = \gamma_j$, with anticommutation relations $\{\gamma_j, \gamma_{j'}\} = \delta_{jj'}$.

The island Hamiltonian is given by

$$H_{\text{island}} = E_C(Q - n_g)^2 - E_J \cos \Xi, \tag{4.2}$$

where E_C is the charging energy, Q the total electron number on the island (with contributions from both Cooper pairs and occupied Majorana states), n_g the backgate parameter (assumed to be close to an integer) determined by the voltage across the capacitor, E_J the Josephson energy for the coupling between the island and the bulk superconductor, where Ξ is their phase difference (we will take the phase of the island to be Ξ, canonically conjugate to Q). The system on the island inherits a superconducting gap Δ_{sc} due to proximity.

The coupling between the lead electrons and the Majorana modes on the island is given by the tunneling Hamiltonian[103,117]

$$H_t = \sum_{j=1}^{N} \lambda_j e^{-i\Xi/2} \psi_j^\dagger(0) \gamma_j + \text{h.c.}, \tag{4.3}$$

where we choose the couplings λ_j to be real and positive. This lead-Majorana tunneling gives a hybridization energy of $\Gamma_j = 2\pi\nu_0\lambda_j^2$, where $\nu_0 = 1/\pi v_F$ is the density of states for the unperturbed leads.

In the following we will be interested in two limiting cases, where the low-energy solution of the problem simplifies[56,109]: for $E_J = 0$, the low-energy (i.e., for $T, V \ll E_C, \Delta_{\text{sc}}, \min \Gamma_j$) behavior is governed by an $SO_2(N)$ topological Kondo effect, whereas when E_J is the largest energy energy scale, the topological Kondo effect has symmetry group $SO_1(N)$.

IV.1.2. Low-energy theory without Josephson coupling

In the absence of Josephson coupling, i.e., with $E_J = 0$, the physics at low energies ($T, V \ll E_C, \Delta_{\text{sc}}, \min \Gamma_j$) is governed by virtual transitions of electrons hopping onto the dot, leading to an effective low-energy Hamiltonian

$H = H_{\rm leads} + H_K^{(1)}$, where[56]

$$H_K^{(1)} = \sum_{i\neq j} J_{jk}^{+}\gamma_j\gamma_k\psi_k^\dagger(0)\psi_j(0) - \sum_j J_{jj}^{-}\psi_j^\dagger(0)\psi_j(0), \tag{4.4}$$

for the tunneling between the leads. The (positive) coupling constants are given by $J_{jk}^{\pm} \approx \lambda_j\lambda_k/E_C$. The first term in $H_K^{(1)}$ shows a non-local quantum impurity set up by the products $\gamma_j\gamma_k$, exchange-coupled to the spin object formed by the lead electron products $\psi_k^\dagger(0)\psi_j(0)$. The resulting entanglement gives rise to a multichannel topological Kondo effect below the energy scale defined by the Kondo temperature T_K; here $T_K \sim E_C e^{-1/\nu_0 J}$ when assuming isotropic $J_{jk}^{+} = J$.

Including electron-electron interactions, the leads are conveniently treated using bosonization,[112] which expresses the lead Hamiltonian as

$$H_{\rm leads} = \frac{v}{2\pi}\sum_{j=1}^{N}\int_0^\infty {\rm d}x\left[g(\partial_x\phi_j)^2 + \frac{1}{g}(\partial_x\vartheta_j)^2\right], \tag{4.5}$$

where ϕ_j and ϑ_j are non-chiral bosonic fields with commutation relation $[\phi_i(x), \partial_y\vartheta_j(y)] = 2\pi{\rm i}\delta(x-y)\delta_{ij}$, g is the Luttinger-liquid interaction parameter (with $g=1$ in the absence of interactions, and $g<1$ for repulsive interactions) and v the interaction-renormalized Fermi velocity. The bosonized form of the electron operator is then given by $\psi_{j,L/R} = \chi_j(2\pi a)^{-1/2}e^{{\rm i}(\phi_j \mp \vartheta_j)}$, where a is the short-distance cut-off, and χ_j is the Klein factor (a Majorana fermion). This Majorana fermion from bosonization can be hybridized with the localized Majorana fermion γ_j coupled to the lead, such that one simply replaces $\gamma_j\chi_j$ with a number $\pm i$ which is gauged away, see Refs. [105 and 106]. This leads to a description of the strong-coupling fixed point in terms of the bosonic field $\mathit{\Phi} = (\mathit{\Phi}_1, ..., \mathit{\Phi}_N)$, where $\mathit{\Phi}_j = \phi_j(x=0)$, which is pinned by the potential

$$V^{(1)}[\mathit{\Phi}] \propto -\sum_{j\neq k}\cos(\mathit{\Phi}_j - \mathit{\Phi}_k), \tag{4.6}$$

whose minima form an $N-1$ dimensional triangular lattice. This means that in a rotated basis, the "zero-mode" $\check{\mathit{\Phi}}_0 \equiv (1/\sqrt{N})\sum_j \mathit{\Phi}_j \equiv \mathbf{v}_0\cdot\mathit{\Phi}$, is a free field (physically, this is due to current conservation at the junction), whereas the components $\check{\mathit{\Phi}}_1, ..., \check{\mathit{\Phi}}_{N-1}$, described by vectors $\mathbf{v}_1, ..., \mathbf{v}_{N-1}$ orthogonal to $\mathbf{v}_0$ (spanning the reciprocal $N-1$ dimensional triangular lattice), are fixed. Explicitly, the rotated basis is given by

$$\begin{aligned}
\check{\phi}_0 &= \frac{1}{\sqrt{N}}\sum_{j=1}^{N}\phi_j,\\
\check{\phi}_1 &= \frac{1}{\sqrt{2}}\phi_1 - \frac{1}{\sqrt{2}}\phi_2,\\
\check{\phi}_2 &= \frac{1}{\sqrt{6}}\phi_1 + \frac{1}{\sqrt{6}}\phi_2 - \frac{2}{\sqrt{6}}\phi_3\\
&\vdots\\
\check{\phi}_{N-1} &= \frac{1}{\sqrt{N(N-1)}}\sum_{j=1}^{N-1}\phi_j - \frac{N-1}{\sqrt{N(N-1)}}\phi_N,
\end{aligned} \tag{4.7}$$

where for $N=3$ the last line should be neglected.

Hence at strong coupling we have a theory of Luttinger liquid wires (Eq. [4.5]) connected at a junction ($x=0$), where the field $\check{\phi}_0(x)$ obeys Neumann (free) boundary condition (BC), whereas the orthogonal components $\check{\phi}_1(x), ..., \check{\phi}_{N-1}(x)$ obey Dirichlet (fixed) BCs. By duality, we simultaneously have that $\check{\vartheta}_0(x)$ obeys Dirichlet BC, and that the orthogonal components $\check{\vartheta}_1(x), ..., \check{\vartheta}_{N-1}(x)$ obey Neumann BCs (the $\check{\vartheta}$ fields are obtained from the ϑ fields in the same way as the $\check{\phi}$ fields from the ϕ fields).

Furthermore, instanton tunneling of the pinned fields at strong coupling yields a leading irrelevant operator with scaling dimension[105,106] $\Delta_{LIO} = 2g(N-1)/N$, determining the finite-temperature scaling of the non-local conductance.

IV.1.3. Low-energy theory with strong Josephson coupling

Another type of low-energy topological Kondo effect is obtained in the limit of strong Josephson coupling, more specifically when $\max\Gamma_j \ll \sqrt{8E_C E_J} \lesssim E_J$; see Ref. [109]. The low-energy theory that emerges in this parameter

regime is given by $H = H_{\text{leads}} + H_A + H_K^{(2)}$, where

$$H_A = -\sum_j \lambda_j \gamma_j \psi_j^\dagger(0) + \text{h.c.}, \tag{4.8}$$

$$H_K^{(2)} = \sum_{j\neq k} J_{jk}\gamma_j\gamma_k(\psi_k^\dagger(0)+\psi_k(0))(\psi_j^\dagger(0)+\psi_j(0)), \tag{4.9}$$

where λ_j is the Majorana tunneling coupling in Eq. [4.3] and $J_{jk} \approx \lambda_j\lambda_k/E_J$. Here H_A corresponds to the usual single-lead resonant Andreev reflection processes, while the exchange term $H_K^{(2)}$ contains both the same processes as in Eq. [4.4] as well as crossed Andreev reflection processes.

Performing the same bosonization procedure as above for $H_K^{(1)}$ now leads to a strong-coupling pinning potential[109]

$$V^{(2)}[\Phi] \propto -\sum_j \sqrt{\Gamma_j}\sin\Phi_j - \sqrt{T_K}\sum_{j\neq k}\cos\Phi_j\cos\Phi_k, \tag{4.10}$$

for the Φ field. This implies a manifold of strong-coupling fixed points, tuned by the N parameters $\delta_j \equiv \sqrt{\Gamma_j/T_K}$, where the minima of the potential $V^{(2)}[\Phi]$ form an N dimensional generalization of the body-centered cubic lattice for $\Gamma_j \ll T_K$, with the center-point being shifted as a function of the δ_j parameters. Here the Kondo temperature T_K defines the energy scale below which the Kondo effect develops, given by $T_K \approx \sqrt{8E_JE_C}e^{-E_J/(N-2)\Gamma}$ for isotropic $\Gamma_j = \Gamma$.

Hence in the regime of strong Josephson coupling, the strong-coupling theory is that of Luttinger liquid wires connected at a junction where all the fields $\check{\phi}_0(x), \check{\phi}_1(x), ..., \check{\phi}_{N-1}(x)$ have Dirichlet BCs, and all the dual fields $\check{\vartheta}_0(x), \check{\vartheta}_1(x), ..., \check{\vartheta}_{N-1}(x)$ have Neumann BCs.

The finite-temperature behavior is governed by a leading irrelevant operator with scaling dimension

$$\Delta_{LIO} = \min\left\{2, \frac{1}{2}\sum_{j=1}^{N}\left[1-\frac{2}{\pi}\sin^{-1}\left(\frac{\delta_j}{2(N-1)}\right)\right]^2\right\}, \tag{4.11}$$

arising from instanton tunneling of the fields between adjacent potential minima.

IV.2. Local density of states

The local density of states ρ_i available for electron tunneling into the ith lead is given by

$$\begin{aligned}\rho_i(x,\omega) &= -\frac{1}{\pi}\text{Im}\, G_i^R(x,\omega) \\ &= \frac{1}{\pi}\,\text{Re}\int_0^\infty \text{d}t\, e^{\text{i}\omega t}\langle\psi_i(x,t)\psi_i^\dagger(x,0)\rangle,\end{aligned} \tag{4.12}$$

where $G_i^R(x,\omega)$ is the equal-position retarded Green's function for the electrons in the ith lead. The local density of states ρ_i is directly measurable using scanning tunneling microscopy, as the differential tunneling conductance $G_i(x,V)$ at position x in lead i is directly proportional to this quantity as a function of applied voltage V, i.e. $G_i(x,V) \propto \rho_i(x,\omega = eV)$.

We shall here be concerned with the low-energy behavior of the LDOS, where temperature T and energy ω are well below the Kondo temperature T_K of the system. With the N wires effectively connected at a single junction with a boundary condition due to the topological Kondo effect, see Fig. [23], the problem of finding the LDOS is analogous to that for a junction of several Luttinger liquid wires.[29,30,70,118,119]

IV.2.1. Electron Green's function

The zero-temperature, equal-position Green's function $\langle\psi_i(x,t)\psi_i^\dagger(x,0)\rangle$ for wire i in the N-wire junction system can be calculated following Agarwal *et al.* in Ref. [70]. This amounts to finding the current-splitting matrix $\mathbb{M}$ for the junction, which relates the incoming $j_{i,L}$ and outgoing $j_{i,R}$ currents at the junction through $j_{i,R} = \sum_j \mathbb{M}_{ij}j_{j,L}$.

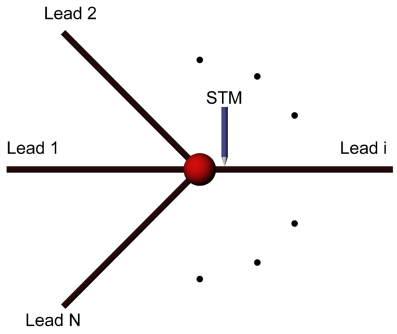

FIG. 23. The topological Kondo problem at low energy is equivalent to an N-wire junction with a splitting matrix $\mathbb{M}$ describing the boundary condition at the junction. With an STM tip the LDOS $\rho_i(x,\omega)$ of wire i is probed.

In terms of the chiral bosonic fields $\phi_{i,L} = \phi_i - \vartheta_i$ and $\phi_{i,R} = \phi_i + \vartheta_i$, such that the electron field is expressed as $\psi_{j,L/R} \propto e^{\mathrm{i}\phi_{j,L/R}}$, the $\mathbb{M}$ matrix is equivalent to the boundary condition

$$\phi_{i,R} = \sum_j \mathbb{M}_{ij}\phi_{j,L}. \tag{4.13}$$

With a Bogoliubov transformation

$$\phi_{j,R/L} = [(1+g)\tilde{\phi}_{j,R/L} + (1-g)\tilde{\phi}_{j,L/R}]/(2\sqrt{g}), \tag{4.14}$$

one obtains the free outgoing/incoming fields $\tilde{\phi}_{j,R/L}$ with commutation relations

$$[\tilde{\phi}_{j,R/L}(x,t), \tilde{\phi}_{j,R/L}(x',t)] = \pm\mathrm{i}\pi\,\mathrm{sgn}(x-x'). \tag{4.15}$$

Their splitting matrix $\tilde{\mathbb{M}}$, which relates $\tilde{\phi}_{i,R}(x) = \sum_j \tilde{\mathbb{M}}_{ij}\tilde{\phi}_{j,L}(-x)$ in the "unfolded picture" (where x is extended to the entire real line) is given by

$$\tilde{\mathbb{M}} = [(1+g)\mathbb{M} - (1-g)\mathbb{L}][(1+g)\mathbb{L} - (1-g)\mathbb{M}]^{-1}, \tag{4.16}$$

where $\mathbb{L}$ is the identity matrix.

The Green's function now follows from

$$\begin{aligned}\langle\psi_i(x,t)\psi_i^\dagger(x,0)\rangle &= \langle\psi_{i,L}(x,t)\psi_{i,L}^\dagger(x,0)\rangle \\ &+ \langle\psi_{i,R}(x,t)\psi_{i,R}^\dagger(x,0)\rangle + e^{\mathrm{i}2k_Fx}\langle\psi_{i,R}(x,t)\psi_{i,L}^\dagger(x,0)\rangle \\ &+ e^{-\mathrm{i}2k_Fx}\langle\psi_{i,L}(x,t)\psi_{i,R}^\dagger(x,0)\rangle,\end{aligned} \tag{4.17}$$

where the two oscillatory terms vanish for lead lengths $L\to\infty$ in the cases we are interested in, since the corresponding Green's functions contain an L dependence $\sim L^{(\mathbb{M}_{ii}-1)g}$. The remaining terms are given by

$$\begin{aligned}\langle\psi_{i,R}(x,t)\psi_{i,R}^\dagger(x,0)\rangle &= \frac{1}{2\pi a}\langle e^{\mathrm{i}\phi_{i,R}(x,t)}e^{-\mathrm{i}\phi_{i,R}(x,0)}\rangle \\ &= \frac{1}{2\pi a}\langle e^{\mathrm{i}[(1+g)\tilde{\phi}_{i,R}(x,t)+(1-g)\tilde{\phi}_{i,L}(x,t)]/(2\sqrt{g})} \\ &\quad\times e^{-\mathrm{i}[(1+g)\tilde{\phi}_{i,R}(x,0)+(1-g)\tilde{\phi}_{i,L}(x,0)]/(2\sqrt{g})}\rangle \\ &= \frac{1}{2\pi a}\langle e^{\mathrm{i}[(1+g)\sum_j\tilde{\mathbb{M}}_{ij}\tilde{\phi}_{j,L}(-x,t)}e^{\mathrm{i}(1-g)\tilde{\phi}_{i,L}(x,t)]/(2\sqrt{g})} \\ &\quad\times e^{-\mathrm{i}[(1+g)\sum_j\tilde{\mathbb{M}}_{ij}\tilde{\phi}_{j,L}(-x,0)}e^{-\mathrm{i}(1-g)\tilde{\phi}_{i,L}(x,0)]/(2\sqrt{g})}\rangle.\end{aligned} \tag{4.18}$$

With the relation $\langle e^{\mathrm{i}\alpha_1\phi(z_1)}\cdots e^{\mathrm{i}\alpha_n\phi(z_n)}\rangle = \prod_{i<j}(z_i-z_j)^{\alpha_i\alpha_j}$ for the expectation value of a product of vertex operators with complex coordinates $z = x + \mathrm{i}\tau$,[120] one arrives at $\langle\psi_{i,R}(x,t)\psi_{i,R}^\dagger(x,0)\rangle = \langle\psi_{i,L}(x,t)\psi_{i,L}^\dagger(x,0)\rangle = \langle\psi_i(x,t)\psi_i^\dagger(x,0)\rangle/2$, with[70]

$$\langle\psi_i(x,t)\psi_i^\dagger(x,0)\rangle =$$

$$= \frac{1}{2\pi a}\left[\frac{\mathrm{i}a}{-vt+\mathrm{i}a}\right]^{(g+1/g)/2} \times \left[\frac{-a^2-4x^2}{(-vt+\mathrm{i}a)^2-4x^2}\right]^{\tilde{\mathbb{M}}_{ii}(1/g-g)/4}. \tag{4.19}$$

Now, close to the junction, where we can put $x \to 0$, as well as far from the junction, where $x \to \infty$, the expressions allow us to compute the LDOS. When $x \to 0$, we have

$$\langle \psi_i(0,t)\psi_i^\dagger(0,0)\rangle = \frac{1}{2\pi a}\left[\frac{\mathrm{i}a}{-vt+\mathrm{i}a}\right]^{\{(1-\tilde{\mathbb{M}}_{ii})g+(1+\tilde{\mathbb{M}}_{ii})/g\}/2}, \tag{4.20}$$

which means that the (chiral) boundary field $\psi_i(0,t)$ has scaling dimension

$$\Delta_i = \{(1-\tilde{\mathbb{M}}_{ii})g + (1+\tilde{\mathbb{M}}_{ii})/g\}/2, \tag{4.21}$$

i.e. $\langle \psi_i(0,\tau)\psi_i^\dagger(0,0)\rangle \sim \tau^{-\Delta_i}$ for imaginary time $\tau \gg a/v$.

Similarly, far away from the junction, where $x \to \infty$, one has

$$\langle \psi_i(x,t)\psi_i^\dagger(x,0)\rangle = \frac{1}{\pi a}\left[\frac{\mathrm{i}a}{-vt+\mathrm{i}a}\right]^{(g+1/g)/2}, \tag{4.22}$$

implying the usual scaling exponent $\Delta_i = (g+1/g)/2$ for bulk (non-chiral) electrons.

IV.2.2. The local density of states

Far away from the junction, putting Eq. [4.22] for the Green's function ($x \to \infty$) into the expression of Eq. [4.12] for the LDOS, we arrive at[70,121]

$$\rho_i(x\to\infty,\omega) = \frac{1}{a\pi\Gamma(\Delta_i)}\left(\frac{a}{v}\right)^{\Delta_i}\omega^{\Delta_i-1}e^{-a\omega/v}H(\omega), \tag{4.23}$$

where Γ is the gamma function and H is the Heaviside step function, and with the above scaling dimension $\Delta_i = (g+1/g)/2$. For non-interacting electrons in the leads this reduces to $\rho_i(x,\omega) = 1/(\pi v) \equiv \nu_0$, i.e. the density of states ν_0 for a bulk spinless quantum wire, as expected.

Considering positive energies $\omega \ll v/a$, we will neglect the factor $e^{-a\omega/v}H(\omega)$ in the discussion below.

An analytical expression can also be obtained for the limit $2x\omega/v \gg 1$, resulting in[116]

$$\begin{aligned}\rho_i(x,\omega) = {} & \frac{1}{\pi v\Gamma((g+1/g)/2)}\left(\frac{a\,\omega}{v}\right)^{(g+1/g)/2-1} \\ & + \frac{2^{2-(g+1/g)/2}\cos(2x\omega/v+\delta)}{\pi v\Gamma(\tilde{\mathbb{M}}_{ii}(1/g-g)/4)} \\ & \times \left(\frac{a\,\omega}{v}\right)^{\tilde{\mathbb{M}}_{ii}(1/g-g)/4-1} \\ & \times \left(\frac{a}{x}\right)^{(3g+1/g)(1+\tilde{\mathbb{M}}_{ii})/8+(g+3/g)(1-\tilde{\mathbb{M}}_{ii})/8}\end{aligned} \tag{4.24}$$

where $\delta \equiv \mathrm{Arg}(\mathrm{i}^{(g+3/g)(1+\tilde{\mathbb{M}}_{ii})/8+(3g+1/g)(1-\tilde{\mathbb{M}}_{ii})/8})$. Note that for fixed ω the second term vanishes as $x \to \infty$, reducing the expression in Eq. [4.24] to that in Eq. [4.23].

Finally and most importantly, namely close to the junction, putting the expression in Eq. [4.20] for the Green's function of the chiral boundary field at the junction ($x = 0$) into the expression in Eq. [4.12] for the LDOS, we arrive at[70]

$$\rho_i(0,\omega) = \frac{1}{a2\pi\Gamma(\Delta_i)}\left(\frac{a}{v}\right)^{\Delta_i}\omega^{\Delta_i-1}, \tag{4.25}$$

with Δ_i now given by Eq. [4.21]. This behavior occurs within a distance of the order of $x < v/(2\omega)$ from the junction.

In order to proceed, we must now see what values for the $\tilde{\mathbb{M}}$ matrix the different boundary conditions in the topological Kondo effect correspond to.

IV.3. Local density of states for topological Kondo systems

IV.3.1. Strong Josephson coupling

The simplest case is for strong Josephson coupling, where all the $\check{\phi}_j$ fields have Dirichlet, and all the $\check{\vartheta}_j$ fields have Neumann BCs, at all strong-coupling fixed points. The electron operator $\psi_{j,L/R} \propto e^{\mathrm{i}(\phi_j \mp \vartheta_j)}$ at the junction at $x = 0$ is then given by

$$\psi_{j,R}(0) \propto e^{\mathrm{i}[\phi_j(0)+\vartheta_j(0)]} = e^{\mathrm{i}c_i} e^{\mathrm{i}\vartheta_j(0)}, \tag{4.26}$$

where c_i, a constant depending on the potential minimum the $\phi_j(0)$ field is trapped in, can be gauged away. Hence $\psi_{j,R}(0) = \psi^\dagger_{j,L}(0)$, meaning that $\tilde{\phi}_{i,R}(0) = -\tilde{\phi}_{i,L}(0)$, i.e. the $\tilde{\mathbb{M}}$ matrix is that for perfect Andreev reflection in each lead separately, namely

$$\tilde{\mathbb{M}} = \begin{pmatrix} -1 & 0 & \dots & 0 \\ 0 & -1 & \dots & 0 \\ \vdots & \vdots & \ddots & \vdots \\ 0 & 0 & \dots & -1 \end{pmatrix}, \tag{4.27}$$

such that $\tilde{\mathbb{M}}_{ii} = -1$ for all i.

Let us now consider the electron Green's function in Eq. [4.19] close to the junction, i.e. letting $x \to 0$. With $\tilde{\mathbb{M}}_{ii} = -1$,

$$\langle \psi_i(x,t)\psi_i^\dagger(x,0)\rangle = \frac{1}{2\pi a}\left[\frac{\mathrm{i}a}{-vt + \mathrm{i}a}\right]^g \tag{4.28}$$

implying a scaling dimension (Eq. [4.21]) equal to $\Delta_i = g$. The lead LDOS at the junction therefore behaves as

$$\rho_i(0,\omega) \sim \omega^{g-1}. \tag{4.29}$$

Hence the LDOS has exactly the same behavior as for a single-wire perfect Andreev reflection,[64] meaning that tunneling spectroscopy follows the same power law for all fixed points appearing, i.e. there is no difference between the Kondo fixed point manifold and the resonant Andreev reflection fixed point.

For non-interacting lead electrons, i.e. with $g = 1$, Eq. [4.25] results in

$$\rho_i(0,\omega) = \frac{1}{2\pi v} = \frac{\nu_0}{2}, \qquad\qquad g = 1, \tag{4.30}$$

such that the electron density of states at the junction is half of that for bulk spinless electrons.

This can be confirmed by the exact solution for a Majorana fermion coupled to a quantum wire. Decomposing the lead electron into two Majorana fermions η and ζ, such that $\psi_j(x) = [\eta_j(x) + \mathrm{i}\zeta_j(x)]/\sqrt{2}$, the Majorana tunneling term (Eq. [4.8]) reads $H_A \propto \sum_j \sqrt{\Gamma_j}\gamma_j\zeta_j(0)$. Hence at the resonant Andreev reflection fixed point ($\Gamma_j \to \infty$), the ζ_j Majorana is hybridized with the γ_j Majorana within a "screening cloud" of size[89] $\xi_M \sim v/\Gamma_j$. In particular, the $x = 0$ Matsubara Green's function G_{ζ_j} for the ζ_j Majorana is given by[122]

$$G_{\zeta_j}(0,\mathrm{i}\omega_n) = \frac{-\mathrm{i}\,\mathrm{sgn}(\omega_n)}{2v}\frac{\mathrm{i}\omega_n}{\mathrm{i}\omega_n + \mathrm{i}\Gamma_j \mathrm{sgn}(\omega_n)}. \tag{4.31}$$

Hence the ζ_j contribution $\propto \mathrm{Im}\, G_{\zeta_j}(0, \mathrm{i}\omega_n \to \omega)$ to the LDOS vanishes as $\Gamma_j \to \infty$.

Therefore, at $x \ll \xi_M$, only the η_j Majorana contributes to the LDOS of the lead electron, which thus is half the bulk value, i.e. $\rho_j(0,\omega) = \nu_0/2$.

IV.3.2. Without Josephson coupling

For the topological Kondo model without Josephson coupling, i.e. the SO_2(N) model of Béri and Cooper,[56] the fields $\check{\phi}_0(x), \check{\vartheta}_1(x), ..., \check{\vartheta}_{N-1}(x)$ have Neumann BCs, and the fields $\check{\vartheta}_0(x), \check{\phi}_1(x), ..., \check{\phi}_{N-1}(x)$ Dirichlet BCs at the strong-coupling fixed point.

The original fields in terms of the rotated ones in Eq. [4.7] are given by

$$\begin{aligned}
\phi_1 &= \frac{1}{\sqrt{N}}\check{\phi}_0 + \frac{1}{\sqrt{2}}\check{\phi}_1 + \frac{1}{\sqrt{6}}\check{\phi}_2 + ... + \frac{1}{\sqrt{N(N-1)}}\check{\phi}_{N-1},\\
\phi_2 &= \frac{1}{\sqrt{N}}\check{\phi}_0 - \frac{1}{\sqrt{2}}\check{\phi}_1 + \frac{1}{\sqrt{6}}\check{\phi}_2 + ... + \frac{1}{\sqrt{N(N-1)}}\check{\phi}_{N-1},\\
\phi_3 &= \frac{1}{\sqrt{N}}\check{\phi}_0 - \frac{2}{\sqrt{6}}\check{\phi}_2 + ... + \frac{1}{\sqrt{N(N-1)}}\check{\phi}_{N-1},\\
&\vdots\\
\phi_N &= \frac{1}{\sqrt{N}}\check{\phi}_0 - \frac{N-1}{\sqrt{N(N-1)}}\check{\phi}_{N-1},
\end{aligned} \tag{4.32}$$

where for $N = 3$ the terms after the dots should be neglected. The change of basis between ϑ_j and $\check{\vartheta}_j$ is the same.

Hence, the electron operator $\psi_{j,L/R} \propto e^{\mathrm{i}(\phi_j \mp \vartheta_j)}$ at the junction at $x = 0$ is then given by, for simplicity considering lead $j = 1$,

$$\begin{aligned}
\psi_{1,R}(0) &\propto e^{\mathrm{i}[\vartheta_1(0)+\phi_1(0)]} = e^{\mathrm{i}[\frac{1}{\sqrt{N}}\check{\vartheta}_0(0)+...+\frac{1}{\sqrt{N}}\check{\phi}_0(0)+...]}\\
&= e^{\mathrm{i}c_1} e^{\mathrm{i}[\frac{1}{\sqrt{N}}\check{\phi}_0(0)+\frac{1}{\sqrt{2}}\check{\vartheta}_1(0)+...+\frac{1}{\sqrt{N(N-1)}}\check{\vartheta}_{N-1}(0)]},
\end{aligned} \tag{4.33}$$

with c_1 a constant, depending on the pinning value of the fields with Dirichlet BCs, which we gauge away.

From Eqs. [4.18)-(4.20] it follows that the term $\check{\phi}_0/\sqrt{N}$ in the exponent in Eq. [4.33] contributes a term $1/(Ng)$, and each term $\check{\vartheta}_n/\sqrt{n(n+1)}$ contributes a term $g/[n(n+1)]$, in the exponent of $\langle\psi_1(0,t)\psi_1^\dagger(0,0)\rangle$, which gives

$$\begin{aligned}
&\langle\psi_1(0,t)\psi_1^\dagger(0,0)\rangle\\
&\qquad = \frac{1}{\pi a}\left[\frac{\mathrm{i}a}{-vt+\mathrm{i}a}\right]^{\frac{1}{Ng}+\sum_{k=1}^{N-1}\frac{1}{k(k+1)}g}
\end{aligned} \tag{4.34}$$

(see also Appendix [IV.5] for a derivation of the $\tilde{\mathbb{M}}$ matrix). Hence we have the scaling exponent

$$\Delta_i = \frac{1}{Ng} + \frac{N-1}{N}g. \tag{4.35}$$

For $x \ll v/(2\omega)$, the lead LDOS therefore goes as

$$\rho_i(x \to 0, \omega) \sim \omega^{\frac{1}{Ng}+\frac{N-1}{N}g-1}. \tag{4.36}$$

Thus, for $\frac{1}{N-1} < g < 1$, we have a diverging LDOS at zero energy in the vicinity of the junction. For non-interacting lead electrons, $g = 1$, we get $\Delta_i = 1$, again giving the result $\rho_i(0,\omega) = \frac{\nu_0}{2}$ according to Eq. [4.25].

Note also, that in the $2x\omega/v \gg 1$ limit, there is an unusual exponent in the x dependence of the subleading oscillatory term in Eq. [4.24], which has an envelope decaying as $\sim x^{-3/(4g)-(g-1/g)/(2N)}$ as a function of distance x from the junction, and diverging as $\sim \omega^{(1-2/N)(g-1/g)/4-1}$ as function of energy.

IV.4. Discussion and conclusions

In this work, we have investigated the tunneling spectroscopy of topological Kondo systems, providing a route complementary to transport measurements in the search for experimental signatures of the predicted non-Fermi liquid behavior.

We have found that for the minimal topological Kondo setup of Béri and Cooper,[56] with a strong-coupling $SO_2(N)$ Kondo fixed point, the LDOS of the effectively spinless electrons in lead i in the immediate neighborhood of the junction (meaning that the distance x from the junction is less than $v/(2\omega)$) follows the power law in Eq. [4.36], i.e. it goes as $\sim \omega^{\frac{1}{Ng}+\frac{N-1}{N}g-1}$ as a function of energy ω. For non-interacting leads, $g = 1$, the LDOS close to the junction is a constant, equal to half the bulk value, i.e. $1/(2\pi v)$. However, for interacting lead electrons, $g < 1$, the scaling dimension (Eq. [4.35]) controlling the LDOS and hence the tunneling conductance of an STM tip probing lead

i, depends on the number N of leads. An experimental signature of the topological Kondo fixed point is therefore obtained by, using gate voltages, changing the number N of leads coupling to the Majoranas on the island, and then observing how the scaling exponent of the tunneling conductance in lead i changes.

In the topological Kondo system with a strong Josephson coupling, realizing an $SO_1(N)$ topological Kondo fixed point together with a resonant Andreev reflection fixed point and a continuous manifold of fixed points where Kondo and resonant Andreev reflection processes coexist,[109] we find that the LDOS of the lead electrons close to the junction instead follows the power law $\sim \omega^{g-1}$ as a function of energy, also with the constant value $1/(2\pi v)$ for $g = 1$. Hence in the strong Josephson coupling case, an STM experiment cannot distinguish the Kondo fixed point, or the coexistence manifold, from the pure resonant Andreev reflection fixed point.

The only trace of the topological Kondo physics in the LDOS in the $SO_1(N)$ case would come from the corrections due to the leading irrelevant operators at the fixed points. With scaling dimension $\Delta_{\rm LIO} > 1$, given by Eq. [4.11], these operators contribute terms $\sim \omega^{\Delta_{\rm LIO}-1}$ to the LDOS at $x \to 0$. Hence in these subleading corrections there is a difference between the resonant Andreev reflection fixed point where $\Delta_{\rm LIO} = 2$ and in the Kondo fixed point manifold, where $1 < \Delta_{\rm LIO} \leq 3/2$ ($1 < \Delta_{\rm LIO} \leq 2$) for $N = 3$ ($N > 3$). However, any repulsive interaction among the lead electrons renders the LDOS (Eq. [4.29]) divergent at zero energy, obscuring the subleading corrections which vanish as $\omega \to 0$.

In summary, we have provided analytical expressions for the LDOS of the leads in Majorana devices hosting the topological Kondo effect. This provides a clear signature, complementary to previously proposed transport measurements, to look for in experiments.

IV.5. Appendix A: Splitting matrix for topological Kondo

Let us here compute the $\tilde{\mathbb{M}}$ matrix for the topological Kondo effect of Béri and Cooper.[56]

First, note that the non-chiral and chiral bosonic fields (see Sec. IV.IV.2.1) are related by

$$\begin{aligned}\tilde{\vartheta}_i(x) &= \frac{1}{\sqrt{g}}\vartheta_i(x) = \left(\tilde{\phi}_{R,i} - \tilde{\phi}_{L,i}\right)/2 \\ &= \frac{1}{\sqrt{g}}\left(\phi_{R,i} - \phi_{L,i}\right)/2, \end{aligned} \tag{4.37}$$

$$\begin{aligned}\tilde{\phi}_i(x) &= \sqrt{g}\phi_i(x) = \left(\tilde{\phi}_{L,i} + \tilde{\phi}_{R,i}\right)/2 \\ &= \sqrt{g}\left(\phi_{L,i} + \phi_{R,i}\right)/2. \end{aligned} \tag{4.38}$$

The topological Kondo BC, i.e. the fields $\check{\phi}_0(x), \check{\vartheta}_1(x), ..., \check{\vartheta}_{N-1}(x)$ having Neumann BCs and the fields $\check{\vartheta}_0(x), \check{\phi}_1(x), ..., \check{\phi}_{N-1}(x)$ Dirichlet BCs, means that we pin the following vector (cf. Refs. [29 and 30])

$$\begin{pmatrix} \frac{1}{\sqrt{N}}[\tilde{\vartheta}_1(x=0) + \tilde{\vartheta}_2(x=0) + \tilde{\vartheta}_3(x=0) + \ldots + \tilde{\vartheta}_N(x=0)] \\ \frac{1}{\sqrt{2}}[\tilde{\phi}_1(x=0) - \tilde{\phi}_2(x=0)] \\ \frac{1}{\sqrt{6}}[\tilde{\phi}_1(x=0) + \tilde{\phi}_2(x=0) - 2\tilde{\phi}_3(x=0)] \\ \frac{1}{\sqrt{12}}[\tilde{\phi}_1(x=0) + \tilde{\phi}_2(x=0) + \tilde{\phi}_3(x=0) - 3\tilde{\phi}_4(x=0)] \\ \vdots \\ \frac{1}{\sqrt{(N-1)N}}[\tilde{\phi}_1(x=0) + \tilde{\phi}_2(x=0) + \tilde{\phi}_3(x=0) + \tilde{\phi}_4(x=0) + \cdots - (N-1)\tilde{\phi}_N(x=0)] \end{pmatrix} = \overrightarrow{0} \tag{4.39}$$

to a value that we set to be the null vector $\vec{0}$. With the notation $\tilde{\Phi}_j \equiv \tilde{\phi}_j(x=0)$ and $\tilde{\Theta}_j = \tilde{\vartheta}_j(x=0)$, we write this as

$$\begin{pmatrix} \frac{1}{\sqrt{N}}(\tilde{\Theta}_1 + \tilde{\Theta}_2 + \tilde{\Theta}_3 + \ldots + \tilde{\Theta}_N) \\ \frac{1}{\sqrt{2}}(\tilde{\Phi}_1 - \tilde{\Phi}_2) \\ \frac{1}{\sqrt{6}}(\tilde{\Phi}_1 + \tilde{\Phi}_2 - 2\tilde{\Phi}_3) \\ \frac{1}{\sqrt{12}}(\tilde{\Phi}_1 + \tilde{\Phi}_2 + \tilde{\Phi}_3 - 3\tilde{\Phi}_4) \\ \vdots \\ \frac{1}{\sqrt{(N-1)N}}(\tilde{\Phi}_1 + \tilde{\Phi}_2 + \tilde{\Phi}_3 + \tilde{\Phi}_4 + \cdots - (N-1)\tilde{\Phi}_N) \end{pmatrix} = \overrightarrow{0}. \tag{4.40}$$

From Eqs. [4.38] and [4.37] we have

$$\begin{pmatrix} (\tilde{\Phi}_{R,1}-\tilde{\Phi}_{L,1}+\tilde{\Phi}_{R,2}-\tilde{\Phi}_{L,2}+\tilde{\Phi}_{R,3}-\tilde{\Phi}_{L,3}+\ldots+\tilde{\Phi}_{R,N}-\tilde{\Phi}_{L,N}) \\ (\tilde{\Phi}_{R,1}+\tilde{\Phi}_{L,1}-\tilde{\Phi}_{R,2}-\tilde{\Phi}_{L,2}) \\ (\tilde{\Phi}_{R,1}+\tilde{\Phi}_{L,1}+\tilde{\Phi}_{R,2}+\tilde{\Phi}_{L,2}-2\tilde{\Phi}_{R,3}-2\tilde{\Phi}_{L,3}) \\ (\tilde{\Phi}_{R,1}+\tilde{\Phi}_{L,1}+\tilde{\Phi}_{R,2}+\tilde{\Phi}_{L,2}+\tilde{\Phi}_{R,3}+\tilde{\Phi}_{L,3}-3\tilde{\Phi}_{R,4}-3\tilde{\Phi}_{L,4}) \\ \vdots \\ (\tilde{\Phi}_{R,1}+\tilde{\Phi}_{L,1}+\tilde{\Phi}_{R,2}+\tilde{\Phi}_{L,2}+\tilde{\Phi}_{R,3}+\tilde{\Phi}_{L,3}+\tilde{\Phi}_{R,4}+\tilde{\Phi}_{L,4}+\cdots-(N-1)\tilde{\Phi}_{R,N}-(N-1)\tilde{\Phi}_{L,N}) \end{pmatrix} = \overrightarrow{0}, \quad (4.41)$$

where $\tilde{\Phi}_{R/L,j} = \tilde{\phi}_{R/L,j}(x=0)$. Hence

$$\begin{pmatrix} \tilde{\Phi}_{R,1}+\tilde{\Phi}_{R,2}+\tilde{\Phi}_{R,3}+\tilde{\Phi}_{R,N} \\ \tilde{\Phi}_{R,1}-\tilde{\Phi}_{R,2} \\ \tilde{\Phi}_{R,1}+\tilde{\Phi}_{R,2}-2\tilde{\Phi}_{R,3} \\ \tilde{\Phi}_{R,1}+\tilde{\Phi}_{R,2}+\tilde{\Phi}_{R,3}-3\tilde{\Phi}_{R,4} \\ \vdots \\ \tilde{\Phi}_{R,1}+\tilde{\Phi}_{R,2}+\tilde{\Phi}_{R,3}+\tilde{\Phi}_{R,4}+\cdots-(N-1)\tilde{\Phi}_{R,N} \end{pmatrix} = \begin{pmatrix} \tilde{\Phi}_{L,1}+\tilde{\Phi}_{L,2}+\tilde{\Phi}_{L,3}+\tilde{\Phi}_{L,N} \\ -\tilde{\Phi}_{L,1}+\tilde{\Phi}_{L,2} \\ -\tilde{\Phi}_{L,1}-\tilde{\Phi}_{L,2}+2\tilde{\Phi}_{L,3} \\ -\tilde{\Phi}_{L,1}-\tilde{\Phi}_{L,2}-\tilde{\Phi}_{L,3}+3\tilde{\Phi}_{L,4} \\ \vdots \\ \tilde{\Phi}_{L,1}+\tilde{\Phi}_{L,2}+\tilde{\Phi}_{L,3}+\tilde{\Phi}_{L,4}+\cdots-(N-1)\tilde{\Phi}_{L,N} \end{pmatrix} \quad (4.42)$$

$$\Leftrightarrow \begin{pmatrix} 1 & 1 & 1 & 1 & \cdots & 1 \\ 1 & -1 & 0 & 0 & \cdots & 0 \\ 1 & 1 & -2 & 0 & \cdots & 0 \\ 1 & 1 & 1 & -3 & \cdots & 0 \\ \vdots & \vdots & \vdots & \vdots & \ddots & \vdots \\ 1 & 1 & 1 & 1 & \cdots & -(N-1) \end{pmatrix} \begin{pmatrix} \tilde{\Phi}_{R,1} \\ \tilde{\Phi}_{R,2} \\ \tilde{\Phi}_{R,3} \\ \tilde{\Phi}_{R,4} \\ \vdots \\ \tilde{\Phi}_{R,N} \end{pmatrix} = \begin{pmatrix} 1 & 1 & 1 & 1 & \cdots & 1 \\ -1 & 1 & 0 & 0 & \cdots & 0 \\ -1 & -1 & 2 & 0 & \cdots & 0 \\ -1 & -1 & -1 & 3 & \cdots & 0 \\ \vdots & \vdots & \vdots & \vdots & \ddots & \vdots \\ -1 & -1 & -1 & -1 & \cdots & (N-1) \end{pmatrix} \begin{pmatrix} \tilde{\Phi}_{L,1} \\ \tilde{\Phi}_{L,2} \\ \tilde{\Phi}_{L,3} \\ \tilde{\Phi}_{L,4} \\ \vdots \\ \tilde{\Phi}_{L,N} \end{pmatrix}. \quad (4.43)$$

It follows that

$$\begin{pmatrix} \tilde{\Phi}_{R,1} \\ \tilde{\Phi}_{R,2} \\ \tilde{\Phi}_{R,3} \\ \tilde{\Phi}_{R,4} \\ \vdots \\ \tilde{\Phi}_{R,N} \end{pmatrix} = \underbrace{\begin{pmatrix} \frac{1}{N} & \frac{1}{2} & \frac{1}{6} & \frac{1}{12} & \cdots & \frac{1}{N(N-1)} \\ \frac{1}{N} & -\frac{1}{2} & \frac{1}{6} & \frac{1}{12} & \cdots & \frac{1}{N(N-1)} \\ \frac{1}{N} & 0 & -\frac{1}{3} & \frac{1}{12} & \cdots & \frac{1}{N(N-1)} \\ \frac{1}{N} & 0 & 0 & -\frac{1}{4} & \cdots & \frac{1}{N(N-1)} \\ \vdots & \vdots & \vdots & \vdots & \ddots & \vdots \\ \frac{1}{N} & 0 & 0 & 0 & \cdots & -\frac{1}{N} \end{pmatrix} \begin{pmatrix} 1 & 1 & 1 & \cdots & \cdots & 1 \\ -1 & 1 & 0 & 0 & \cdots & 0 \\ -1 & -1 & 2 & 0 & \cdots & 0 \\ -1 & -1 & -1 & 3 & \cdots & 0 \\ \vdots & \vdots & \vdots & \vdots & \ddots & \vdots \\ -1 & -1 & -1 & -1 & \cdots & (N-1) \end{pmatrix}}_{=\tilde{\mathbb{M}}} \begin{pmatrix} \tilde{\Phi}_{L,1} \\ \tilde{\Phi}_{L,2} \\ \tilde{\Phi}_{L,3} \\ \tilde{\Phi}_{L,4} \\ \vdots \\ \tilde{\Phi}_{L,N} \end{pmatrix}. \quad (4.44)$$

Thus the splitting matrix $\tilde{\mathbb{M}}$ for the topological Kondo effect is

$$\tilde{\mathbb{M}} = \begin{pmatrix} 2/N-1 & 2/N & \cdots & 2/N \\ 2/N & 2/N-1 & \cdots & 2/N \\ \vdots & \vdots & \ddots & \vdots \\ 2/N & 2/N & \cdots & 2/N-1 \end{pmatrix}. \quad (4.45)$$

For Fermi-liquid leads ($g=1$, i.e. $\tilde{\mathbb{M}} = \mathbb{M}$), this agrees[105,106] with the expression $G_{ij} = (e^2/h)(\delta_{ij} - \mathbb{M}_{ij})$ for the $g=1$ conductance tensor.

Hence, according to Eq. [4.21], the scaling dimension for electron tunneling into a lead, close to the junction, is

$$\begin{aligned}\Delta_i &= \{(1-\tilde{\mathbb{M}}_{ii})g + (1+\tilde{\mathbb{M}}_{ii})/g\}/2 \\ &= (N-1)g/N + 1/(Ng). \end{aligned} \tag{4.46}$$

This thesis was funded with support from the European Commission, the European Social Fund and Regione Calabria. This thesis only reflects the views of the author. The Commission cannot be held responsible for any use which may be made of the information contained herein.

---

[1] K. Inoue, K. Kimura, K. Maehashi, S. Hasegawa, H. Nakashima, M. Iwane, O. Matsuda, and K. Murase, Journal of Crystal Growth **127**, 1041 (1993).
[2] R. Ntzela, Q. Gonga, M. Ramsteinerb, U. Jahnb, K. J. Friedlandb, and K. Ploog, Microelectronics Journal **33**, 573 (2002).
[3] D. Pan, M. Fu, X. Yu, X. Wang, L. Zhu, S. Nie, S. Wang, Q. Chen, P. Xiong, S. Molnr, and J. Zhao, Nano Lett. **14**, 1214 (2014).
[4] H. Ishii, H. Kataura, H. Shiozawa, H. Yoshioka, H. Otsubo, Y. Takayama, T. Miyahara, S. Suzuki, Y. Achiba, M. Nakatake, T. Narimura, M. Higashiguchi, K. Shimada, H. Namatame, and M. Taniguchi, Nature **426**, 540 (2003).
[5] M. Bockrath, D. H. Cobden, J. Lu, A. G. Rinzler, R. E. Smalley, L. Balents, and P. L. McEuen, Nature **397**, 598 (1999).
[6] D. S. Bethune, C. H. Kiang, M. S. Vries, G. Gorman, R. Savoy, J. Vazquez, and R. Beyers, Nature **363**, 605 (1993).
[7] P. Segovia, D. Purdie, M. Hengsberger, and Y. Baer, Nature **402**, 504 (1999).
[8] I. Barke, T. K. Rugheimer, F. Zheng, and F. Himpsel, Applied Surface Science **254**, 4 (2007).
[9] L. D. Landau, Sov. Phys. JETP **3**, 920 (1957).
[10] L. D. Landau, Sov. Phys. JETP **5**, 101 (1957).
[11] L. D. Landau, Sov. Phys. JETP **8**, 70 (1958).
[12] A. A. Abrikosov, L. P. Gorkov, and I. E. Dzyaloshinski, *Methods of Quantum field theory in statistical physics* (Dover, New York, 1963).
[13] M. P. A. Fisher and L. I. Glazman, in *Mesoscopic Electron Transport*, edited by G. S. L. Kouwenhoven and L. Sohn (NATO ASI Series E, Kluwer Ac. Publ., Dordrecht, 1997).
[14] A. J. Schofield, Contemporary Physics **40**, 95 (1999).
[15] P. Nozières, *Theory of interacting Fermi systems* (Addison-Wesley, Reading (MA), 1964).
[16] J. Sólyom, Adv. Phys. **28**, 201 (1979).
[17] R. Shankar, Rev. Mod. Phys. **66**, 129 (1994).
[18] J. Polchinski, in *Proceedings of 1992 Theoretical Advanced Studies Institute in Elementary Particle Physics*, edited by J. Harvey and J. Polchinski (World Scientific, Singapore, 1993).
[19] S. Tomonaga, Prog. Theor. Phys. **13**, 467 (1955).
[20] J. M. Luttinger, J. Math. Phys. **4**, 1154 (1963).
[21] F. D. M. Haldane, J. Phys. C: Solid State Phys. **14**, 2585 (1981).
[22] F. D. M. Haldane, Phys. Rev. Lett. **47**, 1840 (1981).
[23] S. Das, S. Rao, and D. Sen, Phys. Rev. B **74**, 045322 (2006).
[24] D. N. Aristov, Phys. Rev. B **83**, 115446 (2011).
[25] C. L. Kane and M. P. A. Fisher, Phys. Rev. Lett. **68**, 1220 (1992).
[26] C. L. Kane and M. P. A. Fisher, Phys. Rev. B **46**, 15233 (1992).
[27] A. Furusaki and N. Nagaosa, Phys. Rev. B **47**, 4631 (1993).
[28] C. Chamon, M. Oshikawa, and I. Affleck, Phys. Rev. Lett. **91**, 206403 (2003).
[29] M. Oshikawa, C. Chamon, and I. Affleck, J. Stat. Mech. **P02008** (2006), 10.1088/1742-5468/2006/02/P02008.
[30] C.-Y. Hou and C. Chamon, Phys. Rev. B **77**, 155422 (2008).
[31] C.-Y. Hou, A. Rahmani, A. E. Feiguin, and C. Chamon, Phys. Rev. B **86**, 075451 (2012).
[32] A. Rahmani, C.-Y. Hou, A. Feiguin, C. Chamon, and I. Affleck, Phys. Rev. Lett. **105**, 226803 (2010).
[33] A. Rahmani, C.-Y. Hou, A. Feiguin, M. Oshikawa, C. Chamon, and I. Affleck, Phys. Rev. B **85**, 045120 (2012).
[34] N. Sedlmayr, D. Morath, J. Sirker, S. Eggert, and I. Affleck, Phys. Rev. B **89**, 045133 (2014).
[35] A. E. Feiguin and S. R. White, Phys. Rev. B **72**, 220401(R) (2005).
[36] C. Karrasch, J. H. Bardarson, and J. E. Moore, Phys. Rev. Lett. **108**, 227206 (2012).
[37] K. A. Matveev, D. Yue, and L. I. Glazman, Phys. Rev. Lett. **71**, 3351 (1993).
[38] D. Yue, L. I. Glazman, and K. A. Matveev, Phys. Rev. B **49**, 1966 (1994).
[39] S. Lal, S. Rao, and D. Sen, Phys. Rev. B **66**, 165327 (2002).
[40] Y. V. Nazarov and L. I. Glazman, Phys. Rev. Lett. **91**, 126804 (2003).
[41] V. Meden, S. Andergassen, W. Metzner, U. Schollwöck, and K. Schönhammer, Europhys. Lett. **64**, 769 (2003).
[42] S. Andergassen, T. Enss, V. Meden, , W. Metzner, U. Schollwöck, and K. Schönhammer, Phys. Rev. B **70**, 075102 (2004).
[43] V. Meden, T. Enss, S. Andergassen, W. Metzner, and K. Schönhammer, Phys. Rev. B **71**, 041302(R) (2005).
[44] T. Enss, V. Meden, S. Andergassen, X. Barnabe-Theriault, W. Metzner, and K. Schönhammer, Phys. Rev. B **71**, 155401 (2005).
[45] S. Andergassen, T. Enss, V. Meden, W. Metzner, U. Schollwöck, and K. Schönhammer, Phys. Rev. B **73**, 045125 (2006).
[46] X. Barnabe-Theriault, A. Sedeki, V. Meden, and K. Schönhammer, Phys. Rev. Lett. **94**, 136405 (2005).
[47] V. Meden, S. Andergassen, T. Enss, H. Schöller, and K. Schönhammer, New Journal of Physics **10**, 045012 (2006).
[48] X. Barnabe-Theriault, A. Sedeki, V. Meden, and K. Schönhammer, Phys. Rev. B **71**, 205327 (2005).
[49] K. Janzen, V. Meden, and K. Schönhammer, Phys. Rev. B **74**, 085301 (2006).

[50] S. G. Jakobs, V. Meden, H. Schöller, and T. Enss, Phys. Rev. B **75**, 035126 (2007).
[51] M. Titov, M. Müller, and W. Belzig, Phys. Rev. Lett. **97**, 237006 (2006).
[52] D. N. Aristov and P. Wölfle, Phys. Rev. B **86**, 035137 (2012).
[53] D. N. Aristov and P. Wölfle, Phys. Rev. B **88**, 075131 (2013).
[54] D. N. Aristov and P. Wölfle, Phys. Rev. B **84**, 155426 (2011).
[55] D. Giuliano and A. Nava, Phys. Rev. B **92**, 125138 (2015).
[56] B. Béri and N. Cooper, Phys. Rev. Lett. **109**, 156803 (2012).
[57] E. Eriksson, A. Nava, C. Mora, and R. Egger, Phys. Rev. B **90**, 245417 (2014).
[58] I. Affleck, "Quantum impurity problems in condensed matter physics," Lecture Notes, Les Houches (2008).
[59] G. S. Grest, Phys. Rev. B **14**, 5114 (1976).
[60] T. Sugiyama, Prog. Theor. Phys. **64**, 406 (1980).
[61] I. Affleck and D. Giuliano, J. Stat. Mech. **P06011** (2012), 10.1088/1742-5468/2013/06/P06011.
[62] M. Cvetic, G. W. Gibbons, H. L, and C. N. Pope, Phys. Rev. D **65**, 106004 (2002).
[63] P. Dita, J. Phys. A: Math. Gen. **15**, 3465 (1982).
[64] L. Fidkowski, J. Alicea, N. H. Lindner, R. M. Lutchyn, and M. P. A. Fisher, Phys. Rev. B **85**, 245121 (2012).
[65] A. Lande, *From Dualism to Unity in Quantum Physics* (Cambridge U. P., 1960).
[66] C. Rovelli, Int. J. of Theor. Phys. **35**, 1637 (1996).
[67] A. Khrennikov, J. Phys. **34**, 1 (2001).
[68] G. Tanner, J. Phys. A **34**, 8485 (2001).
[69] K. Zyczkowski, M. Kus, W. Sirker, Slomczynski, and H.-J. Sommers, J. Phys. A **36**, 3425 (2003).
[70] A. Agarwal, S. Das, and D. Sen, Phys. Rev. B **81**, 035324 (2010).
[71] I. Bengtsson, "The importance of being unistochastic," USITP 03-12 (2003).
[72] I. Bengtsson, A. Ericsson, M. Kus, W. Tadej, and K. Zyczkowski, Commun. Math. Phys. **259**, 307 (2005).
[73] G. Birkhoff, Univ. Nac. Tucuman Rev. A **5**, 147 (1946).
[74] B. Jokanovic and A. Marincic, in *TELSIKS 2003. 6th International Conference in Telecommunications in Modern Satellite, Cable and Broadcasting Service, 2003.* (2003).
[75] F. M. Ghannouchi and A. Mohammadi, *The Six-Port Technique with Microwave and Wireless Applications* (ARTECH HOUSE, 2009).
[76] L. Arnaut and L. Davis, in *1995. 25th European Microwave Conference* (1995).
[77] S. Das and S. Rao, Phys. Rev. B **78**, 205421 (2008).
[78] D. N. Aristov and P. Wölfle, Phys. Rev. B **80**, 045109 (2009).
[79] Z. Shi and I. Affleck, "New results on y-junctions through yue et al.s approach," Private communication.
[80] D. G. Polyakov and I. V. Gornyi, Phys. Rev. B **68**, 035421 (2003).
[81] T. L. Schmidt, A. Imambekov, and L. I. Glazman, Phys. Rev. B **82**, 245104 (2010).
[82] J. Chardy, Encyclopedia of Mathematical Physics (2006).
[83] D. L. Maslov and M. Stone, Phys. Rev. B **52**, R5539 (1995).
[84] H. J. Schulz, Phys. Rev. B **22**, 5274 (1980).
[85] J. von Delft and H. Schoeller, Annalen Phys. **7**, 225 (1998).
[86] S. Das, S. Rao, and A. Saha, Phys. Rev. B **77**, 155418 (2008).
[87] D. Giuliano and I. Affleck, J. Stat. Mech. **P02034** (2013), 10.1088/1742-5468/2013/02/P02034.
[88] D. Giuliano and I. Affleck, Phys. Rev. B **90**, 045133 (2014).
[89] I. Affleck and D. Giuliano, J. Stat. Phys. , Special Issue in Memory of K. G. Wilson **157**, 666 (2014).
[90] J. Alicea, Rep. Prog. Phys. **75**, 076501 (2012).
[91] M. Leijnse and K. Flensberg, Semicond. Sci. Techn. **27**, 124003 (2012).
[92] C. Beenakker, Annu. Rev. Condens. Matter Phys. **4**, 113 (2013).
[93] V. Mourik, K. Zuo, S. Frolov, S. Plissard, E. Bakkers, and L. Kouwenhoven, Science **336**, 1003 (2012).
[94] L. Rokhinson, X. Liu, and J. Furdyna, Nat. Phys. **8**, 795 (2012).
[95] A. Das, Y. Ronen, Y. Most, Y. Oreg, M. Heiblum, and H. Shtrikman, Nat. Phys. **8**, 887 (2012).
[96] M. Deng, C. Yu, G. Huang, M. Larsson, P. Caroff, and H. Xu, Nano Lett. **12**, 6414 (2012).
[97] H. Churchill, V. Fatemi, K. Grove-Rasmussen, M. Deng, P. Caroff, H. Xu, and C. Marcus, Phys. Rev. B **87**, 241401(R) (2013).
[98] E. Lee, X. Jiang, M. Houzet, R. Aguado, C. Lieber, and S. De Franceschi, Nature Nanotech. **267**, 79 (2014).
[99] A. Kitaev, Ann. Phys. (N.Y.) **303**, 2 (2003).
[100] L. Fu and C. Kane, Phys. Rev. Lett. **100**, 096407 (2008).
[101] J. Sau, R. Lutchyn, T. S., and S. Das Sarma, Phys. Rev. Lett. **104**, 040502 (2010).
[102] Y. Oreg, G. Refael, and F. von Oppen, Phys. Rev. Lett. **105**, 177002 (2010).
[103] L. Fu, Phys. Rev. Lett. **104**, 056402 (2010).
[104] M. R. Galpin, A. K. Mitchell, J. Temaismithi, D. E. Logan, B. Béri, and N. R. Cooper, Phys. Rev. B **89**, 045143 (2014).
[105] B. Béri, Phys. Rev. Lett. **110**, 216803 (2013).
[106] A. Altland and R. Egger, Phys. Rev. Lett **110**, 196401 (2013).
[107] A. Altland, B. Béri, R. Egger, and A. M. Tsvelik, Phys. Rev. Lett **113**, 076401 (2014).
[108] A. Altland, B. Béri, R. Egger, and A. M. Tsvelik, J. Phys. A. **47**, 265001 (2014).
[109] E. Eriksson, C. Mora, A. Zazunov, and R. Egger, Phys. Rev. Lett. **113**, 076404 (2014).
[110] A. M. Tsvelik, Phys. Rev. Lett **110**, 147202 (2013).

[111] A. Zazunov, A. Altland, and R. Egger, New J. Phys. **16**, 015010 (2014).
[112] A. O. Gogolin, A. A. Nersesyan, and A. M. Tsvelik, *Bosonization and Strongly Correlated Systems* (Cambridge University Press, 2004).
[113] S. Eggert, Phys. Rev. Lett. **84**, 4413 (2000).
[114] P. Kakashvili, H. Johannesson, and S. Eggert, Phys. Rev. B **74**, 085114 (2006).
[115] C. Winkelholz, R. Fazio, F. Hekking, and G. Schön, Phys. Rev. Lett. **77**, 3200 (1996).
[116] D. Liu and A. Levchenko, Phys. Rev. B **88**, 155315 (2013).
[117] A. Zazunov, A. Yeyati, and R. Egger, Phys. Rev. B **84**, 165440 (2011).
[118] C. Nayak, M. P. A. Fisher, A. W. W. Ludwig, and H. H. Lin, Phys. Rev. B **59**, 15694 (1999).
[119] S. Chen, B. Trauzettel, and R. Egger, Phys. Rev. Lett. **89**, 226404 (2002).
[120] P. Di Francesco, P. Mathieu, and D. Sénéchal, *Conformal Field Theory* (Springer Verlag, New York, 1997).
[121] H. Bruus and K. Flensberg, *Many-Body Quantum Theory in Condensed Matter Physics* (Oxford University Press, Oxford, 2004).
[122] C. Mora and K. Le Hur, Phys. Rev. B **88**, 241302(R) (2013).